



## Topical Report

# Hydraulic Fracture Model Comparison Study: Complete Results

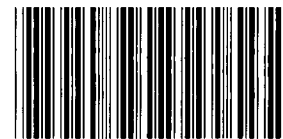
*Prepared by:*

*N. R. Warpinski, Sandia National Laboratories*

*I. S. Abou-Sayed, Mobil Exploration and Production Services*

*Z. Moschovidis, AMOCO Production Company*

*C. Parker, CONOCO*



\*8574884\*

**SANDIA NATIONAL  
LABORATORIES  
TECHNICAL LIBRARY**

**Gas Research Institute**

*Tight Sands and Gas Processing Research Department  
February 1993*

**HYDRAULIC FRACTURE MODEL COMPARISON STUDY:  
COMPLETE RESULTS**

**TOPICAL REPORT  
(February, 1993)**

Prepared by  
N. R. Warpinski Sandia National Laboratories  
I.S. Abou-Sayed Mobil Exploration and Production Services  
Z. Moschovidis AMOCO Production Company  
C. Parker CONOCO

Prepared at  
Sandia National Laboratories  
Division 6114  
P.O. Box 5800  
Albuquerque, New Mexico 87185

For  
GAS RESEARCH INSTITUTE  
Contract No. 5089-211-2059

GRI Project Manager  
Steve Wolhart  
Tight Gas Sands Field Evaluation

February 1993

## **GRI DISCLAIMER**

**LEGAL NOTICE** This report was prepared by Sandia National Laboratories as an account of work sponsored by the Gas Research Institute (GRI). Neither GRI, members of GRI, nor any person acting on behalf of either:

- a. **Makes any warranty or representation, express or implied, with respect to the accuracy, completeness, or usefulness of the information contained in this report, or that the use of any apparatus, method, or process disclosed in this report may not infringe privately owned rights; or**
- b. **Assumes any liability with respect to the use of, or for damages resulting from the use of, any information, apparatus, method, or process disclosed in this report.**

<b>REPORT DOCUMENTATION PAGE</b>	<b>1. REPORT NO.</b> GRI-93/0109	<b>2.</b>	<b>3. Recipient's Accession No.</b>
<b>4. Title and Subtitle</b> Hydraulic Fracture Model Comparison Study: Complete Results			<b>5. Report Date</b> 2/17/93 Preparation
<b>7. Author(s)</b> N.R. Warpinski, I.S. Abou-Sayed, C. Parker, Z. Moschovidis			<b>6.</b>
<b>9. Performing Organization Name and Address</b> Sandia National Laboratories Division 6253 P.O. Box 5800 Albuquerque, New Mexico 87185			<b>8. Performing Organization Rept. No.</b> SAND93-7042
<b>12. Sponsoring Organization Name and Address</b> Gas Research Institute 8600 Bryn Mawr Avenue Chicago, Illinois 60631			<b>10. Project/Task/Work Unit No.</b>
			<b>11. Contract(C) or Grant(G) No.</b> (C) 5089-211-2059 (G)
			<b>13. Type of Report &amp; Period Covered</b> Topical Report
<b>15. Supplementary Notes</b> Topical report on the results of the Fracture Propagation Modeling Forum			<b>14.</b>
<b>16. Abstract (Limit: 200 words)</b> This study is a comparison of hydraulic fracture models run using test data from the GRI Staged-Field Experiment #3 (SFE-3). Models compared include: (1) PKN and GDK constant-height versions; (2) 3-layer pseudo-3-D models; and (3) 5-layer 3-D or pseudo-3D models. Model calculations were provided by several consulting companies, oil producing companies, service companies, and academia. Modelers were given the measured stress and material property data obtained at SFE-3 and fluid properties approximating those used during SFE-3 stimulations. Companies were allowed to run any or all of the three cases (constant height, 3 layer, or 5 layer) using their own models or commercial models they had purchased. Included with the results are brief discussions of each model. This paper documents the differences in length, height, width, pressure, and efficiency predicted by the various models for each of the three cases. Well-known differences in length between 2-D PKN and GDK models are shown, but so are differences between the pseudo-3-D and fully-3-D models. For example, two of the models yield much shorter lengths than other 3-D models. Overall, efficiencies varied between 40% and 97%, and net pressures ranged from about 700 to 1600 psi for the 3-layer and 5-layer cases. Heights varied from 300-700 ft. These comparisons clearly show that fracture design models give widely varying results. These results provide the petroleum engineer a practical comparison of the various available design models for an actual field test.			
<b>17. Document Analysis a. Descriptors</b> Tight gas sands, hydraulic fracturing, fracture modeling			
<b>b. Identifiers/Open-Ended Terms</b> SFE No. 3, fracture height, Fracpro, Trifrac, Stimplan, MFRAC-II, GOHFER, HYFRAC3D, TerraFrac, Enerfrac			
<b>c. COSATI Field/Group</b>			
<b>18. Availability Statement</b> Release unlimited		<b>19. Security Class (This Report)</b> unclassified	<b>21. No. of Pages</b>
		<b>20. Security Class (This Page)</b>	<b>22. Price</b>

<b>Title</b>	<b>Hydraulic Fracture Model Comparison Study: Complete Results</b>
<b>Contractor</b>	<b>Sandia National Laboratories</b>  <b>GRI Contract Number: 5089-211-2059</b>
<b>Principal Investigator</b>	<b>N. R. Warpinski</b>
<b>Report Period</b>	<b>February 1991-February, 1993</b> <b>Topical Report</b>
<b>Objective</b>	<b>To develop a comparative study of hydraulic-fracture simulators in order to provide stimulation engineers with the necessary information to make rational decisions on the type of models most suited for their needs.</b>
<b>Technical Perspective</b>	<b>Large quantities of natural gas exist in low permeability reservoirs throughout the US. Characteristics of these reservoirs, however, make production difficult and often economic and stimulation is required. Hydraulic fracturing is one of the most important stimulation techniques available to the petroleum engineer, being used extensively in tight gas sandstones, coalbed methane, high permeability sandstones in Alaska, very weak sandstones off the US. gulf coast, in horizontal wells in chalks, and in many other applications from waste disposal to geothermal reservoirs. Because of this diversity of application, hydraulic fracture design models must be able to account for widely varying rock properties, reservoir properties, in situ stresses, fracturing fluids, and proppant loads. As a result, fracture simulation has emerged as a highly complex endeavor that must be able to describe many different physical processes.</b>  <b>In addition, many modelers have added ad-hoc features to their models to simulate mechanisms that are not well understood at this time. Such mechanisms include tip effects, wall roughness, complex fracturing, and some aspects of height growth. As a result, fracture models have become heteromorphic with no standard of comparison. Engineers are thus faced with</b>

a difficult choice in selecting a model that is appropriate for their needs.

**Technical Approach**

The technical approach was to collect and integrate the results of the Fracture Model Propagation Forum into a comparative study of the similarity and differences of hydraulic-fracture model output run on the same input data. Participating modelers were given two treatment data sets (one Newtonian fluid, one power-law fluid) and four different geometries (constant-height PKN, constant-height GDK, 3-layer, 5-layer) and asked to provide length, height, maximum width at the wellbore, average width at the wellbore, average width in the whole fracture, net pressure, and efficiency at 25 minute intervals throughout the fracture treatment (total time of 200 minutes). These results were assembled by a four member committee into plots and tables of comparative data.

**Results**

This report is a comparison of the fracture modeling results of twelve different simulators, some of them run in different modes for eight separate design cases. Comparisons of length, width, height, net pressure, maximum width at the wellbore, average width at the wellbore, and average width in the fracture have been made, both for the final geometry and as a function of time. For the models in this study, differences in fracture length, height and width are often greater than a factor of two. In addition, several comparisons of the same model with different options show a large variability in model output depending upon the options chosen. Two comparisons were made of the same model run by different companies; in both cases the agreement was good.

## Table of Contents

1.0 RESEARCH OBJECTIVES	1
2.0 RATIONALE	2
3.0 BACKGROUND - BASIC MODELING DISCUSSION	3
3.1 Planar 3-D Models	4
3.2 Planar 3-D Finite Difference Model - GOHFER	4
3.3 Pseudo-3-D Models	5
3.4 Classic PKN and GDK Models	5
4.0 FRACTURE MODELS	6
4.1 S.A. Holditch & Assoc. (TRIFRAC)	6
4.2 Meyer & Associates (MFRAC-II)	6
4.3 Advani (Lehigh HYFRAC3D)	7
4.4 Shell (ENERFRAC)	7
4.5 Halliburton (PROP)	8
4.6 Chevron	8
4.7 Conoco	9
4.8 Marathon (GOHFER)	9
4.9 ARCO (using TerraFrac)	9
4.10 NSI (STIMPLAN)	10
4.11 Resources Engineering Systems (FRAPRO)	10
4.12 Texaco (using FRACPRO)	11
5.0 SFE-3 FORMATION AND TREATMENT DATA	12
6.0 TEST CASES	13
7.0 MODEL RESULTS	14
7.1 2-D Results (Cases 1-4)	14
7.2 3-Layer Results	16
7.3 5-Layer Results	16
8.0 DISCUSSION	17
9.0 CONCLUSIONS	19
10.0 RECOMMENDATIONS	20
11.0 REFERENCES	21
APPENDIX A	107
APPENDIX B	116
APPENDIX C	125
APPENDIX D	134
APPENDIX E	136
APPENDIX F	145
APPENDIX G	155

## List of Tables

- Table 1 Rock and Reservoir Data
- Table 2 Treatment Data
- Table 3 2-D Results at End of Pump
- Table 4 3-Layer Results at End of Pump
- Table 5 5-layer Results at End of Pump
- Table 6 Time to breakthrough into lower layer
- Table 7 S.A Holditch & Assoc. - GDK Constant height  $\mu=200$  cp
- Table 8 S.A Holditch & Assoc. - GDK Constant height  $n'=0.5$ ,  $k'=0.06$
- Table 9 S.A Holditch & Assoc. - PKN Constant height  $\mu=200$  cp
- Table 10 S.A Holditch & Assoc. - PKN Constant height  $n'=0.5$ ,  $k'=0.06$
- Table 11 S.A. Holditch & Assoc. - 3-layer  $\mu=200$  cp
- Table 12 S.A. Holditch & Assoc. - 3-layer  $n'=0.05$ ,  $k'=0.06$
- Table 13 S.A. Holditch & Assoc. - 5-layer  $\mu=200$  cp
- Table 14 S.A. Holditch & Assoc. - 5-layer  $n'=0.05$ ,  $k'=0.06$
- Table 15 Meyer & Assoc. - GDK Constant height  $\mu=200$  cp Base Case
- Table 16 Meyer & Assoc. - GDK Constant height  $n'=0.5$ ,  $k'=0.06$  Base Case
- Table 17 Meyer & Assoc. - PKN Constant height  $\mu=200$  cp Base Case
- Table 18 Meyer & Assoc. - PKN Constant height  $n'=0.5$ ,  $k'=0.06$  Base Case
- Table 19 Meyer & Assoc. - 3-layer  $\mu=200$  cp Base Case
- Table 20 Meyer & Assoc. - 3-layer  $n'=0.5$ ,  $k'=0.06$  Base Case
- Table 21 Meyer & Assoc. - 5-layer  $\mu=200$  cp Base Case
- Table 22 Meyer & Assoc. - 5-layer  $n'=0.5$ ,  $k'=0.06$  Base Case
- Table 23 Meyer & Assoc. - GDK Constant height  $\mu=200$  cp Knobs on
- Table 24 Meyer & Assoc. - GDK Constant height  $n'=0.5$ ,  $k'=0.06$  Knobs on
- Table 25 Meyer & Assoc. - PKN Constant height  $\mu=200$  cp Knobs on
- Table 26 Meyer & Assoc. - PKN Constant height  $n'=0.5$ ,  $k'=0.06$  Knobs on
- Table 27 Meyer & Assoc. - 3-layer  $\mu=200$  cp Knobs on
- Table 28 Meyer & Assoc. - 3-layer  $n'=0.5$ ,  $k'=0.06$  Knobs on
- Table 29 Meyer & Assoc. - 5-layer  $\mu=200$  cp Knobs on
- Table 30 Meyer & Assoc. - 5-layer  $n'=0.5$ ,  $k'=0.06$  Knobs on
- Table 31 Advani - PKN Constant Height  $\mu=200$  cp
- Table 32 Advani - PKN Constant Height  $n'=0.5$ ,  $k'=0.06$
- Table 33 Advani - 3-Layer  $\mu=200$  cp
- Table 34 Advani - 3-Layer  $n'=0.5$ ,  $k'=0.06$
- Table 35 Advani - 5-Layer  $\mu=200$  cp
- Table 36 Advani - 5-Layer  $n'=0.5$ ,  $k'=0.06$
- Table 37 Shell - GDK Constant Height  $\mu=200$  cp
- Table 38 Shell - GDK Constant Height  $n'=0.5$ ,  $k'=0.06$
- Table 39 Shell - PKN Constant Height  $\mu=200$  cp
- Table 40 Shell - PKN Constant Height  $n'=0.5$ ,  $k'=0.06$
- Table 41 Shell ENERFRAC  $\mu=200$  cp Base Case
- Table 42 Shell ENERFRAC  $n'=0.5$ ,  $k'=0.06$  Base Case
- Table 43 Shell ENERFRAC  $\mu=200$  cp Overpressure=500 psi

Table 44 Shell ENERFRAC  $n'=0.5$ ,  $k'=0.06$  Overpressure=500 psi  
Table 45 Shell ENERFRAC  $\mu=200$  cp Overpressure=1000 psi  
Table 46 Shell ENERFRAC  $n'=0.5$ ,  $k'=0.06$  Overpressure=1000 psi  
Table 47 Shell ENERFRAC  $\mu=200$  cp Overpressure=1500 psi  
Table 48 Shell ENERFRAC  $n'=0.5$ ,  $k'=0.06$  Overpressure=1500 psi  
Table 49 Shell ENERFRAC  $\mu=200$  cp Overpressure=2000 psi  
Table 50 Shell ENERFRAC  $n'=0.5$ ,  $k'=0.06$  Overpressure=2000 psi  
Table 51 Halliburton GDK Constant Height  $\mu=200$  cp  
Table 52 Halliburton GDK Constant Height  $n'=0.5$ ,  $k'=0.06$   
Table 53 Chevron GDK Constant Height  $\mu=200$  cp  
Table 54 Chevron PKN Constant Height  $\mu=200$  cp  
Table 55 Conoco GDK Constant Height  $\mu=200$  cp  
Table 56 Conoco GDK Constant Height  $n'=0.5$ ,  $k'=0.06$   
Table 57 Conoco PKN Constant Height  $\mu=200$  cp  
Table 58 Conoco PKN Constant Height  $n'=0.5$ ,  $k'=0.06$   
Table 59 Marathon GOHFER Constant Height  $\mu=200$  cp  
Table 60 Marathon GOHFER Constant Height  $n'=0.5$ ,  $k'=0.06$   
Table 61 Marathon GOHFER 3-Layer  $\mu=200$  cp  
Table 62 Marathon GOHFER 3-Layer  $n'=0.5$ ,  $k'=0.06$   
Table 63 Marathon GOHFER 5-Layer  $\mu=200$  cp  
Table 64 Marathon GOHFER 5-Layer  $n'=0.5$ ,  $k'=0.06$   
Table 65 ARCO Stimplan 3-Layer  $\mu=200$  cp  
Table 66 ARCO Stimplan 3-Layer  $n'=0.5$ ,  $k'=0.06$   
Table 67 ARCO Stimplan 5-Layer  $\mu=200$  cp  
Table 68 ARCO Stimplan 5-Layer  $n'=0.5$ ,  $k'=0.06$   
Table 69 ARCO TerraFrac 5-Layer  $n'=0.5$ ,  $k'=0.06$   
Table 70 NSI Tech. Stimplan 3-Layer  $\mu=200$  cp  
Table 71 NSI Tech. Stimplan 3-Layer  $n'=0.5$ ,  $k'=0.06$   
Table 72 NSI Tech. Stimplan 5-Layer  $\mu=200$  cp  
Table 73 NSI Tech. Stimplan 5-Layer  $n'=0.5$ ,  $k'=0.06$   
Table 74 RES Fracpro 3-Layer  $\mu=200$  cp  
Table 75 RES Fracpro 3-Layer  $n'=0.5$ ,  $k'=0.06$   
Table 76 RES Fracpro 5-Layer  $\mu=200$  cp  
Table 77 RES Fracpro 5-Layer  $n'=0.5$ ,  $k'=0.06$   
Table 78 Texaco Fracpro GDK Constant Height  $\mu=200$  cp  
Table 79 Texaco Fracpro PKN Constant Height  $\mu=200$  cp  
Table 80 Texaco Fracpro 3-Layer  $\mu=200$  cp  
Table 81 Texaco Fracpro 5-Layer  $\mu=200$  cp  
Table 82 Texaco Fracpro 5-Layer  $n'=0.5$ ,  $k'=0.06$   
Table 83 Texaco Fracpro 5-Layer  $n'=0.5$ ,  $k'=0.06$  No tip effects

## List of Figures

- Figure 1 Length comparison for cases 1-4
- Figure 2 Net pressure comparison for cases 1-4
- Figure 3 Efficiency comparison for cases 1-4
- Figure 4 Comparison of maximum width at wellbore for cases 1-4
- Figure 5 Comparison of average width at wellbore for cases 1-4
- Figure 6 Comparison of average width in fracture for cases 1-4
- Figure 7 Length history for case 1
- Figure 8 Net pressure history for case 1
- Figure 9 History of width at wellbore for case 1
- Figure 10 Length history for case 2
- Figure 11 Net pressure history for case 2
- Figure 12 History of width at wellbore for case 2
- Figure 13 Length history for case 3
- Figure 14 Net pressure history for case 3
- Figure 15 History of width at wellbore for case 3
- Figure 16 Length history for case 4
- Figure 17 Net pressure history for case 4
- Figure 18 History of width at wellbore for case 4
- Figure 19 Length history for other constant height-models - 200 cp
- Figure 20 Net pressure history for other constant height-models - 200 cp
- Figure 21 History of width at wellbore for other constant-height models - 200 cp
- Figure 22 Length history for other constant height-models -  $n'$ ,  $k'$
- Figure 23 Net pressure history for other constant height-models -  $n'$ ,  $k'$
- Figure 24 History of width at wellbore for other constant-height models -  $n'$ ,  $k'$
- Figure 25 Length comparison for cases 5 and 6
- Figure 26 Height comparison for cases 5 and 6
- Figure 27 Net pressure comparison for cases 5 and 6
- Figure 28 Efficiency comparison for cases 5 and 6
- Figure 29 Comparison of maximum width at wellbore for cases 5 and 6
- Figure 30 Comparison of average width at wellbore for cases 5 and 6
- Figure 31 Comparison of average width in fracture for cases 5 and 6
- Figure 32 Length history for case 5
- Figure 33 Height history for case 5
- Figure 34 Net pressure history for case 5
- Figure 35 History of width at wellbore for case 5
- Figure 36 Length history for case 6
- Figure 37 Height history for case 6
- Figure 38 Net pressure history for case 6
- Figure 39 History of width at wellbore for case 6
- Figure 40 Length comparison for cases 7 and 8
- Figure 41 Height comparison for cases 7 and 8
- Figure 42 Net pressure comparison for cases 7 and 8
- Figure 43 Efficiency comparison for cases 7 and 8

- Figure 44 Comparison of maximum width at wellbore for cases 7 and 8
- Figure 45 Comparison of average width at wellbore for cases 7 and 8
- Figure 46 Comparison of average width in fracture for cases 7 and 8
- Figure 47 Length history for case 7
- Figure 48 Height history for case 7
- Figure 49 Net pressure history for case 7
- Figure 50 History of width at wellbore for case 7
- Figure 51 Length history for case 8
- Figure 52 Height history for case 8
- Figure 53 Net pressure history for case 8
- Figure 54 History of width at wellbore for case 8

#### Appendix A

- Figure A1 Height profile - case 5
- Figure A2 Width profile - case 5
- Figure A3 Height profile - case 6
- Figure A4 Width profile - case 6
- Figure A5 Height profile - case 7
- Figure A6 Width profile - case 7
- Figure A7 Height profile - case 8
- Figure A8 Width profile - case 8

#### Appendix B

- Figure B1 Height profile - case 5
- Figure B2 Width profile - case 5
- Figure B3 Height profile - case 6
- Figure B4 Width profile - case 6
- Figure B5 Height profile - case 7
- Figure B6 Width profile - case 7
- Figure B7 Height profile - case 8
- Figure B8 Width profile - case 8

#### Appendix C

- Figure C1 Height profile - case 5
- Figure C2 Width profile - case 5
- Figure C3 Height profile - case 6
- Figure C4 Width profile - case 6
- Figure C5 Height profile - case 7
- Figure C6 Width profile - case 7
- Figure C7 Height profile - case 8
- Figure C8 Width profile - case 8

#### Appendix D

- Figure D1 Height profiles - cases 5-8

## **Appendix E**

- Figure E1 Height profile - case 5**
- Figure E2 Width profile - case 5**
- Figure E3 Height profile - case 6**
- Figure E4 Width profile - case 6**
- Figure E5 Height profile - case 7**
- Figure E6 Width profile - case 7**
- Figure E7 Height profile - case 8**
- Figure E8 Width profile - case 8**

## **Appendix F**

- Figure F1 Height profile (Stimplan) - case 5**
- Figure F2 Width profile (Stimplan) - case 5**
- Figure F3 Height profile (Stimplan) - case 6**
- Figure F4 Width profile (Stimplan) - case 6**
- Figure F5 Height profile (Stimplan) - case 7**
- Figure F6 Width profile (Stimplan) - case 7**
- Figure F7 Height profile (Stimplan) - case 8**
- Figure F8 Width profile (Stimplan) - case 8**
- Figure F9 Height profile (TerraFrac) - case 8**

## **Appendix G**

- Figure G1 Height profile - case 5**
- Figure G2 Width profile - case 5**
- Figure G3 Height profile - case 6**
- Figure G4 Width profile - case 6**
- Figure G5 Height profile - case 7**
- Figure G6 Width profile - case 7**
- Figure G7 Height profile - case 8**
- Figure G8 Width profile - case 8**

## **1.0 RESEARCH OBJECTIVES**

The objective of the GRI Fracture Propagation Modeling Forum and the associated publication of the results in this report is to assemble a comparative study of available hydraulic fracture models. Hydraulic fracturing is one of the most important stimulation techniques available to the petroleum engineer, being used extensively in tight gas sandstones,<sup>1-5</sup> coalbed methane,<sup>6</sup> high permeability sandstones in Alaska,<sup>7</sup> very weak sandstones off the US. gulf coast,<sup>8</sup> in horizontal wells in chalks,<sup>9,10</sup> and in many other applications from waste disposal to geothermal reservoirs. Because of this diversity of application, hydraulic fracture design models must be able to account for widely varying rock properties, reservoir properties, in situ stresses, fracturing fluids, and proppant loads. As a result, fracture simulation has emerged as a highly complex endeavor that must be able to describe many different physical processes.

As the complexity of hydraulic fracturing has increased, many modelers have used ad-hoc features in their models to simulate mechanisms that are not well understood at this time. Such mechanisms include tip effects, wall roughness, complex fracturing, and some aspects of height growth. As a result, fracture models have become heteromorphic with no standard of comparison. Engineers are thus faced with a difficult choice in selecting a model that is appropriate for their needs.

In order to compare models in a reasonable sense, all models must be run with the same input. The purpose of the Forum was to bring concerned modelers together to share results of their models and to agree on a set of rigid input data that all could run for a comparative study. Participating modelers were given two treatment data sets (one Newtonian fluid, one power-law fluid) and four different geometries (constant-height PKN, constant-height GDK, 3-layer, 5-layer) and asked to provide length, height, maximum width at the wellbore, average width at the wellbore, average width in the whole fracture, net pressure, and efficiency at 25 minute intervals throughout the fracture treatment (total time of 200 minutes). This report documents all of the results supplied by the modelers and tabulates and plots those results.

## 2.0 RATIONALE

The petroleum engineer, who must design the fracture treatment, is often confronted with a difficult choice of selecting a suitable hydraulic-fracture model for his/her needs, yet there is very little comparative information available to help in making that choice, particularly with respect to the newer 3-D and pseudo-3-D models. Many experienced engineers will also have their own biases about hydraulic fracture performance and would prefer to find a code whose output is most consistent with the engineers experience. The purpose of this report is to help provide some guidance by comparing many of the available simulators.

This report had its origins in the Fracture Propagation Modeling Forum held February 26-27, 1991, near Houston, TX. This forum, which was sponsored by the Gas Research Institute, was open to all known hydraulic fracturing modelers. Participants were asked to provide fracture designs based on the SPE No. 3 fracture experiment, as well as a history match of the actual pressure data from the treatment. After comparison of the fracture designs and history matches presented at this meeting, a final, revised design data set was given to all participants. Most of the revised data sets were returned by September 1991, although a couple were returned or modified as late as November 1993. The results in this report are derived from the model calculations of the revised design data set. Because of the difficulty in trying to establish any consistency in the use of the actual treatment data (e.g., effects of the breaker, temperature, rate changes, etc.), it was decided that any further attempt to compare history matches would need to be deferred. Thus, publication of forum results is limited to the design phase only.

To publish the results, a four-member committee (the authors) was chosen from forum participants. In assembling this comparison, the members of the committee have purposely attempted to avoid making any judgments about the relative value of different models so as not to inject our biases into this comparison. Only the results and quantifiable comparisons are given.

Since hydraulic fracturing is performed in a large percentage of gas completions (and in recompletions), the benefit to the gas consumer comes from the optimization of this technique when an appropriate model is used. Optimization results in more cost-effective completions, enhanced gas production, lower wellhead costs, and additional supply.

The modelers who participated in the forum and prepared data for this paper deserve special thanks for their efforts. Most importantly, Dr. Steve Holditch of S.A. Holditch & Associates should be singled out for special mention as the prime mover of the forum, a follow-up SPE paper, and this report.

### **3.0 BACKGROUND - BASIC MODELING DISCUSSION**

In recent years, there has been a proliferation of fracturing simulators used in the oil industry. This proliferation was intensified by the availability of personal computers and the need for fast running design simulators for use in the field. Applying these models as "black boxes", without knowing the underlying assumptions may lead to erroneous conclusions, especially for unconfined fracture growth. While specific descriptions of the individual models are given in section 4.0, this section provides a general overview of hydraulic-fracture models and catalogues the various models into similar groupings.

Hydraulic fracturing is a complex non-linear mathematical problem, that involves the mechanical interaction of the propagating fracture with the fluid dynamics of the injected slurry. Several assumptions are commonly made to render the problem tractable: plane fractures, symmetric with respect to the wellbore; elastic formation; linear fracture mechanics for fracture propagation prediction; power law behavior of fracturing fluids and slurries; simplification of fracture geometry, and its representation by few geometric parameters; etc. The reader is referred to the SPE Monograph Volume 12<sup>11</sup> for a detailed description of the governing equations. Although the models predict "trends" of treating pressure behavior; they may not always reliably predict the observed behavior for a given treatment. This discrepancy has been attributed to many complex interactions of the injected fluids with the formation that are not well understood.

An attempt to phenomenologically characterize some of these complex processes occurring within the fracture (e.g., multiple fractures, increased frictional losses) and near the fracture tip (e.g. non-linear formation behavior, microcracking, formation plasticity, dilatancy, plugging, etc.) was made in various simulators by the introduction of additional ad hoc parameters ("knobs"). The choice of values for these parameters is only based on the experience of the modeler, possibly with some guidance from the laboratory, field observations, or from other computational resources (e.g., finite element codes). These knobs are used to match model predictions with field observed behavior, and result in the lack of a standard model response for a given physical problem. This issue was addressed in the forum by having different participants (several different models) simulate common test cases derived from the actual SFE No. 3 well fracturing treatment. These models can be categorized in the order of decreasing complexity as follows:

(1) Planar three-dimensional (3D) models

- \* TerraFrac of TerraTek, Inc.<sup>12-16</sup> run by ARCO
- \* HYFRAC3D by Dr. Advani of Lehigh University<sup>17</sup>

(2) Unique Finite Difference Simulator GOHFER of Marathon Oil Co.<sup>18,19</sup>

### (3) Planar Pseudo three-dimensional models

#### A- "Cell" Approach

STIMPLAN of NSI, Inc.  
ENERFRAC of Shell<sup>20,21</sup>  
TRIFRAC of Holditch & Assoc.

#### B- Overall Fracture Geometry Parameterization

FRACPRO of RES, Inc.<sup>22-25</sup>  
MFRAC-II of Meyer and Assoc.<sup>26-29</sup>

### (4) Classic PKN and GDK Models<sup>30-35</sup>

PROP of Halliburton<sup>34-36</sup>  
Chevron 2-D model<sup>37</sup>  
Conoco 2-D model<sup>38,39</sup>  
Shell 2-D model  
Pseudo-3-D models run in constant-height mode

A discussion of the basics of these models is given to provide some insights on the model assumptions and how they are expected to affect the results.

#### 3.1 Planar 3-D Models

The TerraFrac<sup>12-16</sup> and the HYFRAC3D<sup>17</sup> models employ similar assumptions and formulate the physics rigorously, assuming planar fractures of arbitrary shape in a linearly elastic formation, two dimensional flow in the fracture, power law fluids, and linear fracture mechanics for fracture propagation. Their difference is in the numerical technique to calculate fracture opening. TerraFrac uses an integral equation representation, while the HYFRAC3D model uses the finite element method. Both models use finite elements for two-dimensional fluid flow within the fracture and employ a fracture tip advancement proportional to the stress intensity factor on the fracture tip contour.

#### 3.2 Planar 3-D Finite-Difference Model -GOHFER

Besides the numerical technique used, this model<sup>18,19</sup> is different from the previous models in two fundamental ways: (a) fracture opening is calculated by superposition using the surface displacement of a half space under normal load (Boussinesq Solution); (b) the fracture propagates when the tensile stress normal to the fracturing plane exceeds the tensile strength of the formation at some distance outside the fracture by enforcing the tensile criterion at the centroid of the cells "outside" the

fracturing contour. This model predicts higher treating pressures and shorter and wider fractures as compared with the ones of the previous 3D models.

### 3.3 Pseudo-3-D Models

These models were developed from the PKN model by removing the requirement of constant fracture height. They use equations based on simple geometries (radial, two dimensional, elliptical) to calculate fracture width as a function of position and pressure and apply a fracture propagation criterion to both length and height. Furthermore, they assume one dimensional flow along the length of the fracture.

These models can be divided into two categories: (A) models that divide the fracture along its length into "cells", and use local cell geometry (two-dimensional crack or penny crack) to relate fracture opening with fluid pressure; (B) models that use a parametric representation of the total fracture geometry. As a result of these assumptions, it is expected that each class will have different fracture geometry, even for the simple case of a confined fracture.

The pseudo-3D simulators are extensively used for fracture design because of their efficiency and their availability on personal computers. However, they are directly applicable only for the geometries that are not significantly different from the basic assumptions of the model (e.g., models based on a PKN geometry should have large length/height ratios to be appropriate). For relatively unconfined fracture growth in a complex in situ stress profile, a 3D model is thus more accurate in predicting "trends" of fracture geometry. To avoid this problem, some pseudo-3-D models attempt to include truly 3D fracture behavior in terms of "history" matching or "lumped" parameters determined from fully 3D-solutions of simpler problems or determined from simulations using 3D models.

### 3.4 Classic PKN and GDK Models

The difference in treating pressure behavior and fracture geometry of the PKN and GDK models is well documented in the literature<sup>11,40</sup> and need not be repeated here.

## 4.0 FRACTURE MODELS

This section describes the individual fracture models that were used in this comparison. Short descriptions of the models were provided by the modelers or by the companies who ran commercially available models.

### 4.1 S.A. Holditch & Assoc. (TRIFRAC)

SAH's hydraulic fracturing model TRIFRAC is a pseudo-3-D fracture propagation and proppant transport model that computes created and propped fracture dimensions using a finite-difference numerical approach. It has the capability to handle multiple non-symmetric stress layers with unique values for Young's modulus, Poisson's ratio, fracture toughness, permeability, porosity, and fluid leakoff coefficients for each layer. Properties for a maximum of twenty-two layers can be input currently.

The apparent viscosity of the fracturing fluid is computed based upon the shear rate inside the fracture and changes in  $n'$  and  $k'$  due to variations of temperature and time. A temperature calculation model is thus part of TRIFRAC. Choice of initiating the hydraulic fracture from ten different layers simultaneously is available. Special options are available to input pump schedule for nitrogen foam treatments.

The created geometry computation module is coupled with a rigorous finite difference proppant transport simulator that solves simultaneously for proppant distribution, transport, and settling along with the growth of the fracture. Depending upon the fluid velocity along the height of the fracture and the rate of settling of the proppant, the model computes the proppant profile at each time step during the job.

TRIFRAC also has the simpler two-dimensional geometry computational finite-difference models of Geertsma and DeKlerk, and Perkins, Kern, and Nordgren. Horizontal fracture geometry calculation using the GDK method is also available. All these models are coupled with proppant transport calculation modules.

### 4.2 Meyer & Associates (MFRAC-II)

MFRAC-II<sup>26-29</sup> is a pseudo-3-D hydraulic fracturing simulator. MFRAC-II also includes options for the penny, Geertsma-deKlerk and Perkins-Kern/Nordgren type 2-D fracturing models. Version 7.0, written in C++ and developed under Microsoft Windows 3.x, offers a user interface which takes full advantage of the facilities existing under this operating system. The program's features include intelligent menus, a complete fluid database, flexible units and user customized help screens. This study was run using MFRAC-II, Version 6.1.

MFRAC-II accounts for the coupled parameters affecting fracture propagation and proppant transport. The major fracture, rock and fluid mechanics phenomena include: (1) multi-layer, unsymmetrical confining stress contrast, (2) fracture toughness and

tip/overpressure effects, (3) rock deformation, (4) variable injection rate and time dependent fluid rheology properties, (5) multi-layer leak-off with spurt loss and (6) 2-D proppant transport. The fracture propagation model calculates fracture length, upper and lower heights, width, net pressure, efficiency, and geometry parameters as a function of time. The width variation as a function of height and confining stress is also calculated.

In order to provide applicability over the broadest range of circumstances, MFRAC-II offers numerous options which can be employed by the user. These options and other free parameters ("knobs") allows customization in the modeling approach adopted. MFRAC-II was run in two different modes to demonstrate the effects of some of these parameters. In one case, the base model using the system defaults was run (designated MEYER-1); in a second case (MEYER-2) additional parameters (such as greater friction drop in the fracture) were applied. In both cases, as a default, the viscous thinning assumption was made. Without viscous thinning, the effective friction factor would have increased, resulting in higher net pressures, greater widths and a shorter length. In addition, the fully implicit coupled model for height growth (Ver. 7.0) results in increased development of fracture height and net pressure for certain multi-layer formations.

#### 4.3 Advani (Lehigh HYFRAC3D)

The 3 layer and 5 layer model results (Cases 5 through 8) are obtained from the HYFRAC3D code.<sup>17</sup> This finite element code is based on a set of coupled mass conservation, fluid momentum, constitutive elasticity and fracture mechanics equations governing planar hydraulic fracture propagation in a multilayered reservoir. A mapping technique of the baseline mesh (88 triangular elements representing half of the fracture) defined in a unit circle to arbitrary shaped fracture geometries is utilized in the numerical scheme for tracking the moving fracture front.

The PKN model results (Cases 1 and 2) are also based on a two-dimensional finite element model simulator with standard PKN model equations including vertical stiffness and one-dimensional fluid flow. These simulation results are obtained using 20 line elements for the normalized, time-dependent fracture half-length.

#### 4.4 Shell (ENERFRAC)

ENERFRAC<sup>20,21</sup> is a hydraulic fracture model that predicts fracture dimensions for uncontained (circular) and contained (rectangular) fractures. ENERFRAC incorporates fracture tip effects in addition to the other interacting processes of viscous fluid flow, elastic rock deformation, and fluid loss. Fracture tip effects are accounted for through a direct input of the rock's apparent fracture toughness or the fracture tip net pressure (overpressure). This overpressure is defined as the instantaneous shut-in-pressure minus the closure pressure and can be determined in the field from a microfrac or minifrac test.

Shell also provided 2-D PKN and GDK model results. The ENERFRAC results provided a useful comparison of the effect of free model parameters (the "knobs" discussed earlier) on the results. Shell provided results for typical fracture toughness values measured in lab tests (the base case, designated ENERFRAC-1) and also for a several tip overpressures. The particular case of a tip overpressure of 1000 psi (ENERFRAC-2) is shown in several plots for comparison with the base case. This comparison allows us to see the effect of fracture tip overpressure on fracture geometry and net pressure.

#### 4.5 Halliburton (PROP)

The PROP program<sup>34-36</sup> is a 2-D fracture design model based on Daneshy's numerical solution. Its numerical nature makes the model much more flexible than most analytical models. For example, the program has recently been modified for use of multiple fluids and rates within a single treatment, each fluid with its own set of time- and temperature-dependent rheological parameters. In addition to the power-law model normally used to characterize gelled fracturing fluids, PROP uses the three-parameter Herschel-Bulkley model for fluids containing a nitrogen or carbon dioxide phase. The program's proppant transport calculations are of similar capability.

Although the model originally presented by Daneshy was based on the Khristianovic-Zhel'tov width equation (designated GDK in this paper), the PROP program has since been expanded to include a similar numerical solution of PKN-type geometry with a width profile based on calculated local pressures. The results presented here are for the GDK-type solution only.

#### 4.6 Chevron

Chevron's 2-D fracturing simulator is capable of predicting the propagation of constant height hydraulically induced vertical fractures for a power-law fluid. The simulator also includes a proppant transport model with proppant settling and a production model. The simulator is capable of predicting the created fracture geometry based on either Perkins-Kern-Nordgren (PKN) or the Geertsma-deKlerk (GDK) models. It is most suitable to design fractures where the geologic conditions restrict height growth. In fracture propagation models, the equations describing conservation of mass, conservation of momentum, continuity of fluid flow, and linear elastic deformation of the rock in plane strain are used to calculate mass flux, fracture width, pressure, and length as function of time. The proppant transport model calculates the final propped concentration, width, and bank height given a settlement velocity, and can predict possible problems caused by proppant bridging or screen out.

The fractured well production model is based on an analytic solution developed by Lee and Brockenbrough<sup>37</sup> to study the transient behavior of a well intercepted by a finite conductivity fracture in an infinite reservoir. This production model provides the short

time production results. Combining this solution with the well known semi-log asymptotic solution for longer time periods provides a reliable tool for predicting the potential productivity of the fractured well.

#### 4.7 Conoco

Conoco's fracture design program is a constant-height model (2-D) where either PKN or GDK geometry can be selected, as described by McLeod.<sup>38</sup> It has single inputs for  $n'$ ,  $k'$  and leakoff coefficient. However, the model is capable of calculating the positions and concentrations of progressive fluid/proppant stages. Fracture area can be calculated by either the Howard and Fast Model or an extremely accurate simplification by Crawford.<sup>39</sup>

#### 4.8 Marathon (GOHFER)

Marathon Oil Company's Grid Oriented Hydraulic Fracture Extension Replicator (GOHFER)<sup>18,19</sup> is a planar 3-D fracture geometry simulator with coupled multi-dimensional fluid flow and particle transport. As indicated by the name, the model is based on a regular grid structure which is used for both the elastic rock displacement calculations and as a planar 2-D finite difference grid for the fluid flow solutions. The areal pressure distribution obtained from the fluid flow equations, including proppant transport, is iteratively coupled to the elastic deformation solution. Using the finite difference scheme for fluid flow allows modeling of multiple discrete fluid entry points representing perforations at various locations.

Each grid node can be assigned an individual value of net stress, pore pressure, permeability, porosity, wall-building coefficient, rock strength, Young's Modulus, and Poisson's Ratio, as well as variables describing fracture wall roughness and tortuosity. The displacement of the fracture face at each node is determined by integration of the pressure distribution over all nodes, including the computed tensile stress distribution in the unbroken rock surrounding the fracture. The fracture width equation used is the general formula for displacement of a semi-infinite half-space acted upon by a distributed load, given by Boussinesq. The solution is general enough to allow modeling of multiple fracture initiation sites simultaneously, and is applicable to any planar 3-D geometry from perfect containment to uncontrolled height growth.

#### 4.9 ARCO (using TerraFrac)

TerraFrac<sup>TM</sup> Code<sup>12-16</sup> is a fully three-dimensional hydraulic fracture simulator. It was initiated at Terra Tek in 1978 and its commercial availability was announced in December, 1983. The overall approach used in the model is to subdivide the fracture into discrete elements and to solve the governing equations for these elements. These governing equations consist of (1) 3-D elasticity equations that relate pressure on the crack faces to the crack opening, (2) 2-D fluid flow equations that relate the flow in the fracture to the pressure gradients in the fluid, and (3) a fracture criterion that relates the

intensity of stress state ahead of the crack front to the critical intensity for Mode I fracture growth. TerraFrac provides many distinctive features including (1) 2-D fluid flow for both proppant and temperature distribution, (2) multiple stages having different fluids, proppants, rates, with fluid and proppant properties being functions of temperature if desired, (3) multiple layers, each having different in situ stress, Young's modulus, fracture toughness, Poisson's ratio, and leakoff, (4) poroelastic and thermoelastic capabilities for waterflooding and other applications, (5) a robust mesh generator to handle a wide variety of fracture geometries and a quasi-Newton method to solve the nonlinear system of equations for the fluid pressures (this approach provides for fast convergence and high accuracy), and (6) a post-shut-in calculation capability for which no additional assumptions are made (only the injection rate changes).

#### 4.10 NSI (STIMPLAN)

STIMPLAN is a state-of-the-art 3-D hydraulic-fracture simulator for fracture design and analysis in complex situations involving height growth, proppant settling, foam fluids, tip screen out, etc. The model has complete fluid/proppant tracking that allows for optimum fluid selection and scheduling based on time and temperature history. Fracture height growth is calculated through multiple layers, and includes proppant settling and bridging calculations. A Fracture Analysis/History Matching module provides for history matching of measured net treating pressures to yield the most accurate possible estimation of actual fracture geometry and behavior. Also, simulations during the fracture closure (pressure decline) period aid in pressure decline analysis for fluid loss in complex geologic situations.

#### 4.11 Resources Engineering Systems (FRACPRO)

FRACPRO<sup>22-25</sup> uses measured values of flowrate, proppant concentration, and fluid rheology parameters to calculate the pressure drop down a wellbore of variable deviation and diameter, and the time histories of the fracture growth and the net fracture pressure are calculated. The wellbore model handles non-Newtonian fluids and corrects for the effects of nitrogen foam, carbon dioxide, and proppant phases. The model also accounts for friction variation from entrained proppant.

The fracture model is 3-D, in that spatial variations in reservoir stress, modulus, pressure, and flow distribution are taken into account. However, it does not need to calculate the variations at specific points within the fracture. Instead, the effects are integrated into functional coefficients of governing differential equations, greatly simplifying the calculation of the fracture dimensions. The module can therefore run many times faster than real time, as required for history matching on-site. The coefficients necessary to calculate the spatial variations are calculated from a full three dimensional model and checked against experimental and field test data.

FRACPRO handles up to three modulus zones, up to fifty stress zones, and up to fifty permeable (leakoff) zones. Fluid loss is modeled as one-dimensional flow perpendicular to the fracture face, following Darcy-law behavior, including spurt loss, filtercake buildup on the fracture face, and a compressible reservoir-fluid region. The rise in confining stress due to poroelastic effects (backstress) is included. Heat transfer modeling assumes that there is a cubic-fit temperature distribution between the fracture and the end of the heat transfer region.

FRACPRO models the convection and settling of proppant in a fracture. Proppant convection is a process whereby heavier treatment stages (e.g., proppant stages) displace rapidly downward from the perforations to the bottom of the fracture. Those stages are then replaced by the pad, or by low-concentration proppant stages. Initial laboratory and computer simulations indicate that proppant convection may be the dominant mechanism in propped-fracture stimulations. As well, FRACPRO can be used to model proppant settling. The proppant is carried with the fracturing fluid, and settles. The model takes into account the effects of non-Newtonian fluids, hindered settling rates, and settled bank buildup.

#### 4.12 Texaco (using FRACPRO)

FRACPRO was also run by TEXACO for six different cases. These include single-layer PKN and GDK modes, a 3-layer case with constant frac fluid viscosity, and 5-layer cases for constant fluid viscosity, power-law-fluid behavior, and power-law-fluid behavior with the tip dominated rheology behavior not operating. The 5-layer runs provide a good comparison of tip-dominated vs. conventional rheology results using FRACPRO. The 3-layer and the tip-dominated 5-layer cases provide a good comparison of the results for two different companies using the same model.

#### 4.13 ARCO (using STIMPLAN)

STIMPLAN was also run by ARCO for four different cases. These include both 3-layer and 5-layer cases. These results provide a good comparison of the results for two different companies using the same model.

## 5.0 SFE-3 FORMATION AND TREATMENT DATA

The input data for the fracture modeling comparison is based upon the results obtained at the GRI-sponsored SFE-3 experiment.<sup>3,41</sup> SFE-3 was drilled as the Mobil Cargill Unit No. 15 well in the Waskom Field, Harrison County, Texas. The well was spudded in September, 1988, and drilled to a total depth of 9700 ft (2957 m). Of particular interest was the Cotton Valley Taylor sand which was perforated between 9225-9250 ft (2812-2819 m) and 9285-9330 ft (2830-2844 m). An extensive log program was run on this well and detailed core analyses performed. Both prefrac well-testing and post-frac production testing were performed. Two minifrac and one full-scale treatment were conducted as part of the stimulation program.

The SFE-3 data set was specifically chosen to insure that the model comparison would be performed with actual field data and not for a contrived data set that might favor one type of model over others. In addition, the SFE-3 data set is one of the most complete sets of well information available, and includes stress, rock and reservoir and well-performance results.

For this initial study, the relevant rock and reservoir information are shown in Table 1. As will be described in the next section, three different physical configurations were considered: a single layer, three layers, and five layers. Stress and rock property measurements were averaged over the appropriate depths for each interval to yield the physical data given in Table 1. Most importantly, the stress contrasts range from 1450-1650 psi (10-11.4 MPa), although the lower barrier is only 40 ft (12 m) thick for the five layer configuration. Young's modulus and Poisson's ratio were obtained from sonic measurements, thus accounting for the elevated values of Young's modulus.

The actual SFE-3 treatment was a thirteen-stage procedure using primarily a 40 lb/1000 gal (4.8 kg/m<sup>3</sup>) crosslinked gel with sand stages varying from 1-8 ppg (120 kg/m<sup>3</sup>). For the purpose of this comparison, the treatment was simplified to a single, constant-property, fluid with no proppant, primarily because changes in fluid properties due to temperature or the addition of proppant can not be easily quantified and any resulting comparisons would be of questionable value.

## 6.0 TEST CASES

As noted in the description section, most of the models are capable of accommodating and processing a much broader range of complex data than presented in this data set (i.e., multiple rock properties, leak-off coefficients,  $n'$ ,  $k'$ , etc.). Refer to Tables 1 and 2 for the complete set of data input. However, the data set was arbitrarily restricted to limit as many discretionary inputs as possible to allow a more direct comparison of model performance. The treatment input is also not to be construed as optimum design parameters, but rather an approximation of that from SFE No. 3.

There were a total of eight possible cases each participant could model if they so chose. These were GDK, PKN, 3-layer, and 5-layer cases with separate runs for a constant Newtonian viscosity and a constant  $n'$  and  $k'$  power-law fluid as follows:

Case 1	GDK Constant height - 200 cp fluid
Case 2	GDK Constant height - Power-law fluid ( $n'$ , $k'$ )
Case 3	PKN Constant height - 200 cp fluid
Case 4	PKN Constant height - Power-law fluid ( $n'$ , $k'$ )
Case 5	3-Layer - 200 cp fluid
Case 6	3-Layer - Power-law fluid ( $n'$ , $k'$ )
Case 7	5-Layer - 200 cp fluid
Case 8	5-Layer - Power-law fluid ( $n'$ , $k'$ )

The PKN and GDK cases were run with a constant height (2-D) set at 170 ft (52 m). The 3-layer and 5-layer cases were run using a 3-D or a Pseudo-3-D model allowing fracture height to be determined by the model. Of particular interest was if the fracture broke through zone 4 in the 5-layer case.

The important rock property data for the 3-layer case are shown graphically in Figure 1, and the data for the 5-layer case are shown in Figure 2. These stress and modulus profiles are simplifications of the actual stress and modulus profiles measured at the SFE No. 3 site.

## 7.0 MODEL RESULTS

A short summary of the final geometry at the end of pumping is given in Tables 3-5 for the 2-D, 3-layer, and 5-layer cases respectively. A summary of the time to breakthrough for the 5-layer calculations is given in Table 6. All of the submitted data from the modelers are given in Tables 7-83, in the following order:

S.A. Holditch & Assoc. Trifrac	Tables 7-14
Meyer & Assoc. M-FRAC-II base case (Meyer-1)	Tables 15-22
Meyer & Assoc. M-FRAC-II "knobs" (Meyer-2)	Tables 23-30
Advani HYFRAC3D	Tables 31-36
Shell 2-D Models	Tables 37-40
Shell Enerfrac	Tables 41-50
Halliburton 2-D Prop	Tables 51-52
Chevron 2-D models	Tables 53-54
Conoco 2-D models	Tables 55-58
Marathon GOHFER	Tables 59-64
ARCO (Stimplan)	Tables 65-68
ARCO (TerraFrac)	Table 69
NSI Stimplan	Tables 70-73
RES Fracpro	Tables 74-77
Texaco (Fracpro)	Tables 78-83

The graphs of the data shown in this section were derived from this tabular data set. In addition, some modelers provided additional graphical information on the width and height profiles along the length of the crack. These are given in the following appendices:

S.A. Holditch & Assoc. Trifrac	Appendix A
Meyer & Assoc. M-FRAC-II base case (Meyer-1)	Appendix B
Meyer & Assoc. M-FRAC-II "knobs" (Meyer-2)	Appendix C
Advani HYFRAC3D	Appendix D
Marathon GOHFER	Appendix E
ARCO (Stimplan and TerraFrac)	Appendix F
RES Fracpro	Appendix G

### 7.1 2-D Results (Cases 1-4)

Considering first the 2-D summary results given in Table 1, the final half length for all of the 2-D models are shown in Figure 3. The well-known difference in length estimates between the PKN and GDK models is evident in these results, but some differences between different models in each group become apparent. Presumably, this difference is because of other options included in some models. The effect of the different rheologies is generally small. Besides the PKN and GDK models, GOHFER and ENERFRAC-1 and -2 are also shown.

The reduction in length between ENERFRAC-1 and ENERFRAC-2 is due to increased tip overpressure. Likewise, the reduction in length between MEYER-1 and MEYER-2 is due to options that were included in MEYER-2 which reflect the designers' incorporation of more complex physics into the fracturing process.

The net pressures for the 2-D models, shown in Figure 4, follow a similar pattern to length, with the GDK models giving low pressures and the PKN models providing high net pressures. GOHFER is different in that it predicts short lengths, like the GDK models, but high pressures like the PKN models.

The efficiencies for the 2-D calculations are shown in Figure 5. Values ranged from 70-95%.

The fracture maximum width is shown in Figure 6, while the average width at the wellbore is given in Figure 7, and the average width throughout the whole fracture is shown in Figure 8. As expected, the GDK models provide much greater width than the PKN models. GOHFER's width is more similar to the GDK models while ENERFRAC's width is closer to the PKN models.

The time-history results for Case 1 (GDK with 200-cp fluid) are shown in Figures 9-11 for length, net pressure and width at the wellbore, respectively. It is interesting to note that even for this simple data set there is a significant difference between the various GDK models.

Time-history results for Case 2 (GDK with power-law fluid) are shown in Figures 12-14 for length, net pressure and width at the wellbore, respectively. As with the Case 1 results, there is also a significant difference in the calculations of the various models.

Time history results for Case 3 (PKN with 200-cp fluid) are shown in Figures 15-17 for length, net pressure and maximum width at the wellbore, respectively. Different PKN models also have considerable variation in their calculated output.

Time history results for Case 4 (PKN with power-law fluid) are shown in Figures 18-20 for length, net pressure and maximum width at the wellbore, respectively.

Time history results for other 2-D models using a 200-cp fluid (these do not fit exactly into the Case 1 or 3 categories) are shown in Figures 21-23 for length, net pressure and maximum width at the wellbore, respectively. The effect of tip overpressure is seen by comparing the two ENERFRAC cases.

Time history results for other 2-D models using a power-law fluid are shown in Figures 24-26 for length, net pressure and maximum width at the wellbore, respectively. Tip-overpressure effects can be again seen for a power-law fluid.

## 7.2 3-Layer Results

The 3-layer summary results (Table 4) show considerably more variability than the 2-D cases. A comparison of all 3-Layer length calculations (Cases 5 and 6) is shown in Figure 27. The fracture half length varies from less than 1000 ft for FRACPRO to greater than 3000 ft for the conventional pseudo-3-D models. An interesting and illustrative comparison is seen in the differences between MEYER-1 and -2. MEYER-2, using some features that the modeler believes are more appropriate physics, results in a fracture length that is nearly 1000 ft less than the base case with no options. Many such options have probably been employed on the other models, but were not identified as such for this comparison.

The favorable comparison between ARCO and NSI running Stimplan, and a similar favorable comparison between TEXACO and RES running FRACPRO, show that consistent results can be obtained from a given model even if run by different organizations.

The fracture height comparison, given in Figure 28, shows that much greater height growth is obtained by FRACPRO than by other models. Net pressures, shown in Figure 29, are particularly high in FRACPRO and GOHFER. Efficiencies vary from 40% to greater than 95%, as given in Figure 30.

Fracture maximum widths (at the wellbore) are given in Figure 31, the maximum average width at the wellbore is shown in Figure 32, and the average width in the entire fracture is shown in Figure 33. In all three cases, Fracpro and GOHFER calculate much greater widths than the other models.

Time histories for Case 5 (3-layer with 200-cp fluid) are given in Figures 34-37 for length, height, net pressure and maximum width at the wellbore, respectively. These graphs clearly show that there is an amazing range of output from the different models, even for this relatively simple case.

Time histories for Case 6 (3-layer with power-law fluid) are given in Figures 38-41 for length, height, net pressure and maximum width at the wellbore, respectively. Height growth is extremely fast in FRACPRO, but much better contained in most of the other models.

## 7.3 5-Layer Results

The 5-layer (Cases 7 and 8) summary results (Table 5) are similar to the 3-layer comparison, except that the length in some models is shorter because the height breaks through the lower barrier. The half lengths are shown in Figure 42 and the fracture heights are given in Figure 43. Net pressures range from nearly 700 psi (4.8 MPa) to almost 1400 psi (9.7 MPa), as shown in Figure 44. Efficiencies range from about 60% to 97%, as shown in Figure 45. Again, there is relatively good

agreement between the same model run by two different companies (Stimplan by NSI and ARCO and Fracpro by RES and Texaco).

The maximum fracture width at the wellbore is shown in Figure 46, the fracture average width at the wellbore is given in Figure 47, and the average width throughout the entire fracture is shown in Figure 48. As in the 3-layer case, Fracpro and GOHFER provide the most width development.

Time histories for Case 7 (5-layer with 200-cp fluid) are shown in Figures 49-52 for length, height, net pressure, and maximum width at the wellbore, respectively. The length development in this case is not uniform because height breakthrough into the lower barrier limits growth in some of the models. By comparing all these results with the 3-layer calculations, the effect of breakthrough into the lower low-stress region can be seen.

Time histories for Case 8 (5-layer with power-law fluid) are shown in Figures 53-56 for length, height, net pressure, and maximum width at the wellbore, respectively. One of the interesting results of this study is the behavior of the pressure response as the fracture breaks into the lower barrier. Some models have pressure decreasing, others have pressure remaining flat, while others continue to have pressure increase.

## 8.0 DISCUSSION

The completion engineer now has a wide array of hydraulic models available for both design and analysis of hydraulic-fracture treatments. However, these models calculate widely different fracture geometries for the same input parameters, and it becomes important to choose a model that meets the needs of that particular engineer. The purpose of this comparison study is to evaluate the size of the difference and to provide sufficient information for the engineer to make a studied choice.

It is clear that there are some models that predict results that are significantly different from the majority. Considering the 5-layer cases shown in Figures 42-44, FRACPRO calculates very short fracture lengths and high net pressures and large height. GOHFER also predicts short fracture lengths and high net pressures, but the height growth is not as severe. TRIFRAC, STIMPLAN, TERRAFRAC, and MFRAC-II are all in general agreement, with longer fractures, less height, and somewhat lower net pressures. HYFRAC3D is midway between the two end cases.

MFRAC-II (in 2-D, 3-layer and 5-layer geometries), ENERFRAC (in 2-D geometry), and Texaco's FRACPRO cases (5-layer geometry) were run in two different modes and thus provide a useful assessment of the importance of the options that are available to the fracture designer. In the original formulation of this study, the modelers were asked to run their models in both a base mode (no options) and then with a best-option mode, that is, a mode that reflected their expectations of the options needed to provide the closest simulation of true fracture behavior. Such options may have included tip

effects, higher frictional pressure drops in the fracture, multiple fracture strands, enhanced toughness, or others.

In the three cases mentioned above, the modelers provided such a comparison, and these results can be used to estimate how significantly the engineer can modify the fracture design by trying to incorporate his estimate of the "best physics" possible for a given reservoir. Presumably, such an estimate would be guided by experience with the reservoir. For the 5-layer case with non-Newtonian viscosity, "best physics" results for fracture length differed by about 22% for MFRAC-II and 57% for FRACPRO run by Texaco. For the 2-D case with non-Newtonian rheology, ENERFRAC results differed by about 7%. Since many models have such options, these results should be a useful guideline for estimating the differences in model designs that can be obtained.

The 2-D models, both PKN and GDK, generally provide self-consistent results and the differences between these types of models has been discussed in prior publications.<sup>11,40</sup> Chevron's 2-D model, however, yields considerably shorter lengths than the other PKN and GDK models. GOHFER is also of note because it yields a length typical of the GDK models with the net pressure of the PKN models. Other differences in these 2-D models are minor.

This particular case was chosen because it was a realistic field situation for which detailed data were available. The committee and the modelers all recognize that other formations, with different stress and lithology data, may provide a considerably different comparison of the models. Good examples would be cases where there are minimal stress contrasts and where the stress contrasts are extremely large. It would be beneficial if future model comparison studies investigated those cases as well.

It is also interesting to note that there was general agreement among the modelers at the forum that pressure-history matching (not included in this report) would always result in similar fracture geometries, regardless of the model. This is because a match of the pressure will constrain the width of the fracture, and hence length and height will vary by relatively small amounts. Such an agreement is not the case, however, for design modeling (the results of this report) where the pressure is determined by the model.

Finally, in assembling this comparison, the members of the committee (the authors) have purposely attempted to avoid making any value comparisons between the various models. Only the results and quantifiable comparisons (e.g., model A frac length is greater than model B frac length) are given, as it would take a committee with greater powers than this one has to truly know how the fracture is evolving in the subsurface and, thus, to decide which model is better.

## 9.0 CONCLUSIONS

A comparison study of many of the available hydraulic fracture models has been completed. This study provides information on the relative differences in the models for this one particular case.

These comparisons show that differences in calculated fracture lengths can be large, as much as a factor of three difference. Fracture heights, for the multi-layer cases, can differ by more than 50%. Net pressures also differ by a factor of two.

Calculations from the same model with different options give a useful comparison of the importance of all of the additional physical mechanisms that are continuously being added to the models to explain the wide variety of pressure responses observed in different reservoirs. Such options give the completions engineer considerable flexibility, but also difficult choices of when various options should be used.

## 10.0 RECOMMENDATIONS

Two primary recommendations result from this study.

- It would be beneficial to perform this same type of study for different input conditions. This particular case was chosen because it was a realistic field situation for which detailed data were available. Other warranted cases are those where there are minimal stress contrasts and where the stress contrasts are extremely large
- The pressure-history matches that were performed at the Fracture Propagation Modeling Forum provided many interesting results, but were not suitable for documentation because there was no simple way to compare the various models. However, a comparison of pressure-history matches would be of value.

## 11.0 REFERENCES

1. Holditch, S.A., B.M. Robinson, W.S. Whitehead & J.W. Ely, "The GRI Staged Field Experiment," SPE Form. Eval., 519-533, Sept. 1988.
2. Robinson, B.M., S.A. Holditch & R.E. Peterson, "The Gas Research Institute's 2nd Staged Field Exp.: A Study of Hydraulic Fracturing," SPE 21495, Gas Tech. Symp., Houston, TX, Jan. 1991.
3. Robinson, B.M., S.A. Holditch, W.S. Whitehead & R.E. Peterson, "Hydraulic Fracturing Research in East Texas: Third GRI Staged Field Experiment", JPT, Vol. 44, 78-87, Jan. 1992.
4. Saunders, B.F., B.M. Robinson, S.A. Holditch & R.E. Peterson, "Hydraulic Fracturing Research in the Frontier Formation through the Gas Research Institute's Fourth Staged Field Experiment," SPE 24854, 67th Ann. Tech. Conf., Washington, D.C., 909-922, Oct. 1992.
5. Northrop, D.A. & K-H. Frohne, "The Multiwell Experiment - A Field Laboratory in Tight Gas Sandstone Reservoirs," JPT, Vol. 42, 772-779, June 1990.
6. Cramer, D.D., "The Unique Aspects of Fracturing Western U.S. Coalbeds," JPT, Vol. 44, 1134-1140, Oct. 1992.
7. Martins, P.J., J.C. Abel, C.G. Dyke, C.M. Michel & G. Stewart, "Deviated Well Fracturing and Proppant Production Control in the Prudhoe Bay Field," SPE 24858, 67th Ann. Tech. Conf., Washington, D.C., 955-970, Oct. 1992.
8. Monus, F.L., F.W. Broussard, J.A. Ayoub, & W.D. Norman, "Fracturing Unconsolidated Sand Formations Offshore Gulf of Mexico," SPE 24844, 67th Ann. Tech. Conf., Washington, D.C., 817-831, Oct. 1992.
9. Owens, K.A., S.A. Andersen & M.J. Economides, "Fracturing Pressures for Horizontal Wells," SPE 24822, 67th Ann. Tech. Conf., Washington, D.C., 581-588, Oct. 1992.
10. Meehan, D.N., "Stimulation Results in the Giddings (Austin Chalk) Field," SPE 24783, 67th Ann. Tech. Conf., Washington, D.C., 195-205, Oct. 1992.
11. Gidley, S.A. Holditch, D.E. Nierode, & R.W. Veatch, Editors, "Recent Advances in Hydraulic Fracturing," SPE Monograph Volume 12, Richardson, TX, June 1989.
12. Clifton, R.J. & A.S. Abou-Sayed, "On the Computation of the Three-Dimensional Geometry of Hydraulic Fractures," SPE 7943, SPE/DOE Low Perm. Gas Res. Symp., Denver, CO, May 1979.

13. Clifton, R.J. & A.S. Abou-Sayed, "A Variational Approach to the Prediction of the Three Dimensional Geometry of Hydraulic Fractures," SPE 9879, SPE/DOE Low Perm. Res. Symp., Denver, CO, May 1981.
14. Clifton, R.J. & J.J. Wang, "Multiple Fluids, Proppant Transport, and Thermal Effects in 3-Dimensional Simulation of Hydraulic Fracturing," SPE 18198, 63rd Ann. Tech. Conf., Houston, TX, Oct. 1988.
15. Clifton, R.J. & J.J. Wang, "Modeling of Poroelastic Effects in Hydraulic Fracturing," SPE 21871, Joint Rocky Mt. Regional/Low Perm. Res. Symp., Denver, CO, April 1991.
16. Clifton, R.J. & J.J. Wang, "Adaptive Optimal Mesh Generator for Hydraulic Fracturing Modeling," 32nd U.S. Rock Mech. Symp., 1991.
17. Advani, S.H., T.S. Lee & J.K. Lee, "Three-Dimensional Modeling of Hydraulic Fractures in Layered Media: Part I -Finite Element Formulations," ASME J. Energy Res. Tech., Vol. 112, 1-9, 1990.
18. Barree, R.D. "A Practical Numerical Simulator for Three Dimensional Fracture Propagation in Heterogeneous Media," SPE 12273, Reservoir Simulation Symp., San Francisco, CA, 403-411 Nov. 1983.
19. Barree, R.D. "A New Look at Fracture-Tip Screenout Behavior," JPT, Vol. 43, 138-143, Feb. 1991.
20. Shlyapobersky, J., "Energy Analysis of Hydraulic Fracturing," Proc. 26th U.S. Symp. on Rock Mechanics, Rapid City, SD, June 1985.
21. Shlyapobersky, J., G.K. Wong & W.W. Walhaug, "Overpressure Calibrated Design of Hydraulic Fracture Simulations," SPE 18194, 63rd Ann. Tech. Conf., Houston, TX, October 1988.
22. Cleary, M.P., "Analysis of the Mechanisms and Procedures for Producing Favorable Shapes of Hydraulic Fracturing," SPE 9260, SPE Ann. Tech. Conf., Dallas, TX, Sept. 1980.
23. Cleary, M.P., "Comprehensive Design Formulae for Hydraulic Fracturing," SPE 9259, SPE Ann. Tech. Conf., Dallas, TX, Sept. 1980.
24. Cleary, M.P., C.A. Wright & T.B. Wright, "Experimental and Modeling Evidence for Major Changes in Hydraulic Fracturing Design and Field Procedures," SPE 21494, SPE Gas Tech. Symp., Houston, TX, Jan. 1991.

25. Cleary, M.P. & Amaury Fonseca, "Proppant Convection and Encapsulation in Hydraulic Fracturing: Practical Implications of Computer Laboratory Simulations," SPE 67th Ann. Tech. Conf., Washington, D.C., Oct. 1992.
26. Meyer, B.R., "Design Formulae for 2-D and 3-D Vertical Hydraulic Fractures: Model Comparison and Parametric Studies," SPE 15240, Unconv. Gas Tech. Symp., Louisville, KY, 391-401, May 1986.
27. Meyer, B.R., "Three-Dimensional Hydraulic Fracturing Simulation on Personal Computers: Theory and Comparison Studies," SPE 19329, Eastern Reg. Mtg., Morgantown, WV, p. 213, Oct. 1989.
28. Meyer, B.R., G.D. Cooper & S.G. Nelson, "Real-Time 3-D Hydraulic Fracturing Simulation: Theory and Field Case Studies," SPE 20658, 65th Ann. Tech. Conf., New Orleans, LA, 417-431, Sept. 1990.
29. Hagel, M. & Meyer, B., "Utilizing Mini-Frac Data to Improve Design and Production," CIM 92-40, Pet. Soc. of CIM Ann. Tech. Conf., Calgary, Alberta, June 1992.
30. Kristianovich, S.A. & Y.P. Zheltov, "Formation of Vertical Fractures by Means of Highly Viscous Liquid," Proc. Fourth World Pet. Cong., Rome, Volume II, 579-586, 1955.
31. Perkins, T.K. & L.R. Kern, "Widths of Hydraulic Fractures," JPT, Vol. 13, 937-949, Sept. 1961.
32. Geertsma, J. & F. deKlerk, "A Rapid Method of Predicting Width and Extent of Hydraulic Induced Fractures," JPT, Vol. 21, 1571-1581, Dec. 1969.
33. Nordgren, R.P., "Propagation of Vertical Hydraulic Fractures," SPEJ, Vol. 12, 306-314, Aug. 1972.
34. Daneshy, A.A., "On the Design of Vertical Hydraulic Fractures," JPT, 83-93, Jan. 1973.
35. Daneshy, A.A., "Numerical Solution of Sand Transport in Hydraulic Fracturing," JPT, 132-140, Jan. 1978.
36. Poulsen, D.K. & W.S. Lee, "Fracture Design with Time- and Temperature-Dependent Fluid Properties," SPE 12483, 1984 Formation Damage Control Symp., Bakersfield, CA., Feb 13-14, 1984.

37. Lee, S.T. & J.R. Brockenbrough, "A New Analytical Solution for Finite-Conductivity Vertical Fractures with Real Time and Laplace Space Parameter Estimation," SPE 12013, 58th Annual Tech. Conf., San Francisco, CA, October 5-8, 1983.
38. McLeod, H. O., "A Simplified Approach to Design of Fracturing Treatments Using High Viscosity Cross-Linked Fluids," SPE 11614, Low Perm. Symp., Denver, CO, 121-136., March 1983.
39. Crawford, H.R., "Proppant Scheduling and Calculation of Fluid Lost During Fracturing," SPE 12064, 58th Ann. Tech Conf., San Francisco, CA, Oct. 1983..
40. Geertsma, J. & R. Haafkens, "A Comparison of the Theories for Predicting Width and Extent of Vertical Hydraulically Induced Fractures," ASME J. Energy Res. Tech., Vol. 101, 8-19, March 1979.
41. --"Staged Field Experiment No. 3," GRI-91/0048, GRI Final Report, Feb. 1991.

## Tables and Figures

**Table 1 Rock and Reservoir Data**

Interval	Depth (ft)	Zone Thickness (ft)	In Situ Stress (psi)	Poisson's Ratio	Young's Modulus	Fracture Toughness (psi $\sqrt{\text{in}}$ )
<b>Single-Layer (2-D) Case</b>						
1	9170-9340	170	5700	0.21	$8.5 \times 10^6$	2000
<b>3-Layer (3-D) Case</b>						
1	8990-9170	180	7150	0.30	$6.5 \times 10^6$	2000
2	9170-9340	170	5700	0.21	$8.5 \times 10^6$	2000
3	9340-9650	310	7350	0.29	$5.5 \times 10^6$	2000
<b>5-Layer (3-D) Case</b>						
1	8990-9170	180	7150	0.30	$6.5 \times 10^6$	2000
2	9170-9340	170	5700	0.21	$8.5 \times 10^6$	2000
3	9340-9380	40	7350	0.26	$5.4 \times 10^6$	2000
4	9380-9455	75	5800	0.20	$7.9 \times 10^6$	2000
5	9455-9650	195	8200	0.30	$4.0 \times 10^6$	2000

**Table 2 Treatment Data**

Bottom-hole temperature	246° F
Reservoir pressure	3600 psi
Spurt loss	0.0
Fluid leakoff height	entire fracture height
Fluid leakoff coefficient	$0.00025 \text{ ft}/\sqrt{\text{min}}$
Viscosity - Case A	200 cp
Viscosity - Case B	$n' = 0.5; k' = 0.06$
Fluid volume	10,000 bbls
Injection rate	50 bpm
Proppant	none

Table 3 2-D Results at End of Pump

200 CP	MODEL	LENGTH	HEIGHT	PRESSURE	W MAX	W AVG W	W AVG F	EFFIC
	SAH (GDK)	2542	170	62	0.848	0.849	0.605	85.5
	SAH (PKN)	4855	170	1094	0.502	0.394	0.289	72.3
	MARATHON	2584	204	1685	0.91	0.76	0.73	93
	MEYER1(GDK)	2659	170	70	0.79	0.79	0.62	83.1
	MEYER1(PKN)	4507	170	1188	0.55	0.43	0.32	72.2
	MEYER2(GDK)	2288	170	97	0.94	0.94	0.74	85.4
	MEYER2(PKN)	3803	170	1474	0.68	0.53	0.4	76.6
	SHELL(GDK)	2724	170	53	0.78	0.78	0.61	84
	SHELL(PKN)	4039	170	1377	0.59	0.46	0.37	75
	TEXACO-FP	1898	200	131.9		1.06		94.4
	TEXACO-FP	3587	200	1377		0.72		90
	CHEV(GDK)	1347	170	81.9	0.77	0.77	0.6	81.9
	CHEV(PKN)	2029	170	1380	0.63		0.36	73
	ADVANI	4595	170	1182	0.54	0.43	0.32	73.8
	HALLIB	2212	170	82	0.98	0.98	0.77	85.9
	CONOCO(GDK)	2716	170			0.767	0.6	82.5
	CONOCO(PKN)	3986	170			0.554	0.37	74.4
	ENERFRC-1	3866	170	1595	0.627	0.492	0.387	75
	ENERFRC-2	3556	170	1684	0.704	0.553	0.434	78
n', k'	MODEL	LENGTH	HEIGHT	PRESSURE	W MAX	W AVG W	W AVG F	EFFIC
	SAH (GDK)	2542	170	61.8	0.85	0.85	0.6	61.8
	SAH (PKN)	4629	170	1167.5	0.54	0.42	0.28	73.6
	MARATHON	2516	204	1824	0.98	0.82	0.75	93
	MEYER1(GDK)	2098	170	117	1.04	1.04	0.82	86.4
	MEYER1(PKN)	4118	170	1397	0.64	0.5	0.36	74.3
	MEYER2(GDK)	1808	170	161	1.24	1.24	0.97	88.3
	MEYER2(PKN)	3395	170	1774	0.81	0.64	0.46	79
	SHELL(GDK)	2142	170	89	1.03	1.03	0.81	89
	SHELL(PKN)	3347	170	1754	0.75	0.59	0.47	79
	ADVANI	4046	170	1474	0.68	0.53	0.38	76.9
	HALLIB	2031	170	97	1.07	1.07	0.84	86
	CONOCO(GDK)	2304	170		0.933	0.933	0.733	85.2
	CONOCO(PKN)	3656	170			0.622	0.415	76.5
	ENERFRC-1	3396	170	1880	0.738	0.58	0.456	78
	ENERFRC-2	3155	170	1986	0.817	0.641	0.504	81.7

Table 4 3-Layer Results at End of Pump

200 CP	3-LAYER							
	MODEL	LENGTH	HEIGHT	PRESSURE	W MAX	W AVG W	W AVG F	EFFIC
	SAH	3408	318	1009	0.65	0.35	0.3	77
	NSI	3750	903	283	0.56	0.32	0.25	66
	RES	1744	544	1227	0.9	0.54	0.36	80
	MARATHON	1380	442	1387	1.04	0.68	0.64	96
	MEYER-1	3549	291	987	0.58	0.35	0.29	70.3
	MEYER-2	2692	360	1109	0.72	0.41	0.34	74.3
	ARCO-STIM	3598	306	992	0.57	0.31	0.25	67
	TEXACO-FP	836	740	1561		1.333		89
	ADVANI	2089	357	1113	0.66	0.33	0.25	43
n', k'	3-LAYER							
	MODEL	LENGTH	HEIGHT	PRESSURE	W MAX	W AVG W	W AVG F	EFFIC
	SAH	3259	371	1093	0.75	0.38	0.31	77.6
	NSI	3289	329	1005	0.67	0.35	0.26	68
	RES	902	596	1428	1.1	0.74	0.49	62
	MARATHON	1326	442	1433	1.08	0.71	0.66	96
	MEYER-1	2915	337	1094	0.69	0.4	0.32	72.7
	MEYER-2	2120	413	1212	0.86	0.48	0.4	76.9
	ARCO-STIM	3235	353	1083	0.65	0.33	0.26	69
	ADVANI	2424	435	1171	0.74	0.34	0.21	47

Table 5 5-layer Results at End of Pump

200 CP	5-LAYER							
	MODEL	LENGTH	HEIGHT	PRESSURE	W MAX	W AVG W	W AVG F	EFFIC
	SAH	2905	394	960	0.72	0.42	0.31	80.1
	NSI	3709	361	852	0.63	0.38	0.25	66
	RES	1754	501	1119	0.83	0.6	0.4	82
	MARATHON	1224	476	1250	1.03	0.7	0.65	97
	MEYER-1	2962	328	669	0.5	0.36	0.28	70.5
	MEYER-2	2407	327	768	0.6	0.46	0.35	74.8
	ARCO-STIM	3399	394	944	0.64	0.36	0.24	68
	TEXACO-FP	934	605	934		1.32		89.6
	ADVANI	1594	438	1129	0.81	0.45	0.36	58.1
n', k'	3-LAYER							
	MODEL	LENGTH	HEIGHT	PRESSURE	W MAX	W AVG W	W AVG F	EFFIC
	SAH	2642	430	1035.5	0.82	0.46	0.31	81.8
	NSI	2765	388	935	0.71	0.42	0.25	70
	RES	1042	600	1358	1.18	0.9	0.6	87
	MARATHON	1156	476	1262	1.04	0.71	0.66	93
	MEYER-1	2535	330	766	0.6	0.46	0.37	73.7
	MEYER-2	1980	349	891	0.75	0.57	0.42	77.8
	ARCO-STIM	2926	405	968	0.7			70
	ARCO-TF	3124	449	1160	0.74			62
	TEX-FP	1089	578	1365		1.19		88.5
	TX-FPTIP	1168	614	1285		1.077		87.7
	ADVANI	1870	458	1151	0.85	0.47	0.34	64

Table 6 Time to breakthrough into lower layer

MODEL	Newtonian	n', k'
ARCO TerraFrac		60
ARCO STIMPLAN	63	50
SAH TRIFRAC	70	50
NSI STIMPLAN	140	75
TEXACO FRACPRO	8	6
TEXACO FRACPRO-TIP		7
RES FRACPRO	10	7
MARATHON GHOFER	<25	<25
MEYER MFRAC-II - 1	113	69
MEYER MFRAC-II - 2	44	30
ADVANI	55	40

Table 7 S.A Holditch & Assoc. - GDK Constant height  $\mu=200$  cp

Time (min)	Height (ft)	Half Length (ft)	Net Pressure (psi)	Efficiency (%)	Max. Width (in)	Avg. Width in Frac (in)	Avg. Width at Wellbore (in)
0	170	10	721	99	0.039	0.032	0.039
25	170	661	119	89	0.426	0.284	0.426
50	170	1036	96	88	0.537	0.370	0.537
75	170	1348	84	87	0.614	0.429	0.614
100	170	1624	77	87	0.676	0.475	0.676
125	170	1876	72	86	0.727	0.514	0.727
150	170	2110	68	86	0.772	0.547	0.772
175	170	2332	65	86	0.812	0.578	0.812
200	170	2542	62	86	0.848	0.605	0.848

Table 8 S.A Holditch & Assoc. - GDK Constant height  $n^*=0.5, k^*=0.06$ 

Time (min)	Height (ft)	Half Length (ft)	Net Pressure (psi)	Efficiency (%)	Max. Width (in)	Avg. Width in Frac (in)	Avg. Width at Wellbore (in)
0	170	10	682	99	0.037	0.033	0.037
25	170	626	134	90	0.452	0.267	0.452
50	170	942	118	89	0.597	0.365	0.597
75	170	1195	109	89	0.704	0.436	0.704
100	170	1415	103	89	0.789	0.494	0.789
125	170	1613	99	88	0.863	0.543	0.863
150	170	1796	96	88	0.929	0.587	0.929
175	170	1967	93	88	0.988	0.626	0.988
200	170	2128	91	88	1.04	0.662	1.04

Table 9 S.A Holditch & Assoc. - PKN Constant height  $\mu=200$  cp

Time (min)	Height (ft)	Half Length (ft)	Net Pressure (psi)	Efficiency (%)	Max. Width (in)	Avg. Width in Frac (in)	Avg. Width at Wellbore (in)
0	170	10	42	98	0.079	0.13	0.015
25	170	1067	712	83	0.327	0.157	0.256
50	170	1771	827	80	0.379	0.203	0.298
75	170	2379	901	78	0.413	0.229	0.325
100	170	2934	955	76	0.438	0.247	0.344
125	170	3452	998	75	0.458	0.260	0.360
150	170	3941	1035	74	0.475	0.271	0.373
175	170	4408	1066	73	0.489	0.281	0.382
200	170	4855	1094	72	0.502	0.290	0.394

Table 10 S.A Holditch & Assoc. - PKN Constant height  $n^*=0.5, k^*=0.06$ 

Time (min)	Height (ft)	Half Length (ft)	Net Pressure (psi)	Efficiency (%)	Max. Width (in)	Avg. Width in Frac (in)	Avg. Width at Wellbore (in)
0	170	10	42	98	0.019	0.013	0.015
25	170	1084	699	82	0.321	0.157	0.252
50	170	1764	831	80	0.382	0.192	0.300
75	170	2342	919	78	0.422	0.217	0.331
100	170	2862	989	77	0.452	0.235	0.356
125	170	3341	1042	76	0.478	0.250	0.376
150	170	3793	1089	75	0.500	0.263	0.393
175	170	4220	1131	74	0.519	0.273	0.408
200	170	4629	1168	74	0.536	0.283	0.421

Table 11 S.A. Holditch & Assoc. - 3-layer  $\mu=200$  cp

Time (min)	Height (ft)	Upper Height (ft)	Lower Height (ft)	Half Length (ft)	Net Pressure (psi)	Efficiency (%)	Max. Width (in)	Avg. Width in Frac (in)	Avg. Width at Wellbore (in)
0	172	86	86	15	164	95	0.076	0.059	0.059
25	233	121	112	769	768	84	0.423	0.2227	0.273
50	253	133	120	1288	846	82	0.486	0.248	0.301
75	268	142	126	1720	894	81	0.529	0.264	0.319
100	281	150	131	2105	928	80	0.561	0.275	0.330
125	291	156	135	2458	953	79	0.588	0.283	0.338
150	301	162	139	2792	975	78	0.610	0.290	0.343
175	310	167	142	3107	993	77	0.629	0.296	0.348
200	318	172	145	3408	1009	77	0.647	0.301	0.353

Table 12 S.A. Holditch & Assoc. - 3-layer  $n'=0.05$ ,  $k'=0.06$ 

Time (min)	Height (ft)	Upper Height (ft)	Lower Height (ft)	Half Length (ft)	Net Pressure (psi)	Efficiency (%)	Max. Width (in)	Avg. Width in Frac (in)	Avg. Width at Wellbore (in)
0	172	86	86	16	164	95	0.076	0.059	0.06
25	238	124	114	810	787	84	0.438	0.216	0.280
50	266	141	125	1319	886	82	0.522	0.241	0.316
75	289	155	134	1729	947	81	0.581	0.259	0.336
100	308	166	142	2086	991	80	0.627	0.273	0.347
125	326	177	148	2415	1024	79	0.664	0.283	0.359
150	342	187	155	2717	1051	78	0.696	0.291	0.368
175	357	197	161	2995	1073	78	0.724	0.299	0.377
200	371	206	165	3259	1093	77	0.751	0.306	0.384

Table 13 S.A. Holditch & Assoc. - 5-layer  $\mu=200$  cp

Time (min)	Height (ft)	Upper Height (ft)	Lower Height (ft)	Half Length (ft)	Net Pressure (psi)	Efficiency (%)	Max. Width (in)	Avg. Width in Frac (in)	Avg. Width at Wellbore (in)
0	173	87	86	12	209	96	0.097	0.075	0.075
25	231	120	111	781	760	85	0.420	0.224	0.273
50	250	132	119	1318	836	82	0.480	0.244	0.299
75	269	141	128	1767	883	80	0.522	0.258	0.316
100	328	155	173	2124	912	79	0.604	0.271	0.363
125	369	165	204	2338	930	80	0.660	0.283	0.394
150	387	171	216	2525	943	80	0.689	0.292	0.410
175	391	174	217	2710	953	80	0.705	0.299	0.417
200	394	177	217	2906	960	80	0.716	0.305	0.423

Table 14 S.A. Holditch & Assoc. - 5-layer  $n'=0.05$ ,  $k'=0.06$ 

Time (min)	Height (ft)	Upper Height (ft)	Lower Height (ft)	Half Length (ft)	Net Pressure (psi)	Efficiency (%)	Max. Width (in)	Avg. Width in Frac (in)	Avg. Width at Wellbore (in)
0	173	87	86	12	209	96	0.097	0.075	0.075
25	235	123	113	822	777	84	0.434	0.213	0.279
50	263	139	124	1356	874	81	0.512	0.236	0.312
75	364	164	200	1706	929	81	0.653	0.255	0.391
100	396	178	217	1886	964	81	0.722	0.273	0.425
125	405	186	219	2071	985	82	0.754	0.286	0.438
150	414	194	220	2264	1006	82	0.781	0.295	0.447
175	422	201	221	2442	1021	82	0.801	0.303	0.454
200	430	207	222	2642	1036	82	0.818	0.309	0.461

Table 15 Meyer & Assoc. - GDK Constant height  $\mu=200$  cp Base Case

Time (min)	Height (ft)	Half Length (ft)	Net Pressure (psi)	Efficiency (%)	Max. Width (in)	Avg. Width in Frac (in)	Avg. Width at Wellbore (in)
0	170	0	0	100	0	0	0
25	170	689	138	88	0.402	0.315	0.402
50	170	1082	110	86	0.504	0.395	0.504
75	170	1408	96	85	0.575	0.451	0.575
100	170	1697	88	85	0.631	0.495	0.631
125	170	1961	82	84	0.679	0.532	0.679
150	170	2207	77	84	0.720	0.564	0.720
175	170	2439	73	83	0.757	0.593	0.757
200	170	2659	70	83	0.790	0.619	0.790

Table 16 Meyer & Assoc. - GDK Constant height  $n^*=0.5, k^*=0.06$  Base Case

Time (min)	Height (ft)	Half Length (ft)	Net Pressure (psi)	Efficiency (%)	Max. Width (in)	Avg. Width in Frac (in)	Avg. Width at Wellbore (in)
0	170	0	0	100	0	0	0
25	170	611	178	89	0.459	0.360	0.459
50	170	922	154	88	0.603	0.473	0.603
75	170	1173	142	88	0.708	0.555	0.708
100	170	1391	134	87	0.793	0.621	0.793
125	170	1588	129	87	0.865	0.678	0.865
150	170	1769	124	87	0.930	0.729	0.930
175	170	1939	120	87	0.988	0.774	0.988
200	170	2098	117	86	1.041	0.816	1.041

Table 17 Meyer & Assoc. - PKN Constant height  $\mu=200$  cp Base Case

Time (min)	Height (ft)	Half Length (ft)	Net Pressure (psi)	Efficiency (%)	Max. Width (in)	Avg. Width in Frac (in)	Avg. Width at Wellbore (in)
0	170	0	0	100	0	0	0
25	170	948	813	84	0.373	0.219	0.292
50	170	1605	924	80	0.424	0.248	0.332
75	170	2178	995	78	0.457	0.267	0.358
100	170	2700	1048	77	0.481	0.281	0.377
125	170	3187	1092	75	0.501	0.292	0.393
150	170	3647	1128	74	0.518	0.302	0.406
175	170	4086	1160	73	0.532	0.310	0.417
200	170	4507	1188	72	0.545	0.318	0.427

Table 18 Meyer & Assoc. - PKN Constant height  $n^*=0.5, k^*=0.06$  Base Case

Time (min)	Height (ft)	Half Length (ft)	Net Pressure (psi)	Efficiency (%)	Max. Width (in)	Avg. Width in Frac (in)	Avg. Width at Wellbore (in)
0	170	0	0	100	0	0	0
25	170	934	862	84	0.395	0.222	0.310
50	170	1539	1013	81	0.465	0.260	0.364
75	170	2057	1114	79	0.511	0.286	0.401
100	170	2524	1190	78	0.546	0.305	0.428
125	170	2957	1253	77	0.575	0.321	0.451
150	170	3363	1307	76	0.600	0.335	0.470
175	170	3749	1354	75	0.621	0.347	0.487
200	170	4118	1397	74	0.641	0.358	0.502

Table 19 Meyer & Assoc. - 3-layer  $\mu=200$  cp Base Case

Time (min)	Height (ft)	Upper Height (ft)	Lower Height (ft)	Half Length (ft)	Net Pressure (psi)	Efficiency (%)	Max. Width (in)	Avg. Width in Frac (in)	Avg. Width at Wellbore (in)
0	170	85	85	0	0	100	0	0	0
25	214	110	104	872	740	83	0.385	0.208	0.268
50	234	122	112	1421	826	80	0.445	0.232	0.295
75	249	131	118	1867	876	77	0.482	0.247	0.311
100	260	138	122	2261	910	75	0.510	0.257	0.322
125	270	144	126	2620	935	74	0.532	0.266	0.331
150	278	149	129	2950	956	72	0.550	0.273	0.338
175	284	153	131	3258	973	71	0.566	0.279	0.345
200	291	157	134	3549	987	70	0.580	0.285	0.350

Table 20 Meyer & Assoc. - 3-layer  $n=0.5$ ,  $k=0.06$  Base Case

Time (min)	Height (ft)	Upper Height (ft)	Lower Height (ft)	Half Length (ft)	Net Pressure (psi)	Efficiency (%)	Max. Width (in)	Avg. Width in Frac (in)	Avg. Width at Wellbore (in)
0	170	85	85	0	0	100	0	0	0
25	217	112	105	845	784	84	0.414	0.214	0.286
50	247	130	117	1307	894	80	0.496	0.246	0.323
75	269	143	126	1668	957	78	0.549	0.267	0.345
100	287	154	133	1975	1000	77	0.590	0.282	0.361
125	301	163	138	2244	1032	76	0.622	0.295	0.374
150	315	172	143	2487	1057	75	0.650	0.305	0.385
175	326	179	147	2708	1077	74	0.673	0.314	0.394
200	337	186	151	2915	1094	73	0.694	0.322	0.402

Table 21 Meyer & Assoc. - 5-layer  $\mu=200$  cp Base Case

Time (min)	Height (ft)	Upper Height (ft)	Lower Height (ft)	Half Length (ft)	Net Pressure (psi)	Efficiency (%)	Max. Width (in)	Avg. Width in Frac (in)	Avg. Width at Wellbore (in)
0	170	85	85	0	0	100	0	0	0
25	193	111	104	872	743	83	0.387	0.208	0.268
50	205	124	113	1414	829	80	0.446	0.231	0.294
75	212	132	119	1863	879	77	0.483	0.246	0.310
100	219	139	123	2257	913	75	0.511	0.257	0.321
125	232	144	138	2564	933	73	0.536	0.260	0.321
150	259	143	169	2626	799	72	0.520	0.268	0.336
175	289	132	208	2716	674	71	0.487	0.267	0.341
200	284	123	205	2962	669	71	0.497	0.282	0.364

Table 22 Meyer & Assoc. - 5-layer  $n=0.5$ ,  $k=0.06$  Base Case

Time (min)	Height (ft)	Upper Height (ft)	Lower Height (ft)	Half Length (ft)	Net Pressure (psi)	Efficiency (%)	Max. Width (in)	Avg. Width in Frac (in)	Avg. Width at Wellbore (in)
0	170	85	85	0	0	100	0	0	0
25	219	113	106	842	786	84	0.415	0.214	0.285
50	249	131	118	1303	898	80	0.497	0.246	0.322
75	278	144	134	1643	952	78	0.552	0.263	0.338
100	322	146	176	1725	823	77	0.558	0.282	0.367
125	343	134	209	1844	723	76	0.544	0.296	0.395
150	330	123	207	2099	734	75	0.566	0.316	0.425
175	329	122	207	2327	751	75	0.583	0.327	0.441
200	330	122	208	2535	766	74	0.599	0.336	0.455

Table 23 Meyer & Assoc. - GDK Constant height  $\mu=200$  cp Knobs on

Time (min)	Height (ft)	Half Length (ft)	Net Pressure (psi)	Efficiency (%)	Max. Width (in)	Avg. Width in Frac (in)	Avg. Width at Wellbore (in)
0	170	0	0	100	0	0	0
25	170	589	192	89	0.479	0.376	0.479
50	170	927	153	88	0.601	0.471	0.601
75	170	1208	134	88	0.686	0.538	0.686
100	170	1457	122	87	0.754	0.591	0.754
125	170	1685	114	86	0.811	0.635	0.811
150	170	1898	107	86	0.860	0.674	0.860
175	170	2098	102	86	0.904	0.709	0.904
200	170	2288	97	85	0.944	0.740	0.944

Table 24 Meyer & Assoc. - GDK Constant height  $n'=0.5, k'=0.06$  Knobs on

Time (min)	Height (ft)	Half Length (ft)	Net Pressure (psi)	Efficiency (%)	Max. Width (in)	Avg. Width in Frac (in)	Avg. Width at Wellbore (in)
0	170	0	0	100	0	0	0
25	170	515	255	91	0.556	0.436	0.556
50	170	784	218	90	0.724	0.568	0.724
75	170	1002	199	89	0.846	0.663	0.846
100	170	1192	187	89	0.945	0.741	0.945
125	170	1363	178	89	1.030	0.807	1.030
150	170	1521	171	89	1.105	0.866	1.105
175	170	1669	166	89	1.173	0.919	1.173
200	170	1808	161	88	1.235	0.968	1.235

Table 25 Meyer & Assoc. - PKN Constant height  $\mu=200$  cp Knobs on

Time (min)	Height (ft)	Half Length (ft)	Net Pressure (psi)	Efficiency (%)	Max. Width (in)	Avg. Width in Frac (in)	Avg. Width at Wellbore (in)
0	170	0	0	100	0	0	0
25	170	785	1002	87	0.460	0.273	0.360
50	170	1337	1141	84	0.524	0.310	0.411
75	170	1820	1231	82	0.565	0.334	0.443
100	170	2262	1298	80	0.596	0.352	0.467
125	170	2676	1353	79	0.621	0.367	0.486
150	170	3068	1399	78	0.642	0.379	0.503
175	170	3443	1438	77	0.660	0.390	0.517
200	170	3803	1474	77	0.676	0.399	0.530

Table 26 Meyer & Assoc. - PKN Constant height  $n'=0.5, k'=0.06$  Knobs on

Time (min)	Height (ft)	Half Length (ft)	Net Pressure (psi)	Efficiency (%)	Max. Width (in)	Avg. Width in Frac (in)	Avg. Width at Wellbore (in)
0	170	0	0	100	0	0	0
25	170	741	1110	87	0.509	0.291	0.399
50	170	1238	1298	85	0.595	0.339	0.467
75	170	1667	1422	83	0.652	0.371	0.511
100	170	2056	1517	82	0.696	0.395	0.546
125	170	2417	1596	81	0.732	0.415	0.574
150	170	2759	1662	80	0.763	0.433	0.598
175	170	3083	1721	80	0.790	0.448	0.619
200	170	3395	1774	79	0.814	0.461	0.638

Table 27 Meyer & Assoc. - 3-layer  $\mu=200$  cp Knobs on

Time (min)	Height (ft)	Upper Height (ft)	Lower Height (ft)	Half Length (ft)	Net Pressure (psi)	Efficiency (%)	Max. Width (in)	Avg. Width in Frac (in)	Avg. Width at Wellbore (in)
0	170	85	85	0	0	100	0	0	0
25	235	122	113	696	870	86	0.477	0.255	0.319
50	268	142	126	1109	960	83	0.553	0.283	0.349
75	290	156	134	1446	1008	81	0.599	0.301	0.365
100	307	167	140	1740	1040	79	0.632	0.313	0.377
125	321	176	145	2005	1064	77	0.659	0.323	0.387
150	332	183	149	2250	1082	76	0.680	0.331	0.395
175	343	190	153	2478	1097	75	0.699	0.338	0.401
200	360	195	155	2692	1109	74	0.715	0.344	0.407

Table 28 Meyer & Assoc. - 3-layer  $n'=0.5, k'=0.06$  Knobs on

Time (min)	Height (ft)	Upper Height (ft)	Lower Height (ft)	Half Length (ft)	Net Pressure (psi)	Efficiency (%)	Max. Width (in)	Avg. Width in Frac (in)	Avg. Width at Wellbore (in)
0	170	85	85	0	0	100	0	0	0
25	246	129	117	637	944	87	0.534	0.276	0.352
50	291	156	135	968	1048	84	0.634	0.313	0.392
75	322	175	147	1225	1102	82	0.697	0.335	0.415
100	347	191	156	1444	1138	81	0.743	0.352	0.433
125	367	204	163	1636	1163	80	0.780	0.366	0.447
150	385	216	169	1811	1183	79	0.811	0.378	0.459
175	400	226	174	1971	1199	78	0.837	0.388	0.469
200	413	235	178	2120	1212	77	0.861	0.397	0.478

Table 29 Meyer & Assoc. - 5-layer  $\mu=200$  cp Knobs on

Time (min)	Height (ft)	Upper Height (ft)	Lower Height (ft)	Half Length (ft)	Net Pressure (psi)	Efficiency (%)	Max. Width (in)	Avg. Width in Frac (in)	Avg. Width at Wellbore (in)
0	170	85	85	0	0	100	0	0	0
25	237	124	113	695	874	86	0.479	0.255	0.318
50	282	144	138	1085	949	83	0.556	0.276	0.337
75	346	136	210	1162	687	81	0.517	0.296	0.373
100	325	119	206	1484	708	79	0.537	0.316	0.404
125	325	118	207	1743	727	78	0.556	0.328	0.420
150	325	118	207	1977	743	77	0.572	0.338	0.435
175	326	118	208	2199	757	76	0.586	0.346	0.447
200	327	119	208	2407	748	75	0.598	0.353	0.457

Table 30 Meyer & Assoc. - 5-layer  $n'=0.5, k'=0.06$  Knobs on

Time (min)	Height (ft)	Upper Height (ft)	Lower Height (ft)	Half Length (ft)	Net Pressure (psi)	Efficiency (%)	Max. Width (in)	Avg. Width in Frac (in)	Avg. Width at Wellbore (in)
0	170	85	85	0	0	100	0	0	0
25	249	131	118	633	949	87	0.535	0.276	0.350
50	341	144	197	801	797	84	0.580	0.313	0.399
75	337	128	209	1029	770	83	0.607	0.346	0.455
100	336	127	209	1255	805	81	0.643	0.367	0.487
125	338	127	211	1454	832	80	0.673	0.383	0.513
150	341	129	212	1638	854	79	0.699	0.398	0.533
175	345	132	213	1814	874	79	0.724	0.411	0.551
200	349	135	214	1980	891	78	0.746	0.423	0.567

Table 31 Advani - PKN Constant Height  $\mu=200$  cp

Time (min)	Height (ft)	Half Length (ft)	Net Pressure (psi)	Efficiency (%)	Max. Width (in)	Avg. Width in Frac (in)	Avg. Width at Wellbore (in)
0	170	0	0	100	0	0	0
25	170	968	804	84	0.369	0.216	0.289
50	170	1638	915	81	0.420	0.246	0.329
75	170	5550	987	79	0.453	0.265	0.356
100	170	2752	1041	78	0.478	0.280	0.375
125	170	3248	1085	77	0.498	0.292	0.391
150	170	3718	1121	76	0.515	0.302	0.404
175	170	4165	1153	75	0.529	0.310	0.415
200	170	4595	1182	74	0.542	0.318	0.426

Table 32 Advani - PKN Constant Height  $n=0.5, k'=0.06$ 

Time (min)	Height (ft)	Half Length (ft)	Net Pressure (psi)	Efficiency (%)	Max. Width (in)	Avg. Width in Frac (in)	Avg. Width at Wellbore (in)
0	170	0	0	100	0	0	0
25	170	919	900	85	0.413	0.229	0.324
50	170	1513	1062	83	0.487	0.271	0.383
75	170	2020	1170	81	0.537	0.298	0.421
100	170	2479	1252	80	0.575	0.319	0.451
125	170	2904	1320	79	0.606	0.337	0.475
150	170	3303	1378	78	0.632	0.352	0.496
175	170	3683	1429	78	0.656	0.365	0.515
200	170	4046	1474	77	0.676	0.377	0.531

Table 33 Advani - 3-Layer  $\mu=200$  cp

Time (min)	Height (ft)	Upper Height (ft)	Lower Height (ft)	Half Length (ft)	Net Pressure (psi)	Efficiency (%)	Max. Width (in)	Avg. Width in Frac (in)	Avg. Width at Wellbore (in)
0	170	85	85	0	0	100	0	0	0
25	240	124	116	654	885	67	0.434	0.218	0.267
50	274	143	131	1069	972	58	0.513	0.220	0.298
75	298	158	141	1303	1040	56	0.571	0.245	0.316
100	316	169	147	1501	1048	52	0.598	0.248	0.326
125	328	177	151	1635	1077	51	0.624	0.265	0.329
150	340	185	155	1778	1090	48	0.634	0.265	0.326
175	352	193	159	1983	1112	44	0.649	0.238	0.327
200	357	195	162	2089	1113	43	0.658	0.250	0.331

Table 34 Advani - 3-Layer  $n=0.5, k'=0.06$ 

Time (min)	Height (ft)	Upper Height (ft)	Lower Height (ft)	Half Length (ft)	Net Pressure (psi)	Efficiency (%)	Max. Width (in)	Avg. Width in Frac (in)	Avg. Width at Wellbore (in)
0	170	85	85	0	0	100	0	0	0
25	249	131	117	905	865	71	0.422	0.165	0.251
50	296	157	139	1323	995	64	0.530	0.191	0.286
75	315	169	146	1313	1017	59	0.568	0.198	0.303
100	329	179	151	1790	1048	58	0.598	0.218	0.309
125	361	196	165	2018	1106	54	0.646	0.206	0.318
150	372	202	171	2188	1104	52	0.659	0.213	0.319
175	406	226	180	2381	1142	52	0.706	0.216	0.334
200	435	244	191	2424	1171	47	0.743	0.211	0.339

Table 35 Advani - 5-Layer  $\mu=200$  cp

Time (min)	Height (ft)	Upper Height (ft)	Lower Height (ft)	Half Length (ft)	Net Pressure (psi)	Efficiency (%)	Max. Width (in)	Avg. Width in Frac (in)	Avg. Width at Wellbore (in)
0	170	85	85	0	0	100	0	0	0
25	240	124	116	654	885	67	0.434	0.218	0.267
50	276	144	132	1073	965	58	0.513	0.220	0.299
75	380	151	229	1194	1065	62	0.667	0.295	0.386
100	392	161	231	1227	1051	65	0.702	0.340	0.408
125	403	169	234	1273	1048	63	0.727	0.359	0.421
150	413	177	237	1363	1047	58	0.720	0.337	0.402
175	430	190	241	1506	1076	57	0.749	0.336	0.406
200	438	195	243	1594	1129	58	0.805	0.364	0.445

Table 36 Advani - 5-Layer  $n'=0.5, k'=0.06$ 

Time (min)	Height (ft)	Upper Height (ft)	Lower Height (ft)	Half Length (ft)	Net Pressure (psi)	Efficiency (%)	Max. Width (in)	Avg. Width in Frac (in)	Avg. Width at Wellbore (in)
0	170	85	85	0	0	100	0	0	0
25	249	131	117	905	865	71	0.422	0.165	0.251
50	378	147	231	1150	992	72	0.597	0.244	0.340
75	388	157	231	1159	1021	76	0.662	0.299	0.377
100	398	166	232	1208	1044	70	0.695	0.308	0.396
125	422	187	235	1502	1027	65	0.697	0.278	0.373
150	430	193	237	1751	1035	62	0.704	0.267	0.370
175	449	205	244	1853	1095	61	0.770	0.289	0.410
200	458	210	248	1870	1151	64	0.848	0.337	0.465

Table 37 Shell - GDK Constant Height  $\mu=200$  cp

Time (min)	Height (ft)	Half Length (ft)	Net Pressure (psi)	Efficiency (%)	Max. Width (in)	Avg. Width in Frac (in)	Avg. Width at Wellbore (in)
0	170	0	0	100	0	0	0
25	170	704	104	88	0.396	0.311	0.396
50	170	1107	83	87	0.496	0.390	0.496
75	170	1441	73	86	0.566	0.445	0.566
100	170	1738	66	86	0.622	0.489	0.622
125	170	2007	62	85	0.669	0.525	0.669
150	170	2261	58	85	0.710	0.557	0.710
175	170	2499	55	84	0.746	0.586	0.746
200	170	2725	53	84	0.779	0.612	0.779

Table 38 Shell - GDK Constant Height  $n'=0.5, k'=0.06$ 

Time (min)	Height (ft)	Half Length (ft)	Net Pressure (psi)	Efficiency (%)	Max. Width (in)	Avg. Width in Frac (in)	Avg. Width at Wellbore (in)
0	170	0	0	100	0	0	0
25	170	624	134	90	0.453	0.356	0.453
50	170	942	117	89	0.596	0.466	0.596
75	170	1198	108	89	0.699	0.549	0.699
100	170	1421	102	88	0.784	0.615	0.784
125	170	1622	98	88	0.856	0.672	0.856
150	170	1807	94	88	0.920	0.722	0.920
175	170	1979	91	88	0.977	0.768	0.977
200	170	2142	89	87	1.030	0.809	1.030

Table 39 Shell - PKN Constant Height  $\mu=200$  cp

Time (min)	Height (ft)	Half Length (ft)	Net Pressure (psi)	Efficiency (%)	Max. Width (in)	Avg. Width in Frac (in)	Avg. Width at Wellbore (in)
0	170	0	0	100	0	0	0
25	170	948	848	84	0.358	0.225	0.281
50	170	1540	993	81	0.423	0.266	0.332
75	170	2044	1092	79	0.466	0.293	0.366
100	170	2496	1168	78	0.499	0.314	0.392
125	170	2917	1232	77	0.526	0.331	0.413
150	170	3310	1286	76	0.550	0.345	0.432
175	170	3683	1334	76	0.570	0.358	0.448
200	170	4039	1378	75	0.589	0.370	0.463

Table 40 Shell - PKN Constant Height  $n'=0.5, k'=0.06$ 

Time (min)	Height (ft)	Half Length (ft)	Net Pressure (psi)	Efficiency (%)	Max. Width (in)	Avg. Width in Frac (in)	Avg. Width at Wellbore (in)
0	170	0	0	100	0	0	0
25	170	863	950	85	0.400	0.251	0.314
50	170	1356	1160	83	0.493	0.310	0.387
75	170	1767	1307	82	0.567	0.350	0.437
100	170	2132	1424	81	0.607	0.382	0.477
125	170	2465	1522	80	0.650	0.406	0.511
150	170	2776	1608	80	0.687	0.432	0.540
175	170	3069	1685	79	0.720	0.452	0.565
200	170	3347	1754	79	0.750	0.471	0.589

Table 41 Shell ENERFRAC  $\mu=200$  cp Base Case

Time (min)	Height (ft)	Half Length (ft)	Net Pressure (psi)	Efficiency (%)	Max. Width (in)	Avg. Width in Frac (in)	Avg. Width at Wellbore (in)
0	170	0	0	100	0	0	0
25	170	811	1093	85	0.423	0.261	0.332
50	170	1373	1237	83	0.483	0.296	0.380
75	170	1863	1332	81	0.522	0.322	0.410
100	170	2311	1405	79	0.551	0.340	0.433
125	170	2729	1464	78	0.575	0.354	0.451
150	170	3125	1513	77	0.594	0.367	0.467
175	170	3503	1557	76	0.612	0.377	0.480
200	170	3866	1595	75	0.627	0.387	0.492

Table 42 Shell ENERFRAC  $n'=0.5$ ,  $k'=0.06$  Base Case

Time (min)	Height (ft)	Half Length (ft)	Net Pressure (psi)	Efficiency (%)	Max. Width (in)	Avg. Width in Frac (in)	Avg. Width at Wellbore (in)
0	170	0	0	100	0	0	0
25	170	770	1160	86	0.448	0.276	0.352
50	170	1267	1359	84	0.530	0.327	0.417
75	170	1693	1494	82	0.585	0.361	0.459
100	170	2079	1598	81	0.626	0.386	0.492
125	170	2436	1684	80	0.661	0.408	0.519
150	170	2772	1757	79	0.690	0.426	0.542
175	170	3092	1821	79	0.715	0.441	0.562
200	170	3396	1880	78	0.738	0.456	0.580

Table 43 Shell ENERFRAC  $\mu=200$  cp Overpressure=500 psi

Time (min)	Height (ft)	Half Length (ft)	Net Pressure (psi)	Efficiency (%)	Max. Width (in)	Avg. Width in Frac (in)	Avg. Width at Wellbore (in)
0	170	0	0	100	0	0	0
25	170	772	1120	86	0.448	0.277	0.352
50	170	1322	1259	83	0.506	0.312	0.396
75	170	1806	1353	81	0.543	0.335	0.427
100	170	2249	1424	80	0.571	0.352	0.449
125	170	2663	1482	79	0.594	0.366	0.467
150	170	3054	1531	78	0.613	0.378	0.482
175	170	3429	1574	77	0.630	0.389	0.495
200	170	3789	1612	76	0.645	0.396	0.506

Table 44 Shell ENERFRAC  $n'=0.5$ ,  $k'=0.06$  Overpressure=500 psi

Time (min)	Height (ft)	Half Length (ft)	Net Pressure (psi)	Efficiency (%)	Max. Width (in)	Avg. Width in Frac (in)	Avg. Width at Wellbore (in)
0	170	0	0	100	0	0	0
25	170	730	1200	87	0.477	0.294	0.375
50	170	1220	1392	84	0.556	0.343	0.437
75	170	1642	1524	83	0.608	0.375	0.478
100	170	2024	1626	82	0.649	0.400	0.509
125	170	2379	1710	81	0.682	0.420	0.535
150	170	2714	1782	80	0.710	0.438	0.558
175	170	3031	1846	79	0.735	0.453	0.577
200	170	3336	1903	79	0.757	0.467	0.595

Table 45 Shell ENERFRAC  $\mu=200$  cp Overpressure=1000 psi

Time (min)	Height (ft)	Half Length (ft)	Net Pressure (psi)	Efficiency (%)	Max. Width (in)	Avg. Width in Frac (in)	Avg. Width at Wellbore (in)
0	170	0	0	100	0	0	0
25	170	660	1262	88	0.536	0.332	0.422
50	170	1174	1372	86	0.585	0.361	0.429
75	170	1634	1451	84	0.616	0.380	0.484
100	170	2060	1513	82	0.640	0.395	0.502
125	170	2460	1565	81	0.659	0.407	0.518
150	170	2840	1610	80	0.676	0.417	0.531
175	170	3205	1649	79	0.691	0.426	0.543
200	170	3556	1684	79	0.704	0.434	0.553

Table 46 Shell ENERFRAC  $n'=0.5, k'=0.06$  Overpressure=1000 psi

Time (min)	Height (ft)	Half Length (ft)	Net Pressure (psi)	Efficiency (%)	Max. Width (in)	Avg. Width in Frac (in)	Avg. Width at Wellbore (in)
0	170	0	0	100	0	0	0
25	170	626	1359	89	0.570	0.352	0.448
50	170	1089	1519	86	0.637	0.393	0.500
75	170	1496	1635	85	0.682	0.421	0.536
100	170	1868	1727	84	0.718	0.443	0.564
125	170	2215	1805	82	0.748	0.461	0.587
150	170	2543	1872	82	0.773	0.477	0.607
175	170	2855	1932	81	0.796	0.491	0.625
200	170	3155	1966	80	0.817	0.504	0.641

Table 47 Shell ENERFRAC  $\mu=200$  cp Overpressure=1500 psi

Time (min)	Height (ft)	Half Length (ft)	Net Pressure (psi)	Efficiency (%)	Max. Width (in)	Avg. Width in Frac (in)	Avg. Width at Wellbore (in)
0	170	0	0	100	0	0	0
25	170	524	1591	91	0.695	0.429	0.546
50	170	970	1648	88	0.730	0.450	0.573
75	170	1384	1696	86	0.751	0.463	0.590
100	170	1776	1737	85	0.767	0.473	0.603
125	170	2148	1774	84	0.781	0.482	0.614
150	170	2506	1806	83	0.794	0.490	0.623
175	170	2850	1836	82	0.805	0.496	0.632
200	170	3184	1863	81	0.814	0.502	0.640

Table 48 Shell ENERFRAC  $n'=0.5, k'=0.06$  Overpressure=1500 psi

Time (min)	Height (ft)	Half Length (ft)	Net Pressure (psi)	Efficiency (%)	Max. Width (in)	Avg. Width in Frac (in)	Avg. Width at Wellbore (in)
0	170	0	0	100	0	0	0
25	170	507	1672	91	0.721	0.445	0.566
50	170	920	1776	89	0.774	0.477	0.608
75	170	1297	1862	87	0.809	0.499	0.635
100	170	1647	1934	86	0.837	0.516	0.657
125	170	1977	1998	85	0.861	0.531	0.676
150	170	2291	2054	84	0.882	0.544	0.693
175	170	2591	2105	83	0.901	0.558	0.707
200	170	2881	2152	82	0.918	0.566	0.721

**Table 49 Shell ENERFRAC  $\mu=200$  cp Overpressure=2000 psi**

Time (min)	Height (ft)	Half Length (ft)	Net Pressure (psi)	Efficiency (%)	Max. Width (in)	Avg. Width in Frac (in)	Avg. Width at Wellbore (in)
0	170	0	0	100	0	0	0
25	170	420	2035	93	0.884	0.545	0.694
50	170	878	2059	90	0.921	0.568	0.723
75	170	1141	2061	89	0.937	0.578	0.736
100	170	1482	2102	87	0.947	0.584	0.744
125	170	1813	2122	86	0.956	0.590	0.751
150	170	2133	2141	85	0.963	0.594	0.757
175	170	2446	2159	84	0.970	0.598	0.762
200	170	2750	2175	84	0.976	0.602	0.767

**Table 50 Shell ENERFRAC  $n'=0.5$ ,  $k'=0.06$  Overpressure=2000 psi**

Time (min)	Height (ft)	Half Length (ft)	Net Pressure (psi)	Efficiency (%)	Max. Width (in)	Avg. Width in Frac (in)	Avg. Width at Wellbore (in)
0	170	0	0	100	0	0	0
25	170	413	2088	93	0.900	0.555	0.707
50	170	765	2148	91	0.951	0.586	0.747
75	170	1098	2203	89	0.978	0.603	0.768
100	170	1414	2252	88	0.999	0.616	0.784
125	170	1717	2297	87	1.016	0.627	0.798
150	170	2008	2339	86	1.032	0.637	0.811
175	170	2290	2378	85	1.047	0.646	0.822
200	170	2583	2414	85	1.060	0.654	0.833

Table 51 Halliburton GDK Constant Height  $\mu=200$  cp

Time (min)	Height (ft)	Half Length (ft)	Net Pressure (psi)	Efficiency (%)	Max. Width (in)	Avg. Width in Frac (in)	Avg. Width at Wellbore (in)
0	170	0	0	100	0	0	0
25	170	535	186	91	0.53	0.42	0.53
50	170	858	141	89	0.66	0.52	0.66
75	170	1132	120	88	0.74	0.58	0.74
100	170	1378	108	88	0.80	0.63	0.80
125	170	1605	98	87	0.85	0.67	0.85
150	170	1818	92	87	0.90	0.71	0.90
175	170	2020	86	86	0.94	0.74	0.94
200	170	2212	82	86	0.98	0.77	0.98

Table 52 Halliburton GDK Constant Height  $n'=0.5$ ,  $k'=0.06$ 

Time (min)	Height (ft)	Half Length (ft)	Net Pressure (psi)	Efficiency (%)	Max. Width (in)	Avg. Width in Frac (in)	Avg. Width at Wellbore (in)
0	170	0	0	100	0	0	0
25	170	560	168	91	0.51	0.40	0.51
50	170	861	140	89	0.65	0.51	0.65
75	170	1106	126	88	0.75	0.59	0.75
100	170	1322	117	88	0.84	0.66	0.84
125	170	1518	110	87	0.90	0.71	0.90
150	170	1699	105	87	0.97	0.76	0.97
175	170	1870	101	86	1.02	0.80	1.02
200	170	2031	97	86	1.07	0.84	1.07

**Table 53 Chevron GDK Constant Height  $\mu=200$  cp**

Time (min)	Height (ft)	Half Length (ft)	Net Pressure (psi)	Efficiency (%)	Max. Width (in)	Avg. Width in Frac (in)	Avg. Width at Wellbore (in)
0	170	0	0	100	0	0	0
25	170	386	116	85	0.333	0.262	0.333
50	170	581	102	84	0.438	0.343	0.438
75	170	774	94	83	0.530	0.416	0.530
100	170	906	90	83	0.589	0.462	0.589
125	170	1026	87	83	0.640	0.502	0.640
150	170	1137	84	82	0.585	0.538	0.585
175	170	1241	82	82	0.726	0.570	0.726
200	170	1347	80	82	0.767	0.602	0.767

**Table 54 Chevron PKN Constant Height  $\mu=200$  cp**

Time (min)	Height (ft)	Half Length (ft)	Net Pressure (psi)	Efficiency (%)	Max. Width (in)	Avg. Width in Frac (in)	Avg. Width at Wellbore (in)
0	170	0	0	100	0	0	-
25	170	454	837	82	0.384	0.216	-
50	170	744	988	80	0.453	0.254	-
75	170	1049	1108	77	0.508	0.285	-
100	170	1267	1179	76	0.541	0.304	-
125	170	1470	1239	75	0.569	0.319	-
150	170	1660	1291	74	0.592	0.332	-
175	170	1841	1336	73	0.613	0.344	-
200	170	2029	1380	73	0.633	0.355	-

Table 55 Conoco GDK Constant Height  $\mu=200$  cp

Time (min)	Height (ft)	Half Length (ft)	Net Pressure (psi)	Efficiency (%)	Max. Width (in)	Avg. Width in Frac (in)	Avg. Width at Wellbore (in)
0	170	0	-	100	0	0	0
25	170	704	-	87	0.391	0.307	0.391
50	170	1106	-	86	0.489	0.384	0.489
75	170	1439	-	85	0.558	0.438	0.558
100	170	1734	-	84	0.613	0.481	0.613
125	170	2004	-	84	0.659	0.517	0.659
150	170	2255	-	83	0.699	0.549	0.699
175	170	2492	-	83	0.735	0.577	0.735
200	170	2716	-	83	0.767	0.602	0.767

Table 56 Conoco GDK Constant Height  $n'=0.5, k'=0.06$ 

Time (min)	Height (ft)	Half Length (ft)	Net Pressure (psi)	Efficiency (%)	Max. Width (in)	Avg. Width in Frac (in)	Avg. Width at Wellbore (in)
0	170	0	-	100	0	0	0
25	170	674	-	88	0.411	0.323	0.411
50	170	1015	-	87	0.541	0.424	0.541
75	170	1290	-	86	0.634	0.498	0.634
100	170	1530	-	86	0.711	0.558	0.711
125	170	1745	-	86	0.776	0.609	0.776
150	170	1944	-	86	0.833	0.654	0.833
175	170	2129	-	85	0.886	0.695	0.886
200	170	2304	-	85	0.933	0.733	0.933

Table 57 Conoco PKN Constant Height  $\mu=200$  cp

Time (min)	Height (ft)	Half Length (ft)	Net Pressure (psi)	Efficiency (%)	Max. Width (in)	Avg. Width in Frac (in)	Avg. Width at Wellbore (in)
0	170	0	-	100	-	0	0
25	170	839	-	85	-	0.250	0.375
50	170	1418	-	82	-	0.286	0.428
75	170	1925	-	80	-	0.308	0.462
100	170	2386	-	78	-	0.325	0.488
125	170	2817	-	77	-	0.339	0.508
150	170	3225	-	76	-	0.351	0.526
175	170	3614	-	75	-	0.361	0.541
200	170	3986	-	74	-	0.370	0.554

Table 58 Conoco PKN Constant Height  $n'=0.5, k'=0.06$ 

Time (min)	Height (ft)	Half Length (ft)	Net Pressure (psi)	Efficiency (%)	Max. Width (in)	Avg. Width in Frac (in)	Avg. Width at Wellbore (in)
0	170	0	-	100	-	0	0
25	170	831	-	85	-	0.253	0.380
50	170	1367	-	82	-	0.299	0.448
75	170	1826	-	81	-	0.329	0.493
100	170	2240	-	80	-	0.352	0.528
125	170	2624	-	79	-	0.371	0.557
150	170	2985	-	78	-	0.388	0.581
175	170	3328	-	77	-	0.402	0.603
200	170	3656	-	77	-	0.415	0.622

Table 59 Marathon GHOFER Constant Height  $\mu=200$  cp

Time (min)	Height (ft)	Half Length (ft)	Net Pressure (psi)	Efficiency (%)	Max. Width (in)	Avg. Width in Frac (in)	Avg. Width at Wellbore (in)
0	204	0	0	100	0	0	0.75
25	204	374	1819	97	0.91	0.68	0.75
50	204	714	1742	96	0.91	0.71	0.75
75	204	1054	1668	95	0.88	0.69	0.75
100	204	1360	1694	95	0.90	0.72	0.75
125	204	1666	1683	94	0.90	0.72	0.75
150	204	1972	1684	94	0.91	0.72	0.75
175	204	2312	1678	94	0.90	0.72	0.76
200	204	2584	1685	93	0.91	0.73	0.76

Table 60 Marathon GHOFER Constant Height  $n'=0.5, k'=0.06$ 

Time (min)	Height (ft)	Half Length (ft)	Net Pressure (psi)	Efficiency (%)	Max. Width (in)	Avg. Width in Frac (in)	Avg. Width at Wellbore (in)
0	204	0	0	100	0	0	0
25	204	374	1832	97	0.91	0.68	0.76
50	204	714	1767	96	0.92	0.71	0.76
75	204	1020	1764	95	0.93	0.72	0.77
100	204	1360	1754	95	0.93	0.72	0.77
125	204	1632	1776	94	0.95	0.74	0.78
150	204	1938	1786	94	0.96	0.73	0.79
175	204	2244	1805	94	0.97	0.74	0.80
200	204	2516	1825	93	0.98	0.75	0.82

Table 61 Marathon GHOFER 3-Layer  $\mu=200$  cp

Time (min)	Height (ft)	Upper Height (ft)	Lower Height (ft)	Half Length (ft)	Net Pressure (psi)	Efficiency (%)	Max. Width (in)	Avg. Width in Frac (in)	Avg. Width at Wellbore (in)
0	-	-	-	0	0	100	0	0	0
25	374	204	170	306	1423	98	0.84	0.51	0.55
50	374	238	170	476	1435	97	0.95	0.59	0.66
75	408	238	170	612	1426	97	1.00	0.61	0.67
100	408	238	170	782	1413	97	1.01	0.63	0.68
125	442	238	204	918	1391	97	1.02	0.62	0.67
150	442	238	204	1054	1394	97	1.03	0.63	0.68
175	442	238	204	1190	1396	97	1.04	0.65	0.69
200	442	238	204	1360	1389	96	1.04	0.64	0.68

Table 62 Marathon GHOFER 3-Layer  $n'=0.5, k'=0.06$ 

Time (min)	Height (ft)	Upper Height (ft)	Lower Height (ft)	Half Length (ft)	Net Pressure (psi)	Efficiency (%)	Max. Width (in)	Avg. Width in Frac (in)	Avg. Width at Wellbore (in)
0	-	-	-	0	0	100	0	0	0
25	374	204	170	306	1434	98	0.84	0.51	0.55
50	374	204	170	476	1450	98	0.98	0.59	0.66
75	408	204	170	612	1441	97	1.04	0.61	0.68
100	442	204	204	782	1414	97	1.02	0.61	0.67
125	442	238	204	884	1434	97	1.06	0.64	0.70
150	442	238	204	1020	1434	97	1.07	0.65	0.71
175	442	238	204	1190	1431	97	1.07	0.65	0.72
200	442	238	204	1326	1433	96	1.08	0.66	0.71

Table 63 Marathon GHOFER 6-Layer  $\mu=200$  cp

Time (min)	Height (ft)	Upper Height (ft)	Lower Height (ft)	Half Length (ft)	Net Pressure (psi)	Efficiency (%)	Max. Width (in)	Avg. Width in Frac (in)	Avg. Width at Wellbore (in)
0	-	-	-	0	0	100	0	0	0
25	340	204	170	306	1447	98	0.84	0.53	0.58
50	442	204	238	408	1323	98	0.96	0.59	0.64
75	442	204	238	544	1303	97	1.00	0.63	0.71
100	442	204	238	714	1266	97	0.99	0.63	0.70
125	476	238	238	850	1251	97	1.00	0.63	0.67
150	476	238	238	952	1257	97	1.02	0.64	0.69
175	476	238	238	1088	1254	97	1.03	0.65	0.70
200	476	238	238	1224	1250	97	1.03	0.65	0.70

Table 64 Marathon GHOFER 6-Layer  $n^*=0.5$ ,  $k^*=0.06$ 

Time (min)	Height (ft)	Upper Height (ft)	Lower Height (ft)	Half Length (ft)	Net Pressure (psi)	Efficiency (%)	Max. Width (in)	Avg. Width in Frac (in)	Avg. Width at Wellbore (in)
0	-	-	-	0	0	100	0	0	0
25	308	170	136	306	1455	96	0.84	0.54	0.62
50	442	204	238	408	1316	95	0.95	0.59	0.66
75	442	204	238	544	1289	95	0.98	0.61	0.68
100	442	204	238	680	1285	94	1.01	0.64	0.71
125	442	204	238	816	1268	94	1.01	0.65	0.74
150	476	238	238	918	1265	94	1.03	0.64	0.70
175	476	238	238	1054	1257	93	1.03	0.65	0.70
200	476	238	238	1156	1263	93	1.04	0.66	0.71

Table 65 ARCO Stimplan 3-Layer  $\mu=200$  cp

Time (min)	Height (ft)	Upper Height (ft)	Lower Height (ft)	Half Length (ft)	Net Pressure (psi)	Efficiency (%)	Max. Width (in)	Avg. Width in Frac (in)	Avg. Width at Wellbore (in)
0	170	85	85	0	0	100	0	0	0
25	249	154	96	920	824	80	-	0.19	-
50	259	159	100	1422	868	76	-	0.21	-
75	269	164	105	1850	902	74	-	0.23	-
100	280	171	110	2248	927	73	-	0.23	-
125	288	175	113	2616	955	71	-	0.24	-
150	295	180	116	2960	963	70	-	0.24	-
175	300	182	118	3286	976	68	-	0.25	-
200	306	186	121	3598	992	67	0.57	0.25	0.31

Table 66 ARCO Stimplan 3-Layer  $n'=0.5, k'=0.06$ 

Time (min)	Height (ft)	Upper Height (ft)	Lower Height (ft)	Half Length (ft)	Net Pressure (psi)	Efficiency (%)	Max. Width (in)	Avg. Width in Frac (in)	Avg. Width at Wellbore (in)
0	170	85	85	0	0	100	0	0	0
25	252	155	97	900	845	81	-	0.19	-
50	271	166	105	1356	911	77	-	0.22	-
75	289	176	113	1748	956	75	-	0.23	-
100	305	185	120	2094	990	73	-	0.24	-
125	315	191	124	2409	1016	71	-	0.25	-
150	328	198	130	2703	1043	71	-	0.25	-
175	340	205	135	2976	1061	69	-	0.26	-
200	353	213	141	3235	1083	69	0.65	0.26	0.33

Table 67 ARCO Stimplan 5-Layer  $\mu=200$  cp

Time (min)	Height (ft)	Upper Height (ft)	Lower Height (ft)	Half Length (ft)	Net Pressure (psi)	Efficiency (%)	Max. Width (in)	Avg. Width in Frac (in)	Avg. Width at Wellbore (in)
0	170	85	85	0	0	100	0	0	0
25	251	157	95	926	816	80	-	0.19	-
50	268	168	100	1425	860	77	-	0.21	-
75	354	175	180	1863	881	74	-	0.22	-
100	369	176	194	2225	885	72	-	0.22	-
125	369	176	194	2540	891	70	-	0.24	-
150	380	176	205	2846	900	69	-	0.24	-
175	380	176	205	3118	908	68	-	0.25	-
200	394	180	215	3399	944	68	0.64	0.24	0.36

Table 68 ARCO Stimplan 5-Layer  $n'=0.5, k'=0.06$ 

Time (min)	Height (ft)	Upper Height (ft)	Lower Height (ft)	Half Length (ft)	Net Pressure (psi)	Efficiency (%)	Max. Width (in)	Avg. Width in Frac (in)	Avg. Width at Wellbore (in)
0	170	85	85	0	0	100	0	0	0
25	250	156	94	889	822	80	-	0.19	-
50	328	174	154	1358	890	77	-	0.20	-
75	379	175	204	1718	920	75	-	0.22	-
100	390	178	212	2009	930	74	-	0.24	-
125	396	182	215	2269	932	73	-	0.25	-
150	402	187	216	2497	931	71	-	0.26	-
175	403	188	216	2717	967	71	-	0.26	-
200	405	190	216	2926	968	70	0.70	0.27	0.40

Table 69 ARCO TerraFrac 5-Layer  $n'=0.5$ ,  $k'=0.06$ 

Time (min)	Height (ft)	Upper Height (ft)	Lower Height (ft)	Half Length (ft)	Net Pressure (psi)	Efficiency (%)	Max. Width (in)	Avg. Width in Frac (in)	Avg. Width at Wellbore (in)
0	170	85	85	0	0	100	0	0	0
25	226	142	84	921	864	81	0.37	-	-
50	246	150	96	1371	981	71	0.45	-	-
75	358	170	188	1802	997	73	0.47	-	-
100	370	182	188	2133	1030	67	0.52	-	-
125	399	211	188	2378	1080	67	0.63	-	-
150	408	220	188	2651	1120	65	0.67	-	-
175	423	234	188	2923	1150	64	.07	-	-
200	449	239	210	3124	1160	62	0.74	-	-

Table 70 NSI Tech. Stimplan 3-Layer  $\mu=200$  cp

Time (min)	Height (ft)	Upper Height (ft)	Lower Height (ft)	Half Length (ft)	Net Pressure (psi)	Efficiency (%)	Max. Width (in)	Avg. Width in Frac (in)	Avg. Width at Wellbore (in)
0	170	85	85	0	0	100	0	0	0
25	237	119	118	906	684	81	0.38	0.19	0.23
50	246	122	124	1447	746	75	0.43	0.20	0.26
75	252	124	127	1914	787	73	0.46	0.21	0.28
100	256	126	130	2336	818	71	0.49	0.22	0.29
125	259	127	132	2726	840	69	0.50	0.22	0.30
150	267	131	136	3089	865	68	0.52	0.23	0.31
175	275	135	141	3428	884	67	0.54	0.24	0.31
200	283	138	144	3750	903	66	0.56	0.25	0.32

Table 71 NSI Tech. Stimplan 3-Layer  $n'=0.5$ ,  $k'=0.06$ 

Time (min)	Height (ft)	Upper Height (ft)	Lower Height (ft)	Half Length (ft)	Net Pressure (psi)	Efficiency (%)	Max. Width (in)	Avg. Width in Frac (in)	Avg. Width at Wellbore (in)
0	170	85	85	0	0	100	0	0	0
25	240	120	120	851	696	80	0.40	0.17	0.25
50	253	125	128	1340	798	76	0.47	0.20	0.28
75	265	130	135	1758	862	74	0.52	0.22	0.31
100	284	139	145	2123	910	72	0.56	0.23	0.32
125	298	146	142	2450	945	71	0.60	0.24	0.33
150	308	151	158	2749	970	70	0.63	0.25	0.34
175	322	157	165	3032	1003	69	0.65	0.26	0.34
200	329	160	168	3289	1005	68	0.67	0.26	0.35

Table 72 NSI Tech. Stimplan 5-Layer  $\mu=200$  cp

Time (min)	Height (ft)	Upper Height (ft)	Lower Height (ft)	Half Length (ft)	Net Pressure (psi)	Efficiency (%)	Max. Width (in)	Avg. Width in Frac (in)	Avg. Width at Wellbore (in)
0	170	85	85	0	0	100	0	0	0
25	172	124	105	911	682	78	0.38	0.17	0.24
50	238	125	112	1469	757	76	0.43	0.21	0.27
75	242	126	117	1945	799	74	0.46	0.22	0.29
100	246	126	120	2373	828	72	0.49	0.23	0.31
125	342	149	193	2739	828	70	0.56	0.23	0.33
150	359	153	203	3079	848	68	0.60	0.23	0.35
175	364	157	206	3424	871	67	0.63	0.24	0.38
200	361	155	206	3709	852	66	0.63	0.25	0.38

Table 73 NSI Tech. Stimplan 5-Layer  $n'=0.5$ ,  $k'=0.06$ 

Time (min)	Height (ft)	Upper Height (ft)	Lower Height (ft)	Half Length (ft)	Net Pressure (psi)	Efficiency (%)	Max. Width (in)	Avg. Width in Frac (in)	Avg. Width at Wellbore (in)
0	170	85	85	0	0	100	0	0	0
25	233	125	108	866	708	80	0.40	0.18	0.25
50	244	126	118	1362	810	77	0.47	0.21	0.30
75	354	152	203	1757	848	74	0.61	0.22	0.37
100	365	157	209	2069	878	73	0.65	0.23	0.39
125	375	162	213	2333	904	72	0.66	0.24	0.39
150	381	165	215	2555	850	71	0.66	0.24	0.38
175	384	167	218	2749	924	70	0.70	0.25	0.41
200	388	169	220	2765	935	70	0.71	0.25	0.42

Table 74 RES Fracpro 3-Layer  $\mu=200$  cp

Time (min)	Height (ft)	Upper Height (ft)	Lower Height (ft)	Half Length (ft)	Net Pressure (psi)	Efficiency (%)	Max. Width (in)	Avg. Width in Frac (in)	Avg. Width at Wellbore (in)
0	170	85	85	0	0	100	0	0	0
25	347	218	129	446	1130	92	0.62	0.32	0.48
50	400	262	138	711	1162	89	0.69	0.34	0.51
75	439	294	145	932	1185	87	0.73	0.34	0.51
100	469	319	150	1124	1202	85	0.76	0.35	0.53
125	495	340	155	1300	1215	84	0.78	0.35	0.53
150	516	359	157	1461	1222	82	0.87	0.35	0.53
175	531	373	158	1608	1223	81	0.88	0.36	0.54
200	544	385	159	1744	1227	80	0.90	0.36	0.54

Table 75 RES Fracpro 3-Layer  $n'=0.5, k'=0.06$ 

Time (min)	Height (ft)	Upper Height (ft)	Lower Height (ft)	Half Length (ft)	Net Pressure (psi)	Efficiency (%)	Max. Width (in)	Avg. Width in Frac (in)	Avg. Width at Wellbore (in)
0	170	85	85	0	0	100	0	0	0
25	337	189	148	325	1334	80	0.72	0.39	0.59
50	404	231	173	466	1363	75	0.84	0.43	0.43
75	452	261	191	571	1381	71	0.91	0.44	0.44
100	489	285	204	656	1395	69	0.96	0.46	0.46
125	521	305	216	729	1405	67	1.01	0.47	0.47
150	549	323	226	793	1413	65	1.04	0.48	0.48
175	574	340	234	850	1421	63	1.08	0.48	0.48
200	596	354	242	902	1428	62	1.10	0.49	0.49

Table 76 RES Fracpro 5-Layer  $\mu=200$  cp

Time (min)	Height (ft)	Upper Height (ft)	Lower Height (ft)	Half Length (ft)	Net Pressure (psi)	Efficiency (%)	Max. Width (in)	Avg. Width in Frac (in)	Avg. Width at Wellbore (in)
0	170	85	85	0	0	100	0	0	0
25	396	200	196	408	979	91	0.57	0.30	0.45
50	420	222	198	665	1013	89	0.67	0.34	0.51
75	439	239	200	887	1042	87	0.71	0.36	0.54
100	456	253	203	1086	1064	86	0.75	0.37	0.56
125	469	265	204	1269	1081	85	0.77	0.38	0.57
150	480	275	205	1439	1096	84	0.80	0.39	0.59
175	491	285	206	1600	1109	83	0.81	0.40	0.60
200	501	294	207	1754	1119	82	0.83	0.40	0.60

Table 77 RES Fracpro 5-Layer  $n'=0.5, k'=0.06$ 

Time (min)	Height (ft)	Upper Height (ft)	Lower Height (ft)	Half Length (ft)	Net Pressure (psi)	Efficiency (%)	Max. Width (in)	Avg. Width in Frac (in)	Avg. Width at Wellbore (in)
0	170	85	85	0	0	100	0	0	0
25	406	202	204	293	1263	93	0.74	0.42	0.63
50	475	252	223	424	1317	92	0.91	0.49	0.74
75	516	286	230	535	1343	90	1.01	0.52	0.78
100	545	312	233	632	1360	90	1.09	0.56	0.84
125	569	333	236	719	1375	89	1.14	0.58	0.87
150	583	347	236	846	1355	88	1.14	0.57	0.86
175	592	357	235	952	1352	87	1.16	0.58	0.87
200	600	366	234	1042	1358	87	1.18	0.60	0.90

Table 78 Texaco Fracpro GDK Constant Height  $\mu=200$  cp

Time (min)	Height (ft)	Half Length (ft)	Net Pressure (psi)	Efficiency (%)	Max. Width (in)	Avg. Width in Frac (in)	Avg. Width at Wellbore (in)
0	170	0	0	100	0	0	0
25	170	636	144	91	0.39	0.39	-
50	170	1002	113	89	0.48	0.48	-
75	170	1307	99	88	0.55	0.55	-
100	170	1577	89	88	0.60	0.60	-
125	170	1824	83	87	0.64	0.64	-
150	170	2055	78	87	0.68	0.68	-
175	170	2273	74	86	0.71	0.71	-
200	170	2480	71	86	0.74	0.74	-

Table 79 Texaco Fracpro PKN Constant Height  $\mu=200$  cp

Time (min)	Height (ft)	Half Length (ft)	Net Pressure (psi)	Efficiency (%)	Max. Width (in)	Avg. Width in Frac (in)	Avg. Width at Wellbore (in)
0	170	0	0	100	0	0	0
25	170	849	653	88	0.33	-	-
50	170	1449	732	85	0.39	-	-
75	170	1976	783	83	0.42	-	-
100	170	2460	823	81	0.44	-	-
125	170	2915	854	80	0.46	-	-
150	170	3346	881	79	0.48	-	-
175	170	3759	904	78	0.49	-	-
200	170	4157	925	77	0.50	-	-

Table 80 Texaco Fracpro 3-Layer  $\mu=200$  cp

Time (min)	Height (ft)	Upper Height (ft)	Lower Height (ft)	Half Length (ft)	Net Pressure (psi)	Efficiency (%)	Max. Width (in)	Avg. Width in Frac (in)	Avg. Width at Wellbore (in)
0	170	85	85	0	0	100	0	0	0
25	315	203	112	521	1024	85	0.55	-	-
50	355	236	119	836	1065	80	0.61	-	-
75	377	254	123	1085	1083	76	0.64	-	-
100	392	267	125	1299	1098	74	0.66	-	-
125	404	277	127	1490	1109	72	0.68	-	-
150	315	286	129	1666	1119	71	0.70	-	-
175	426	295	131	1830	1125	69	0.71	-	-
200	435	302	133	1983	1132	68	0.72	-	-

Table 81 Texaco Fracpro 5-Layer  $\mu=200$  cp

Time (min)	Height (ft)	Upper Height (ft)	Lower Height (ft)	Half Length (ft)	Net Pressure (psi)	Efficiency (%)	Max. Width (in)	Avg. Width in Frac (in)	Avg. Width at Wellbore (in)
0	170	85	85	0	0	100	0	0	0
25	367	176	191	463	872	84	0.50	-	-
50	383	190	193	751	915	80	0.57	-	-
75	396	201	195	1000	944	77	0.61	-	-
100	404	208	196	1233	962	75	0.63	-	-
125	411	214	197	1449	976	73	0.64	-	-
150	418	220	198	1649	988	72	0.66	-	-
175	422	224	198	1835	999	70	0.67	-	-
200	428	229	199	2011	1008	69	0.68	-	-

Table 82 Texaco Fracpro 5-Layer  $n=0.5, k=0.06$ 

Time (min)	Height (ft)	Upper Height (ft)	Lower Height (ft)	Half Length (ft)	Net Pressure (psi)	Efficiency (%)	Max. Width (in)	Avg. Width in Frac (in)	Avg. Width at Wellbore (in)
0	170	85	85	0	0	100	0	0	0
25	414	207	207	283	1251	88	0.72	-	-
50	473	255	218	442	1234	85	0.84	-	-
75	505	285	220	580	1235	82	0.91	-	-
100	530	310	220	704	1240	81	0.96	-	-
125	552	330	222	818	1250	79	1.01	-	-
150	571	348	223	926	1257	78	1.05	-	-
175	588	364	224	1028	1263	77	1.08	-	-
200	602	378	224	1125	1270	76	1.11	-	-

Table 83 Texaco Fracpro 5-Layer  $n=0.5, k=0.06$  No tip effects

Time (min)	Height (ft)	Upper Height (ft)	Lower Height (ft)	Half Length (ft)	Net Pressure (psi)	Efficiency (%)	Max. Width (in)	Avg. Width in Frac (in)	Avg. Width at Wellbore (in)
0	170	85	85	0	0	100	0	0	0
25	256	164	92	859	857	80	0.35	-	-
50	286	186	100	1308	930	74	0.40	-	-
75	348	161	187	1603	796	70	0.38	-	-
100	360	171	189	1802	845	67	0.42	-	-
125	370	179	191	2020	876	65	0.44	-	-
150	378	186	192	2234	900	64	0.46	-	-
175	385	192	193	2440	919	63	0.48	-	-
200	391	197	194	2636	934	62	0.49	-	-

# FRACTURE HALF LENGTH CONSTANT HEIGHT MODELS

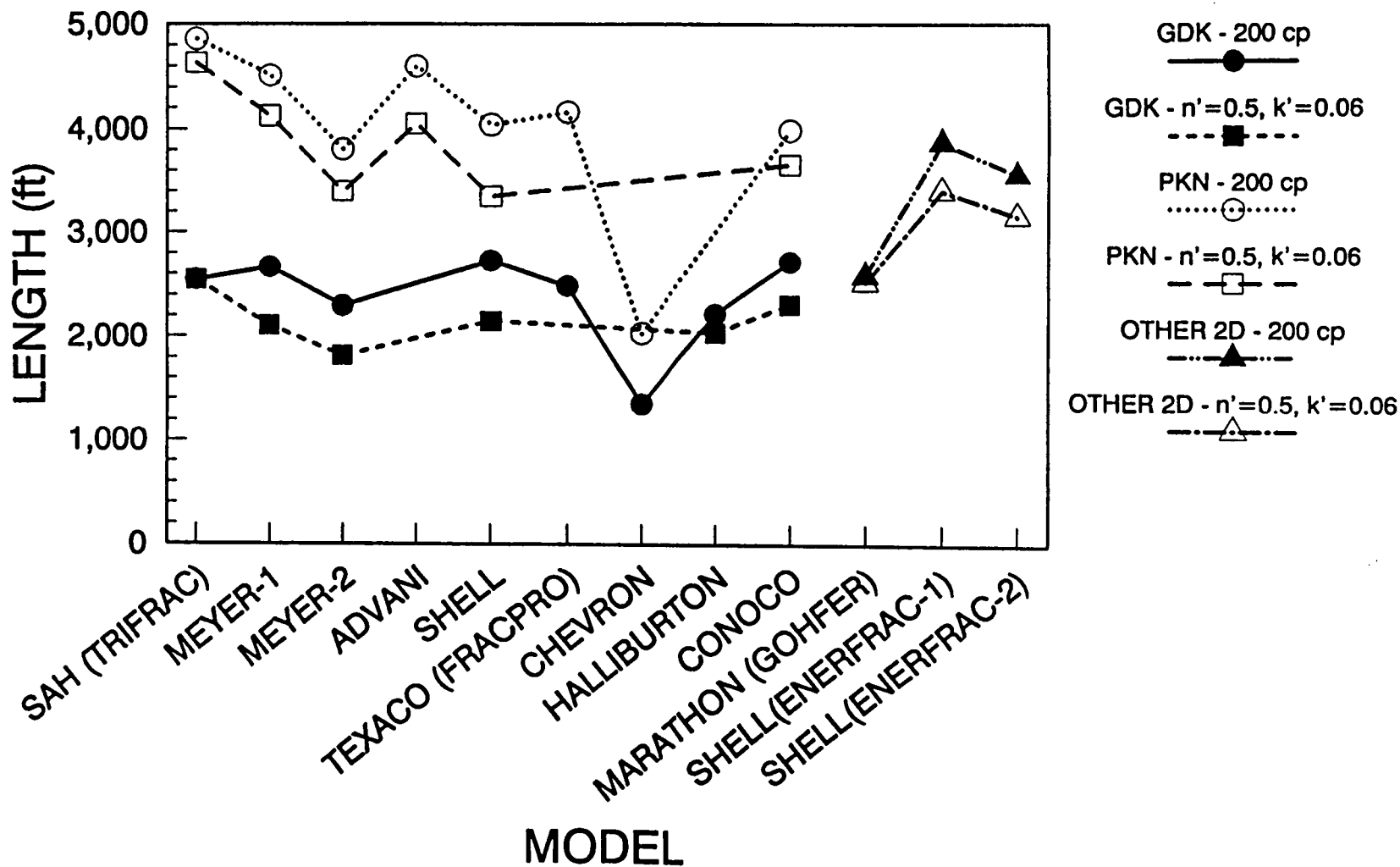


Figure 1 Length comparison for cases 1-4

# FRACTURE NET PRESSURE CONSTANT HEIGHT MODELS

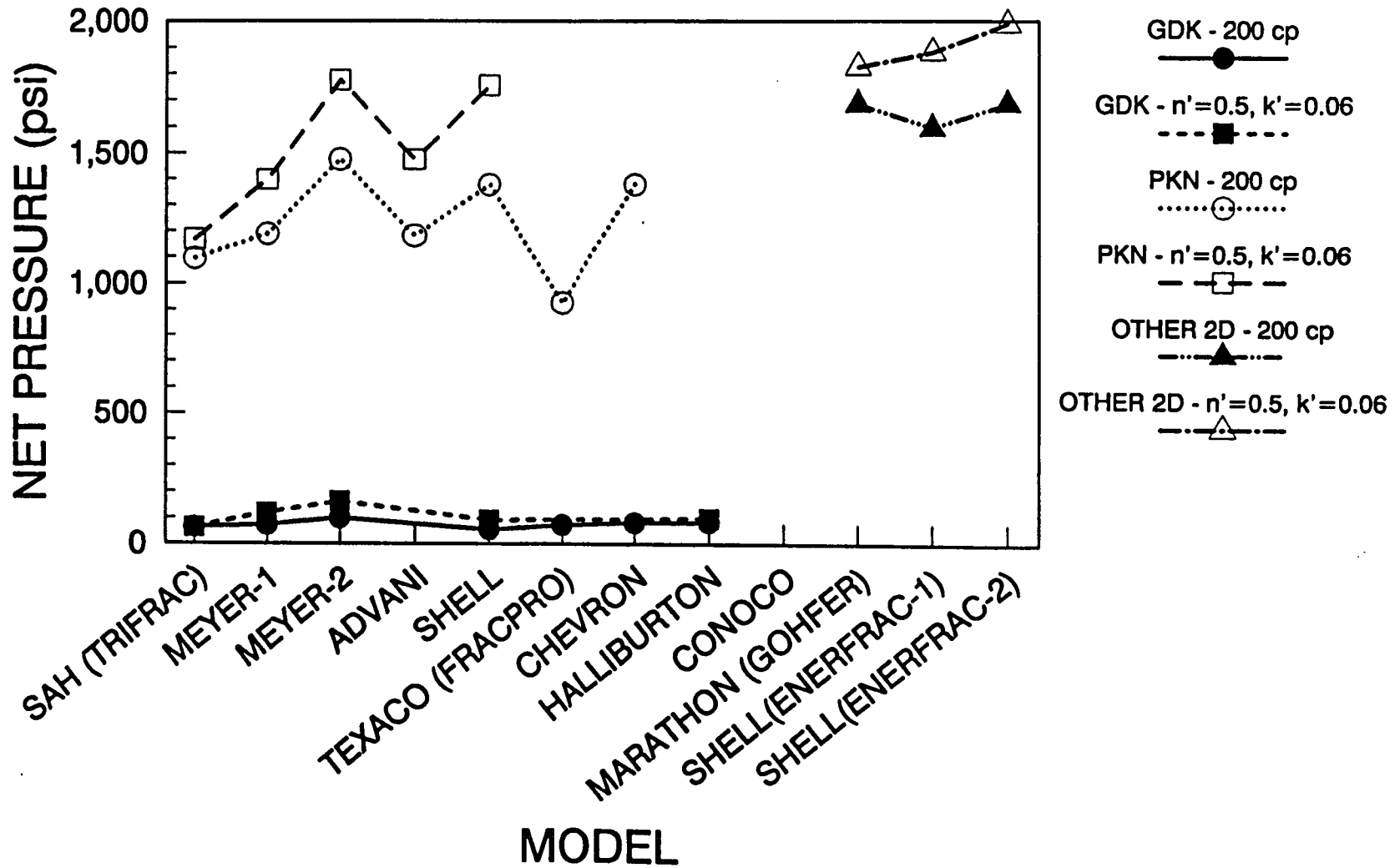


Figure 2 Net pressure comparison for cases 1-4

# FRACTURE EFFICIENCY CONSTANT HEIGHT MODELS

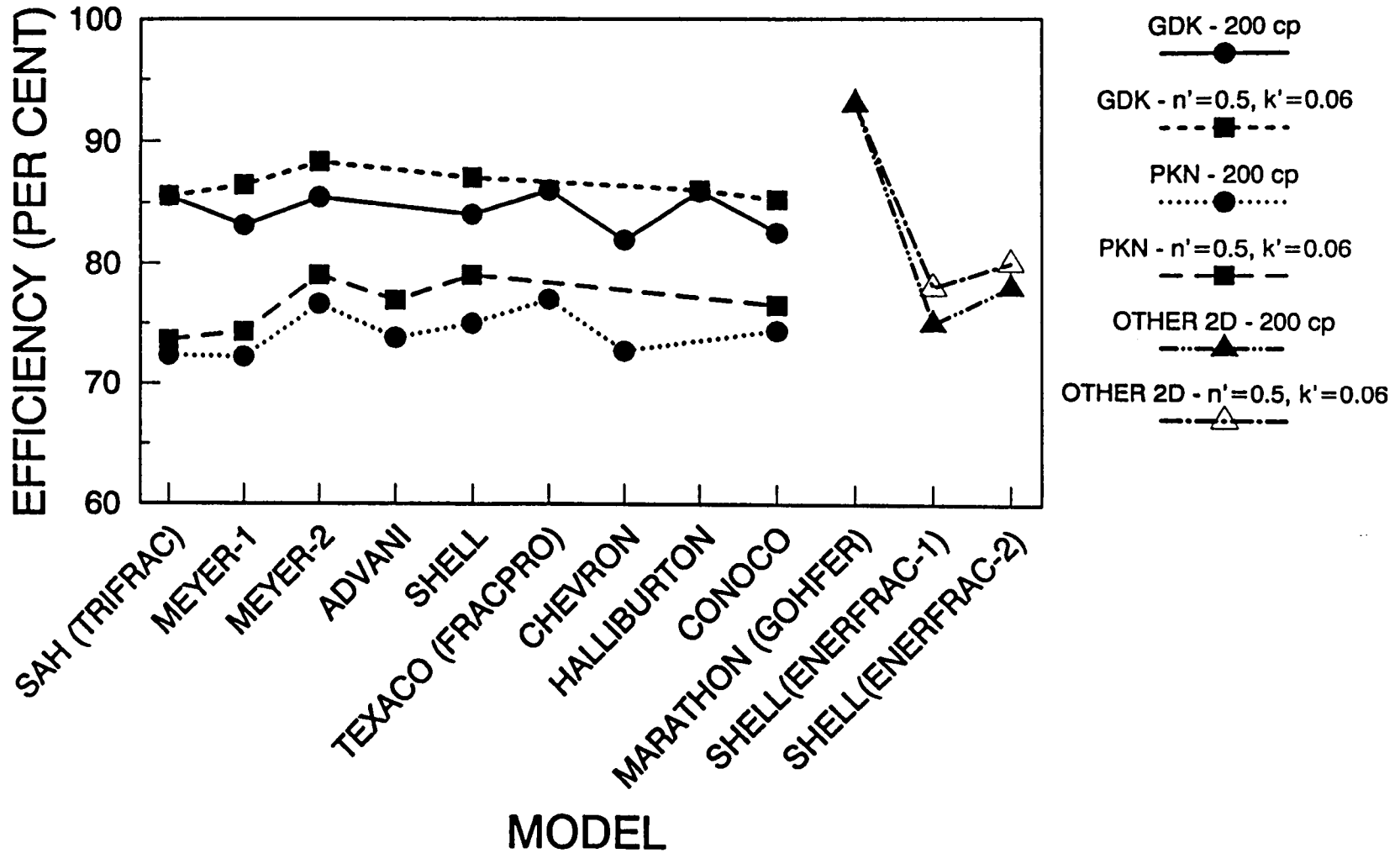


Figure 3 Efficiency comparison for cases 1-4

# FRACTURE MAXIMUM WIDTH

## CONSTANT HEIGHT MODELS

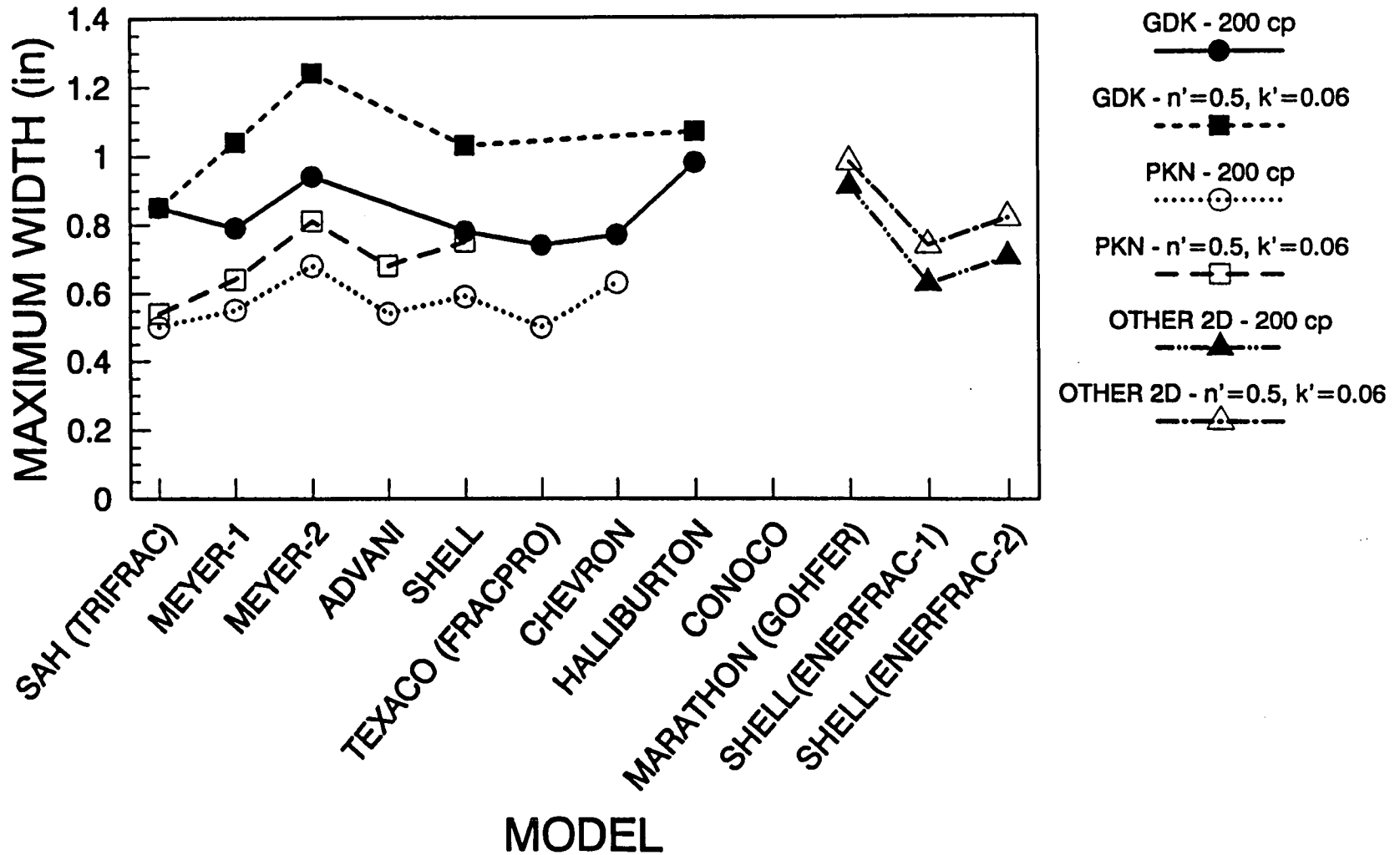


Figure 4 Comparison of maximum width at wellbore for cases 1-4

# FRACTURE AVERAGE WIDTH AT WELLBORE

## CONSTANT HEIGHT MODELS

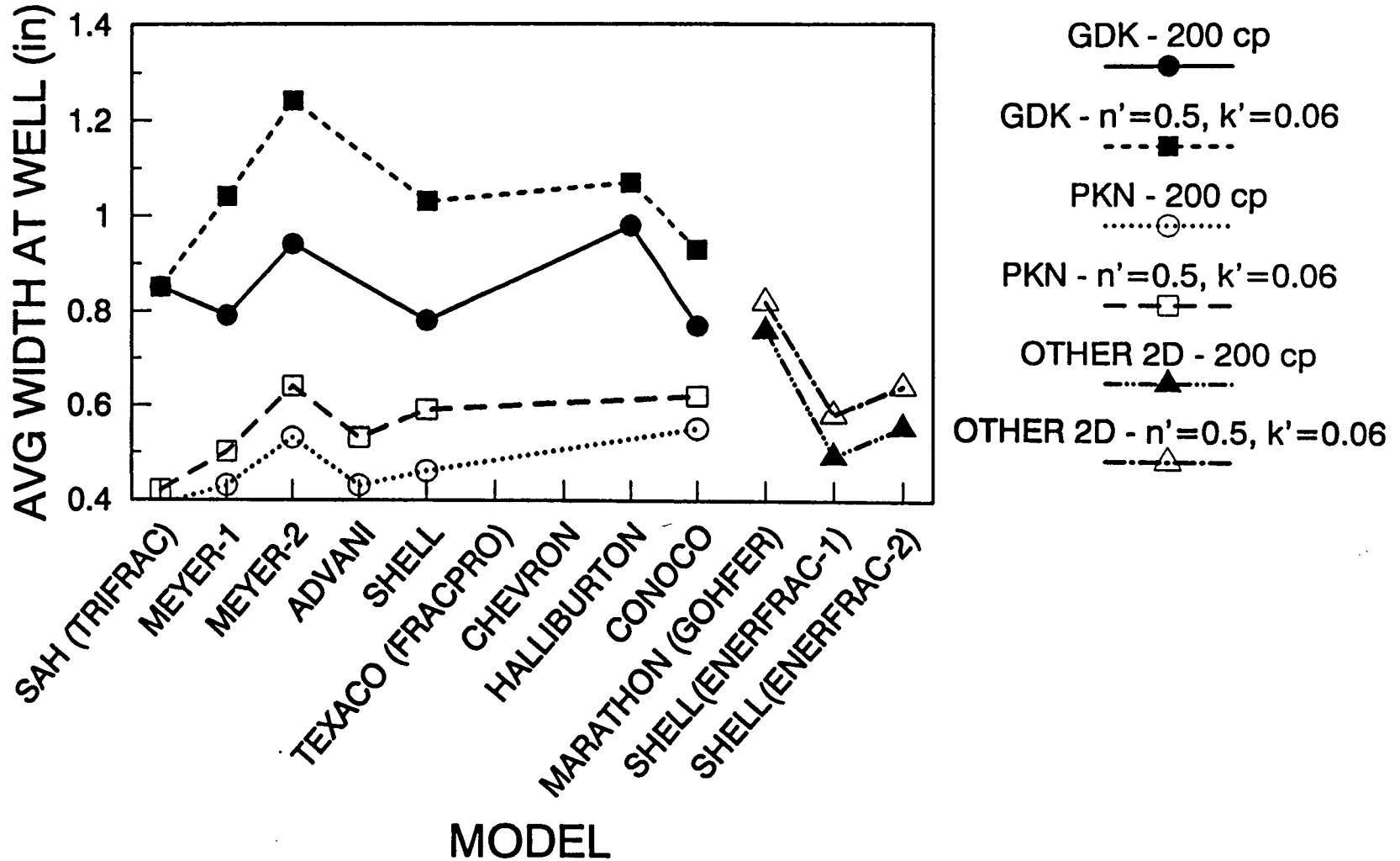


Figure 5 Comparison of average width at wellbore for cases 1-4

# FRACTURE AVERAGE WIDTH

## CONSTANT HEIGHT MODELS

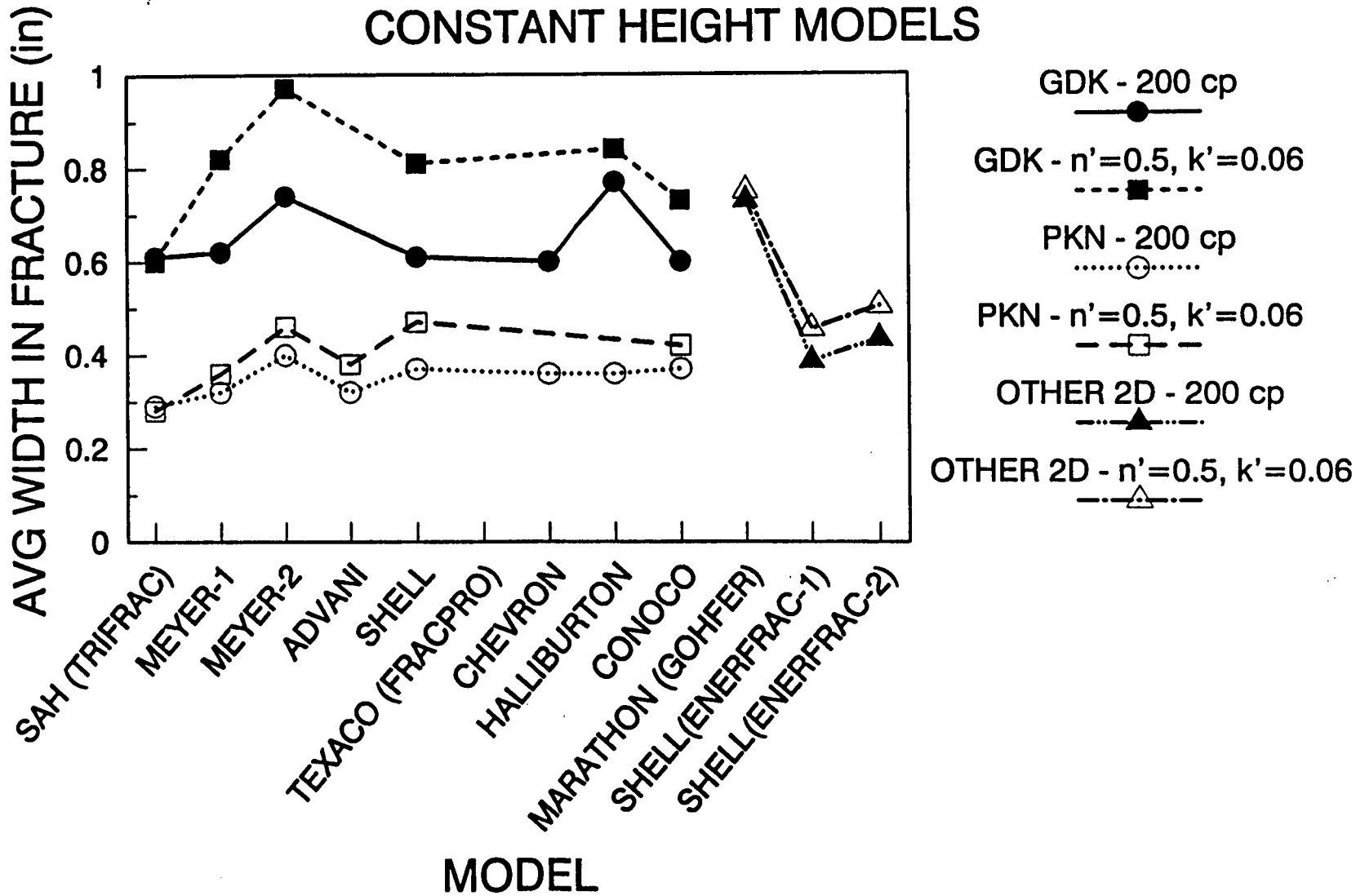


Figure 6 Comparison of average width in fracture for cases 1-4

# GDK-CONSTANT HEIGHT: 200 cp

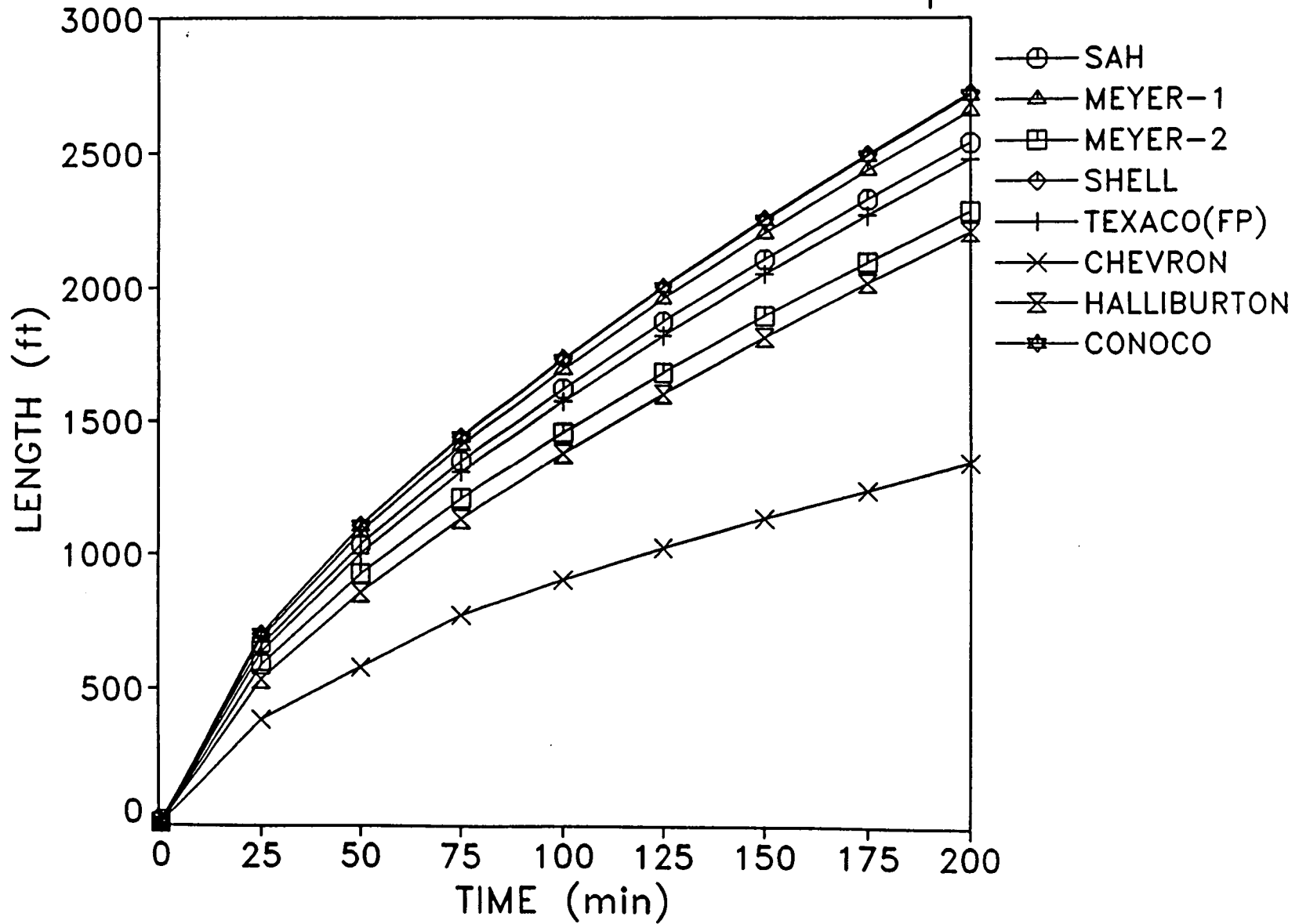


Figure 7 Length history for case 1

GDK-CONSTANT HEIGHT: 200 cp

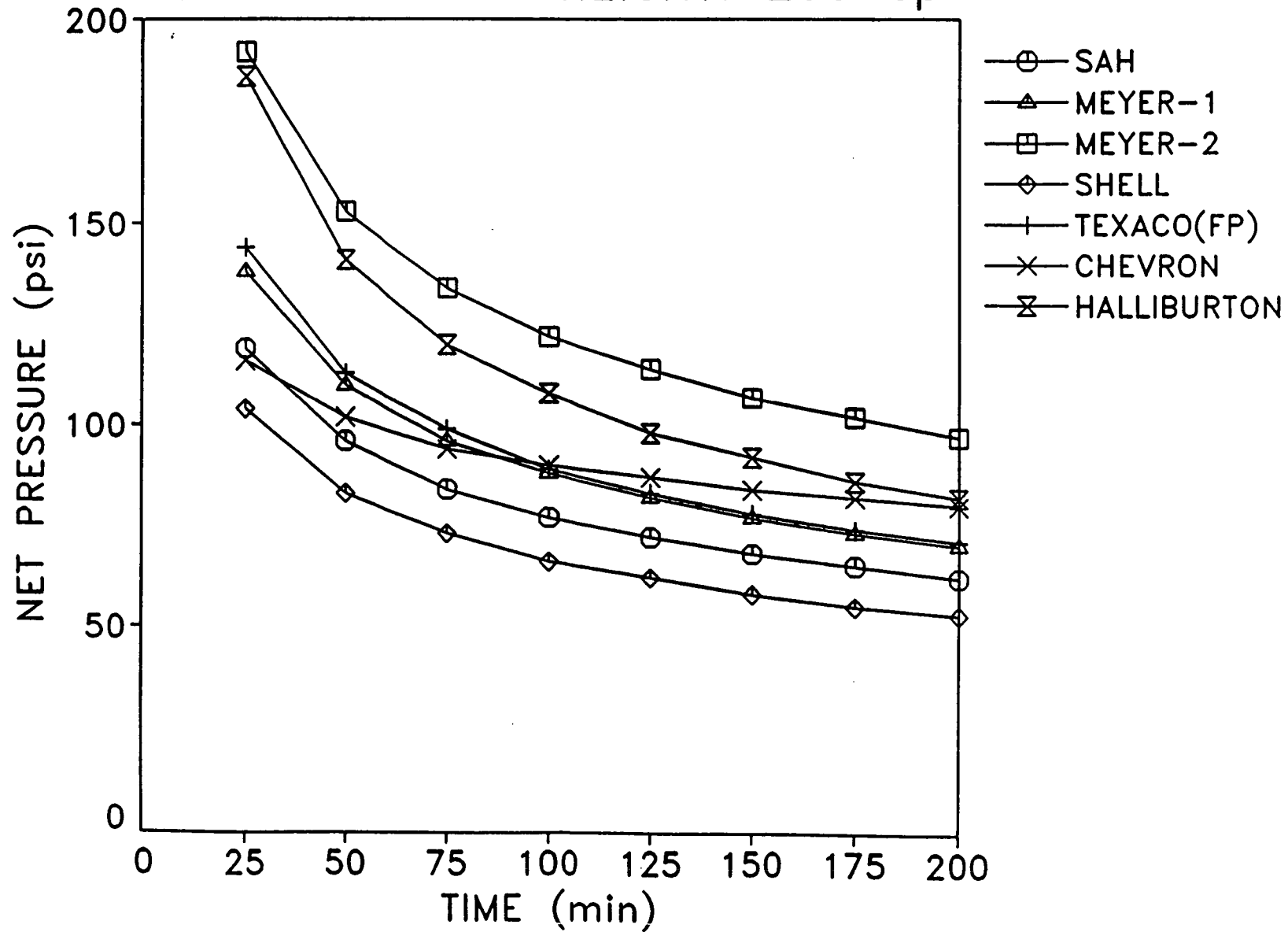


Figure 8 Net pressure history for case 1

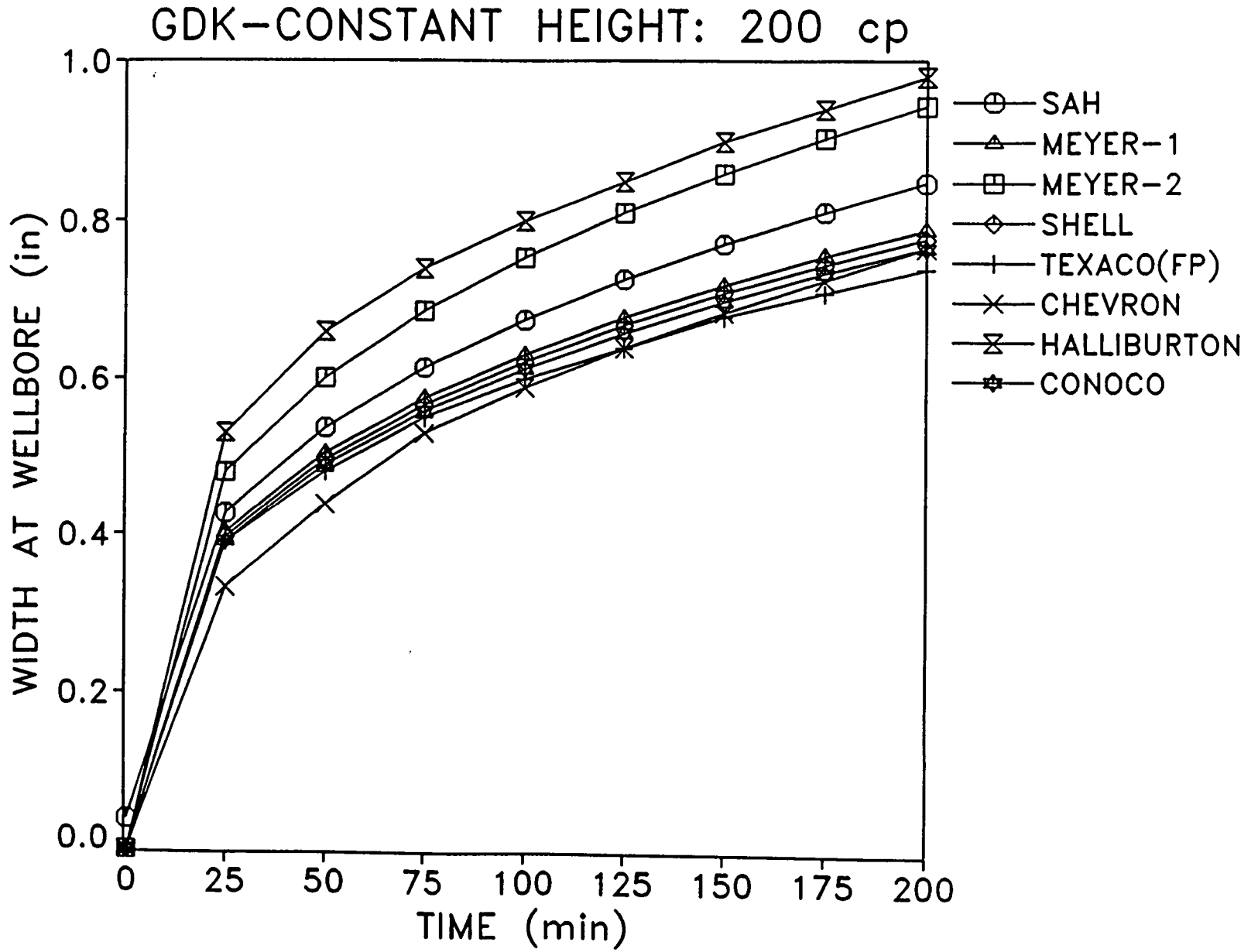


Figure 9 History of width at wellbore for case 1

# GDK-CONSTANT HEIGHT: $n'$ , $k'$

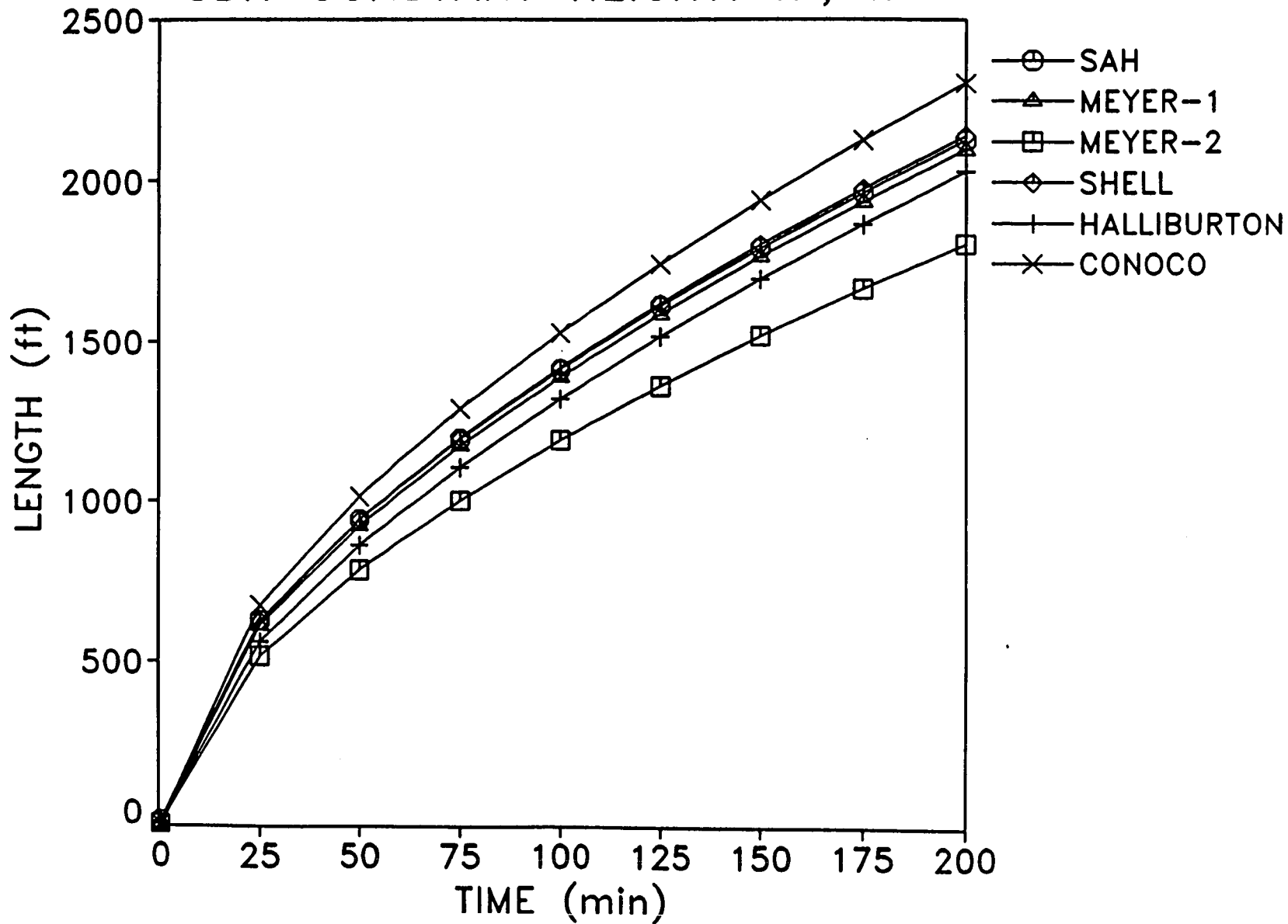


Figure 10 Length history for case 2

# GDK-CONSTANT HEIGHT: $n'$ , $k'$

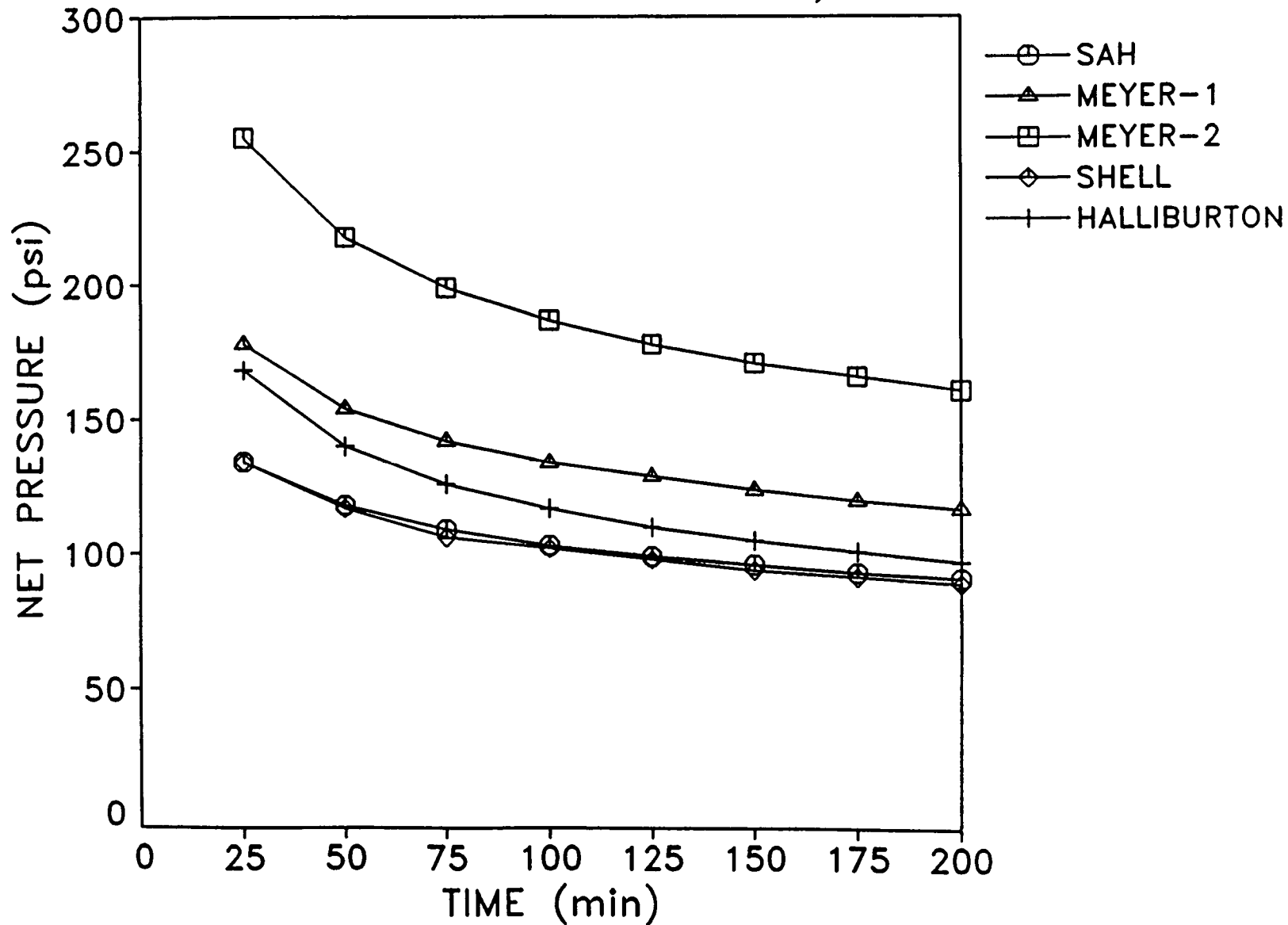


Figure 11 Net pressure history for case 2

GDK-CONSTANT HEIGHT:  $n'$ ,  $k'$

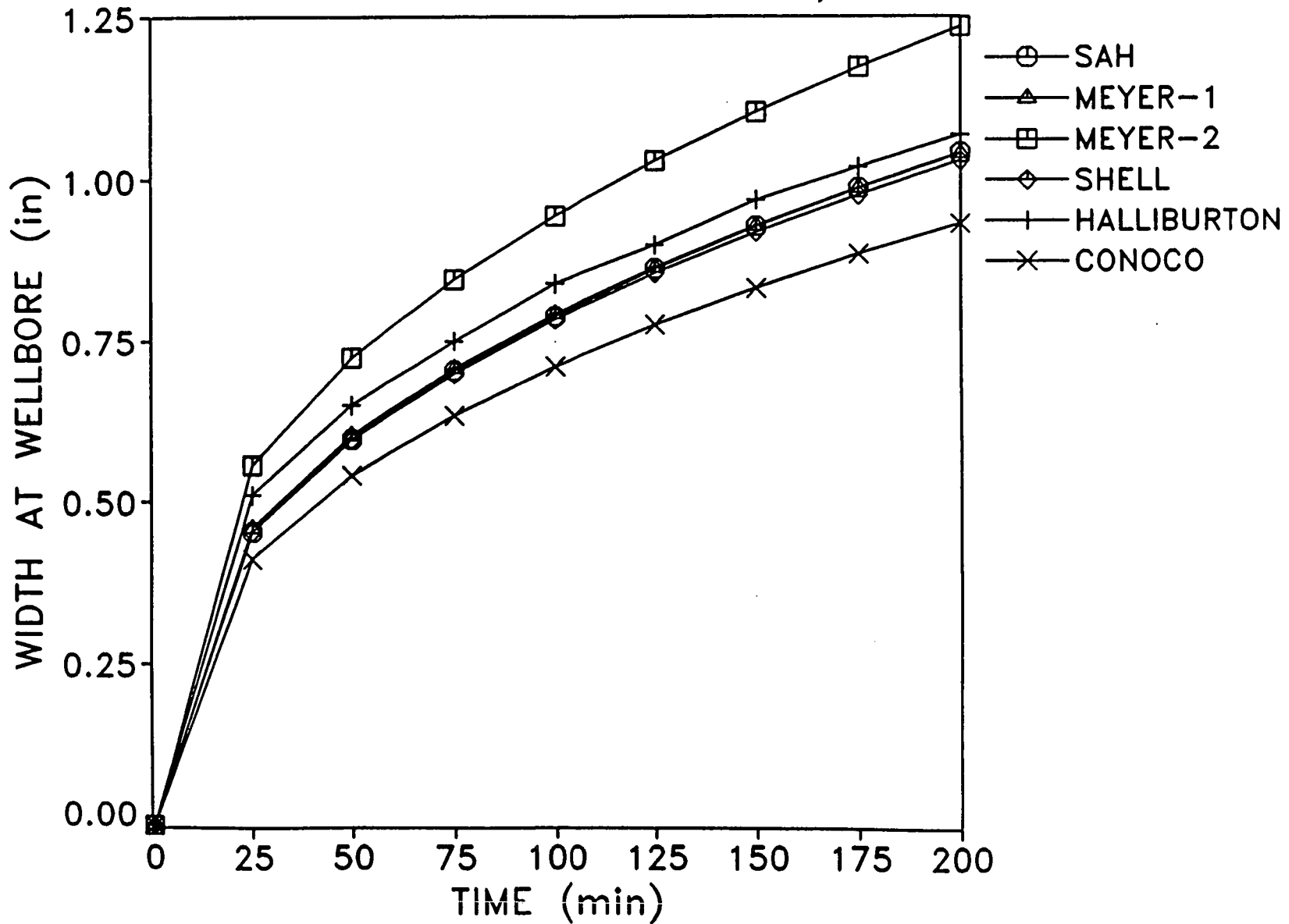


Figure 12 History of width at wellbore for case 2

# PKN-CONSTANT HEIGHT: 200 cp

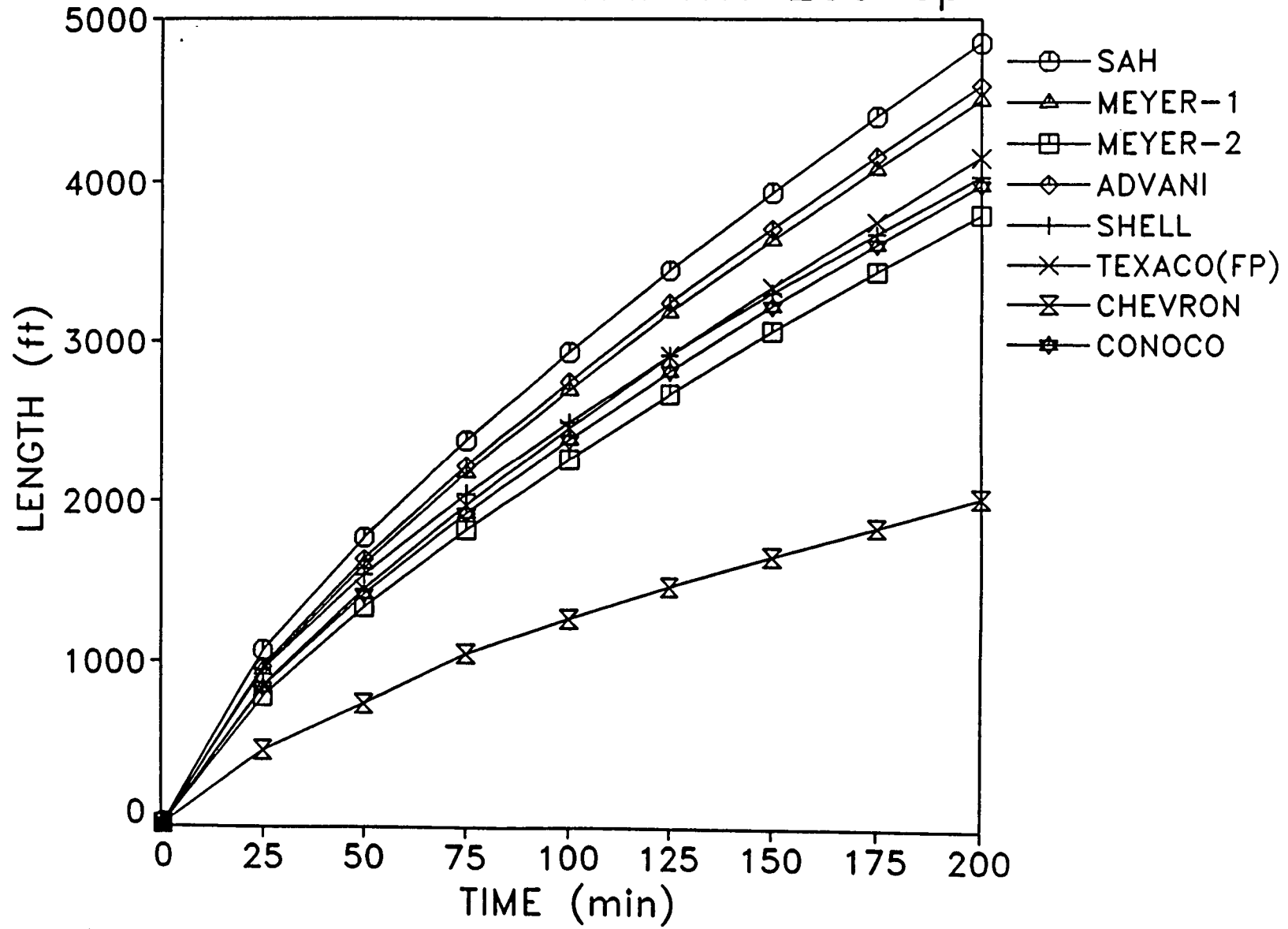


Figure 13 Length history for case 3

# PKN-CONSTANT HEIGHT: 200 cp

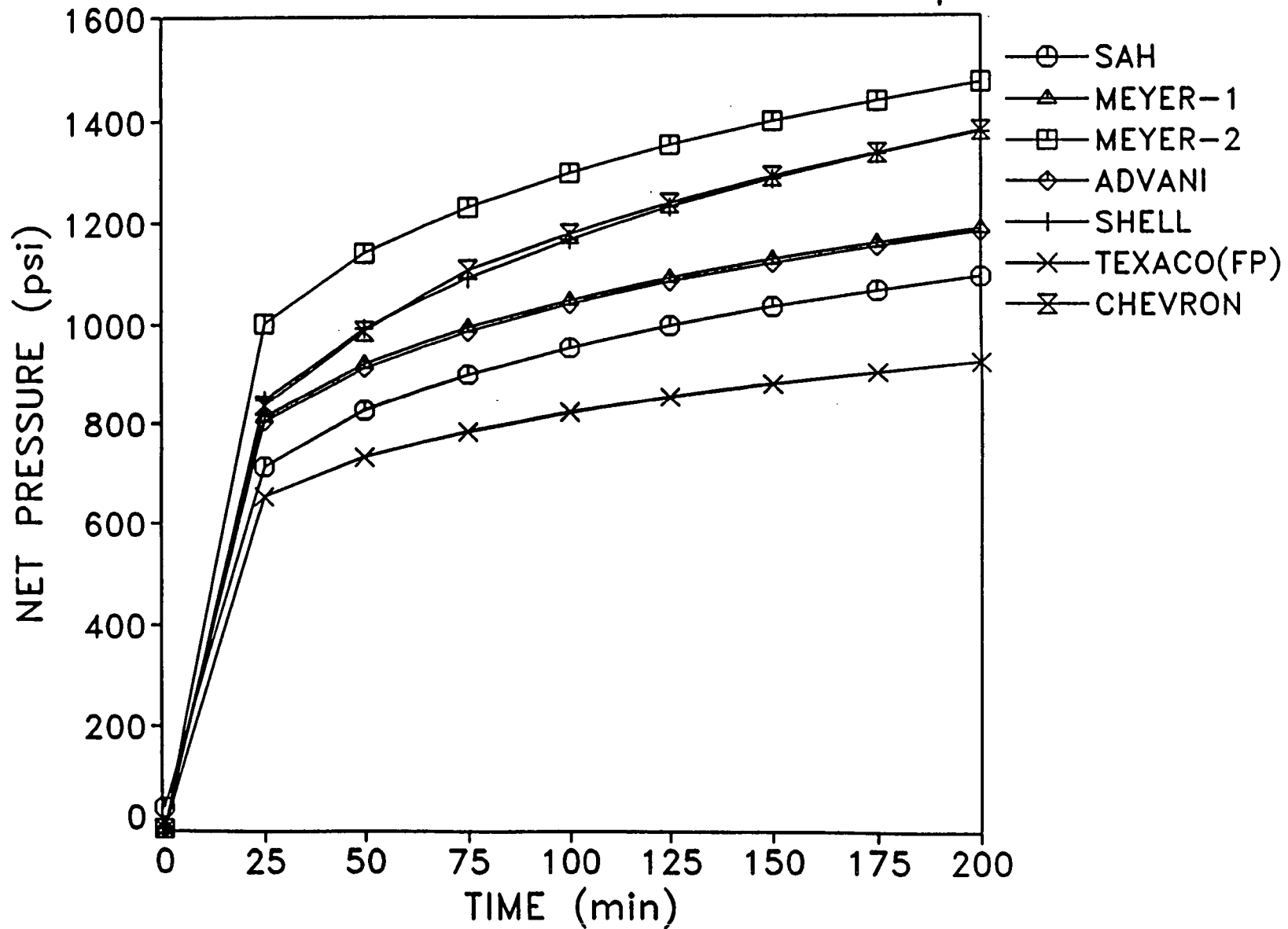


Figure 14 Net pressure history for case 3

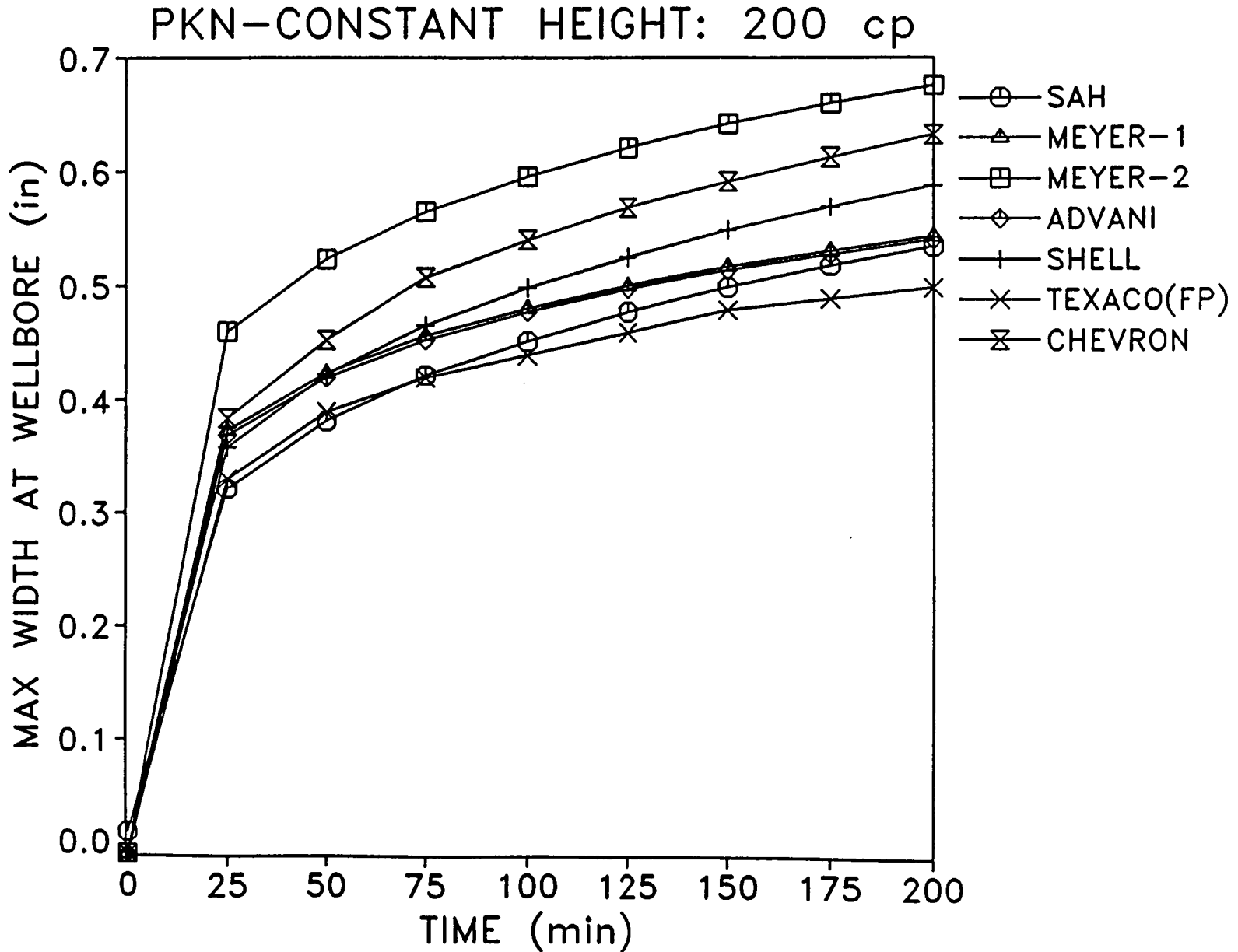


Figure 15 History of width at wellbore for case 3

# PKN-CONSTANT HEIGHT: $n'$ , $k'$

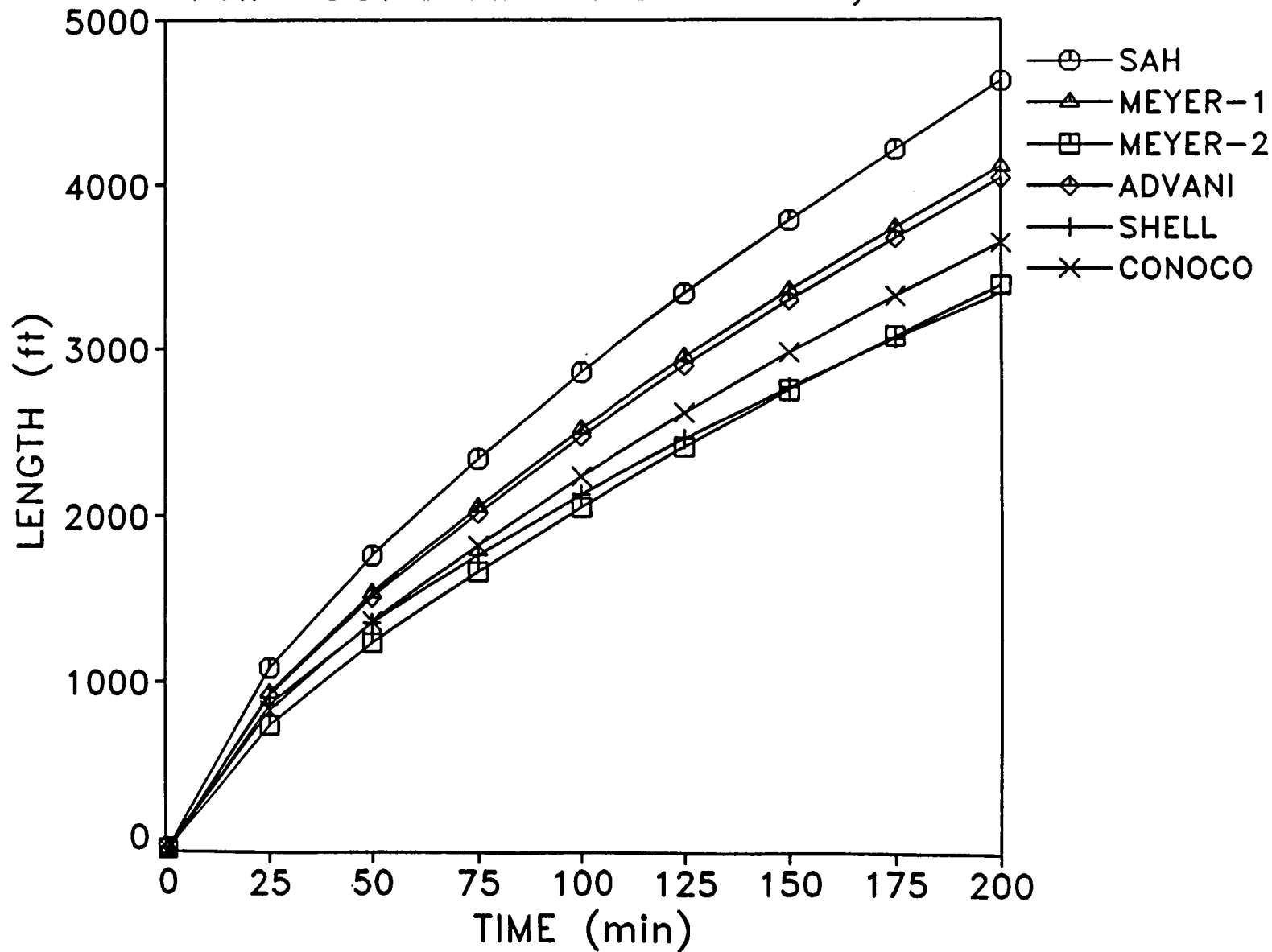


Figure 16 Length history for case 4

# PKN-CONSTANT HEIGHT: $n'$ , $k'$

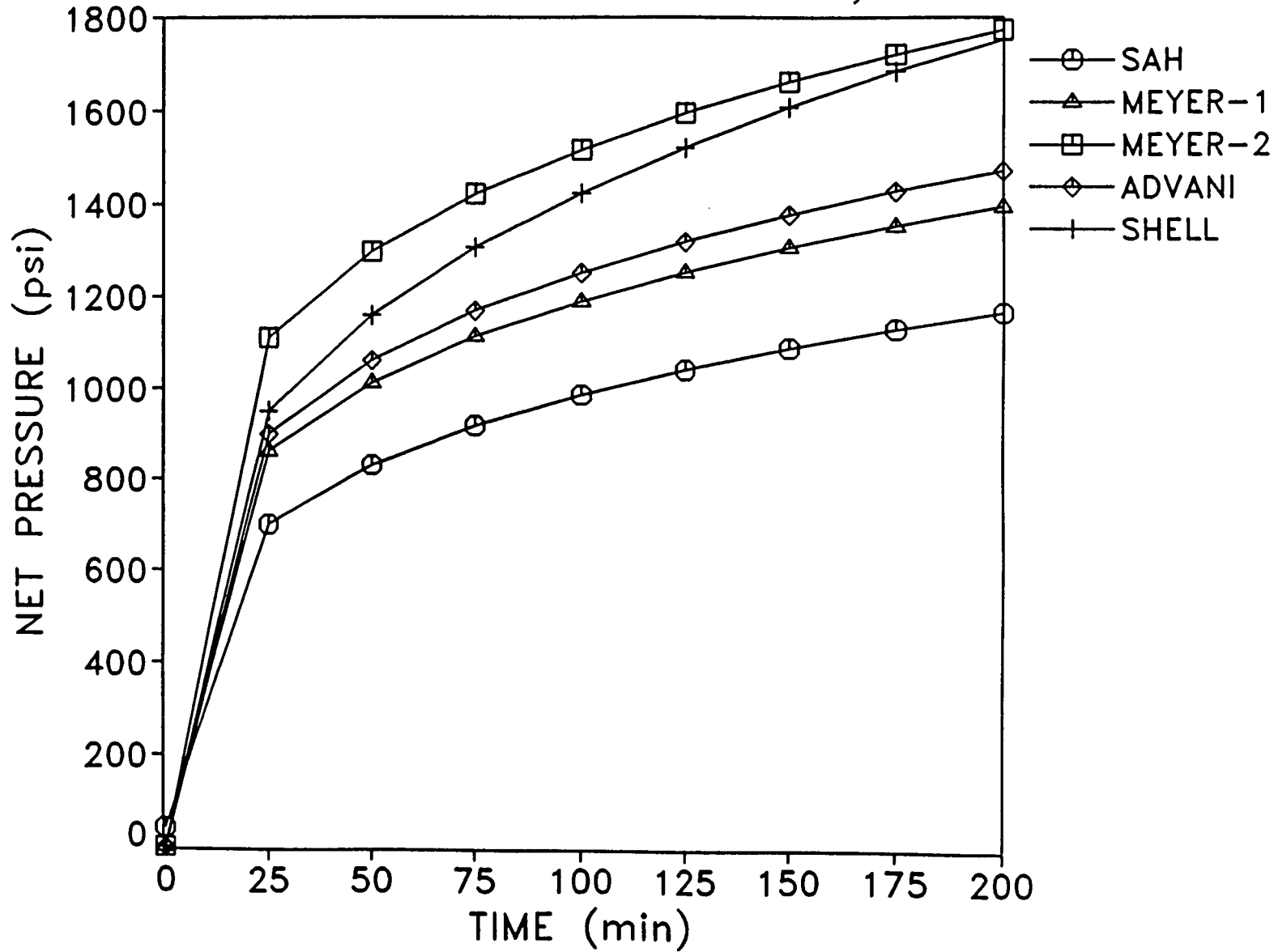


Figure 17 Net pressure history for case 4

# PKN-CONSTANT HEIGHT: $n'$ , $k'$

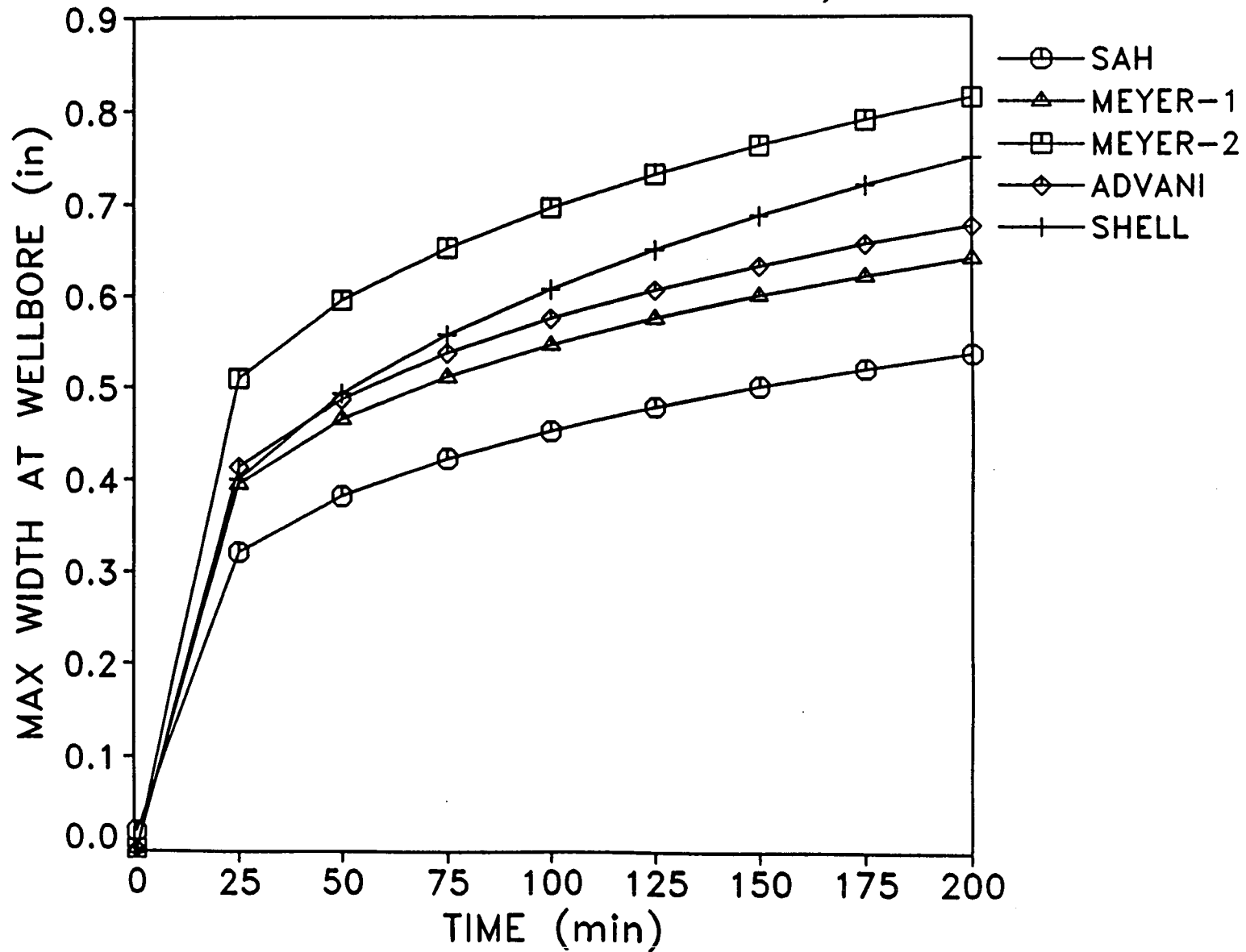


Figure 18 History of width at wellbore for case 4

OTHER 2D-CONSTANT HEIGHT: 200 cp

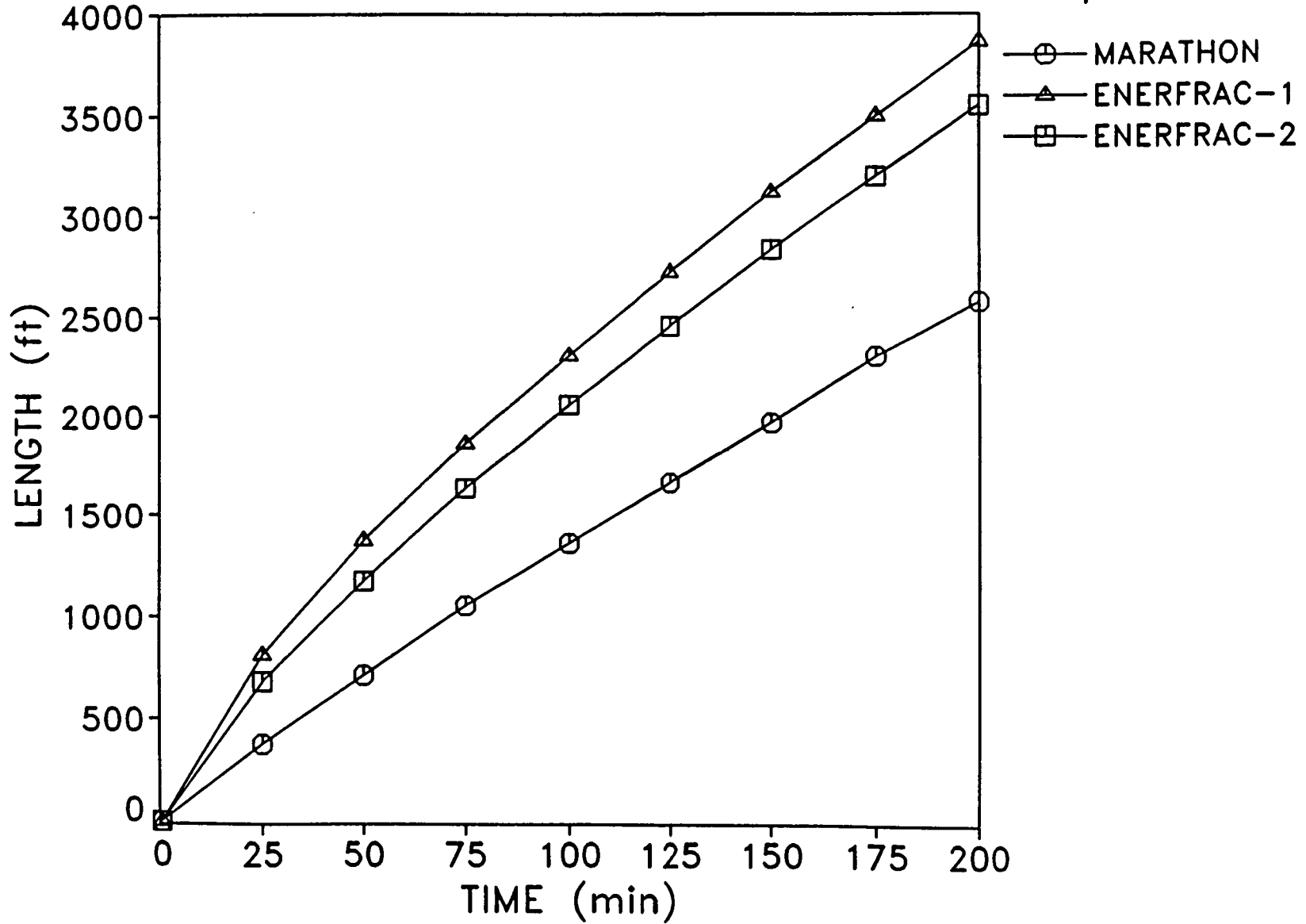


Figure 19 Length history for other constant height-models - 200 cp

OTHER 2D-CONSTANT HEIGHT: 200 cp

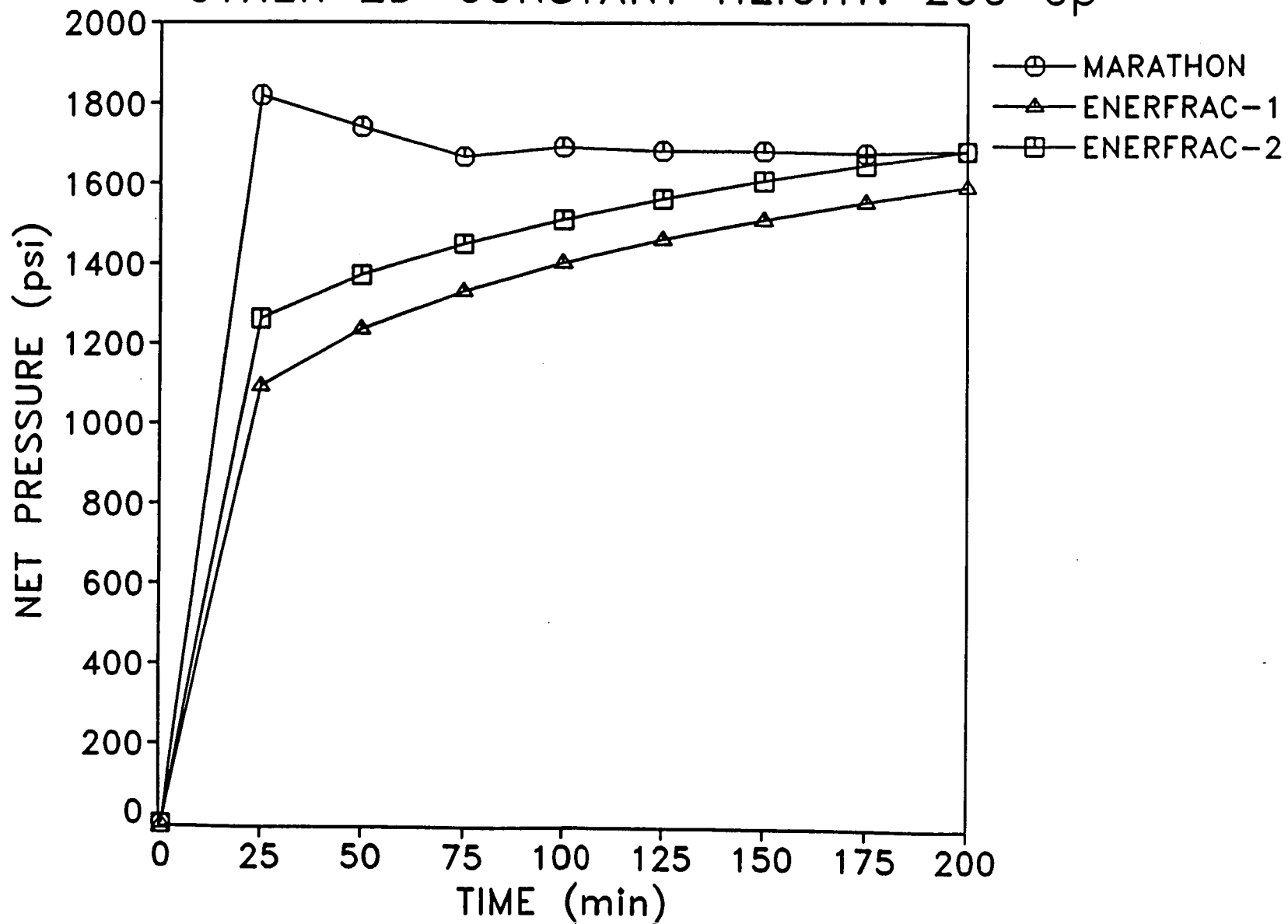


Figure 20 Net pressure history for other constant height-models - 200 cp

OTHER 2D-CONSTANT HEIGHT: 200 cp

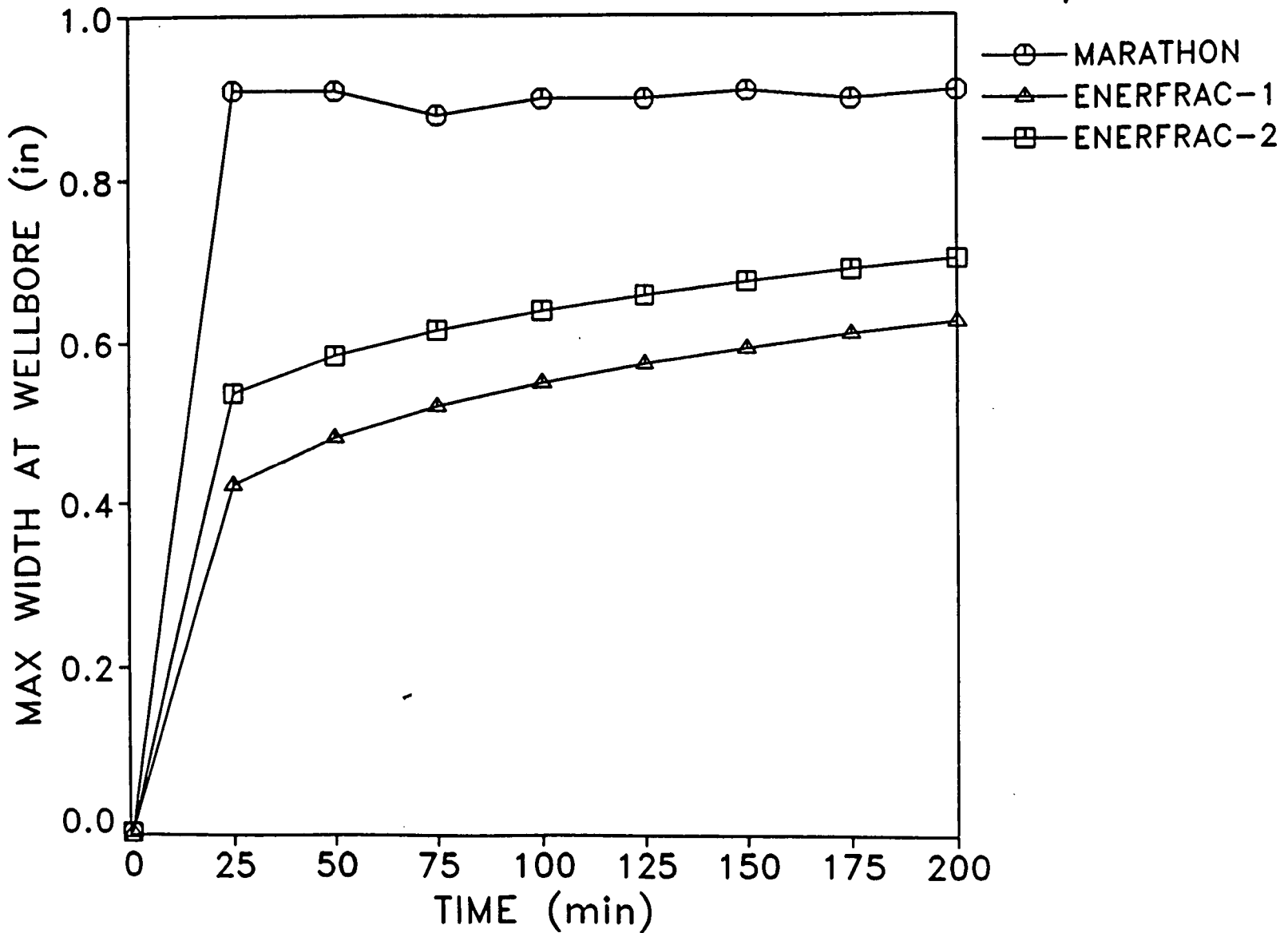


Figure 21 History of width at wellbore for other constant-height models - 200 cp

OTHER 2D-CONSTANT HEIGHT:  $n'$ ,  $k'$

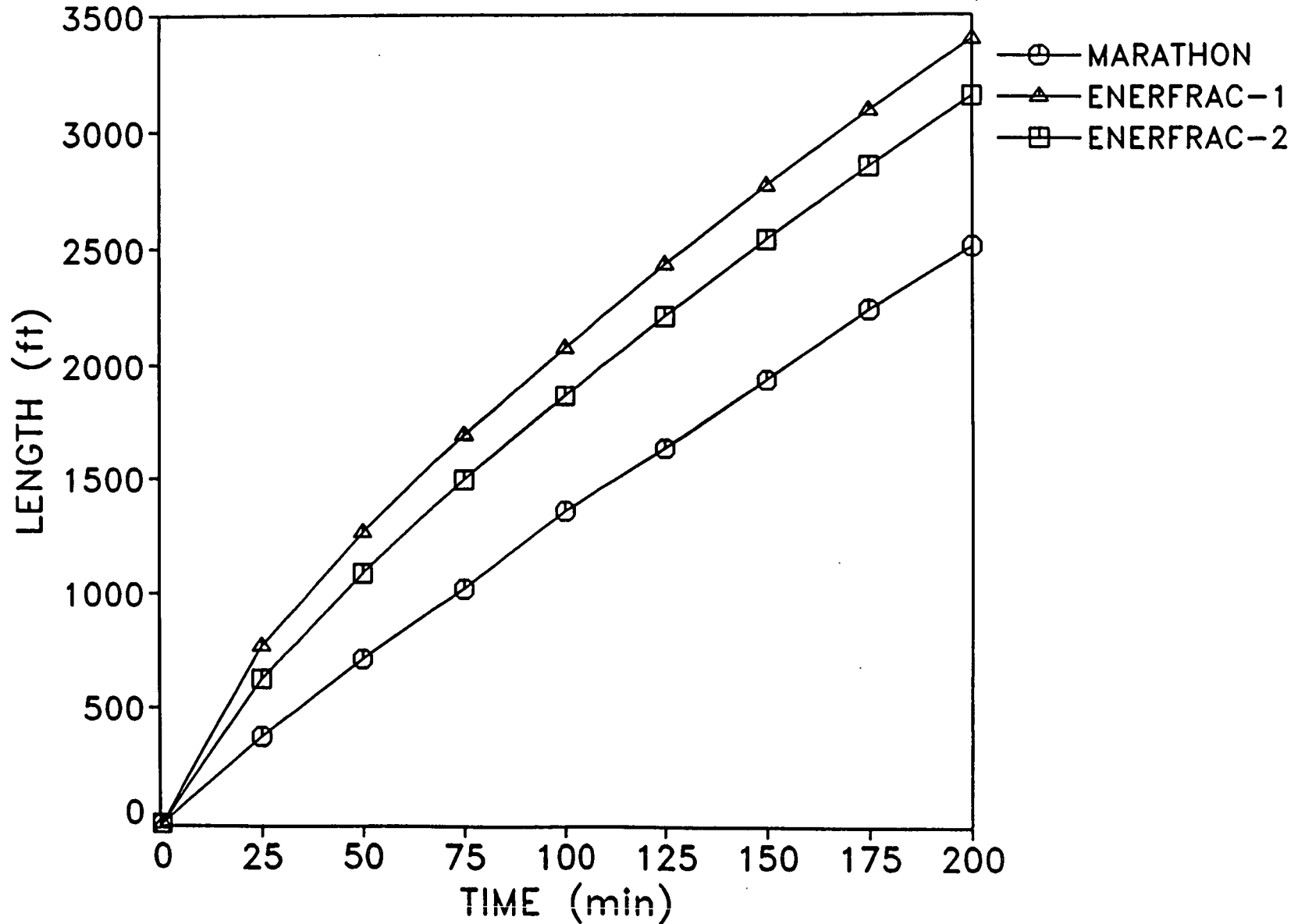


Figure 22 Length history for other constant height-models -  $n'$ ,  $k'$

OTHER 2D-CONSTANT HEIGHT:  $n'$ ,  $k'$

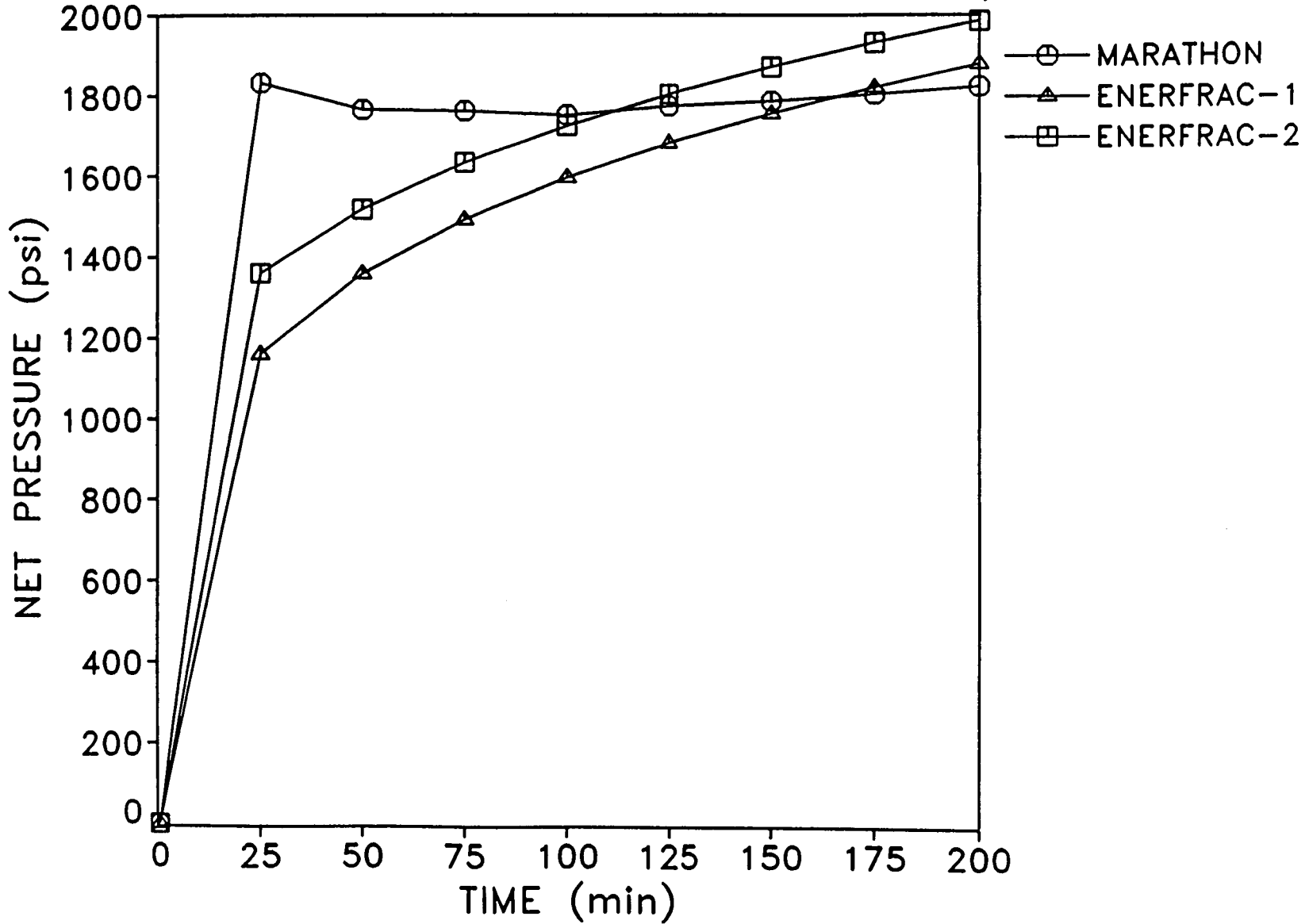


Figure 23 Net pressure history for other constant height-models -  $n'$ ,  $k'$

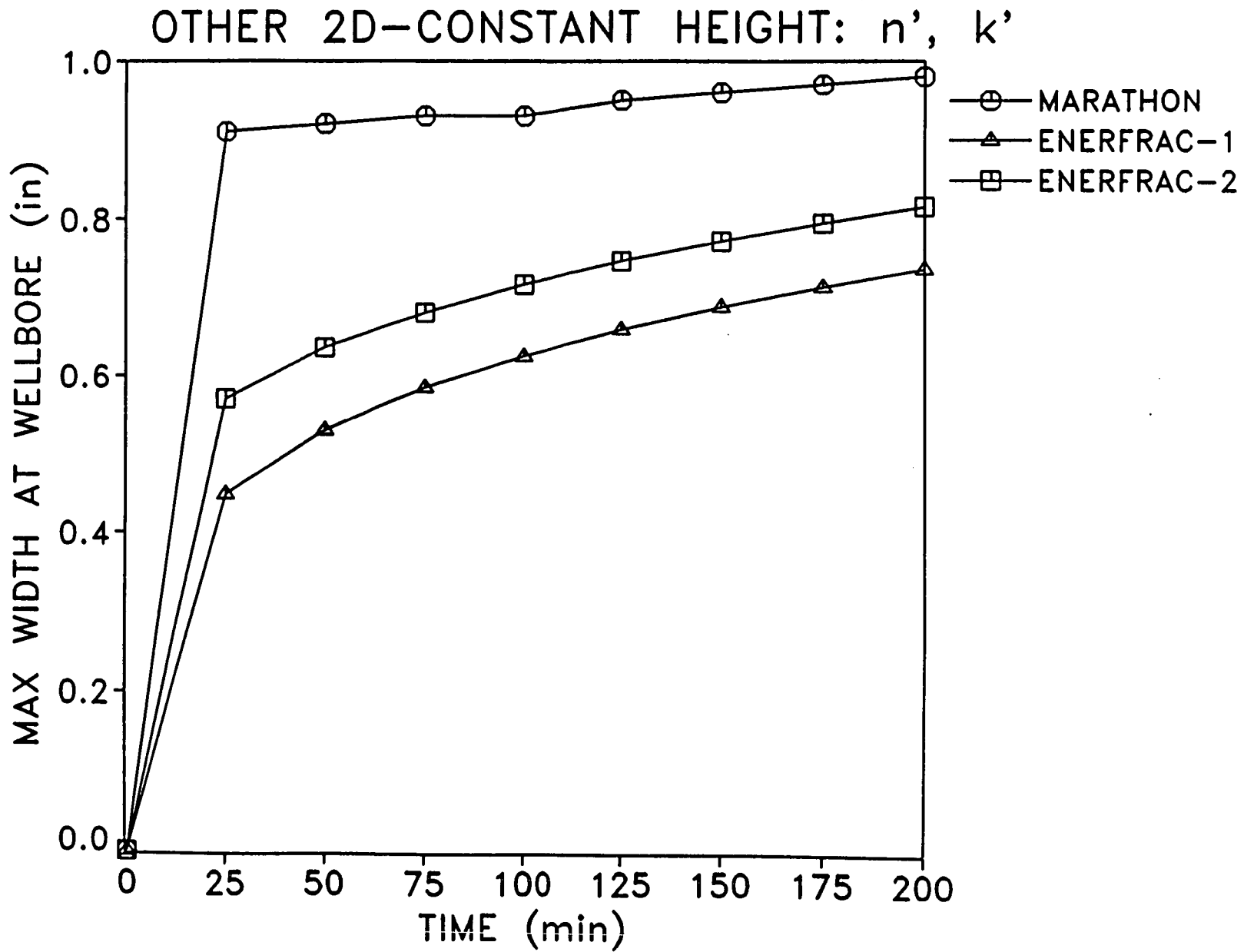


Figure 24 History of width at wellbore for other constant-height models -  $n'$ ,  $k'$

# FRACTURE HALF LENGTH

## 3-LAYER MODELS

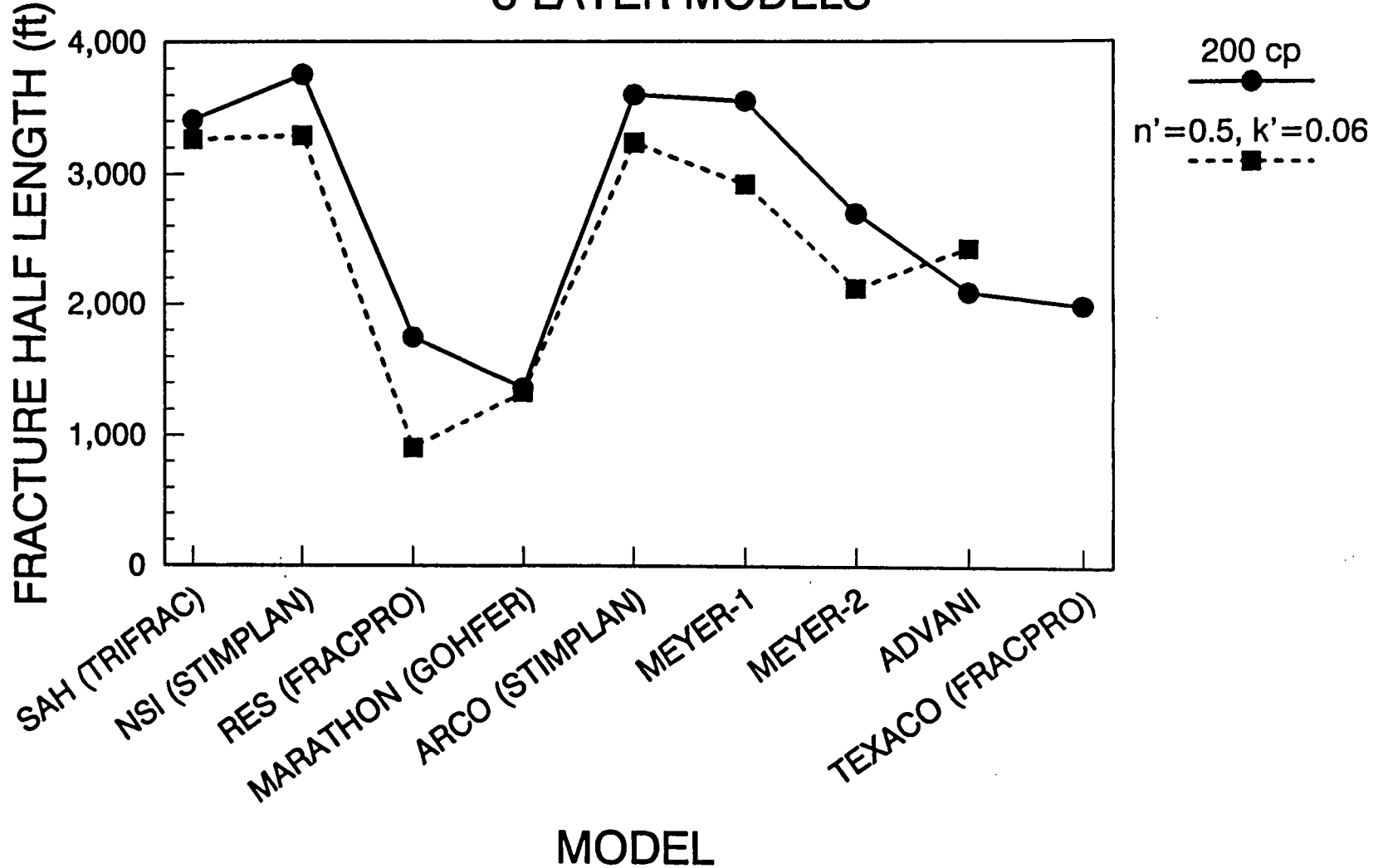


Figure 25 Length comparison for cases 5 and 6

# FRACTURE HEIGHT

## 3-LAYER MODELS

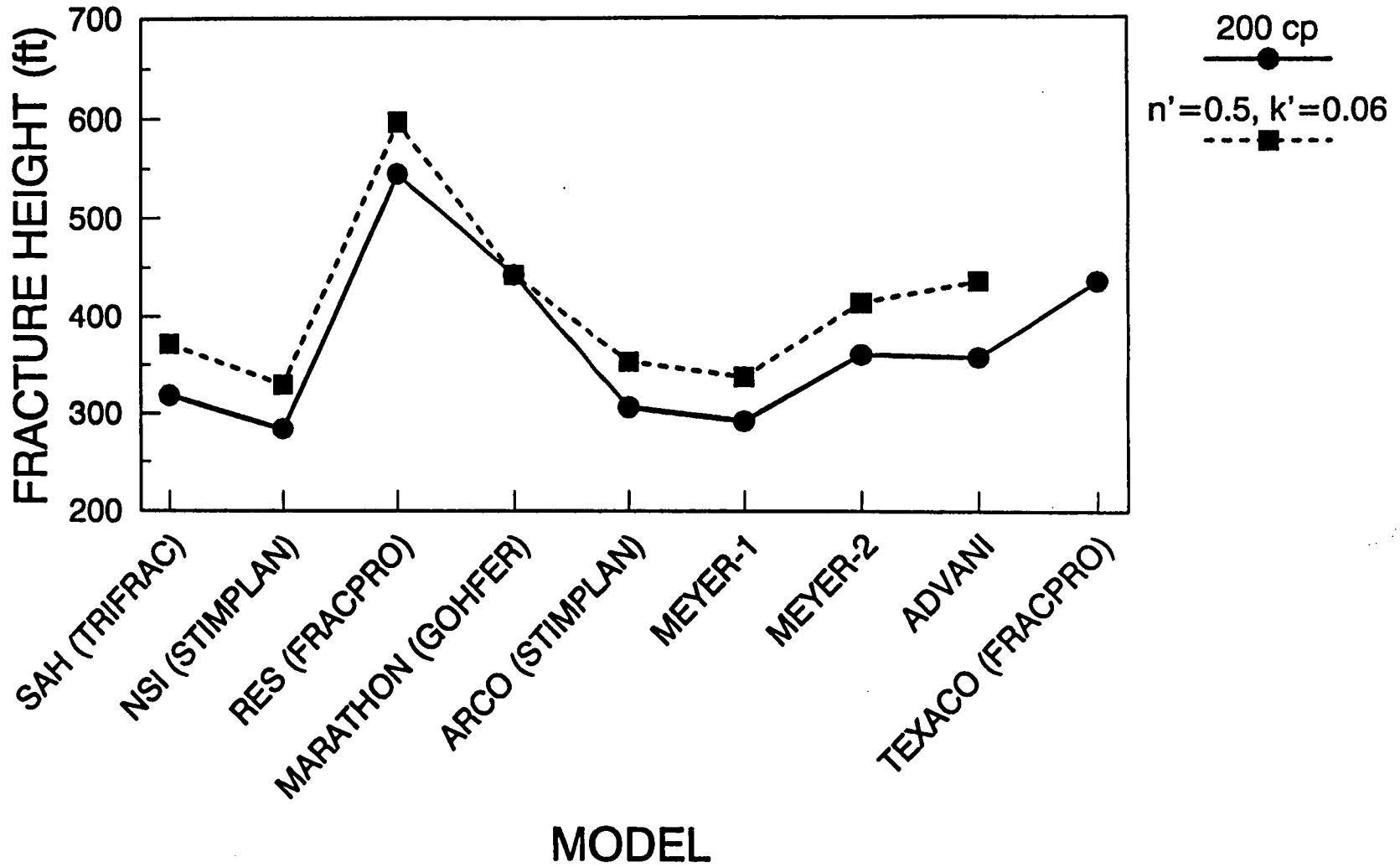


Figure 26 Height comparison for cases 5 and 6

# FRACTURE NET PRESSURE

## 3-LAYER MODELS

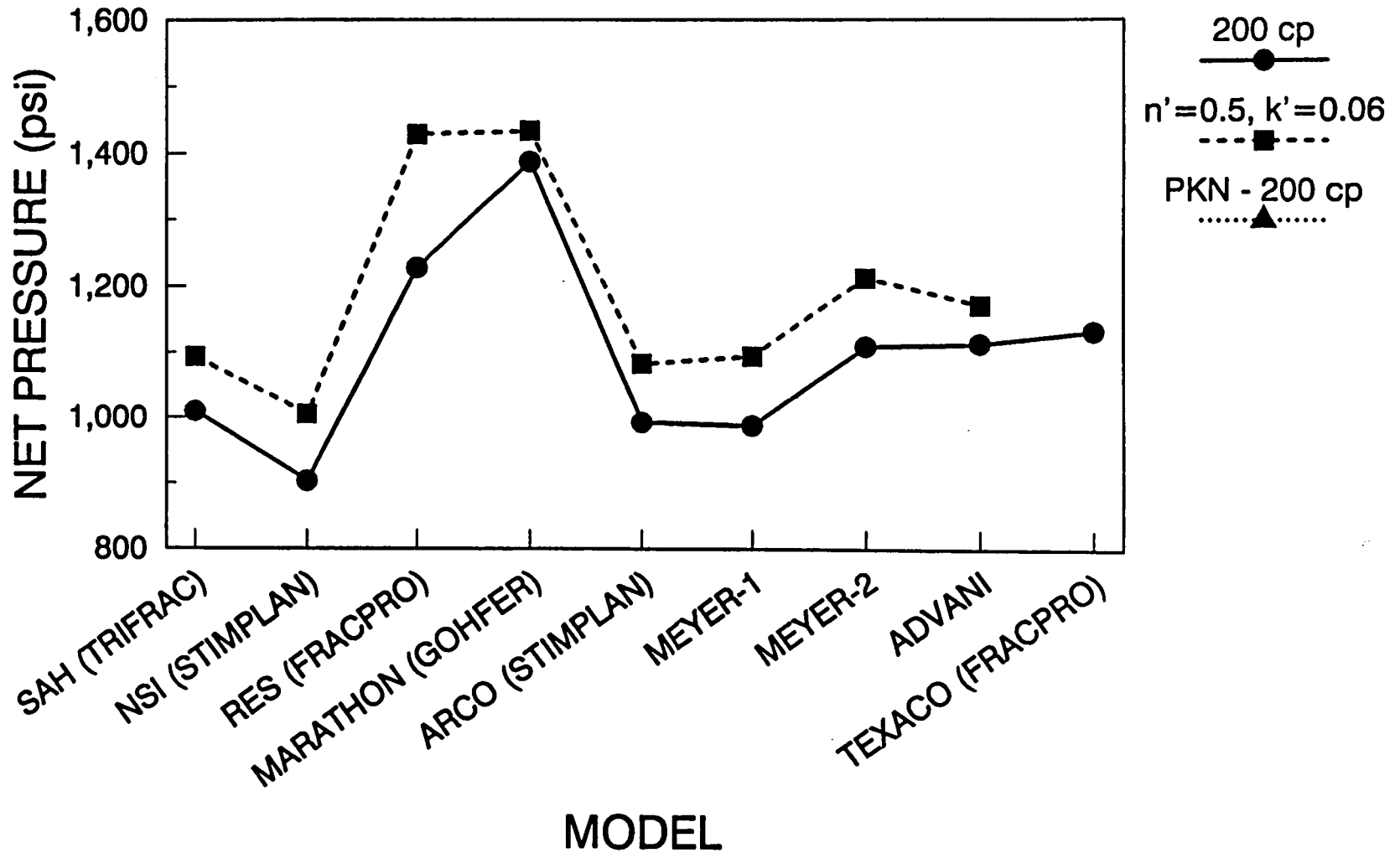


Figure 27 Net pressure comparison for cases 5 and 6

# FRACTURE EFFICIENCY

## 3-LAYER MODELS

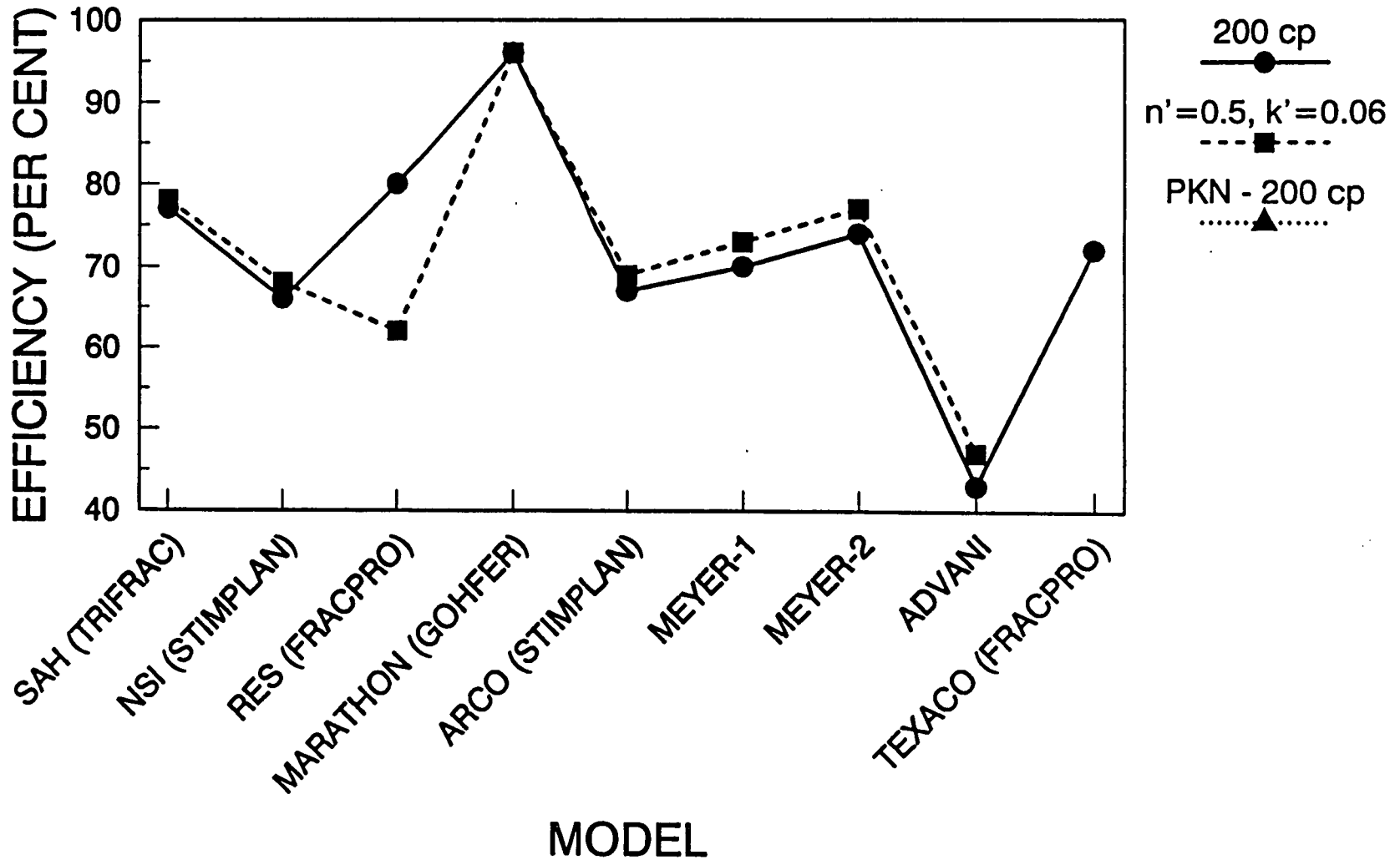


Figure 28 Efficiency comparison for cases 5 and 6

# FRACTURE MAXIMUM WIDTH

## 3-LAYER MODELS

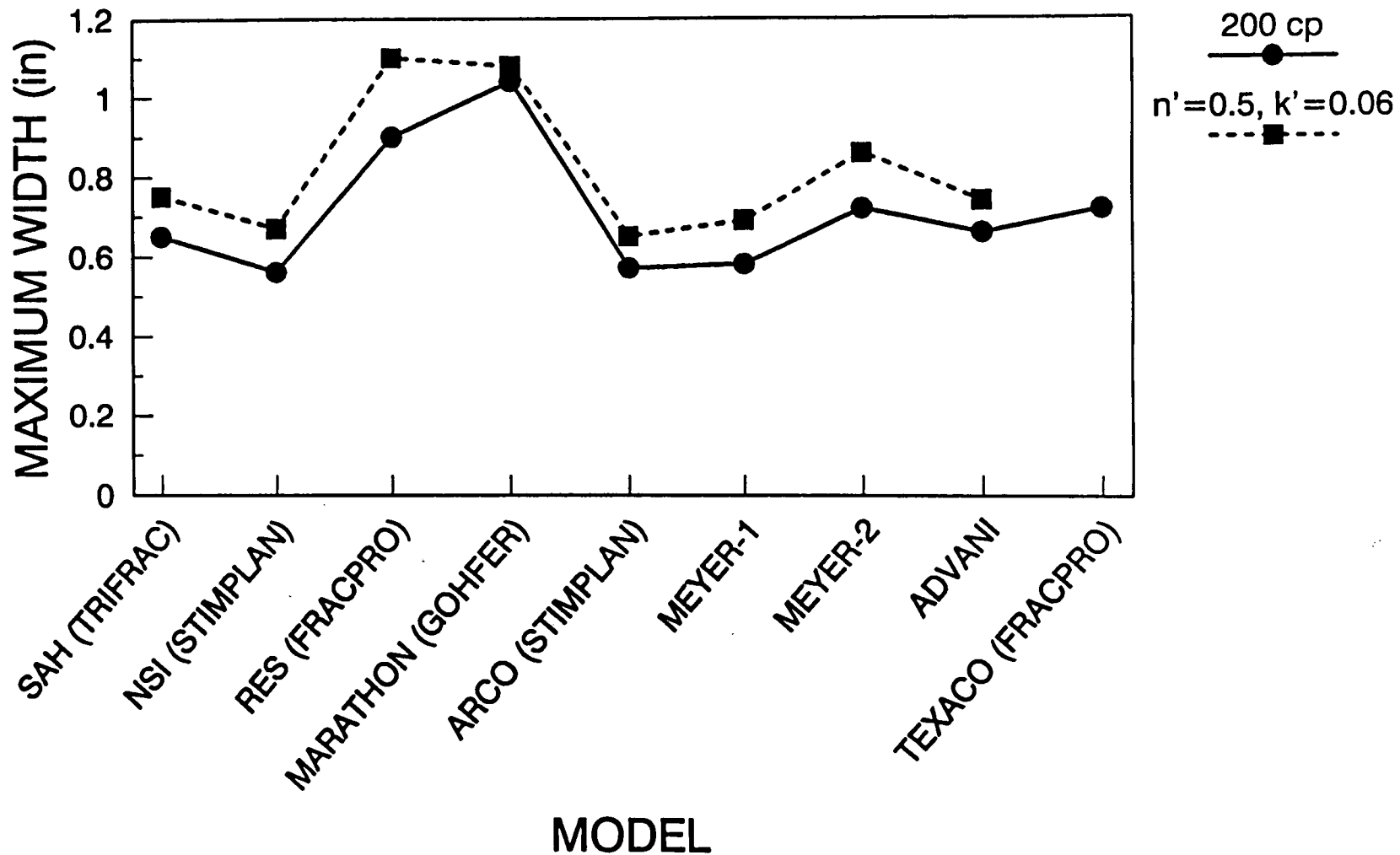


Figure 29 Comparison of maximum width at wellbore for cases 5 and 6

# FRACTURE AVERAGE WIDTH AT WELLBORE

## 3-LAYER MODELS

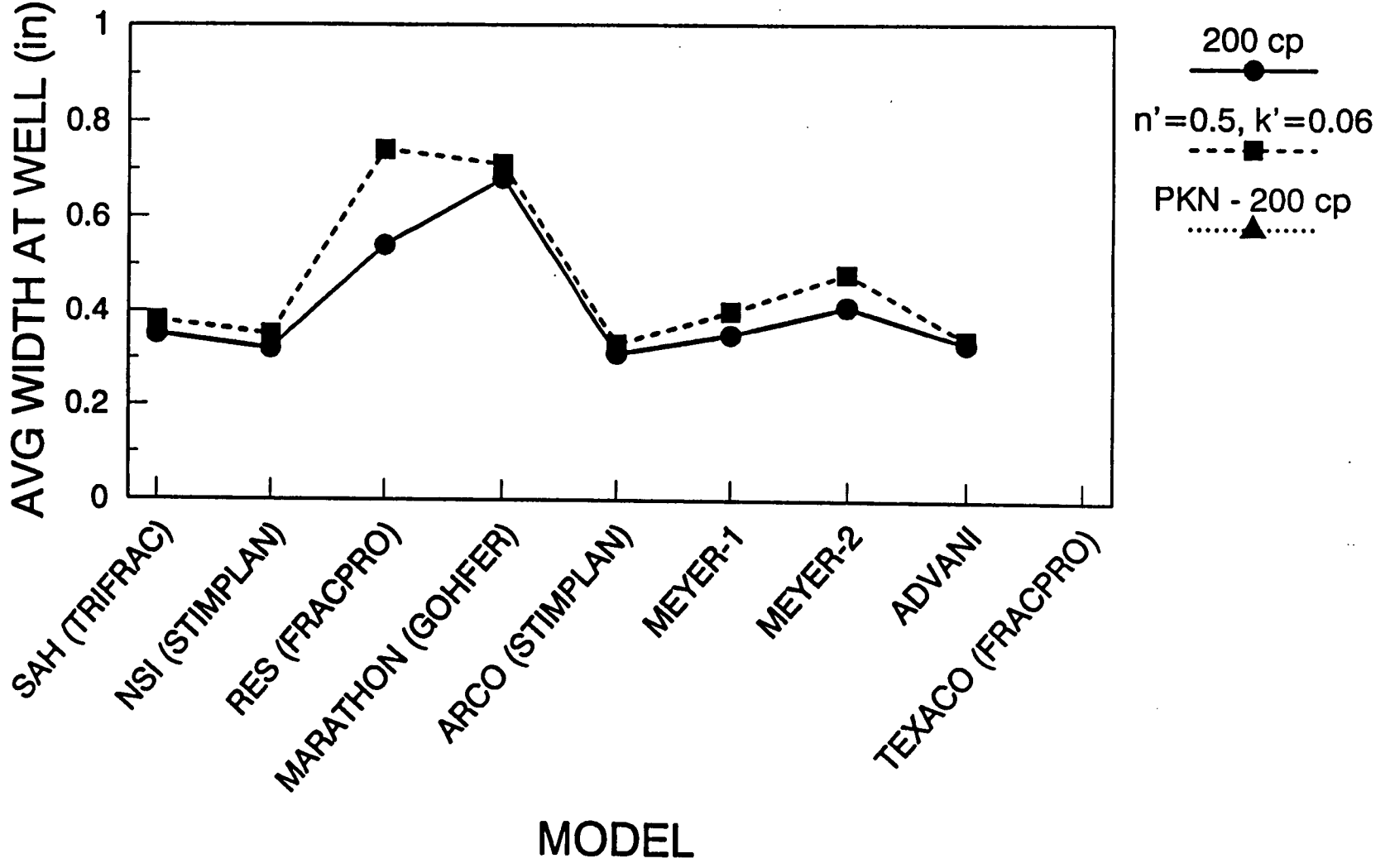


Figure 30 Comparison of average width at wellbore for cases 5 and 6

# FRACTURE AVERAGE WIDTH

## 3-LAYER MODELS

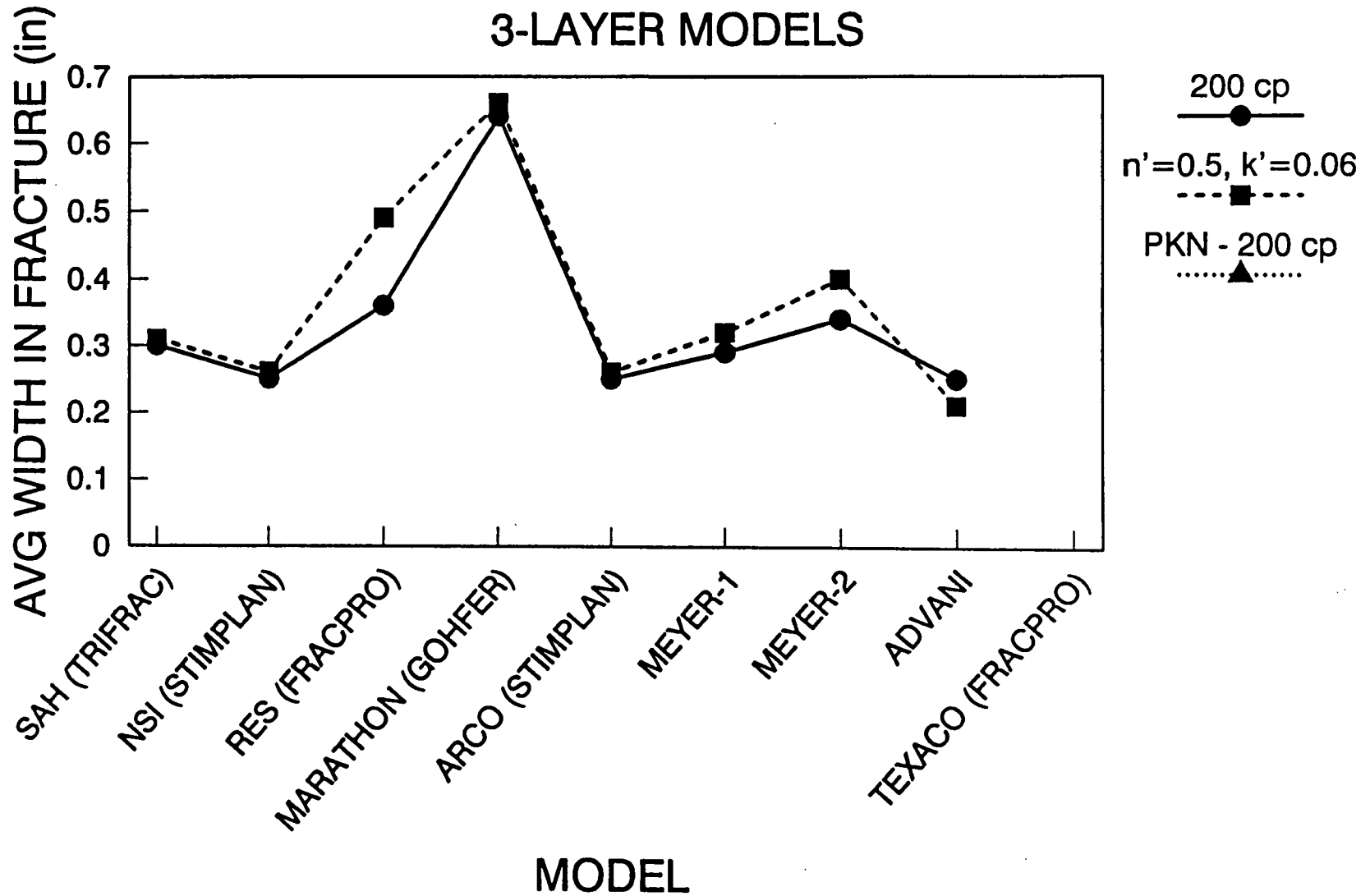


Figure 31 Comparison of average width in fracture for cases 5 and 6

### 3-LAYER MODELS: 200 cp

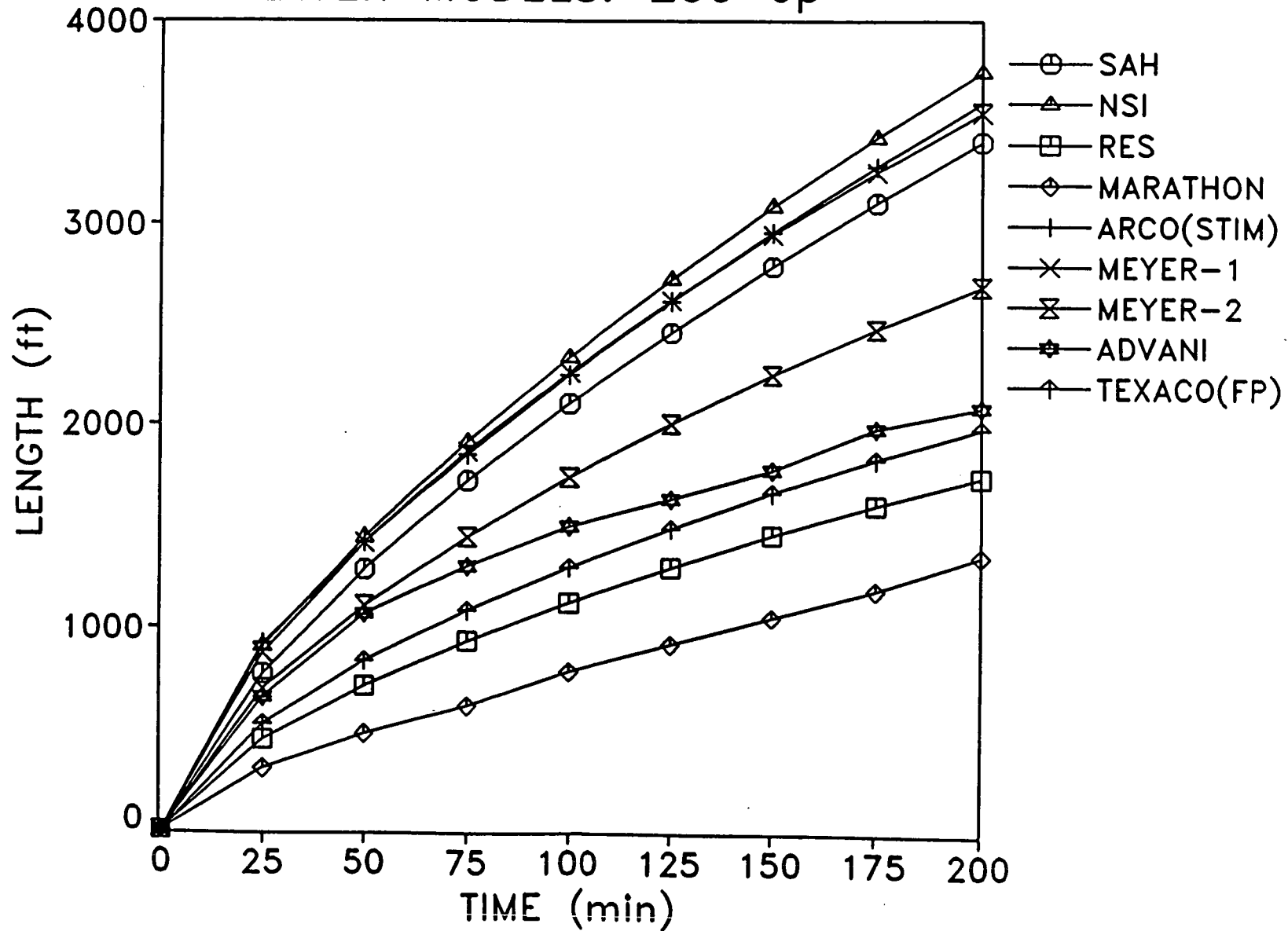


Figure 32 Length history for case 5

### 3-LAYER MODELS: 200 cp

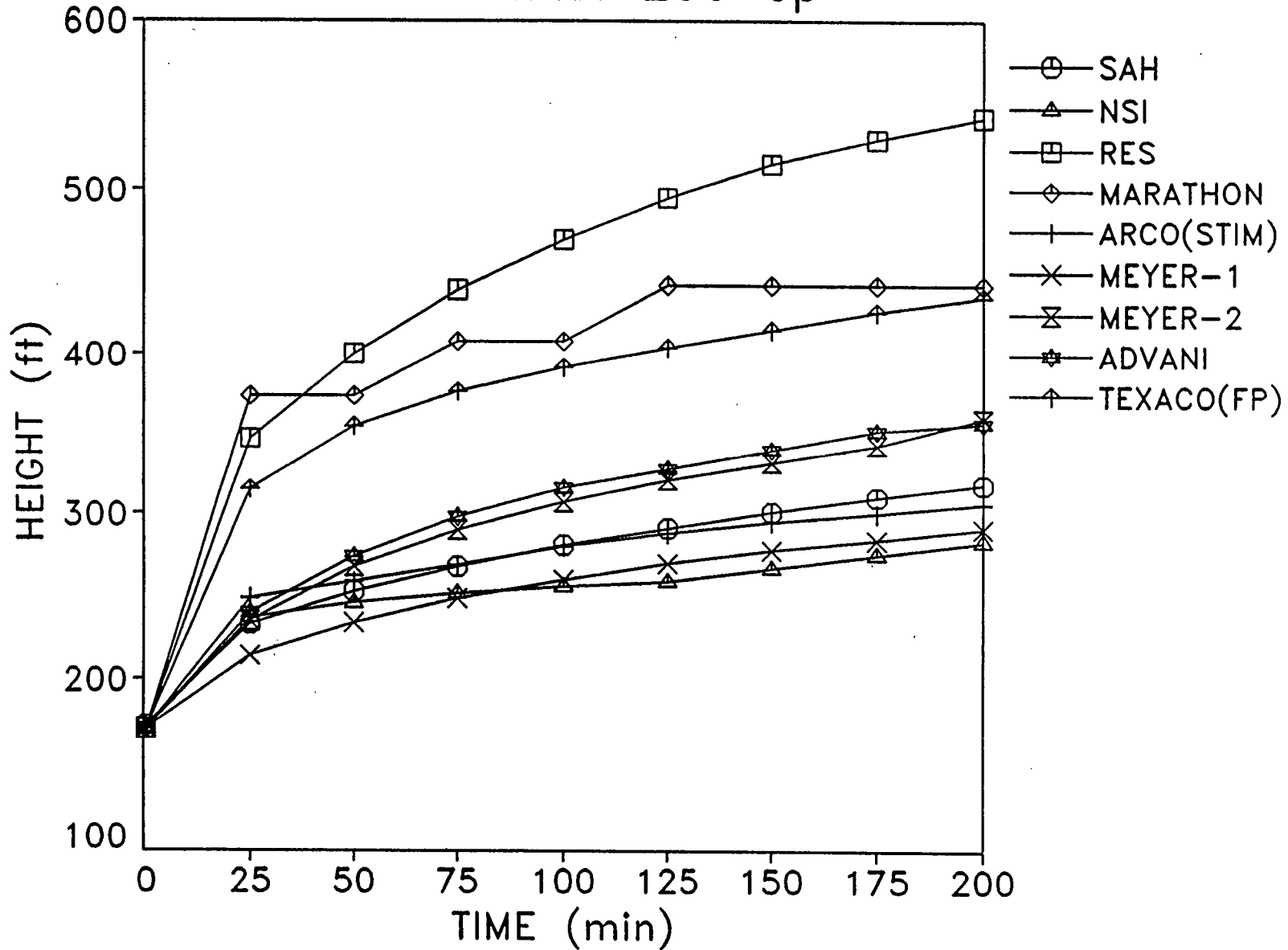


Figure 33 Height history for case 5

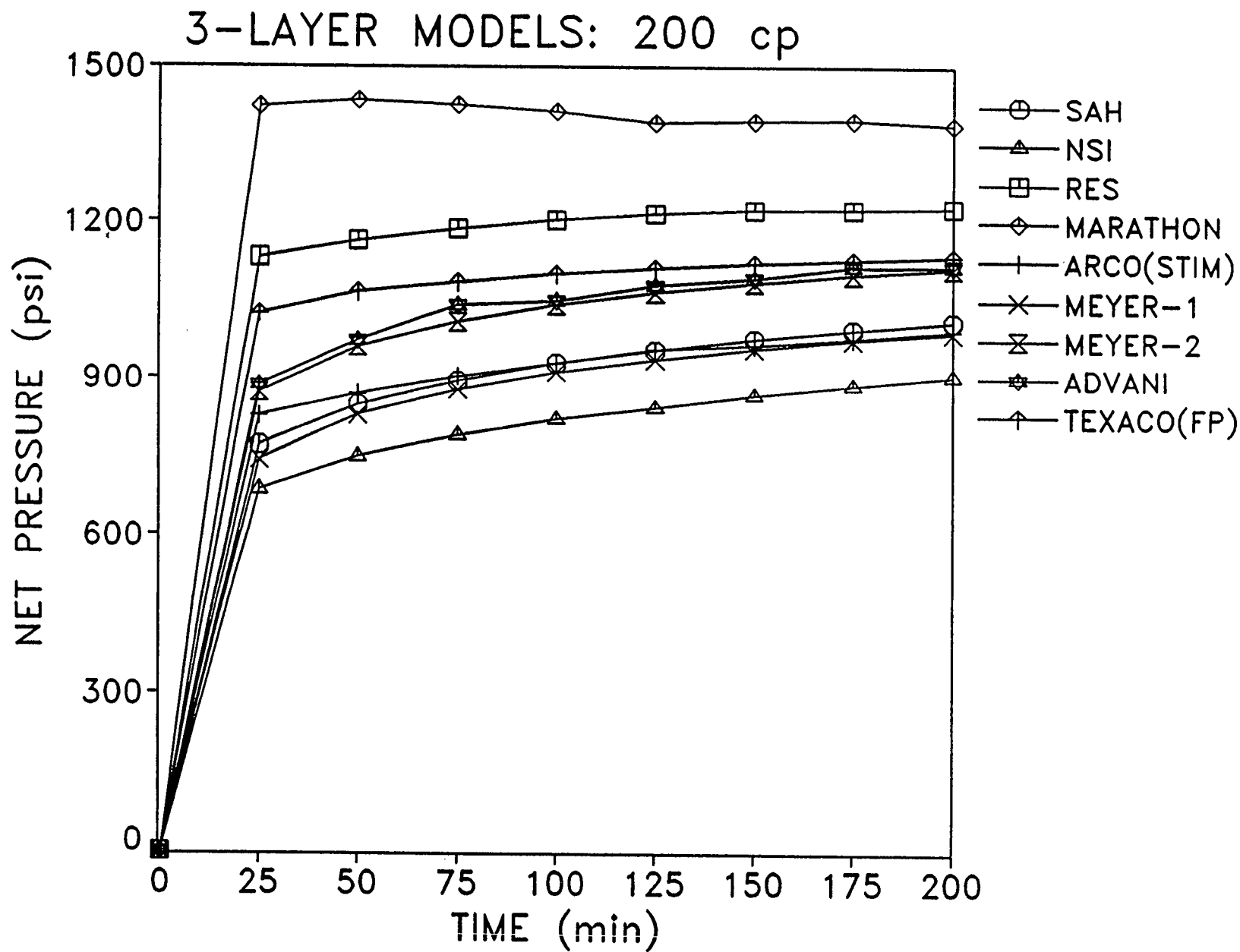


Figure 34 Net pressure history for case 5

### 3-LAYER MODELS: 200 cp

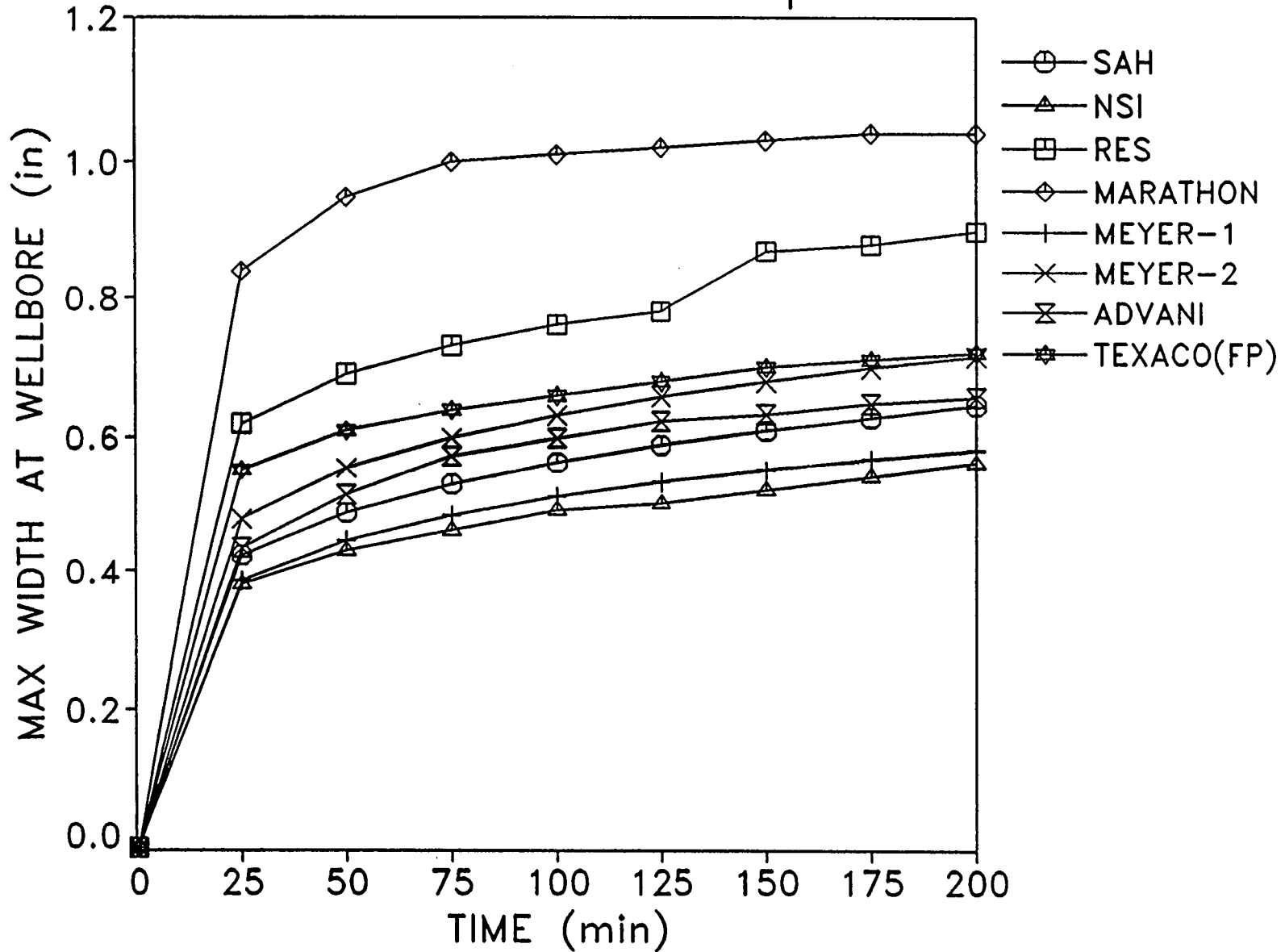


Figure 35 History of width at wellbore for case 5

### 3-LAYER MODELS: $n'$ , $k'$

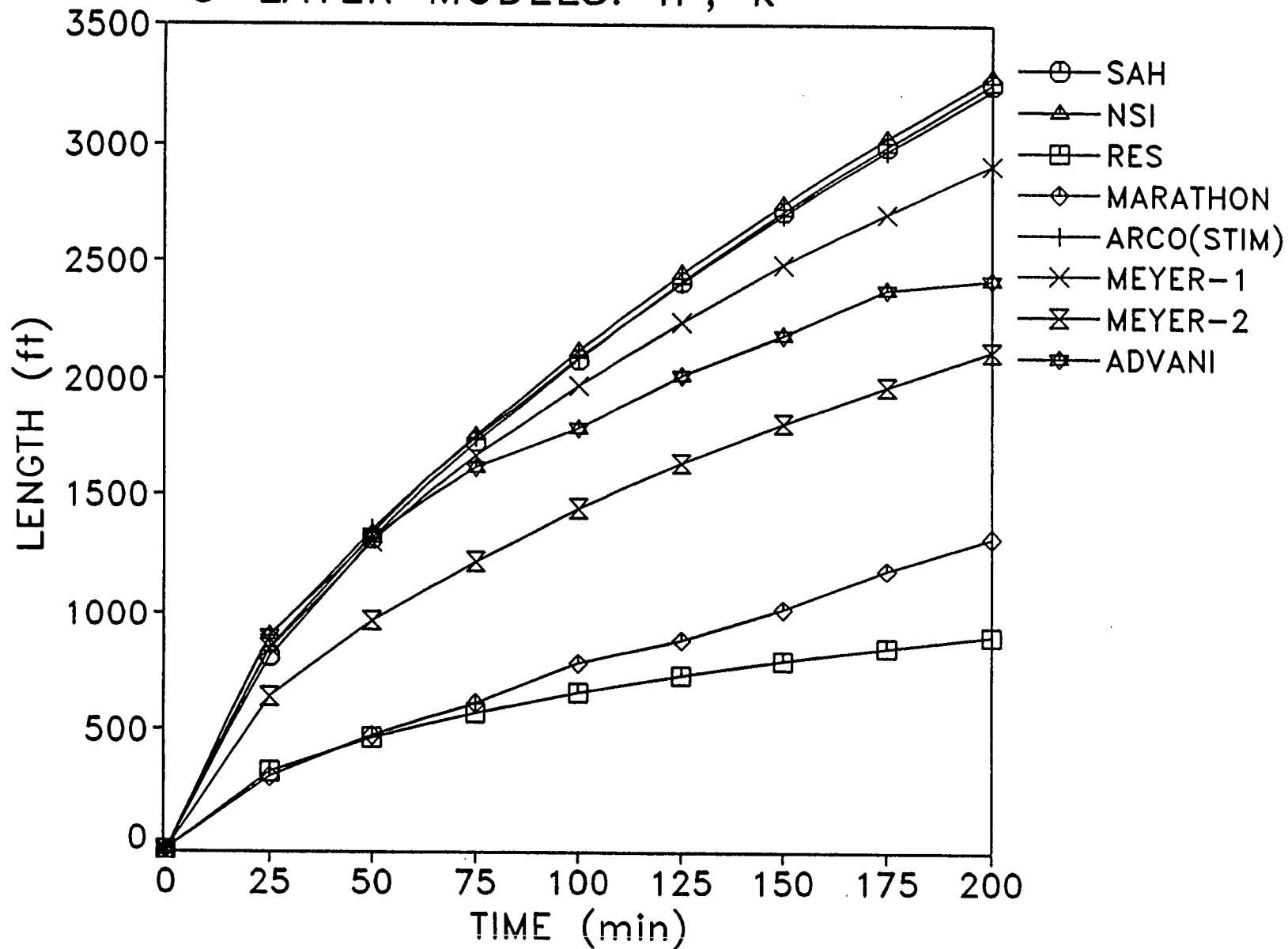


Figure 36 Length history for case 6

### 3-LAYER MODELS: $n'$ , $k'$

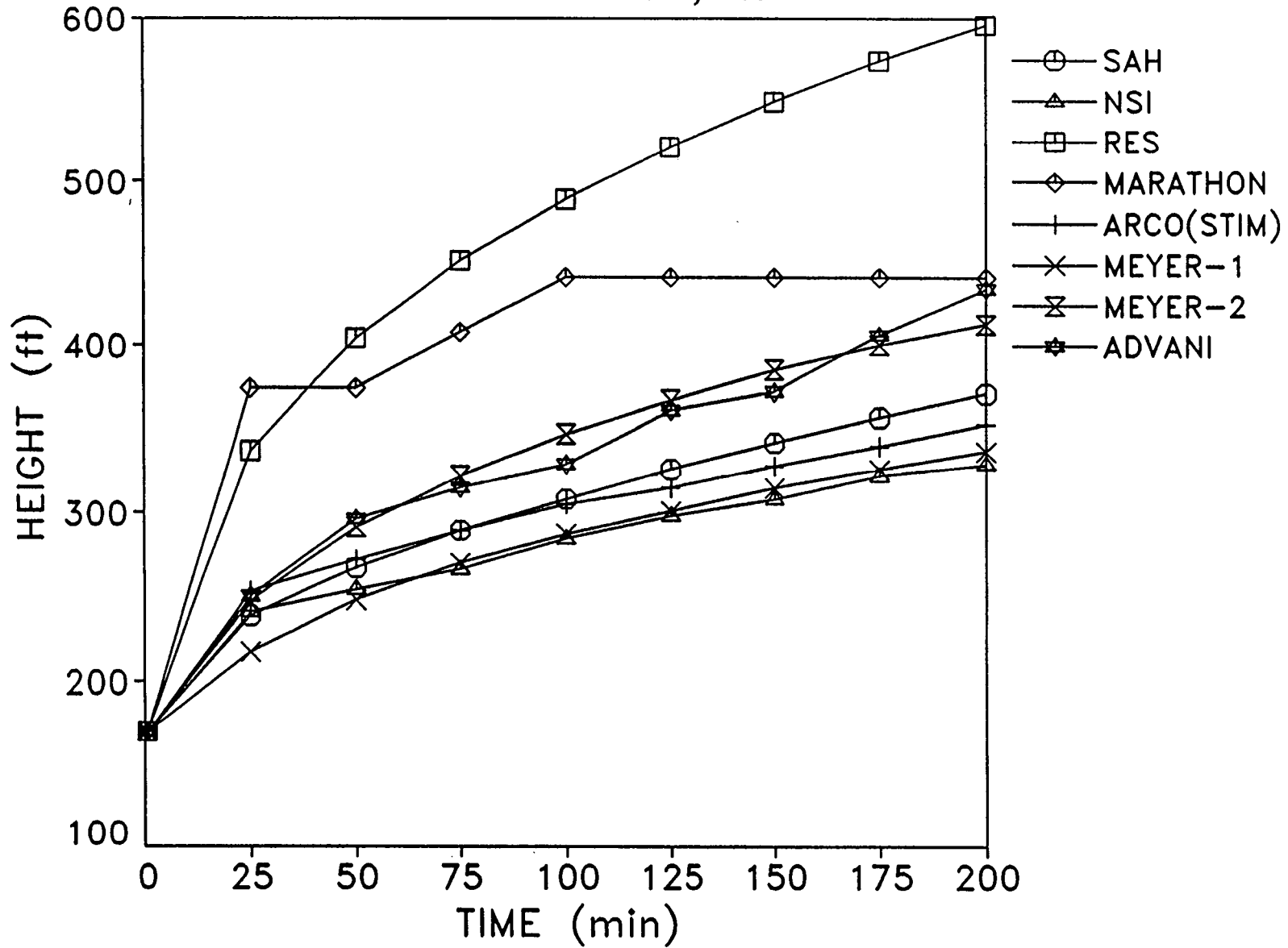


Figure 37 Height history for case 6

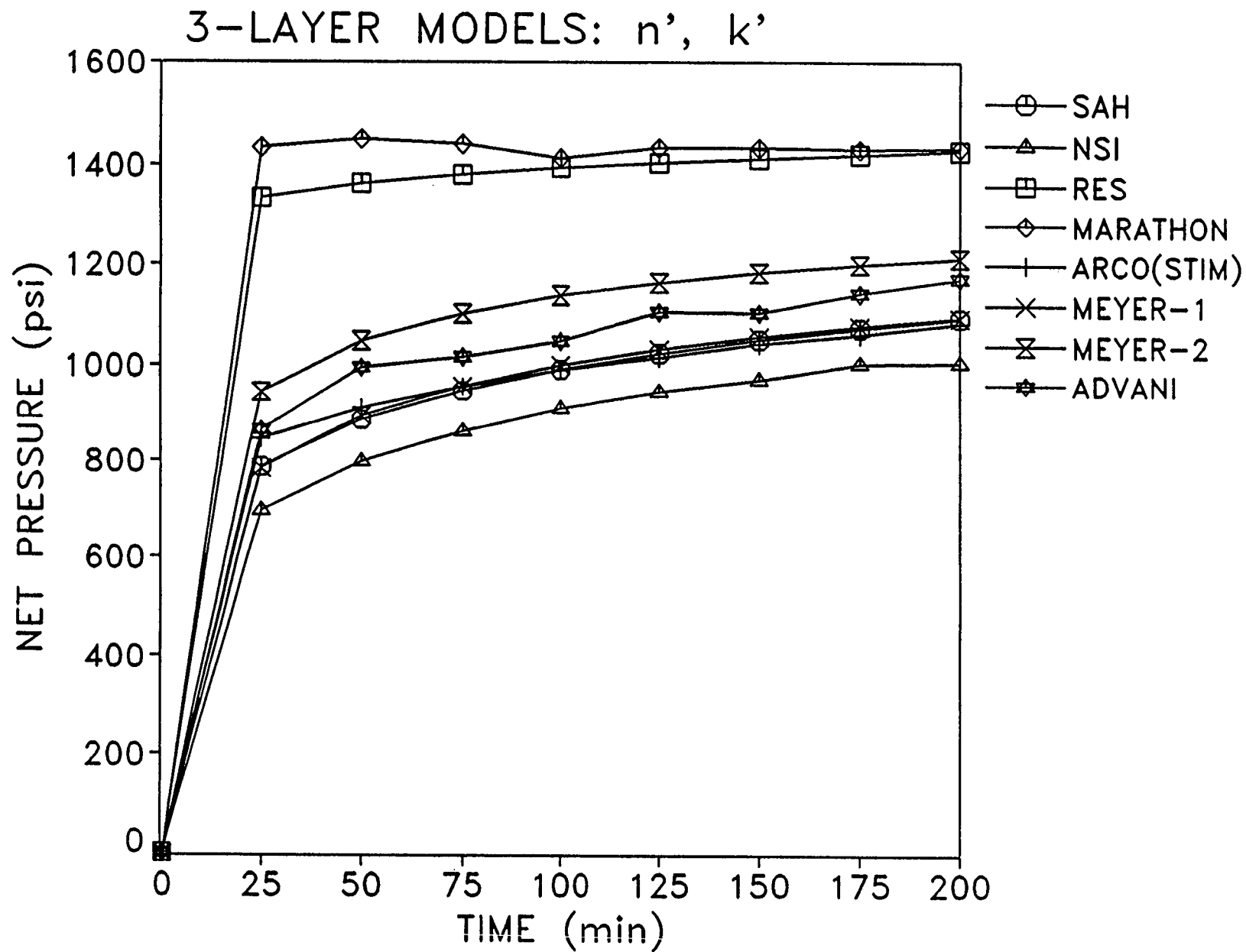


Figure 38 Net pressure history for case 6

### 3-LAYER MODELS: $n'$ , $k'$

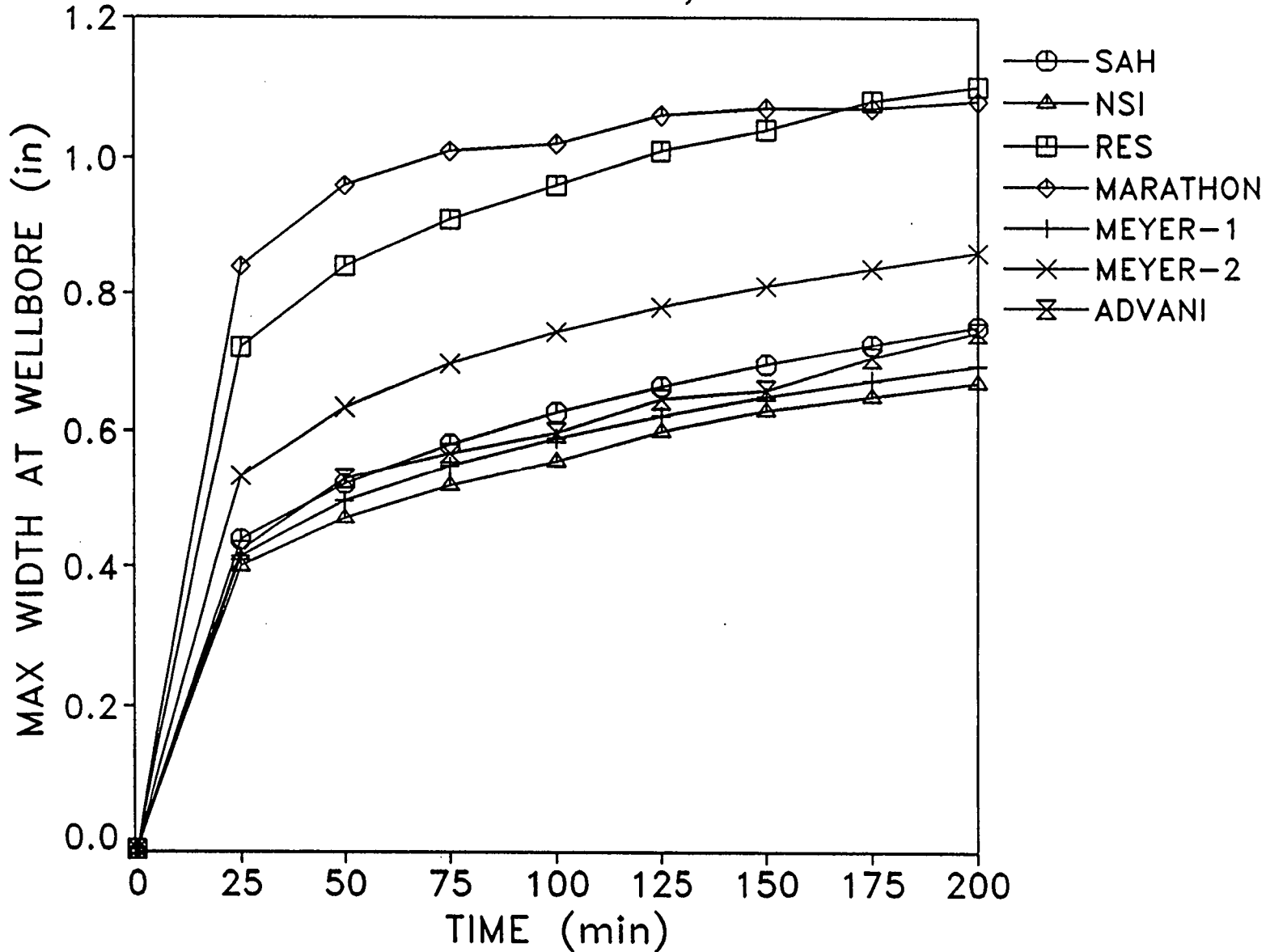


Figure 39 History of width at wellbore for case 6

# FRACTURE HALF LENGTH

## 5-LAYER MODELS

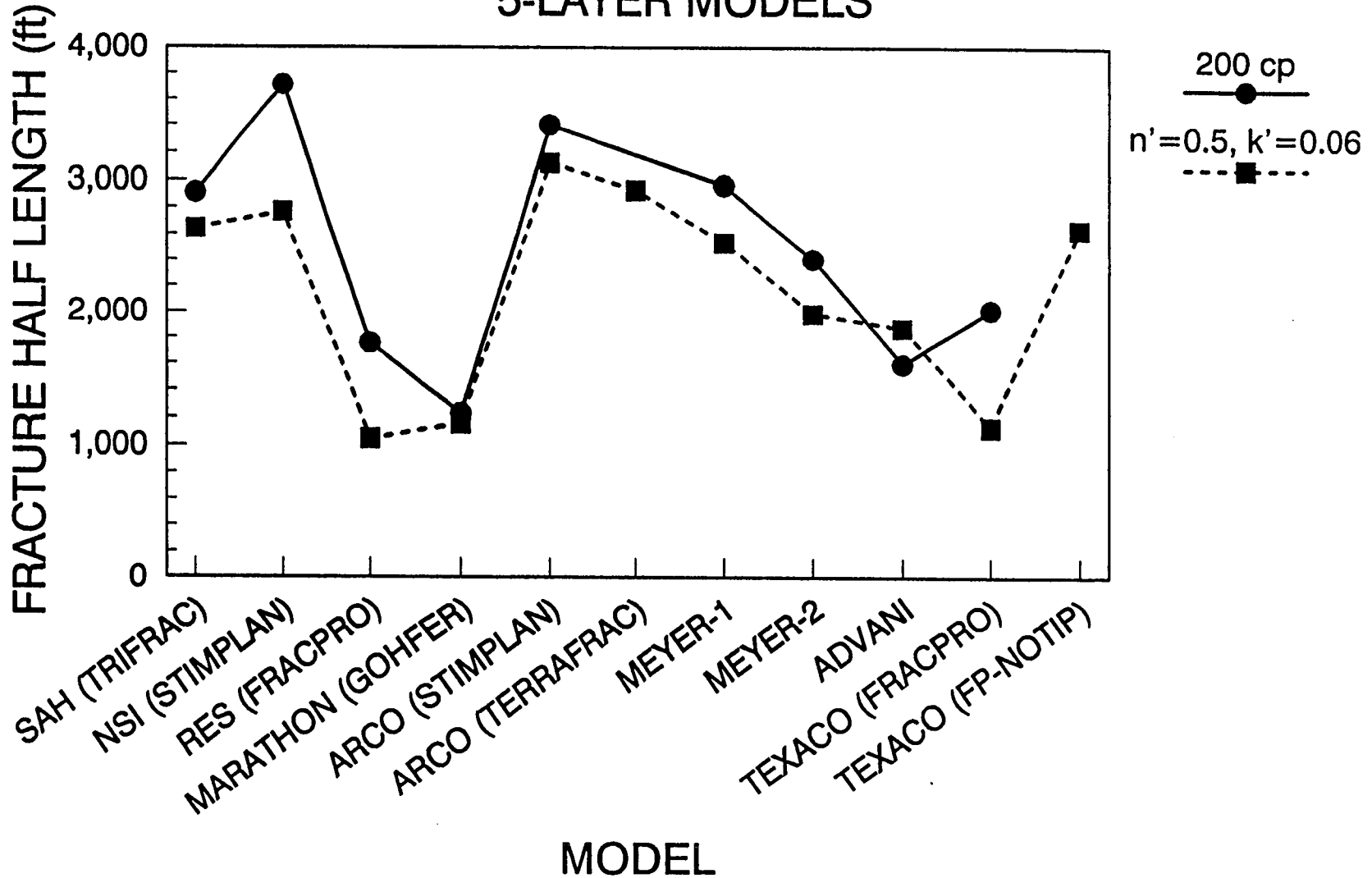


Figure 40 Length comparison for cases 7 and 8

# FRACTURE HEIGHT

## 5-LAYER MODELS

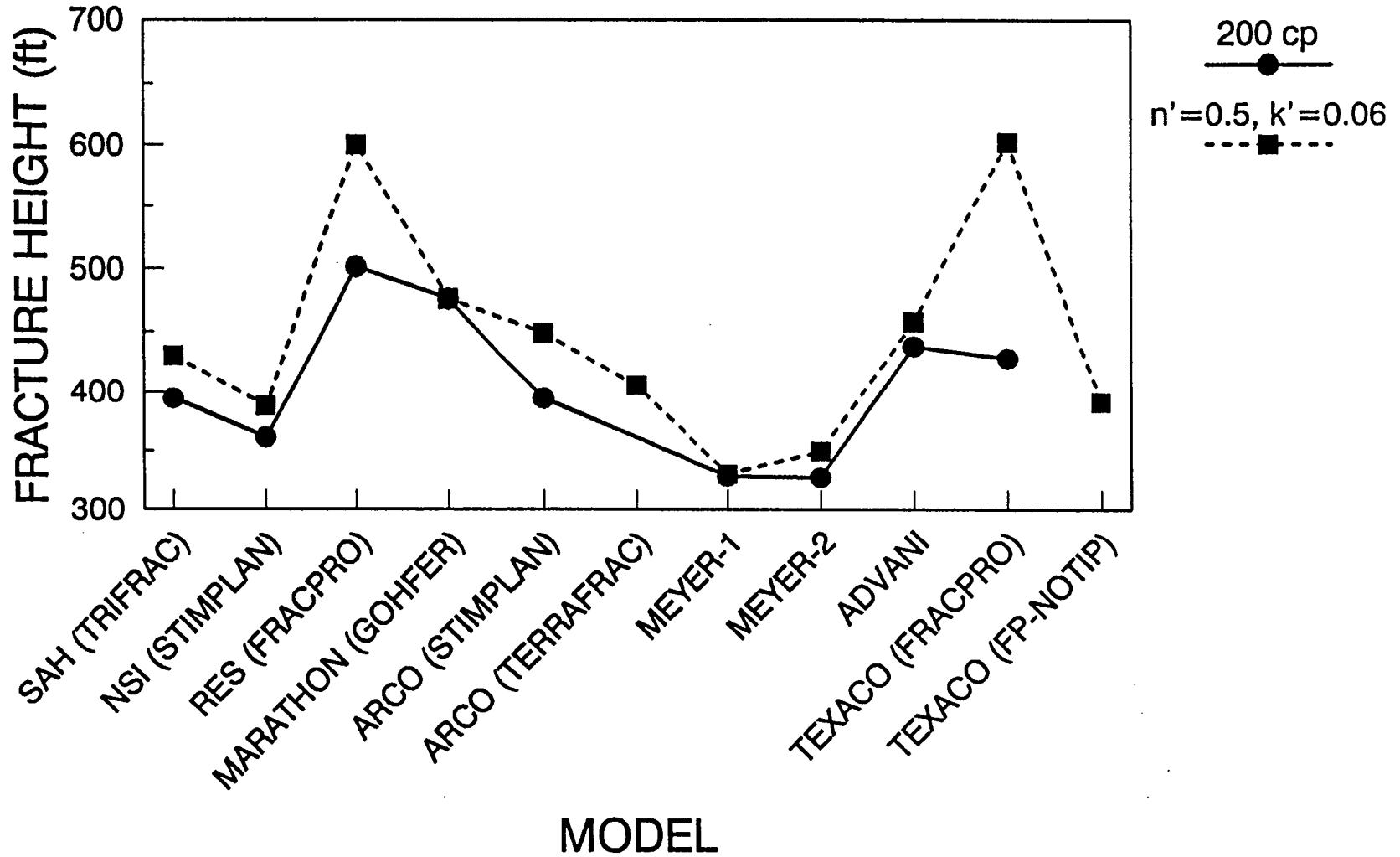


Figure 41 Height comparison for cases 7 and 8

# FRACTURE NET PRESSURE

## 5-LAYER MODELS

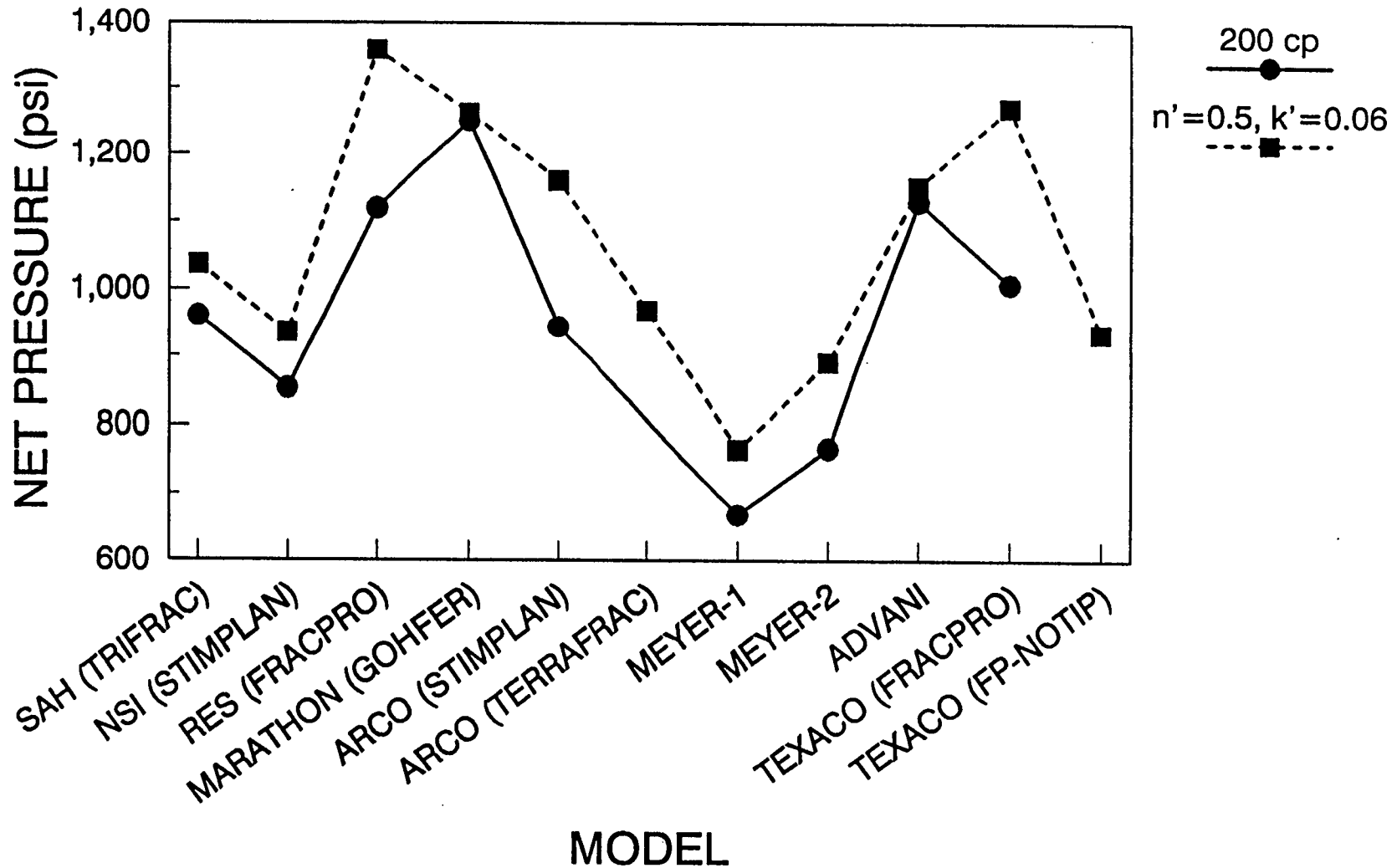


Figure 42 Net pressure comparison for cases 7 and 8

# FRACTURE EFFICIENCY

## 5-LAYER MODELS

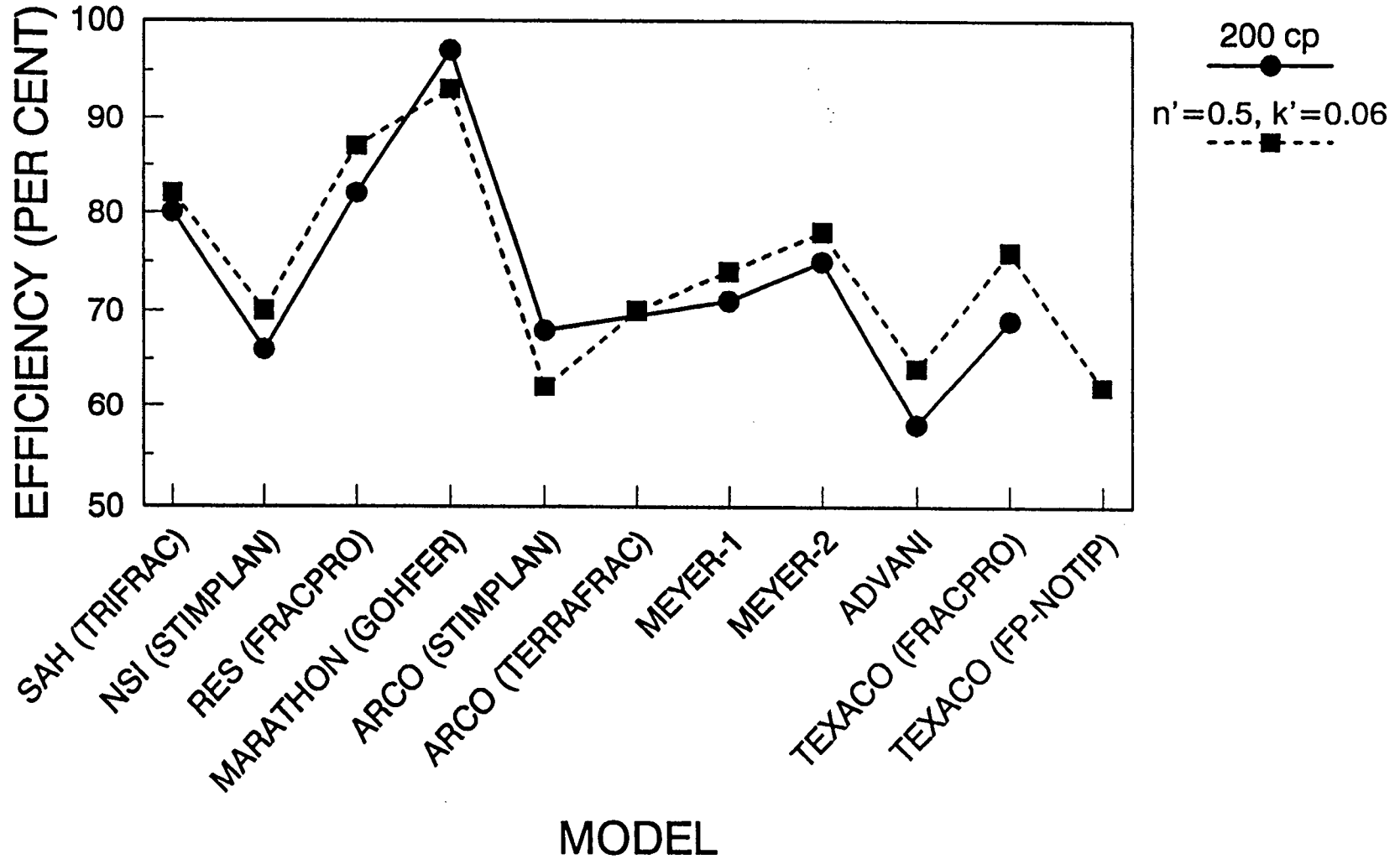


Figure 43 Efficiency comparison for cases 7 and 8

# FRACTURE MAXIMUM WIDTH

## 5-LAYER MODELS

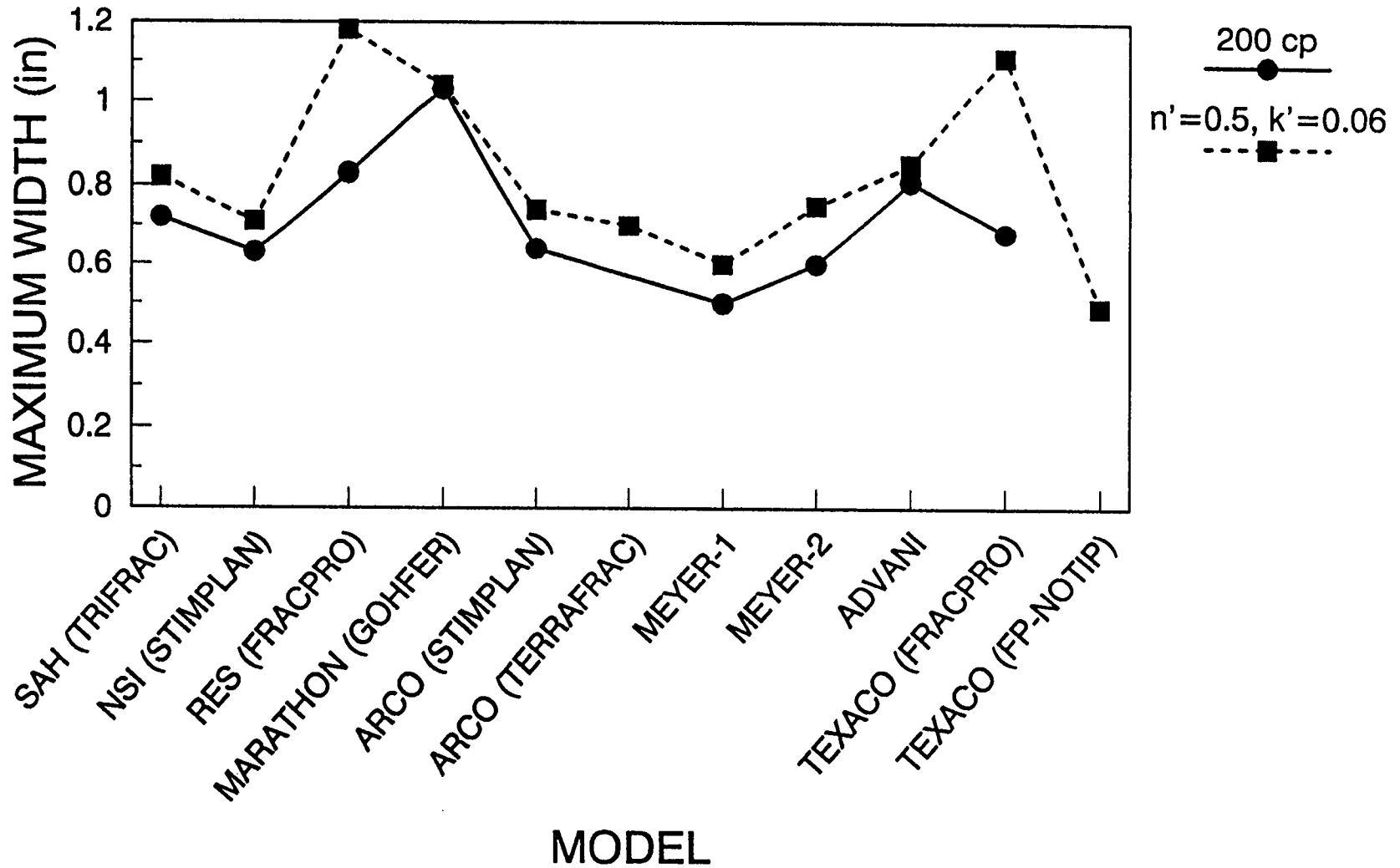


Figure 44 Comparison of maximum width at wellbore for cases 7 and 8

# FRACTURE AVERAGE WIDTH AT WELLBORE

## 5-LAYER MODELS

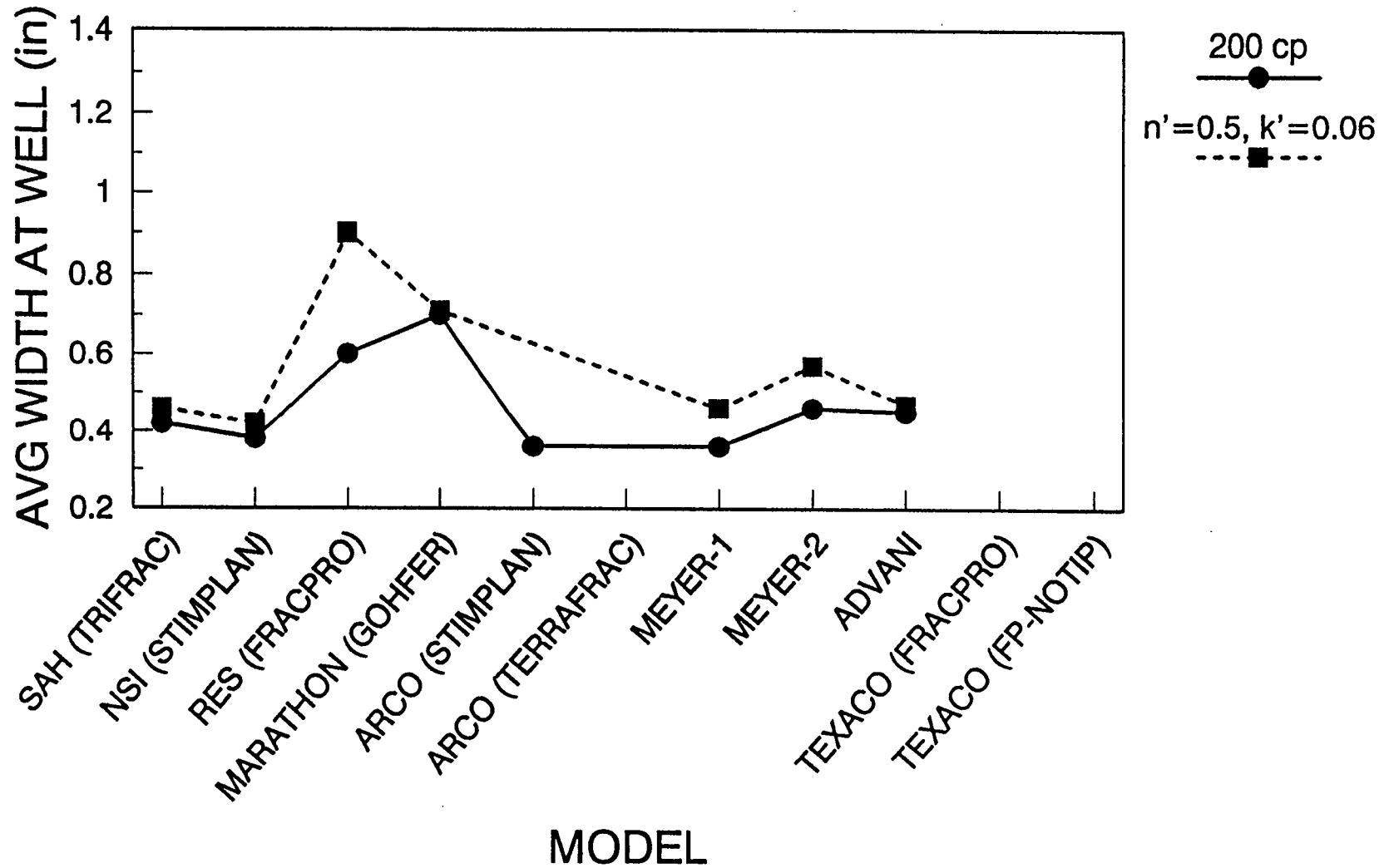


Figure 45 Comparison of average width at wellbore for cases 7 and 8

# FRACTURE AVERAGE WIDTH

## 5-LAYER MODELS

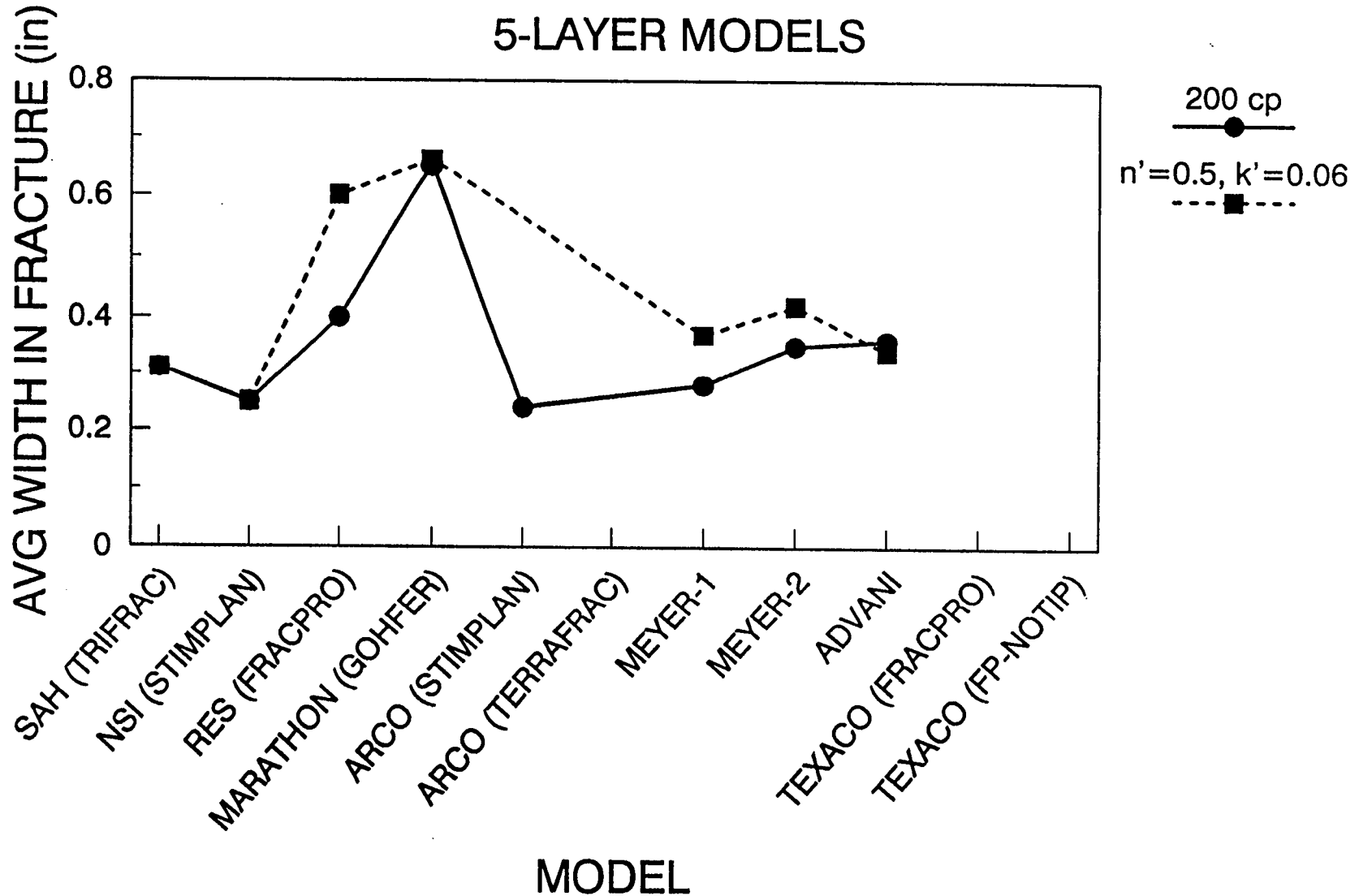


Figure 46 Comparison of average width in fracture for cases 7 and 8

# 5-LAYER MODELS: 200 cp

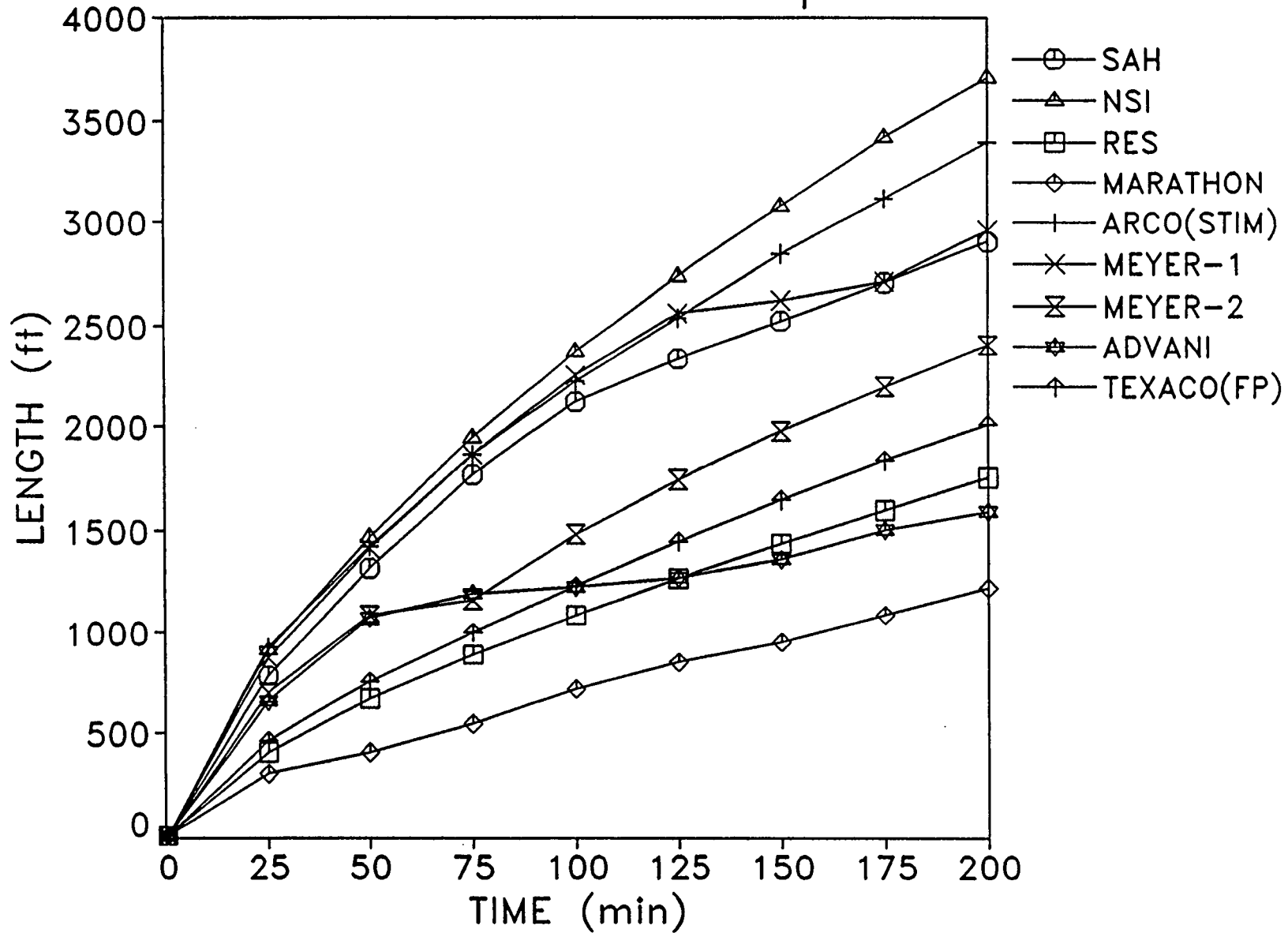


Figure 47 Length history for case 7

# 5-LAYER MODELS: 200 cp

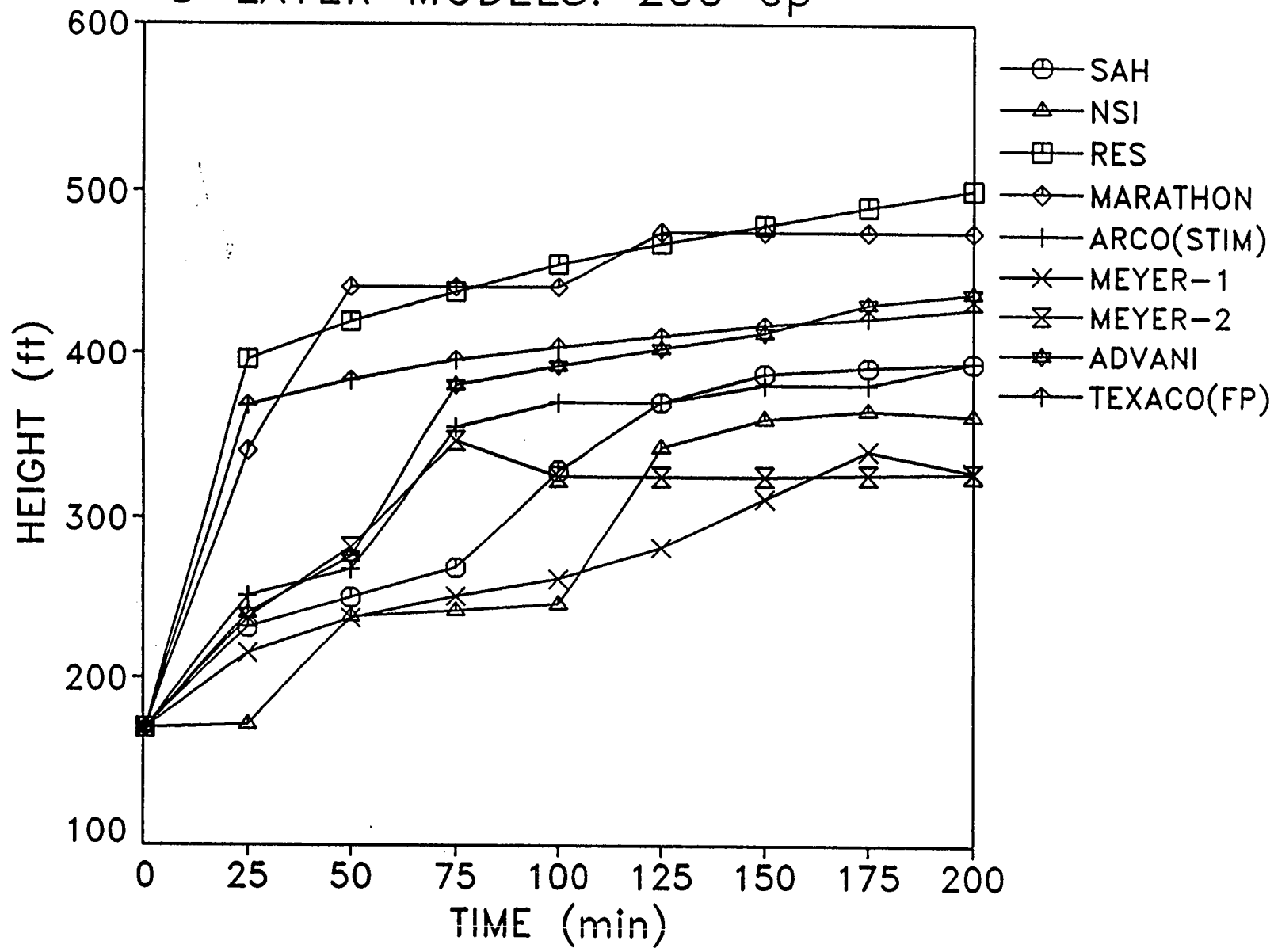


Figure 48 Height history for case 7

### 5-LAYER MODELS: 200 cp

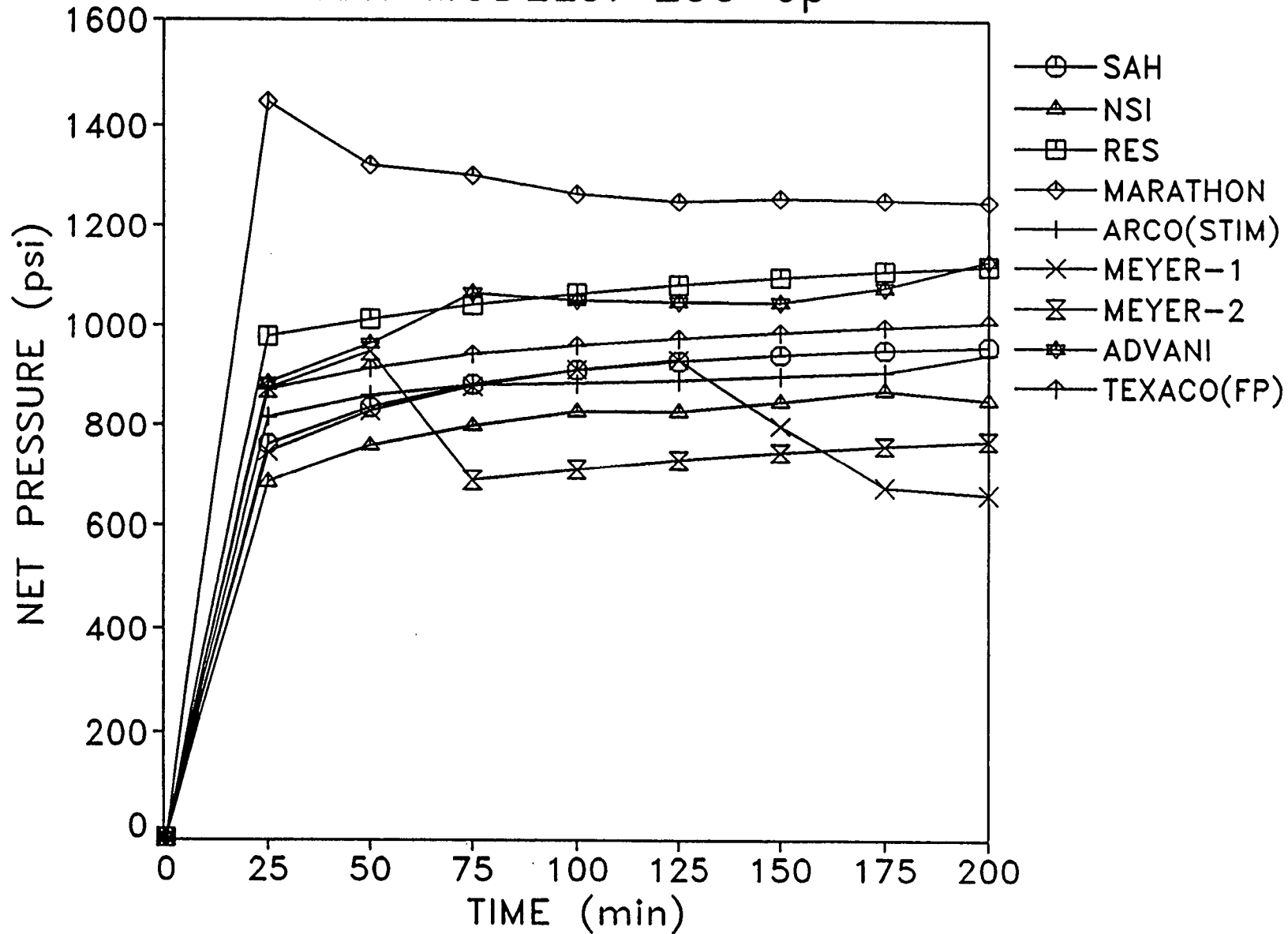


Figure 49 Net pressure history for case 7

# 5-LAYER MODELS: 200 cp

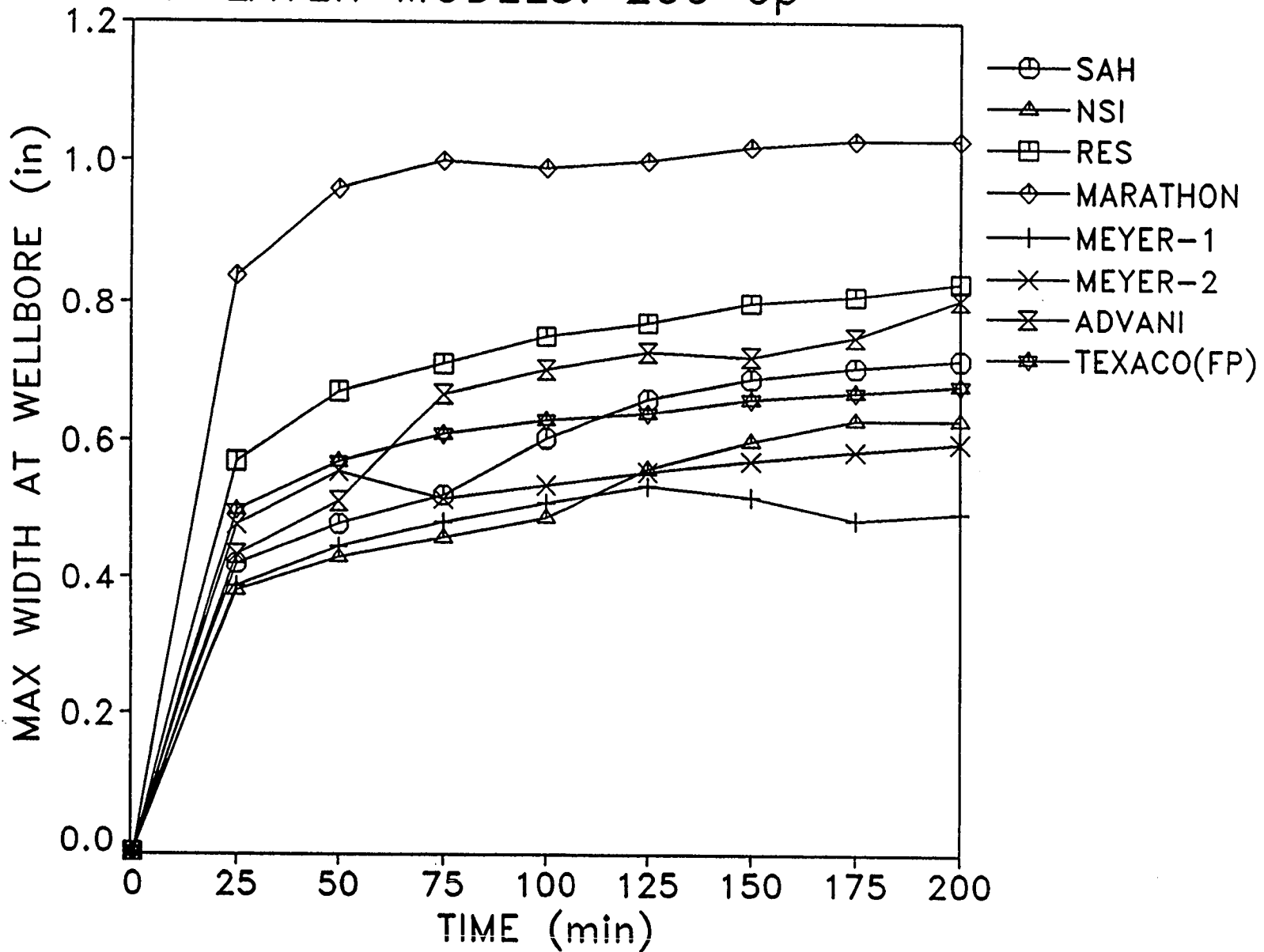


Figure 50 History of width at wellbore for case 7

# 5 LAYER MODELS: n', k'

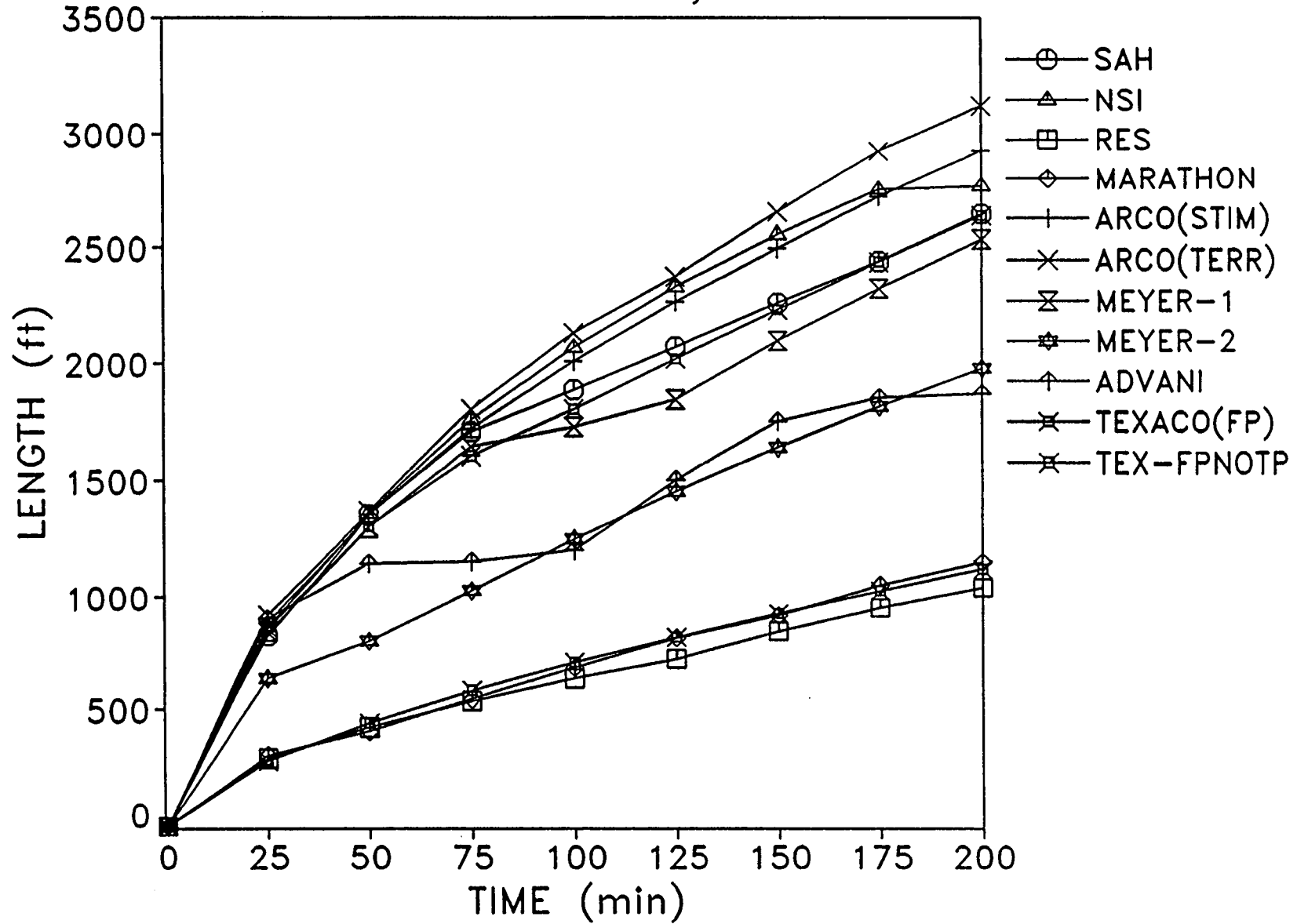


Figure 51 Length history for case 8

# 5-LAYER MODELS: n', k'

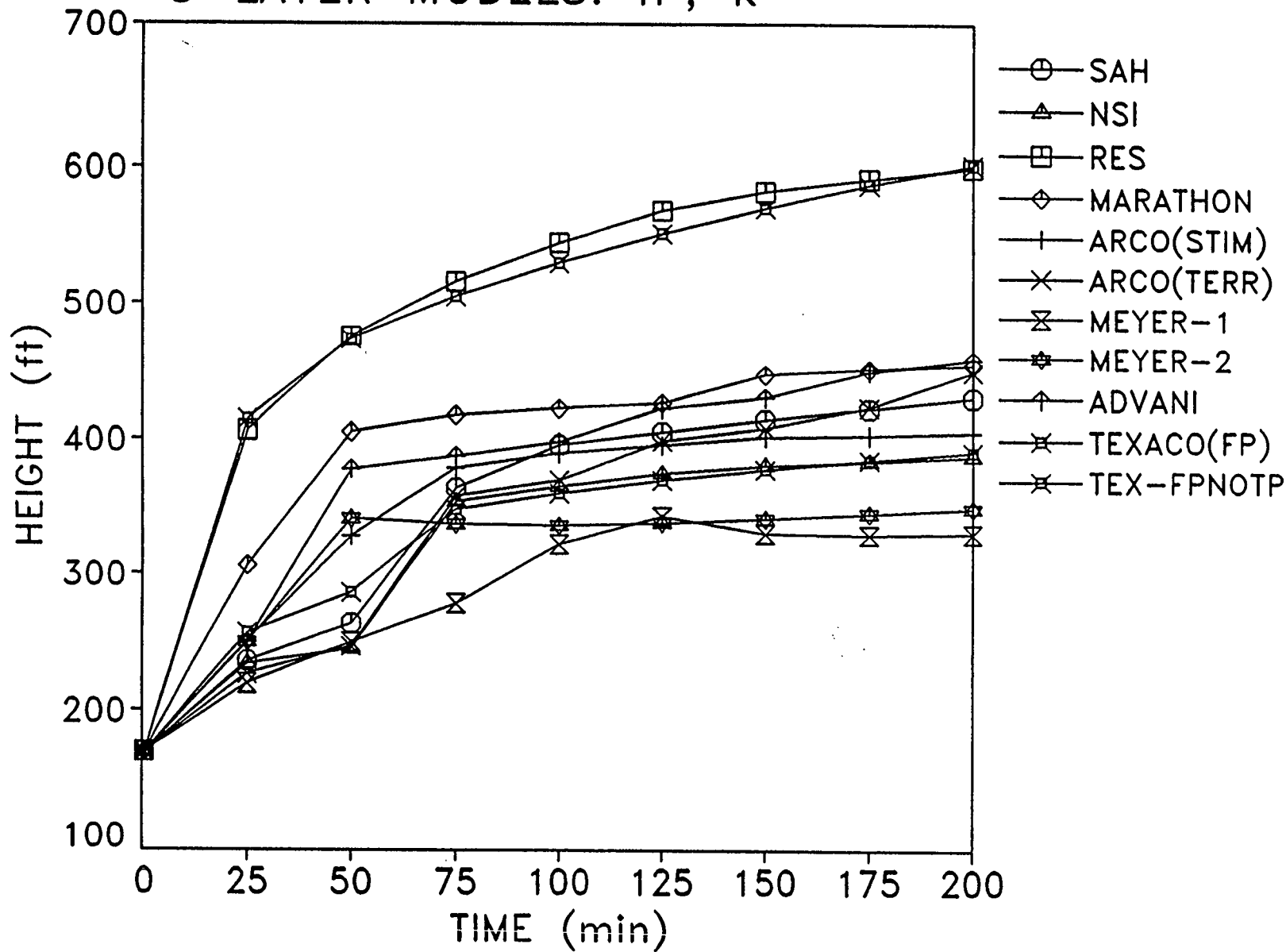


Figure 52 Height history for case 8

### 5-LAYER MODELS: $n'$ , $k'$

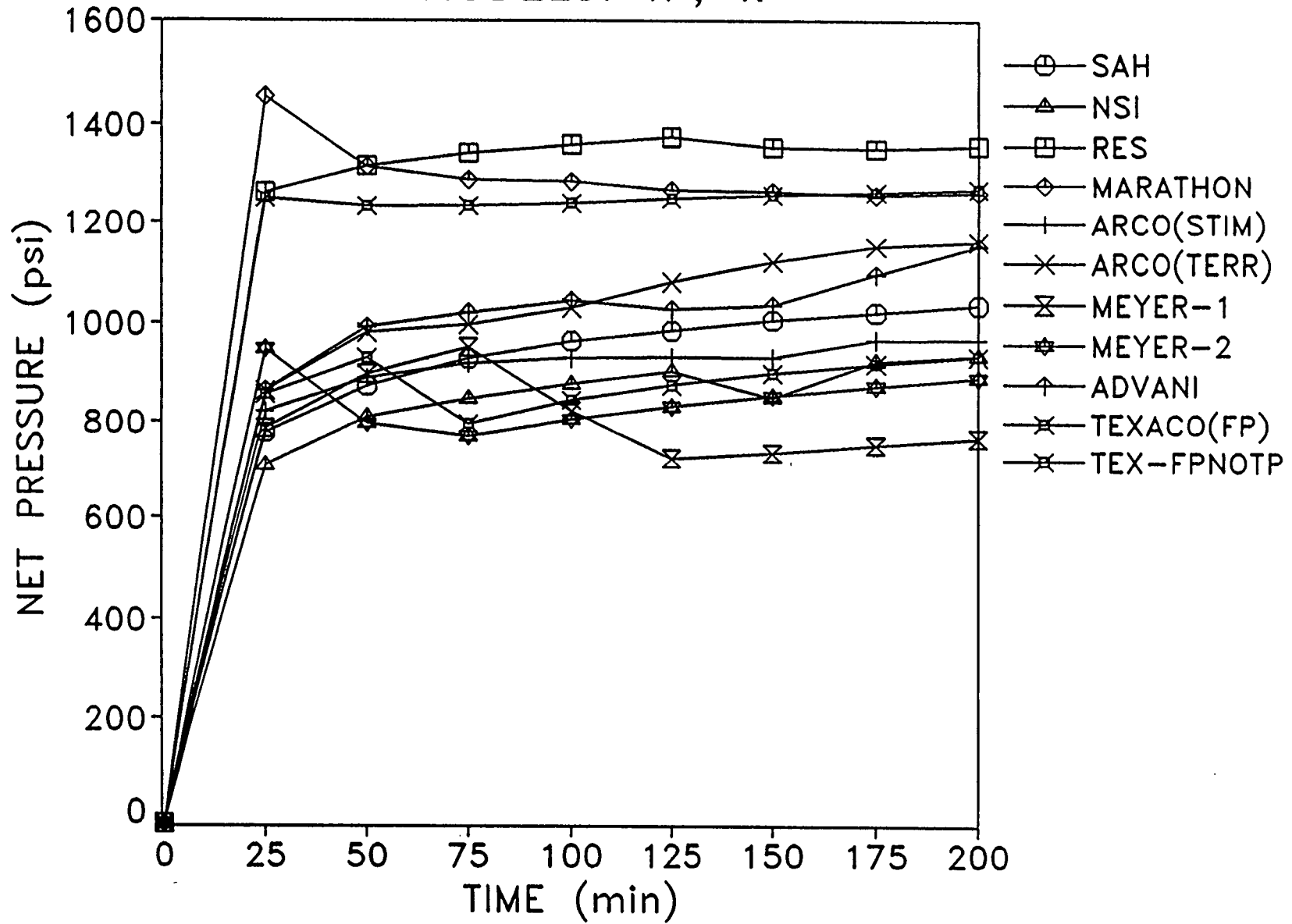


Figure 53 Net pressure history for case 8

# 5-LAYER MODELS: $n'$ , $k'$

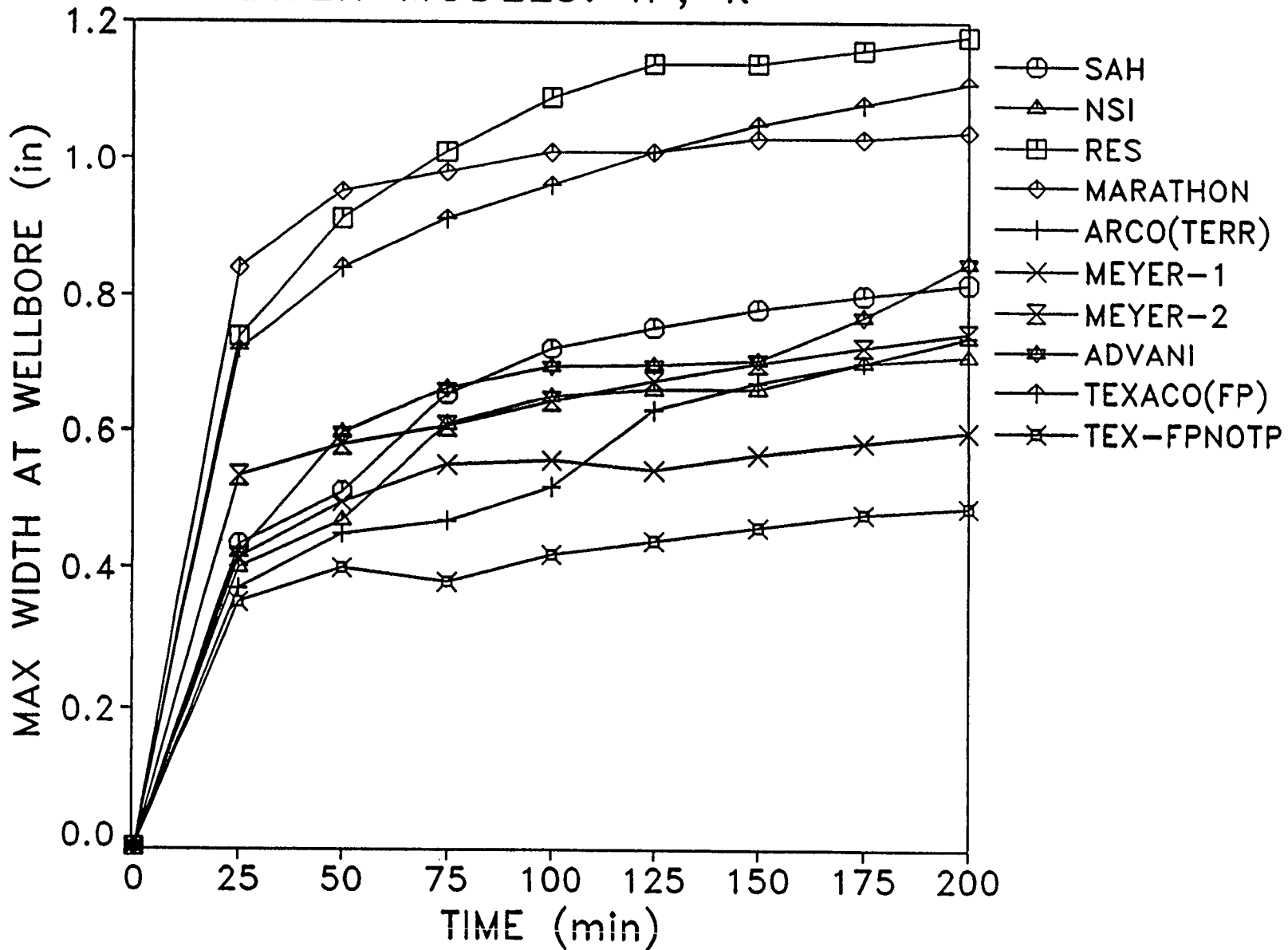


Figure 54 History of width at wellbore for case 8

### **Appendix A Width and height profiles for SAH Trifrac**

Figure A1-A8 give the height profiles and width profiles calculated by Trifrac as a function of length for cases 5-8. These profiles were provided by S.A. Holditch & Assoc. and have not been changed for publication.

Fracture Height Profile Plot  
case a, constant 200 cp fluid (f3-200.DAT)

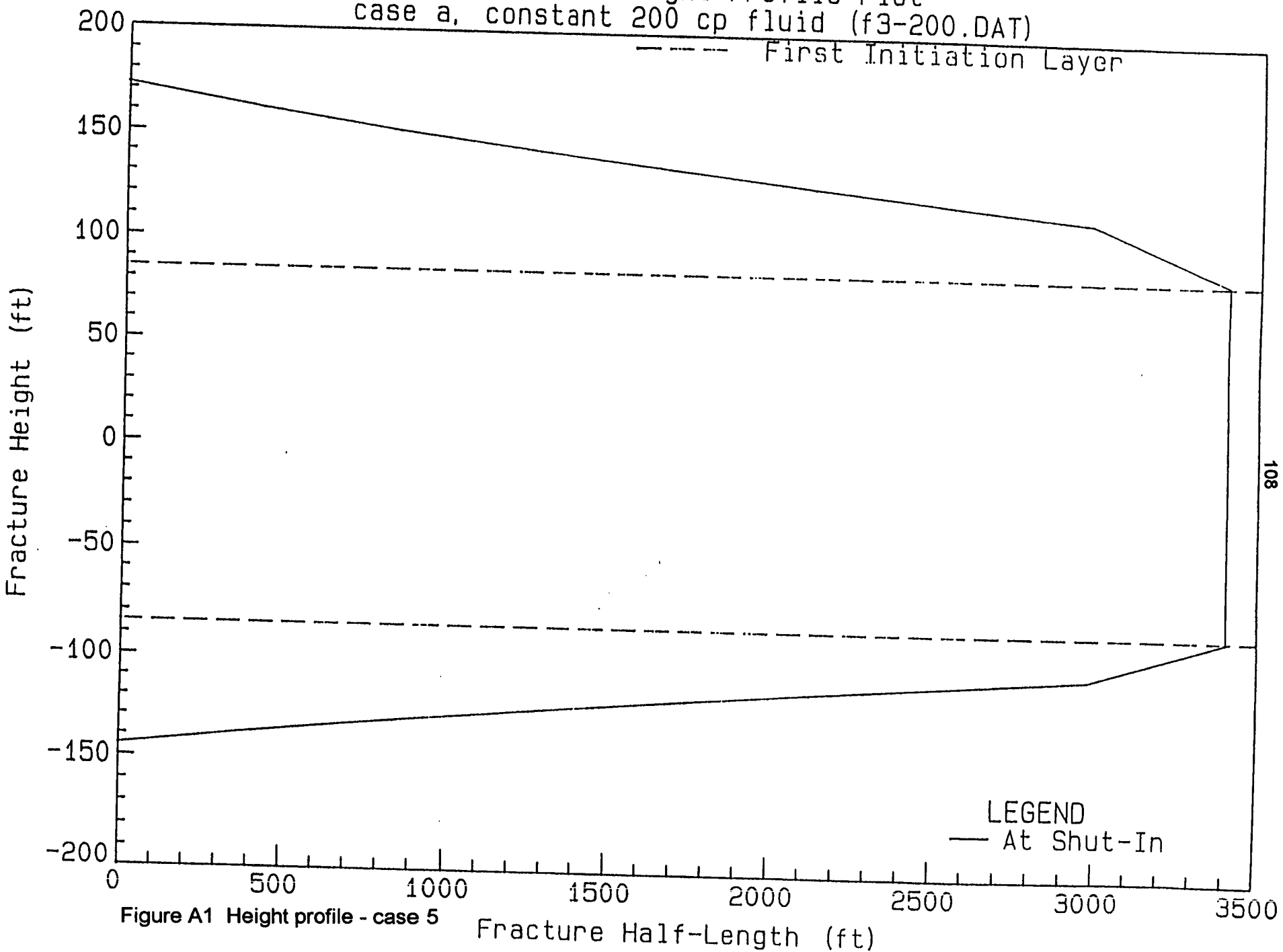
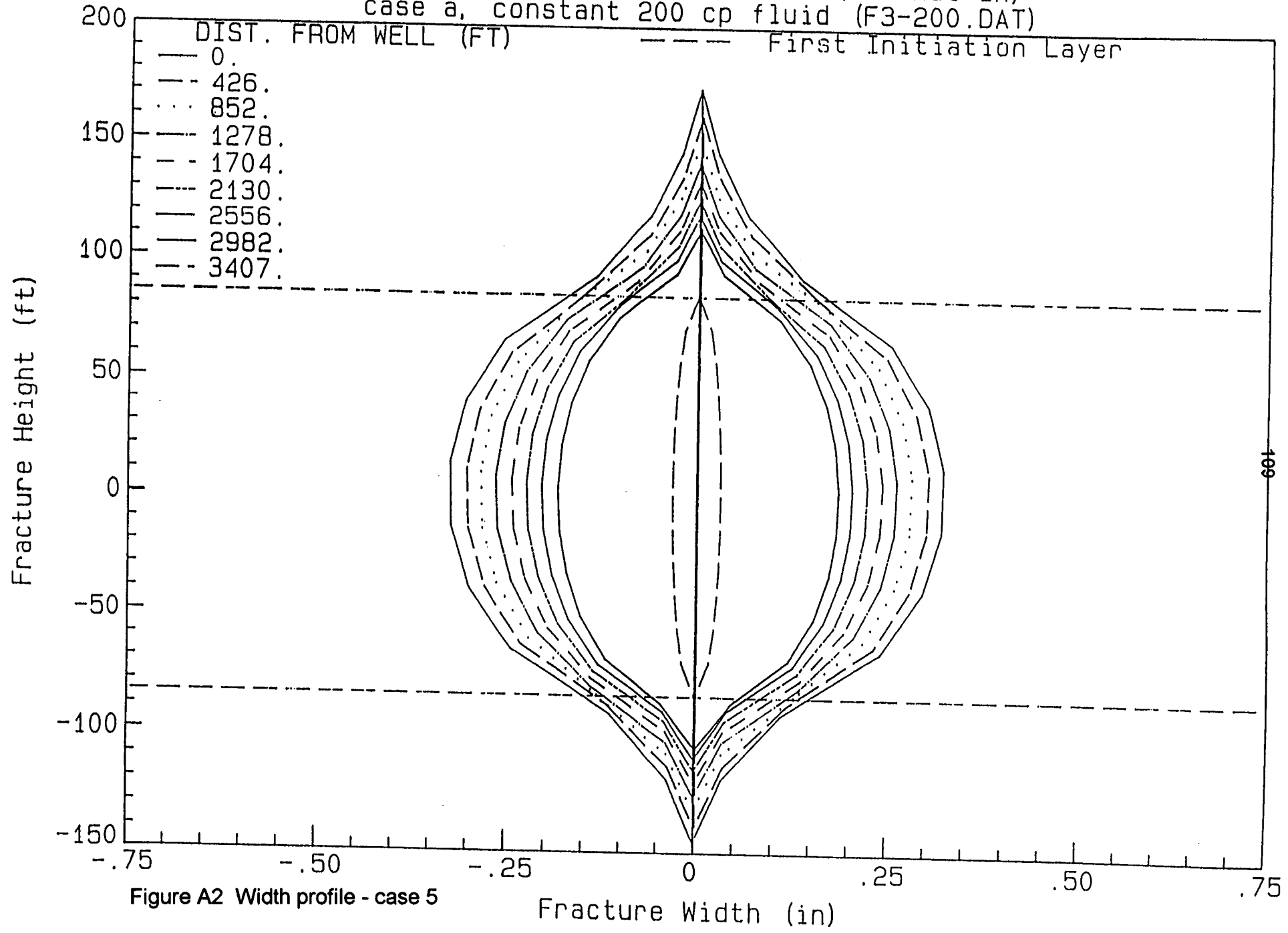


Figure A1 Height profile - case 5

108

Width Profile Down Fracture (At Shut-In)  
case a, constant 200 cp fluid (F3-200.DAT)



Fracture Height Profile Plot  
case b, variable viscosity fluid (f3-v.DAT)

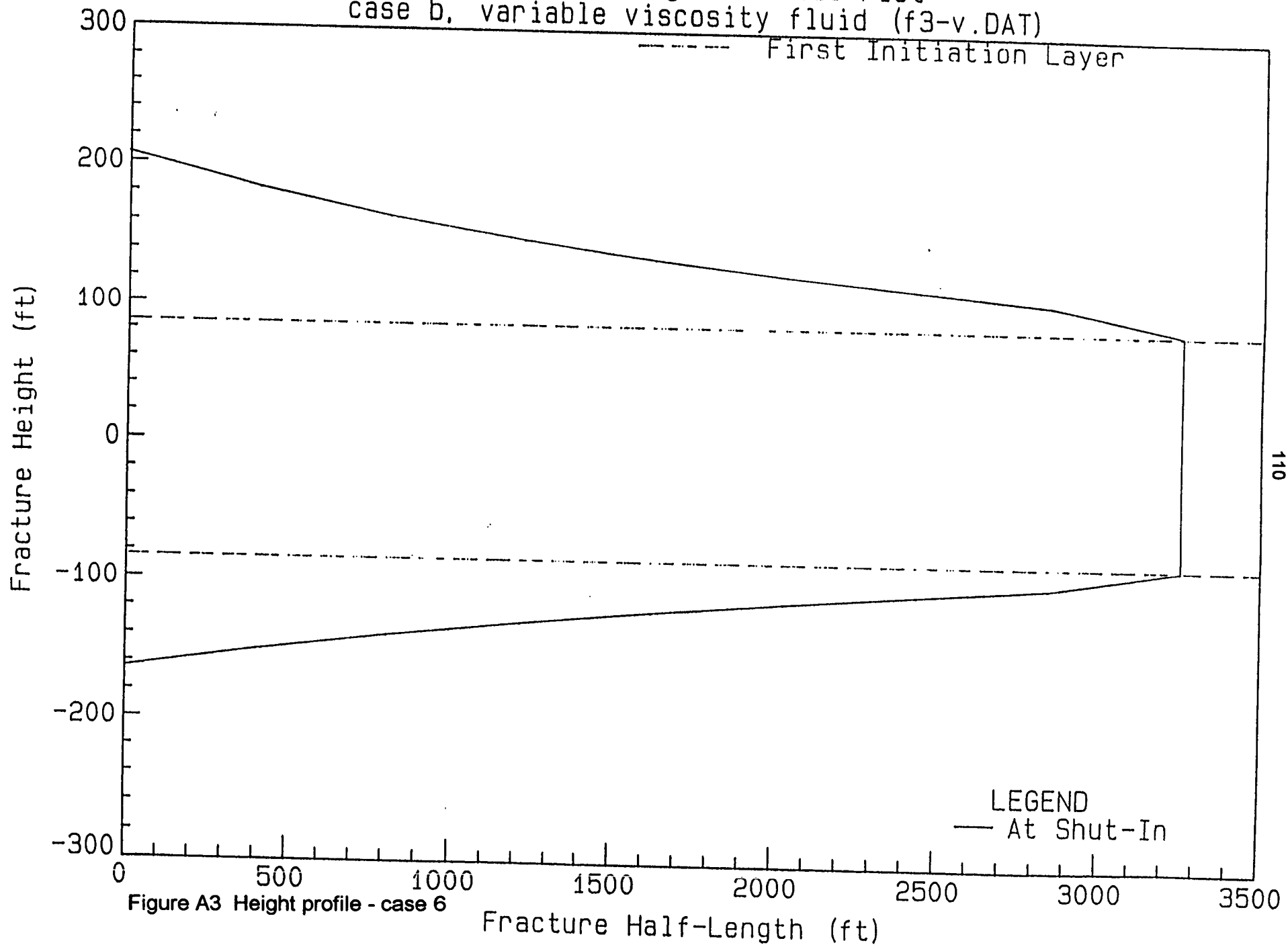
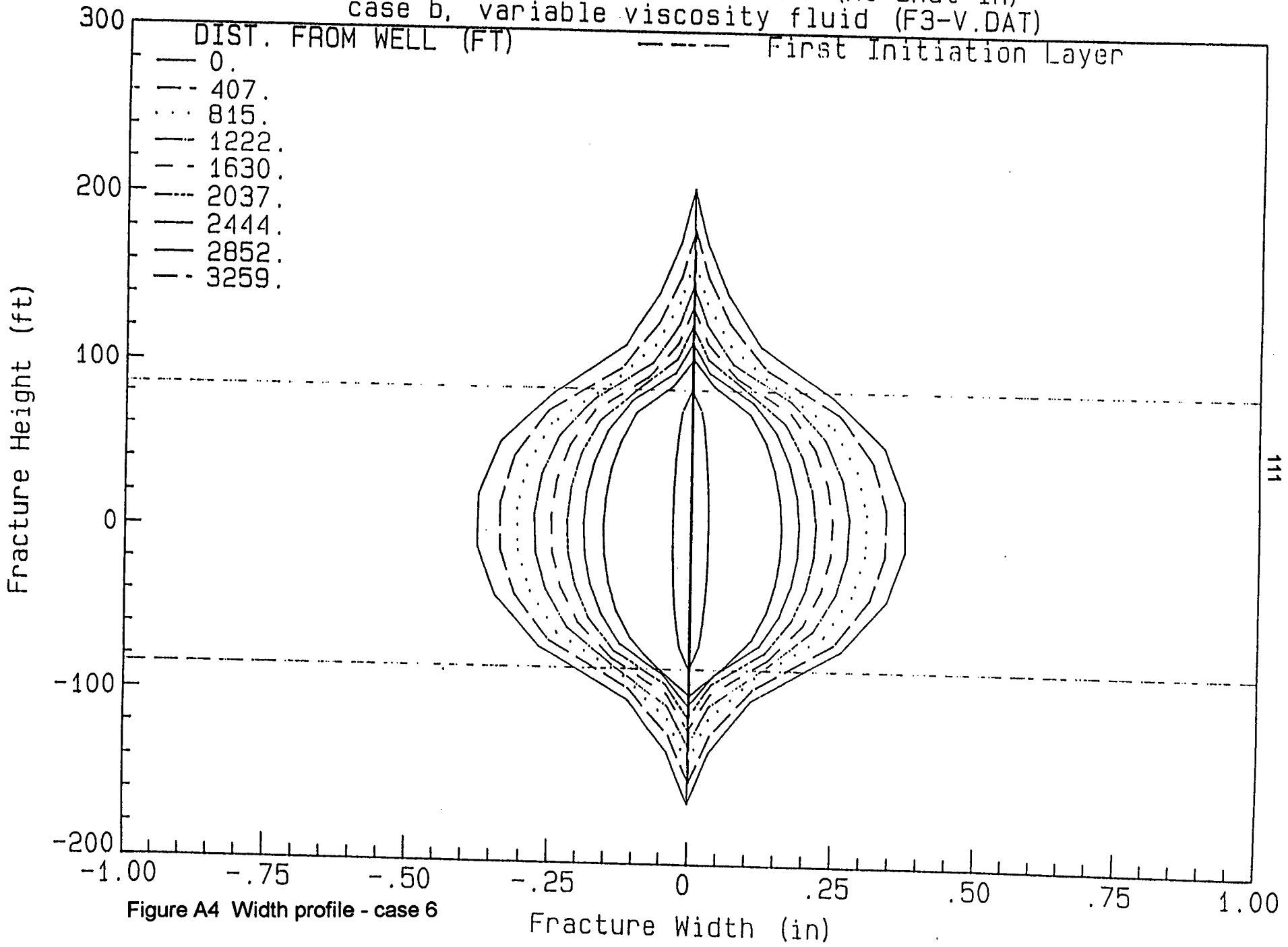


Figure A3 Height profile - case 6

Width Profile Down Fracture (At Shut-In)  
case b, variable viscosity fluid (F3-V.DAT)



Fracture Height Profile Plot  
case b, 200 cp fluid (f5-200.DAT)

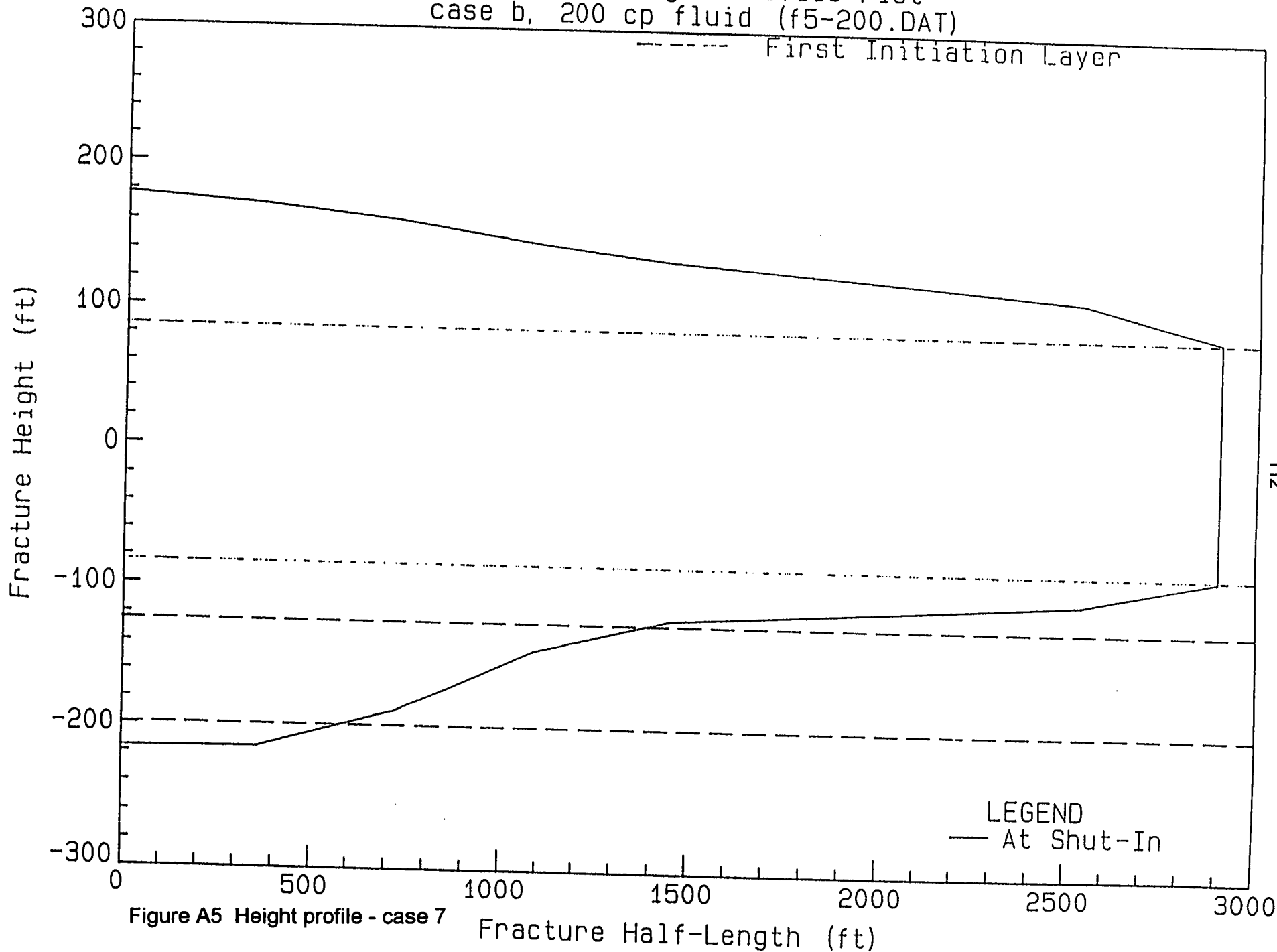


Figure A5 Height profile - case 7

Width Profile Down Fracture (At Shut-In)  
case b, 200 cp fluid (F5-200.DAT)

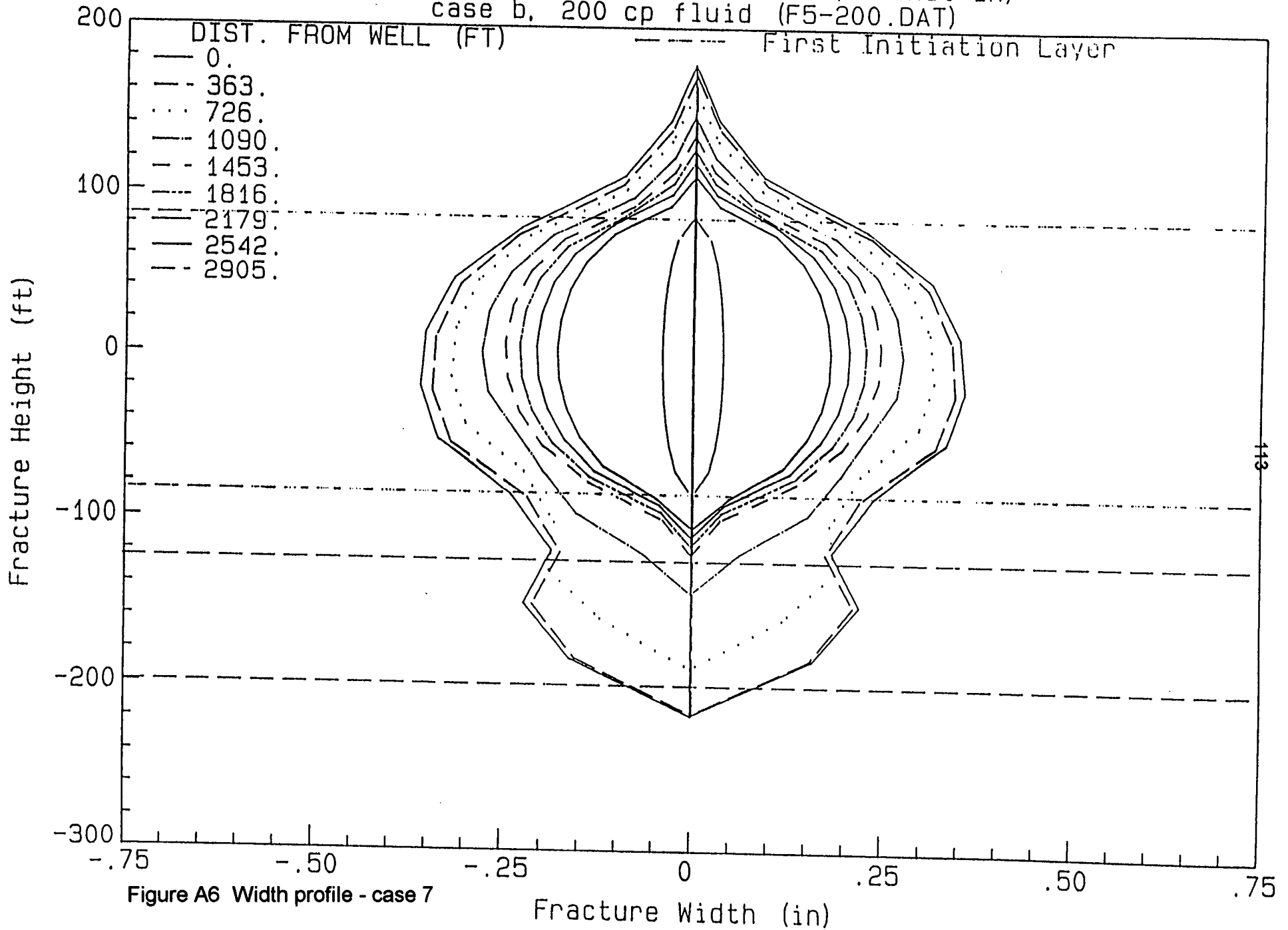


Figure A6 Width profile - case 7

Fracture Height Profile Plot  
case b, variable viscosity fluid (f5-v.DAT)

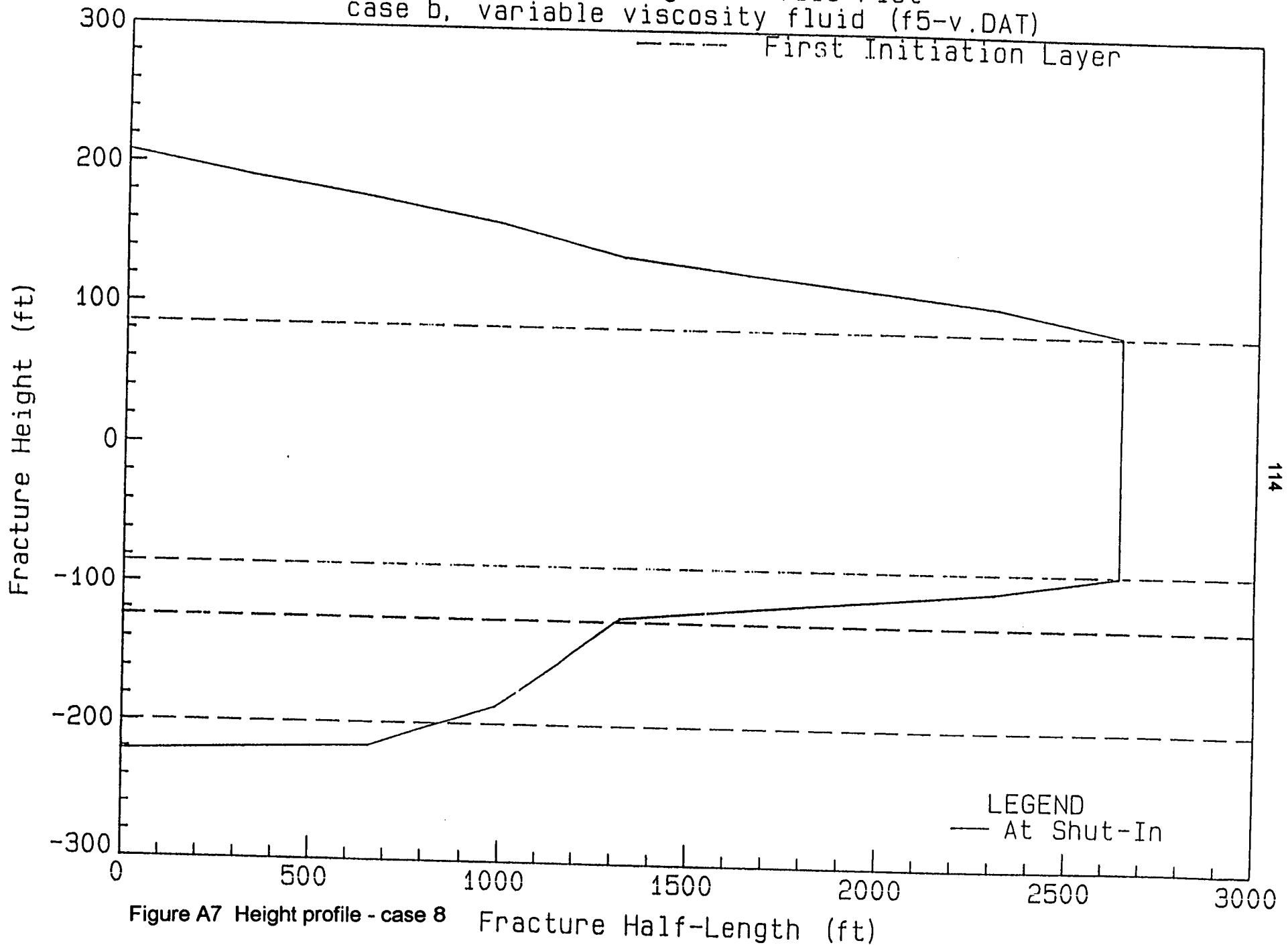
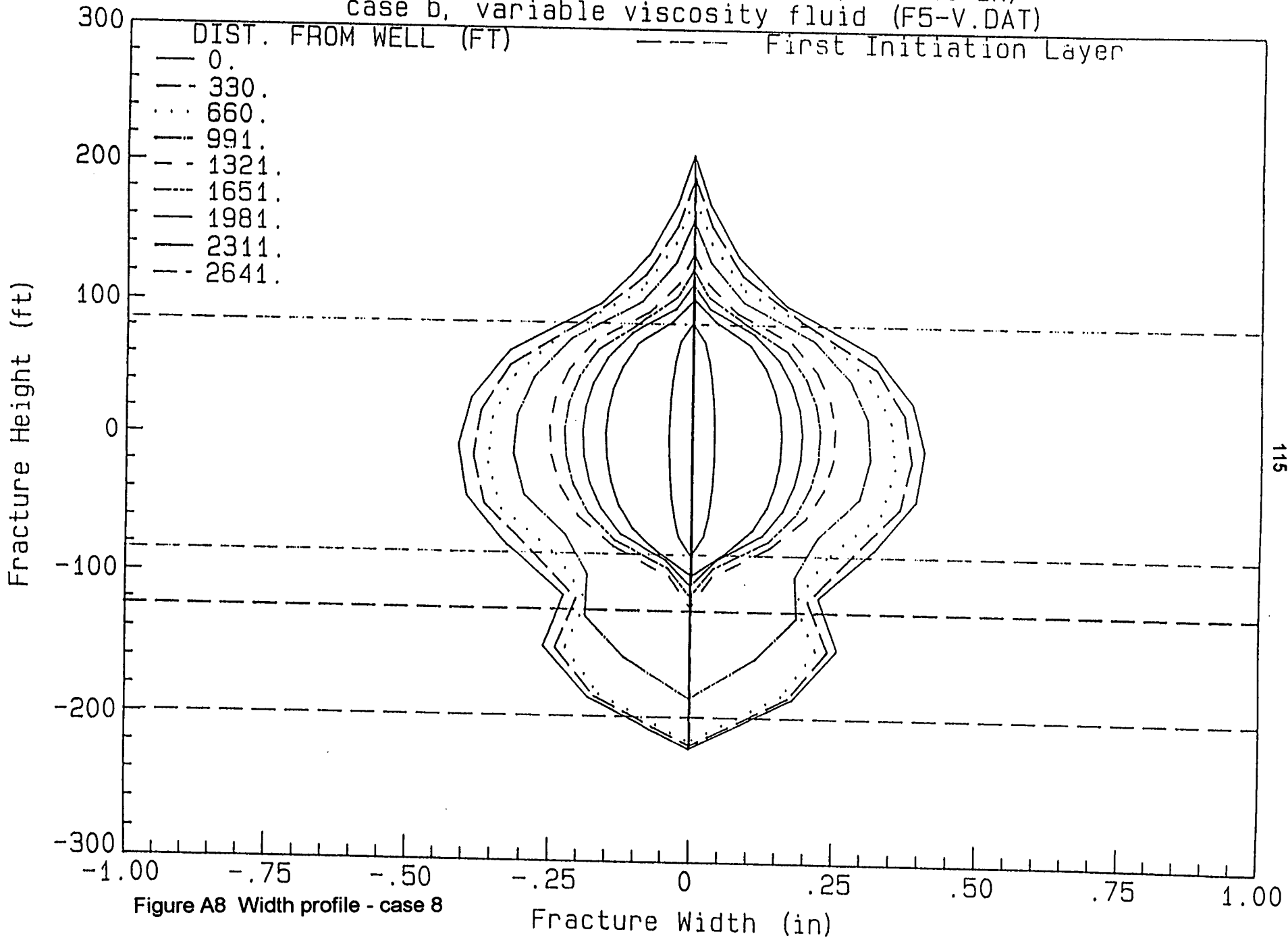


Figure A7 Height profile - case 8

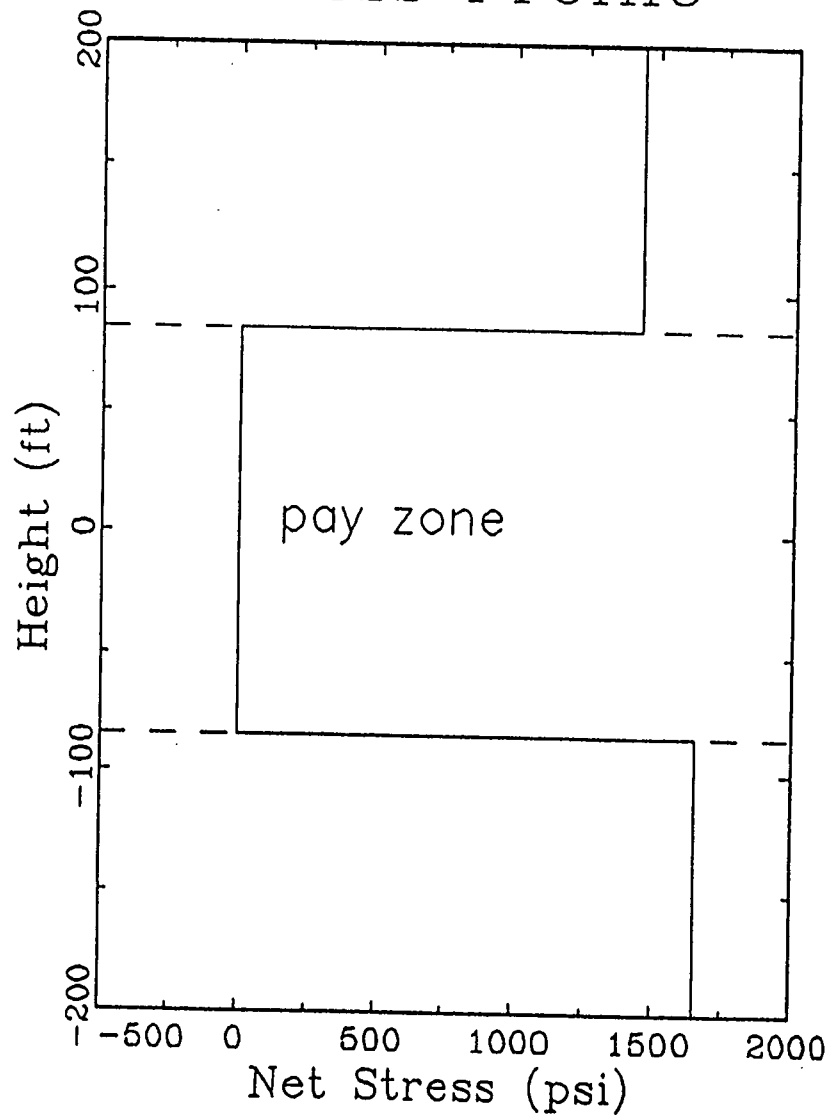
Width Profile Down Fracture (At Shut-In)  
case b, variable viscosity fluid (F5-V.DAT)



**Appendix B Width and height profiles for Meyer-1**

Figure B1-B8 give the height profiles and width profiles calculated by MFRAC-II (no "knobs") as a function of length for cases 5-8. These profiles were provided by Meyer & Assoc. and have not been changed for publication.

# Stress Profile



# Vert. Width Profile

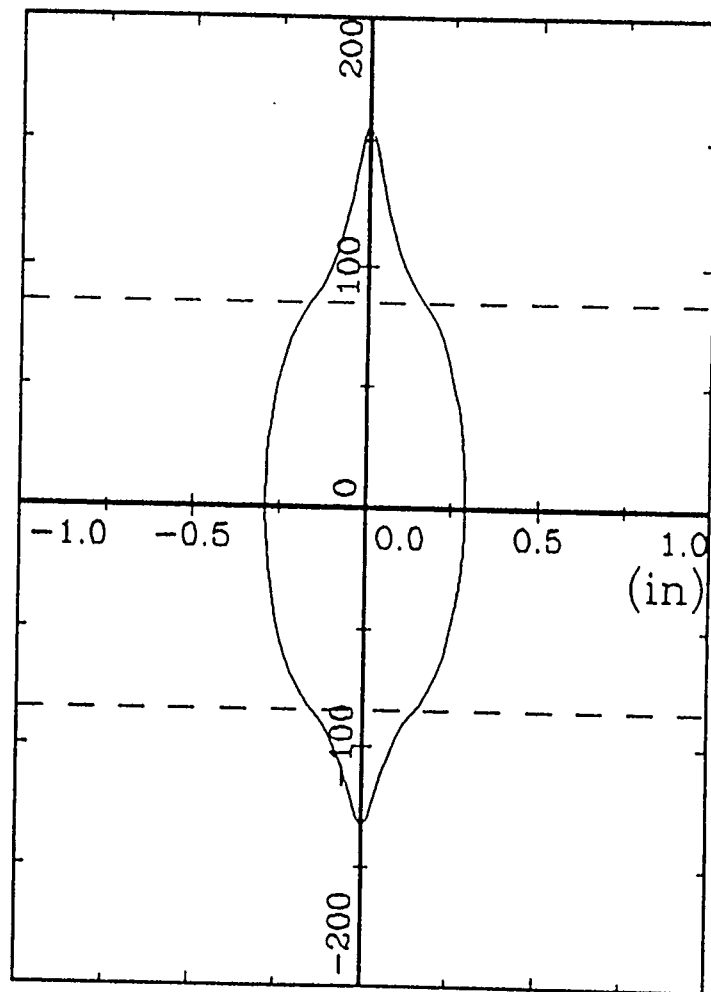


Figure B1 Height profile - case 5

# Width Profile Contours

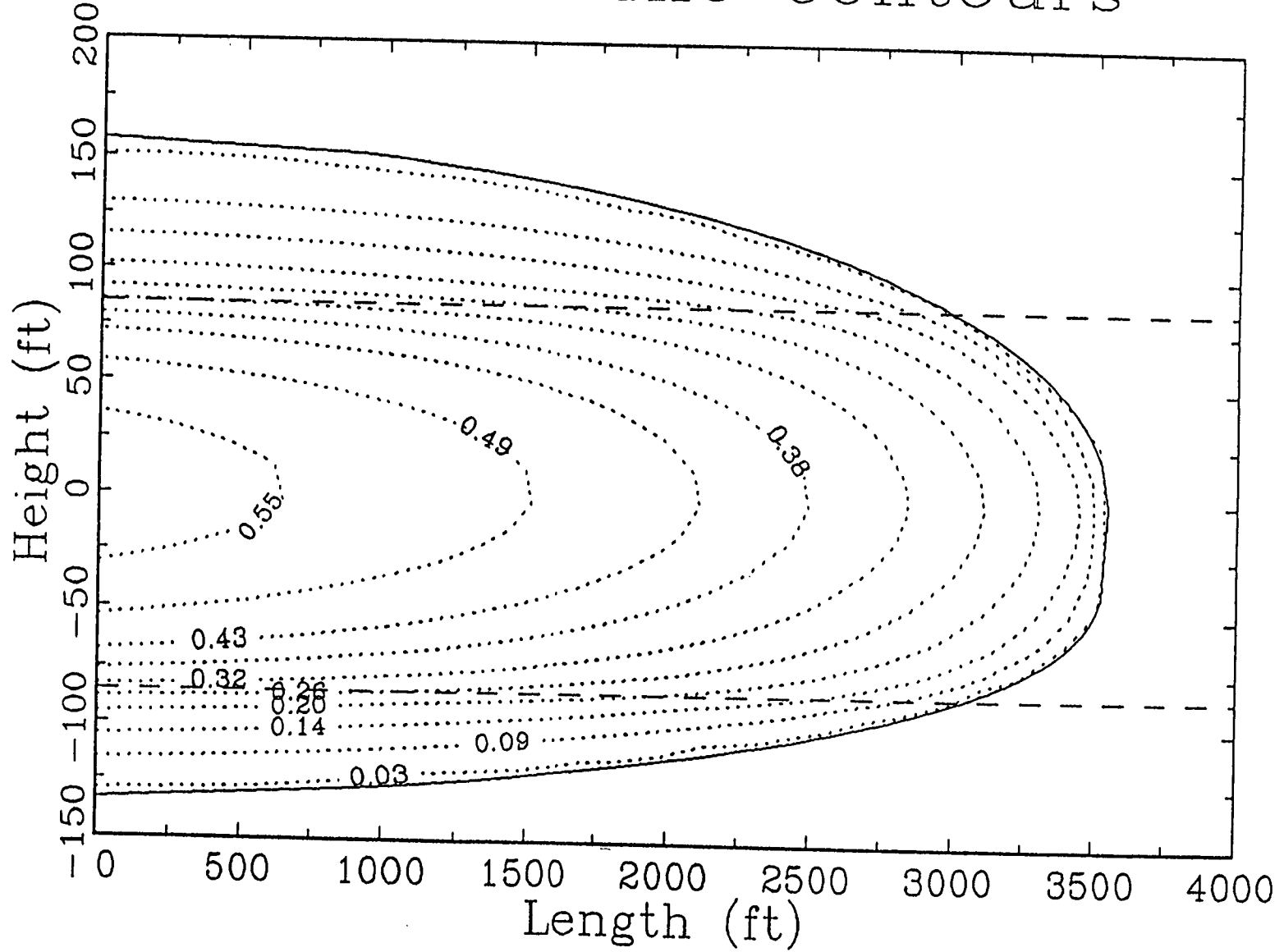
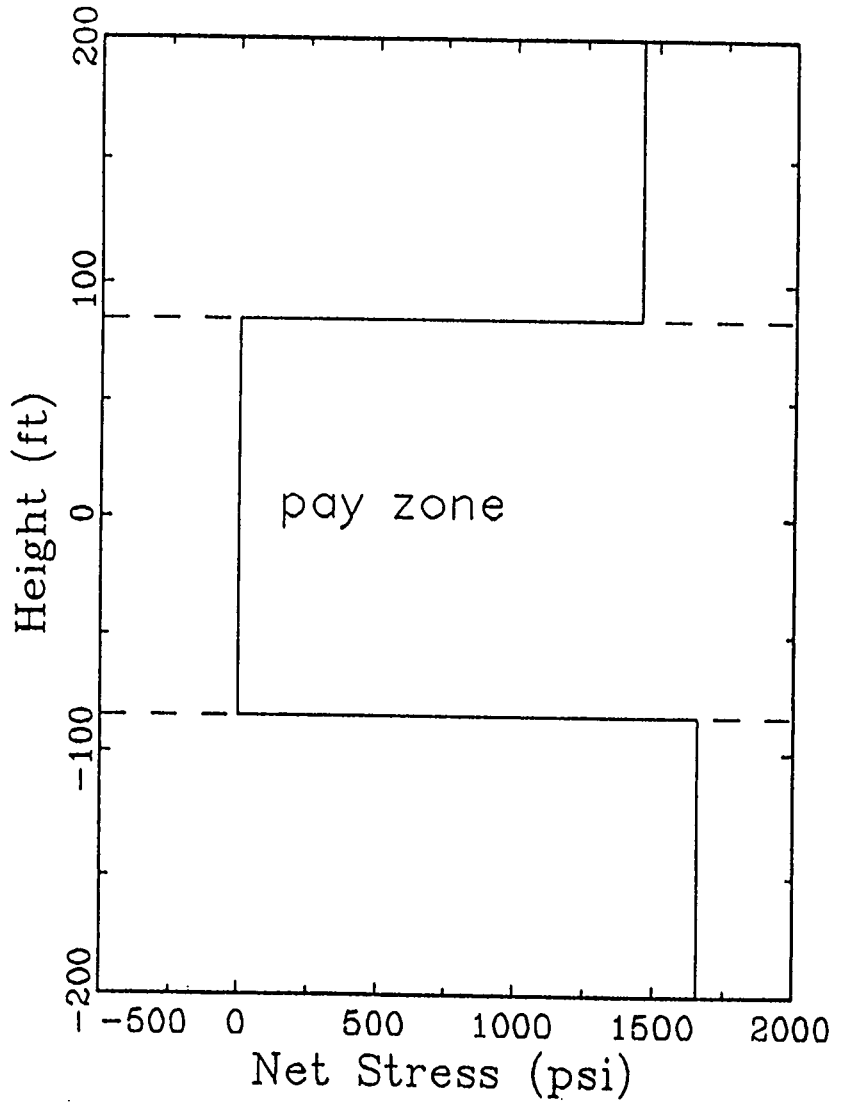


Figure B2 Width profile - case 5

# Stress Profile



# Vert. Width Profile

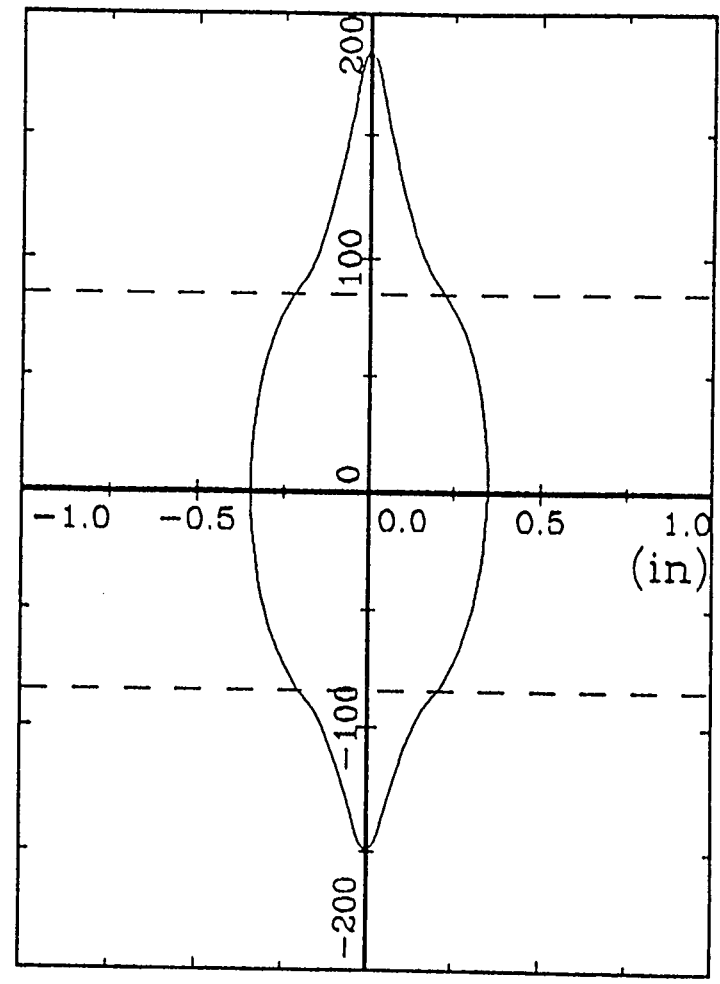


Figure B3 Height profile - case 6

# Width Profile Contours

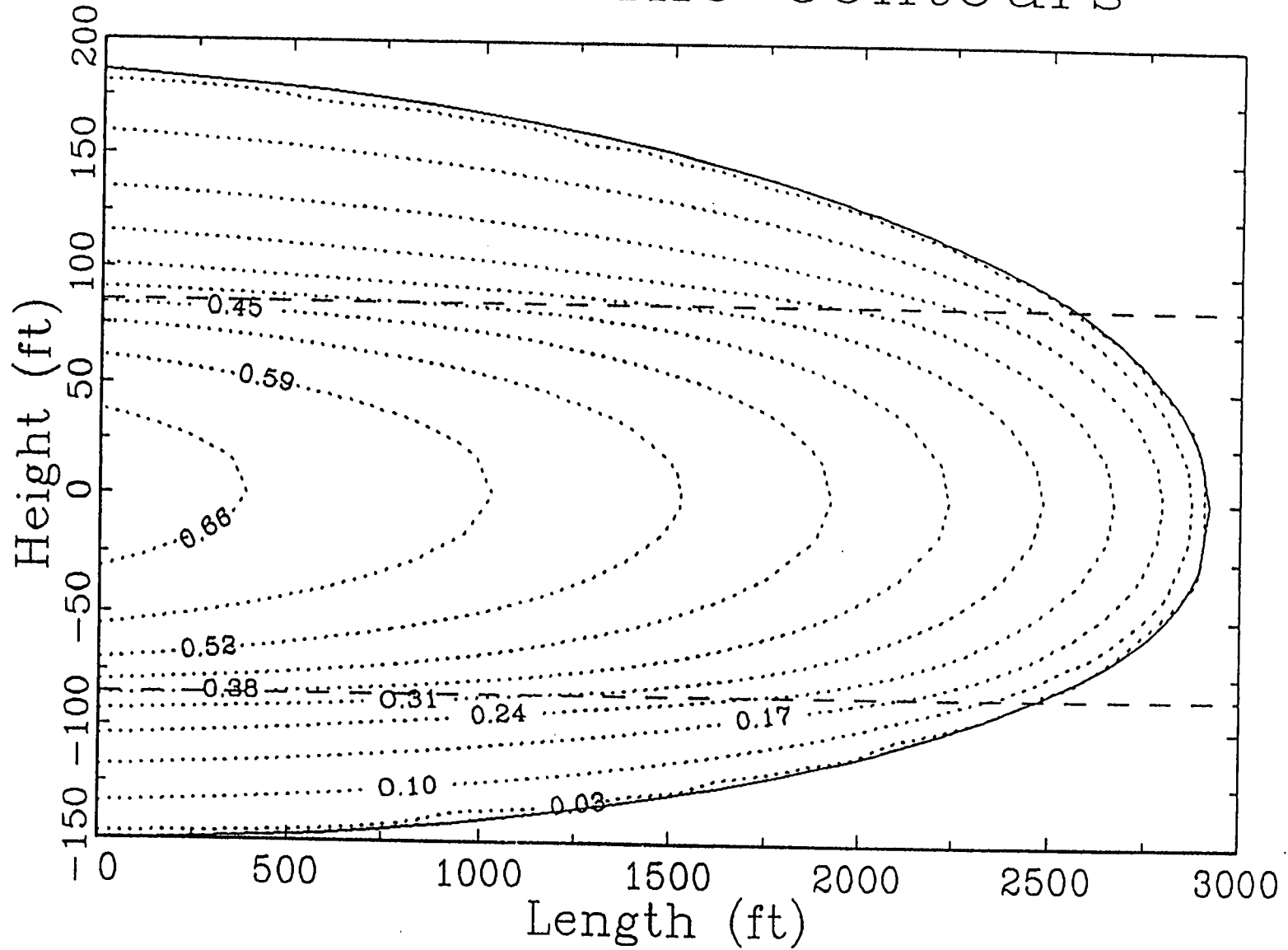


Figure B4 Width profile - case 6

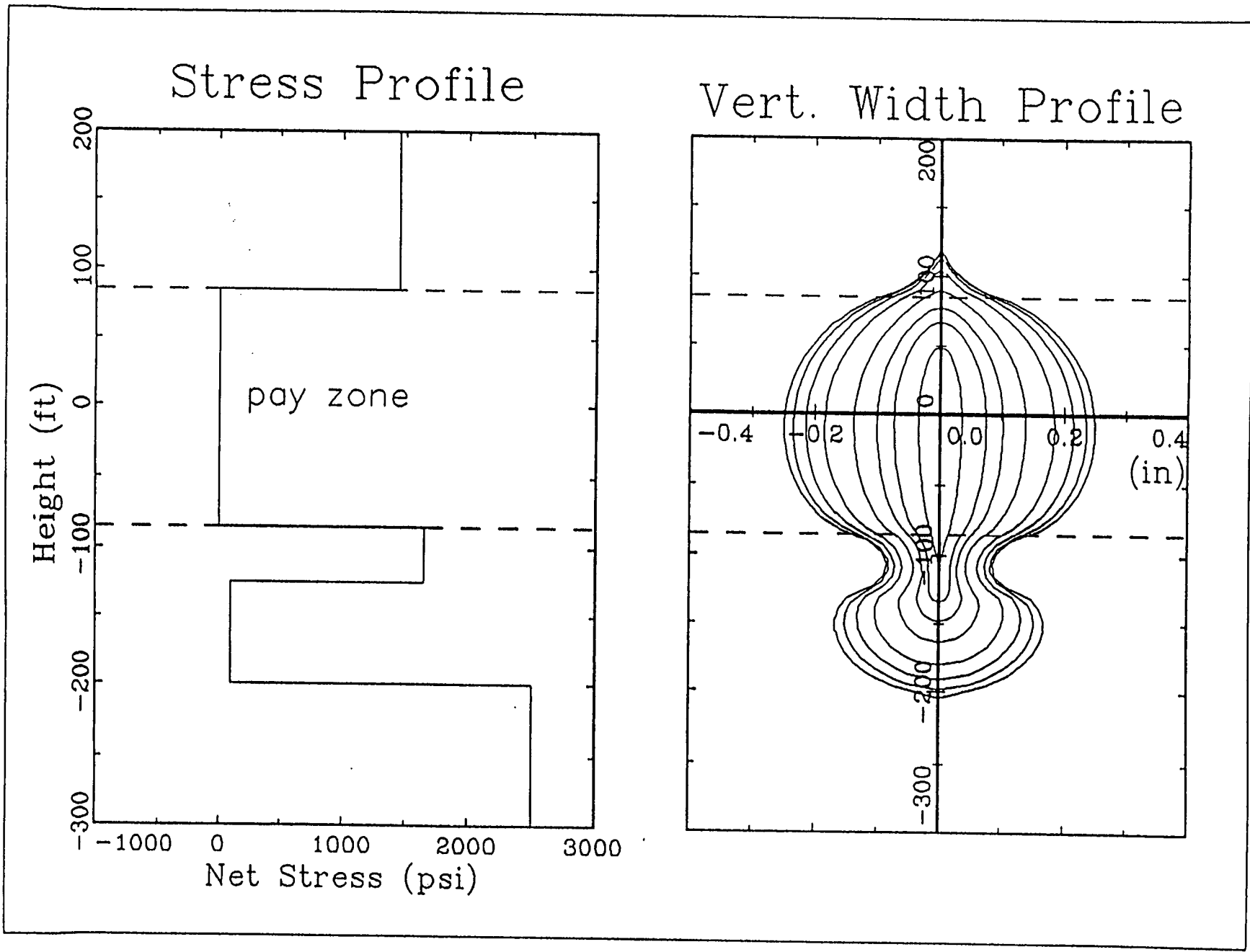


Figure B5 Height profile - case 7

# Width Profile Contours

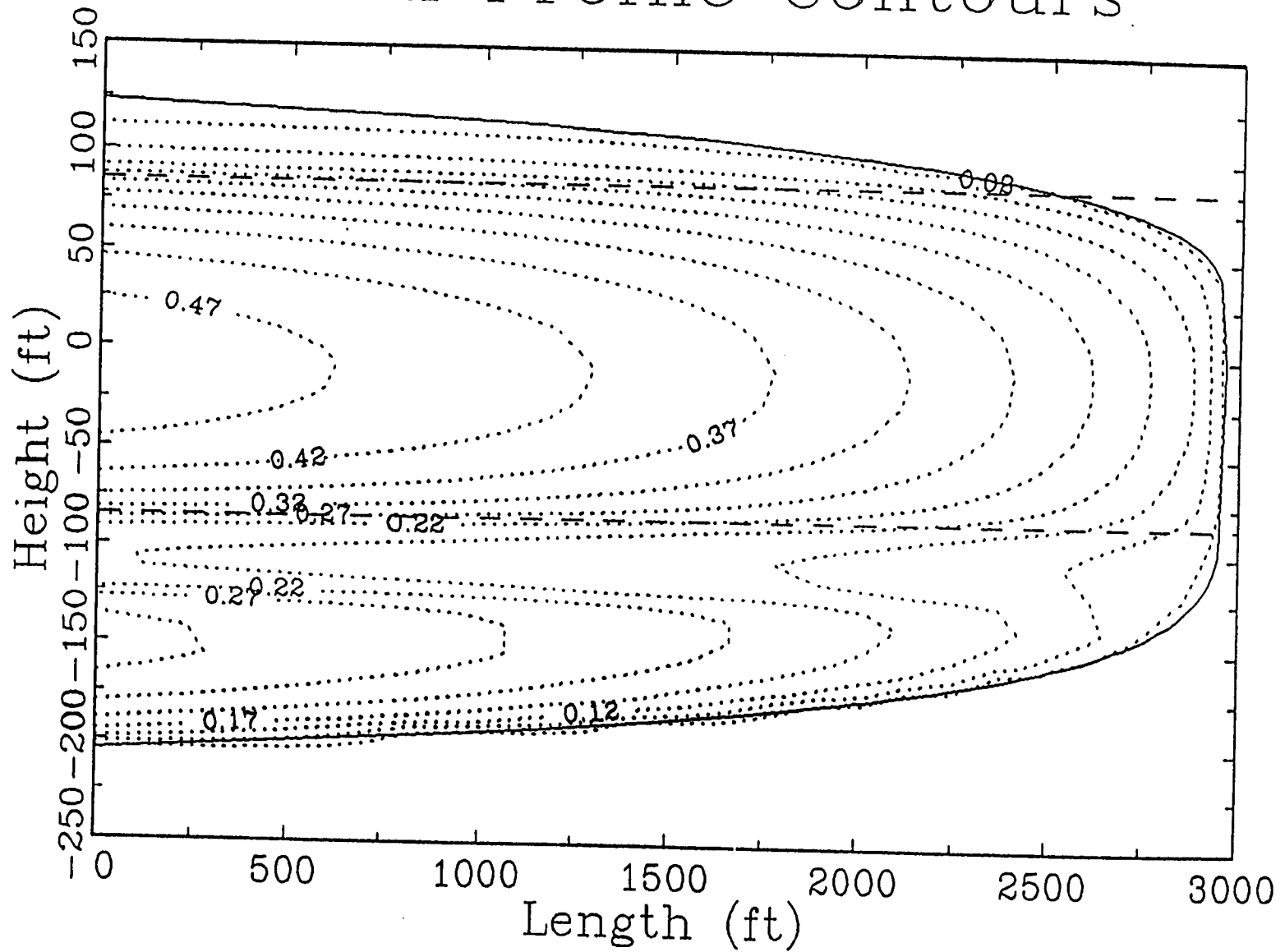
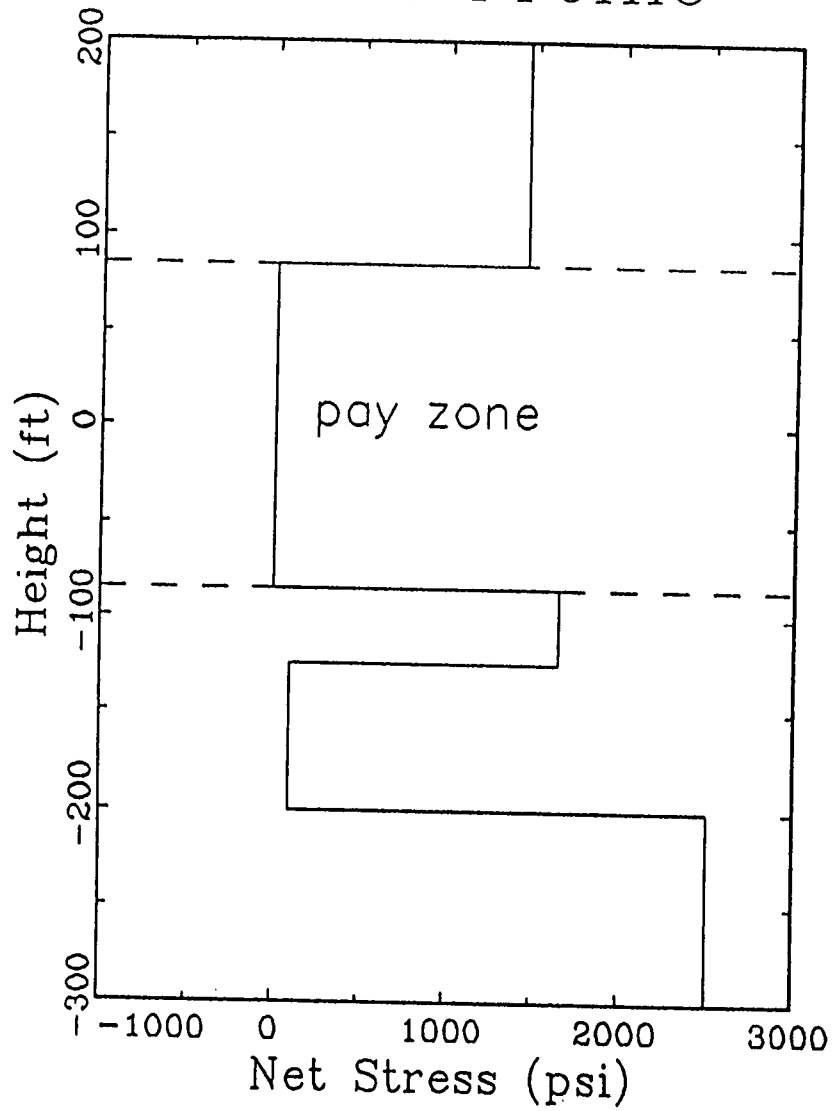


Figure B6 Width profile - case 7

# Stress Profile



# Vert. Width Profile

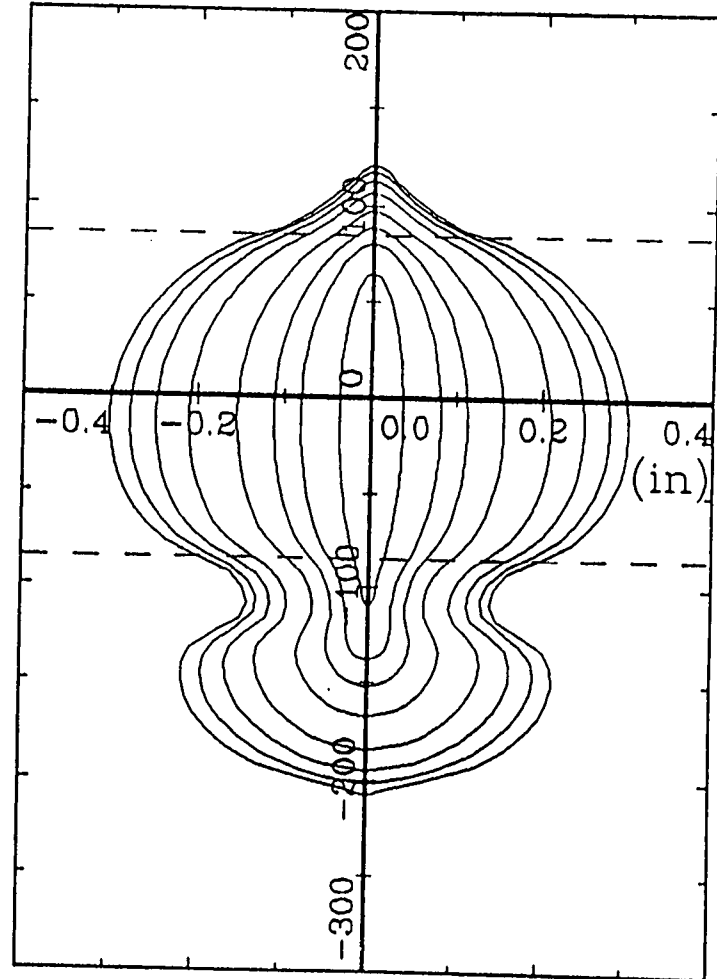


Figure B7 Height profile - case 8

# Width Profile Contours

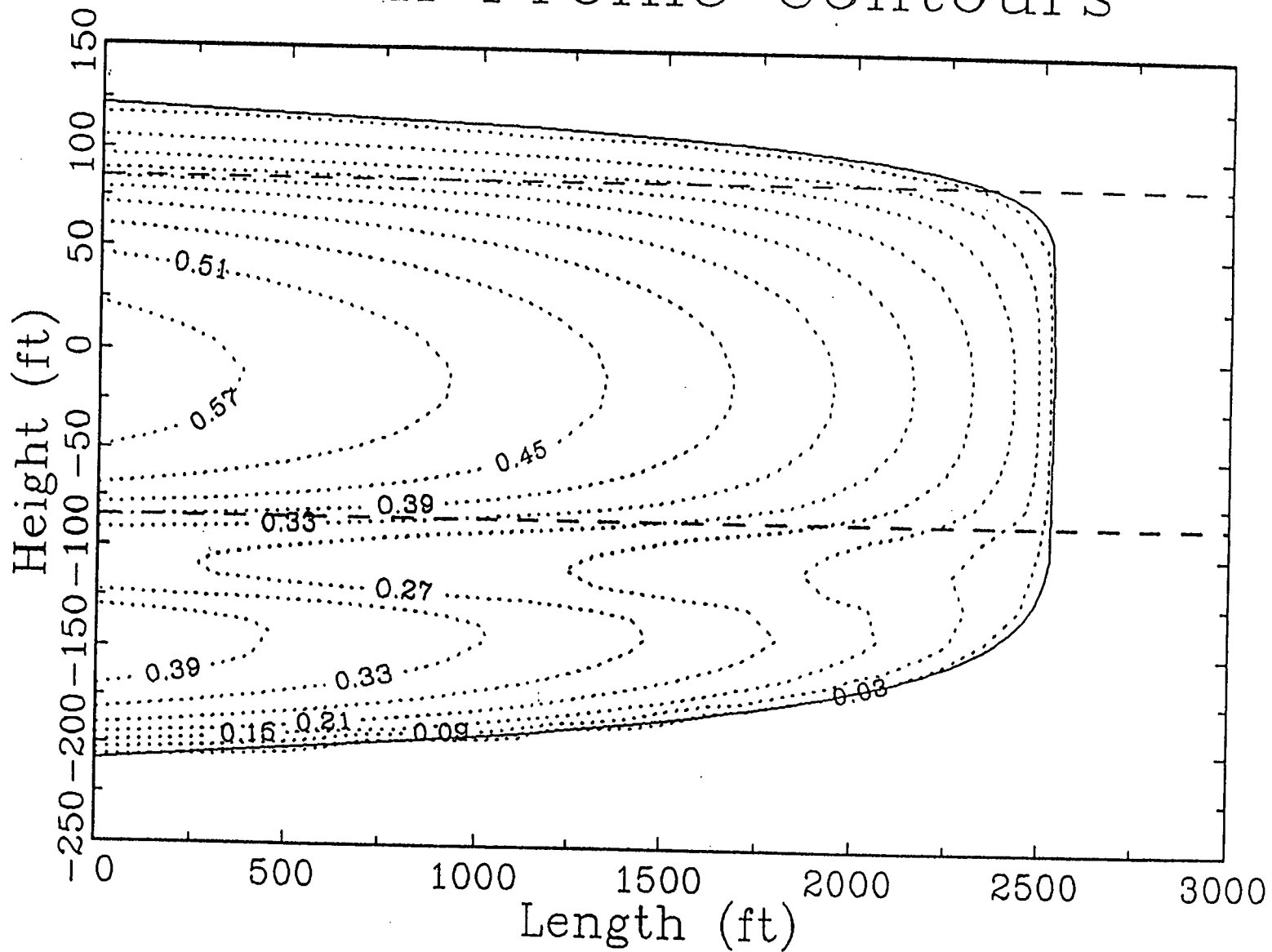


Figure B8 Width profile - case 8

### **Appendix C Width and height profiles for Meyer-2**

Figure C1-C8 give the height profiles and width profiles calculated by MFRAC-II ("knobs" on) as a function of length for cases 5-8. These profiles were provided by Meyer & Assoc. and have not been changed for publication.

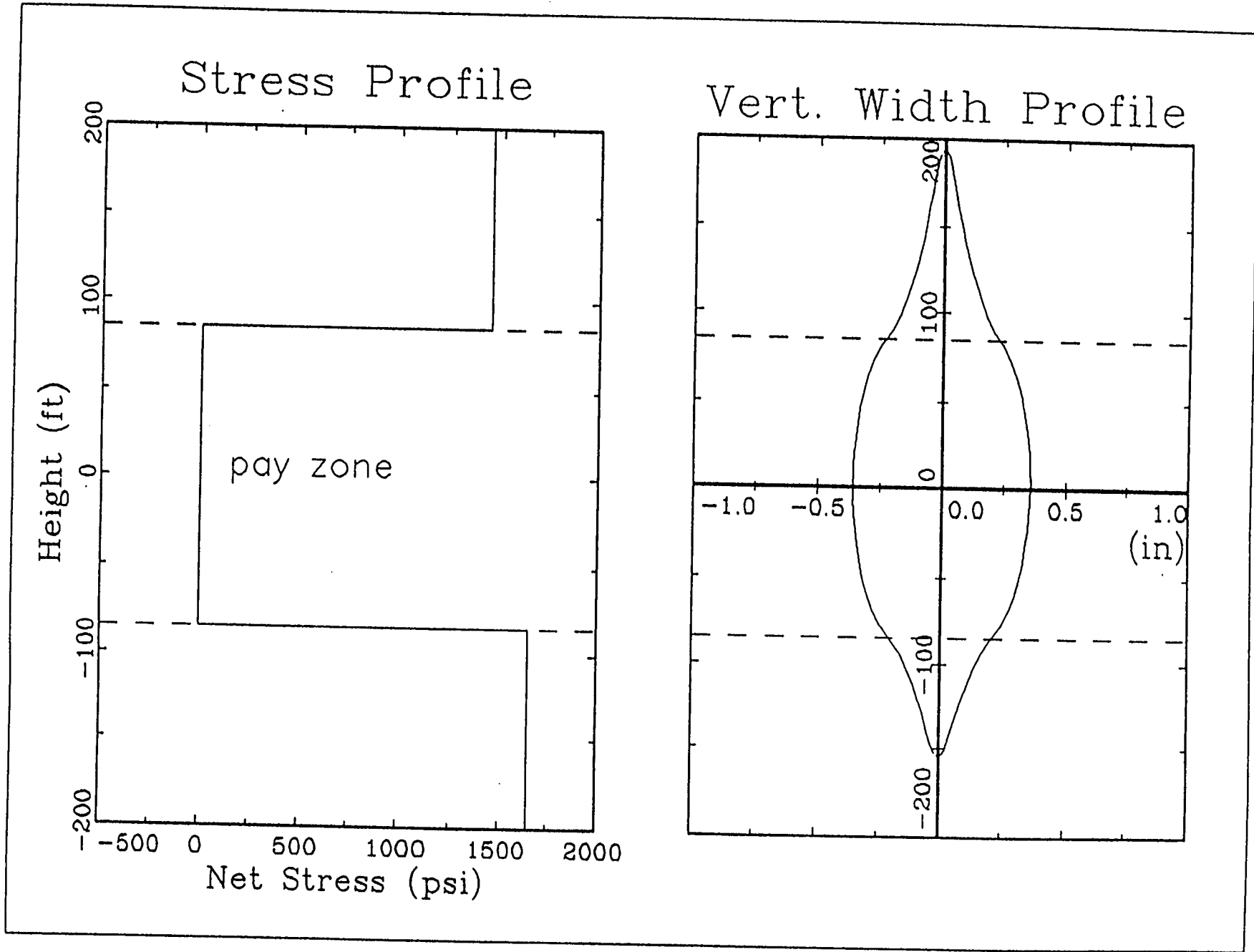


Figure C1 Height profile - case 5

# Width Profile Contours

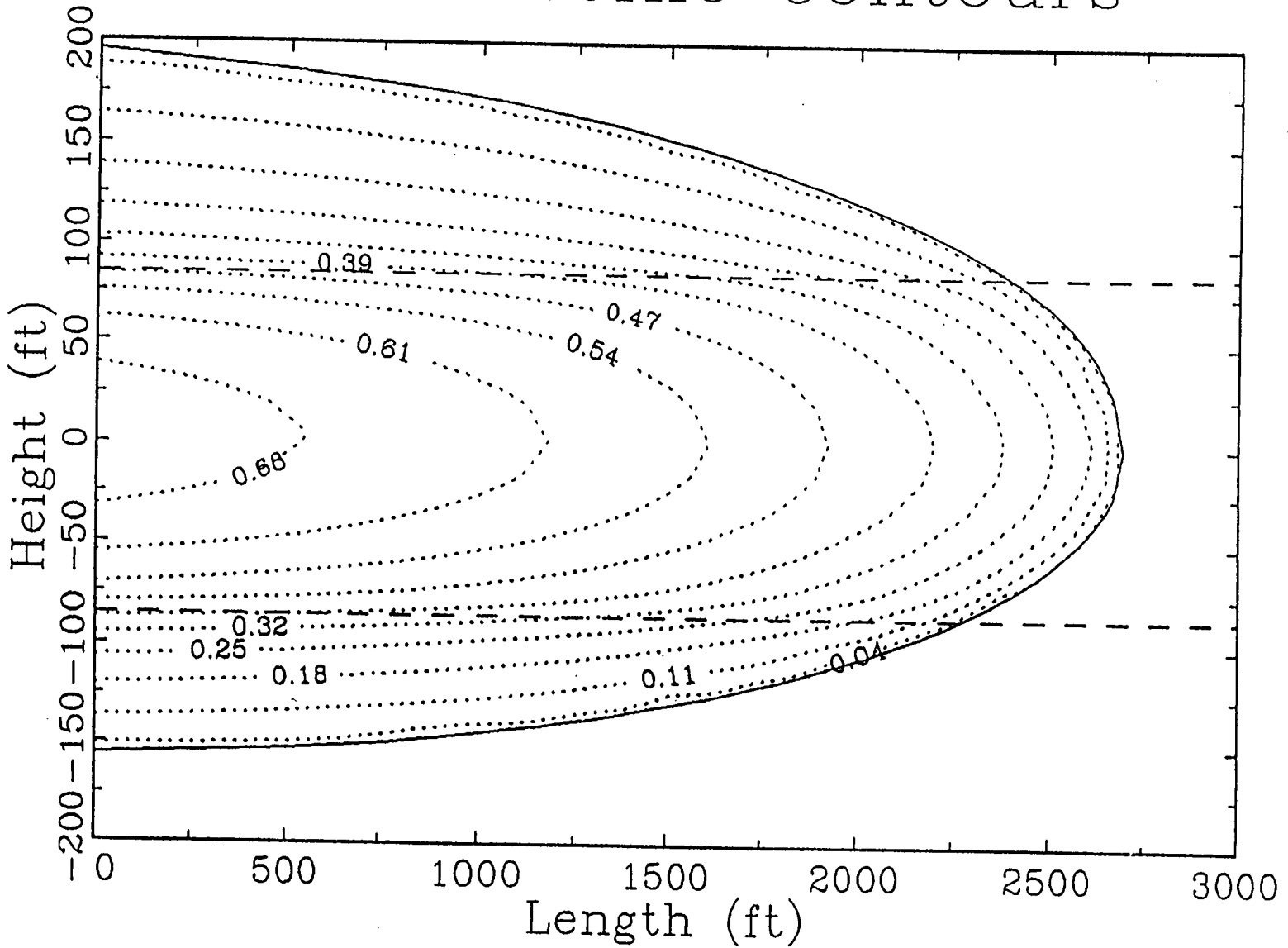
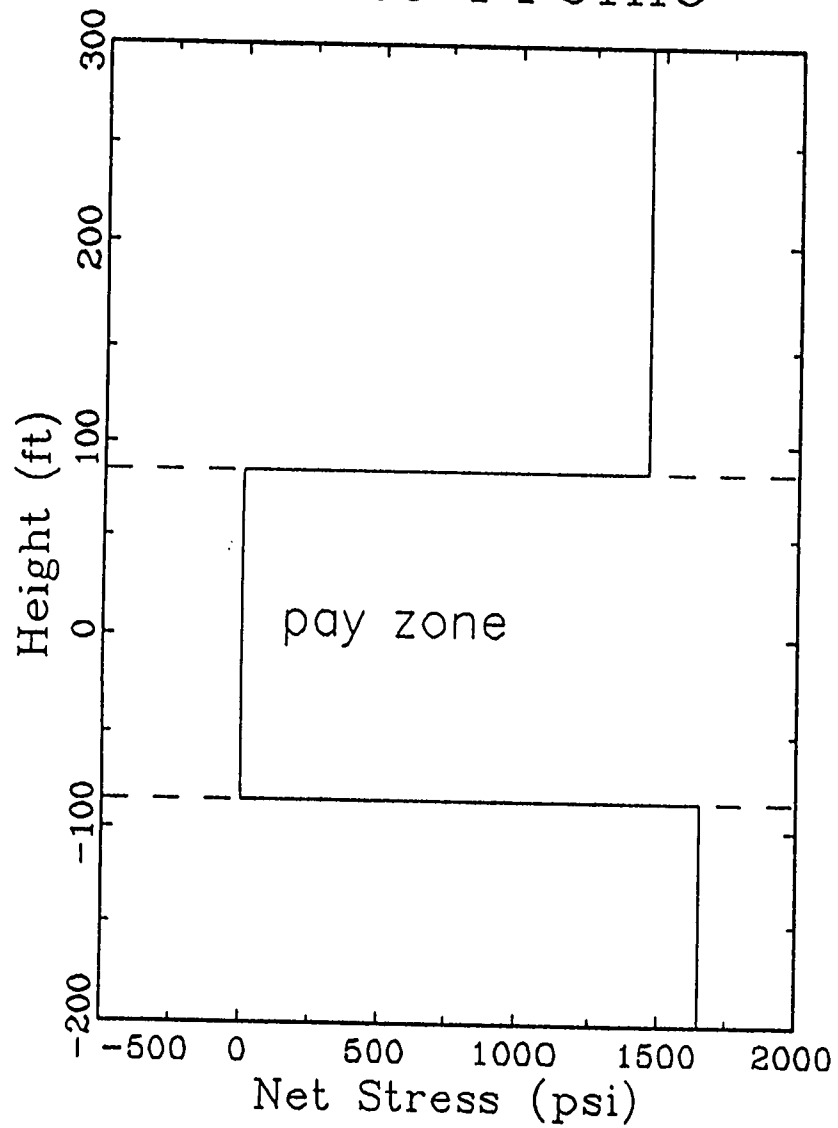


Figure C2 Width profile - case 5

# Stress Profile



# Vert. Width Profile

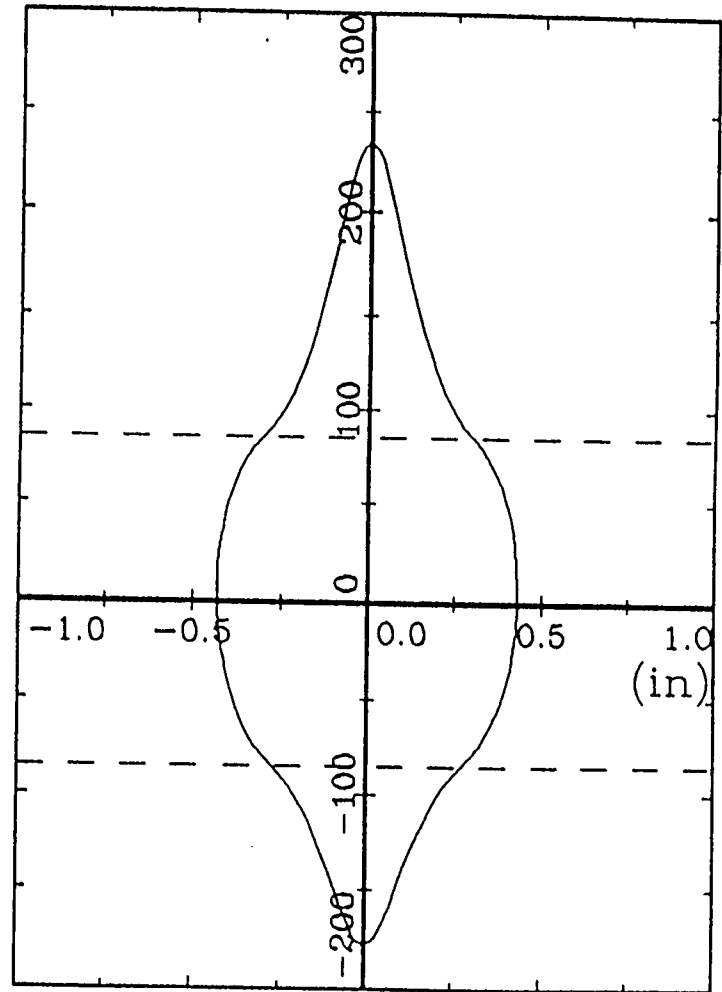


Figure C3 Height profile - case 6

# Width Profile Contours

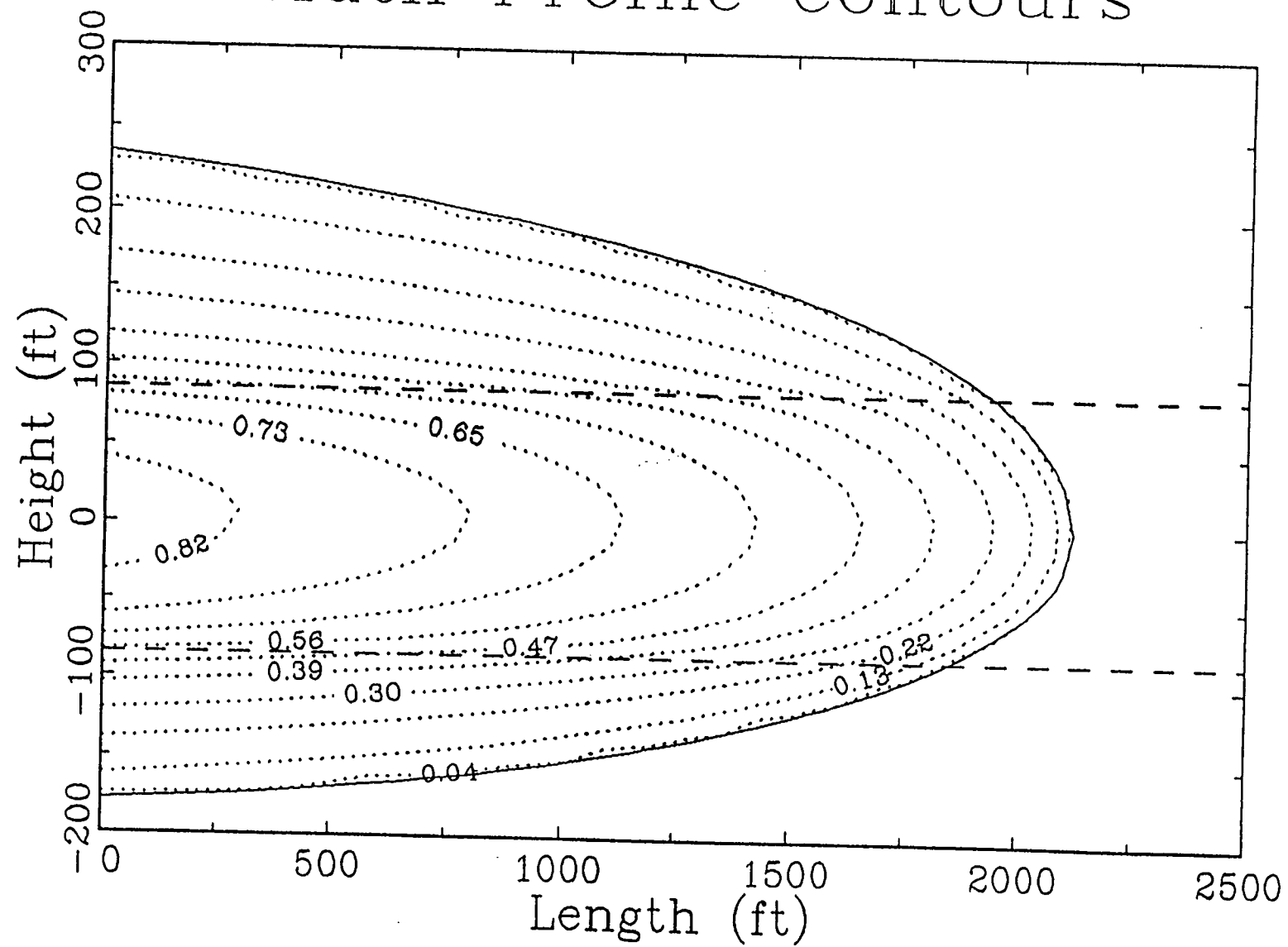


Figure C4 Width profile - case 6

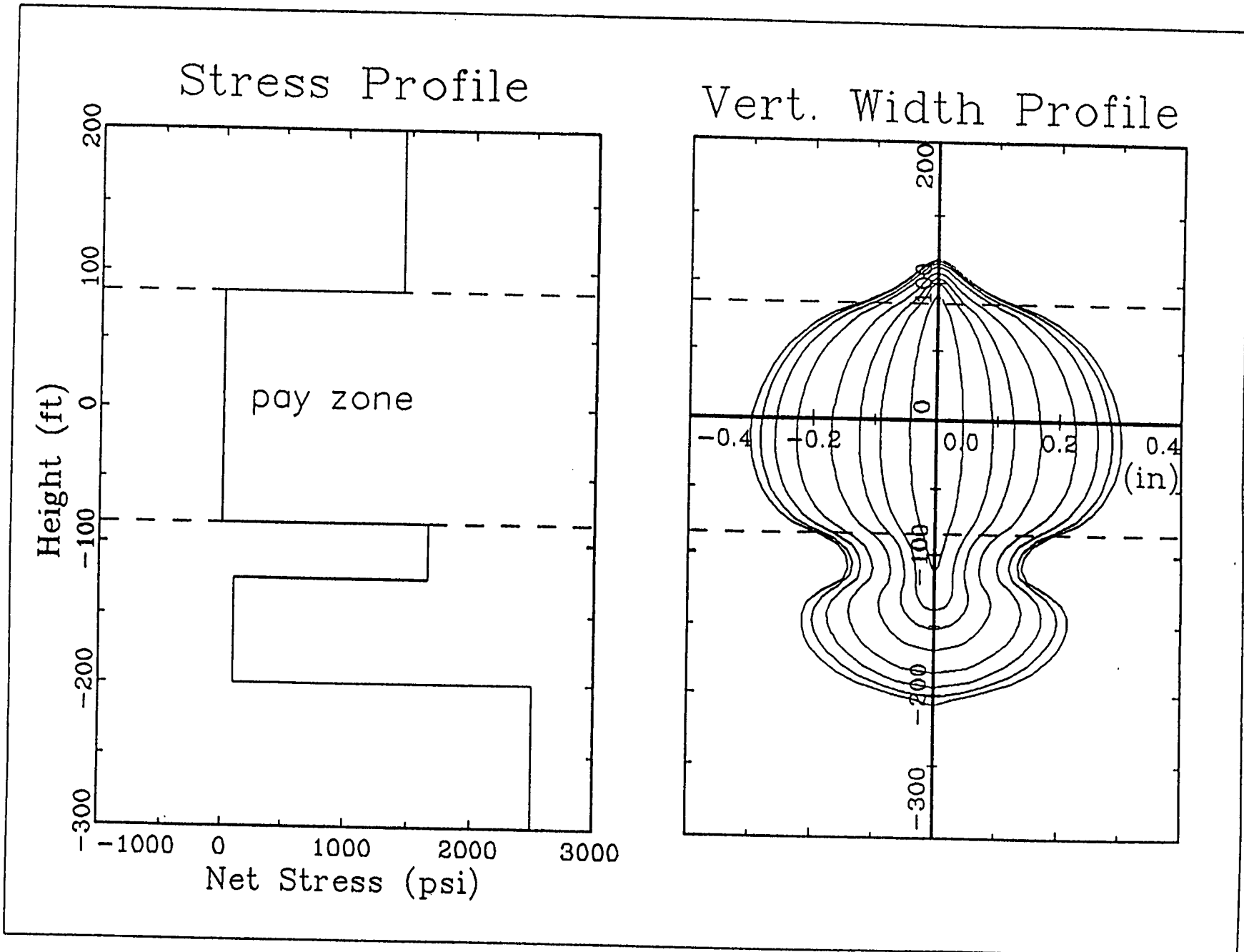


Figure C5 Height profile - case 7

# Width Profile Contours

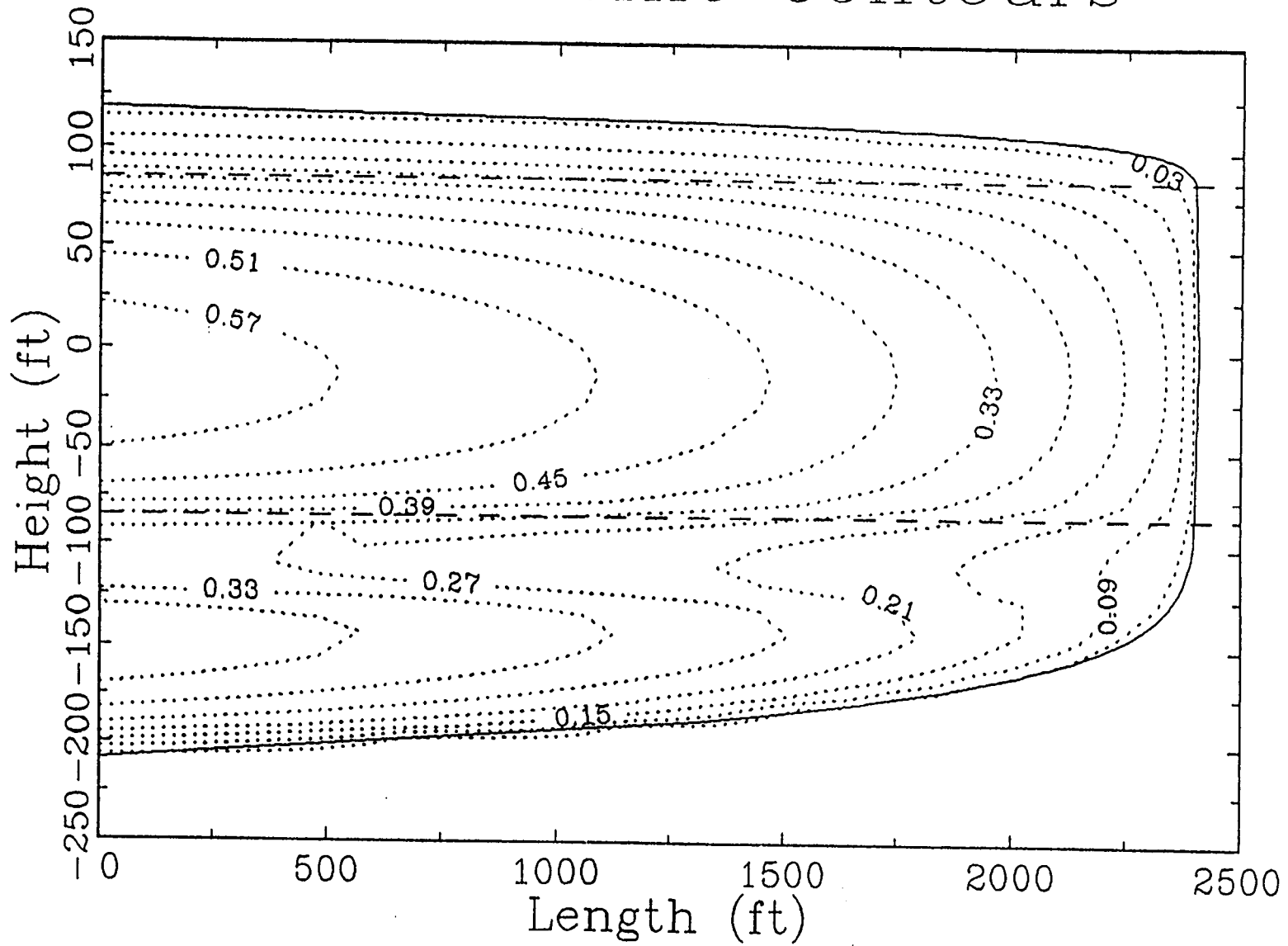


Figure C6 Width profile - case 7

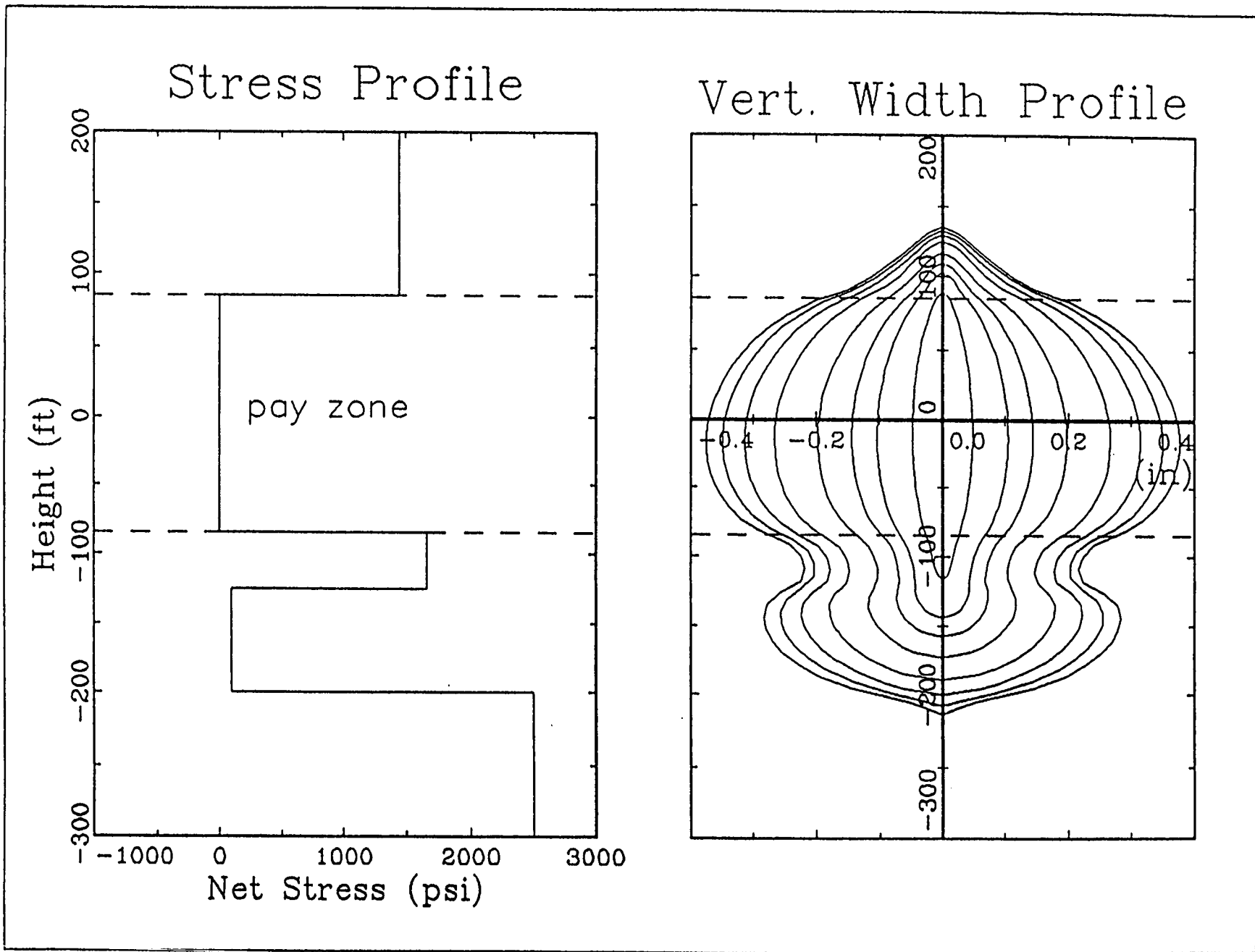


Figure C7 Height profile - case 8

# Width Profile Contours

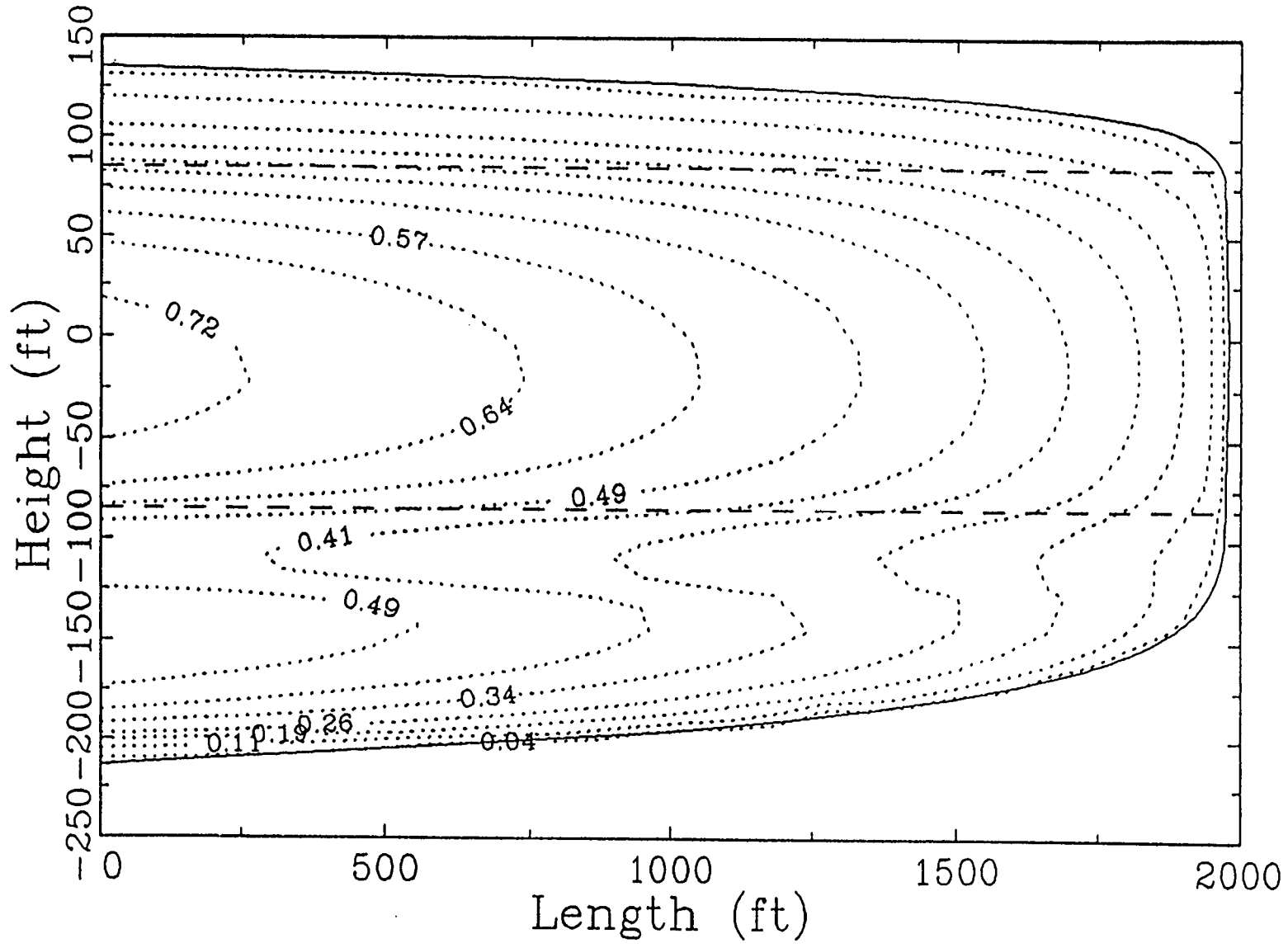


Figure C8 Width profile - case 8

### **Appendix D Width and height profiles for Advani model**

Figure D1 gives the height profiles calculated by HYFRAC3D for cases 5-8. These profiles were provided by S. Advani of Lehigh University and have not been changed for publication.

### SFE NO.3 FRACTURE GEOMETRY

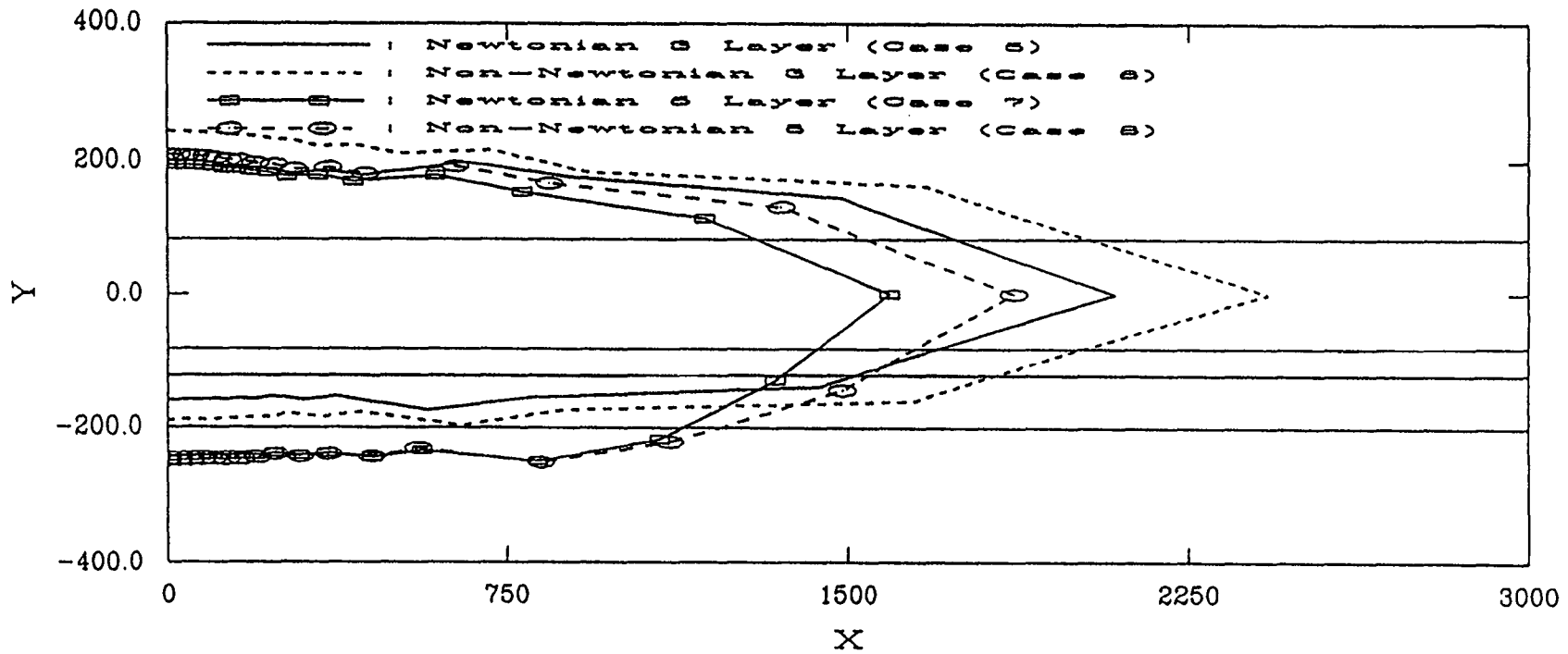


Figure D1 Height profiles - cases 5-8

## **Appendix E Width and height profiles for GOHFER**

Figure E1-E8 give the height profiles and width profiles calculated by GOHFER as a function of length for cases 5-8. These profiles were provided by Marathon. and have not been changed for publication.

GRI/SFE #3 Case 5 - 3 Layer Const. Visc.

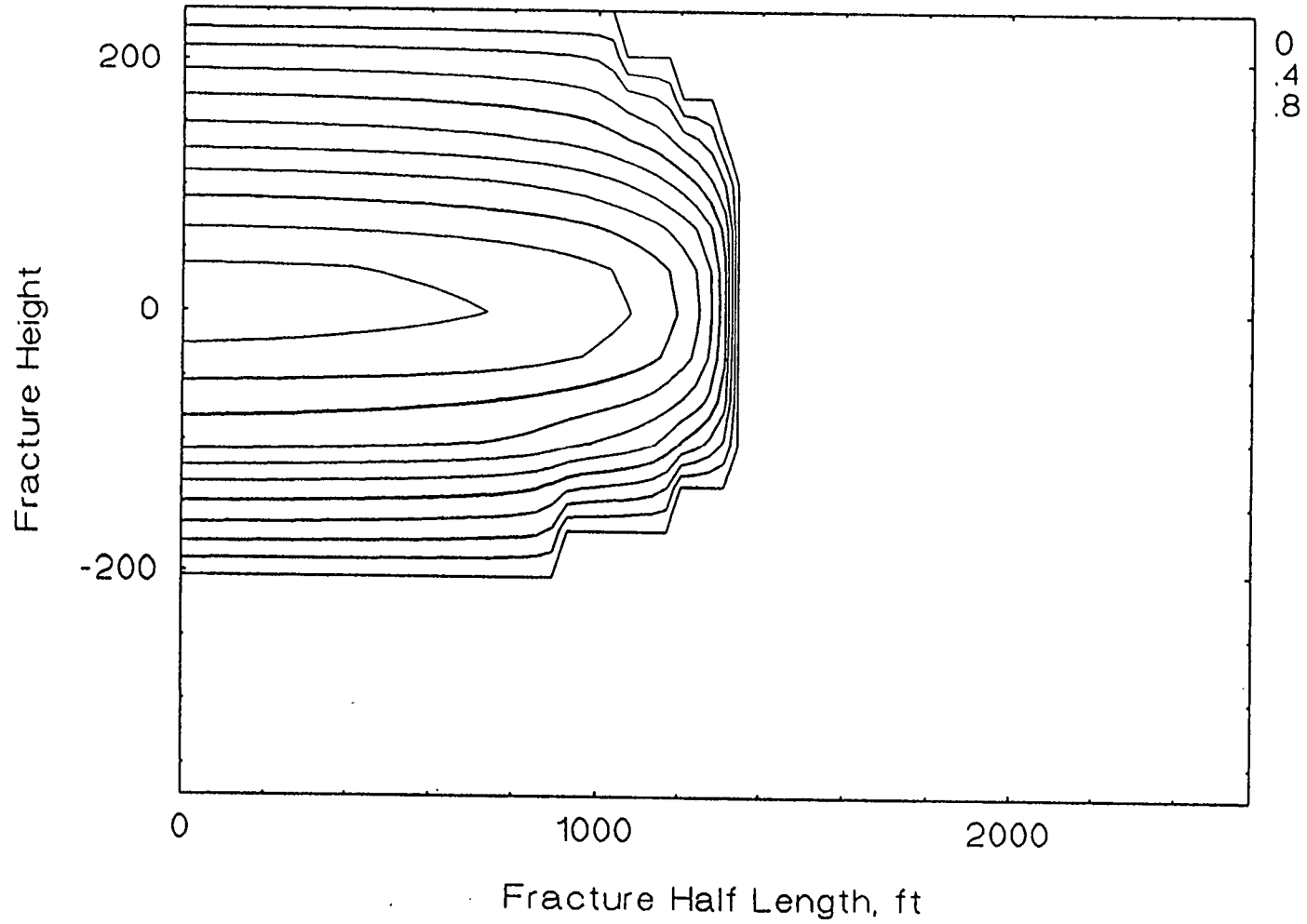


Figure E1 Height profile - case 5

# GRI/SFE #3 Case 5 - 3 Layer Const Visc.

## Width Profile at Well

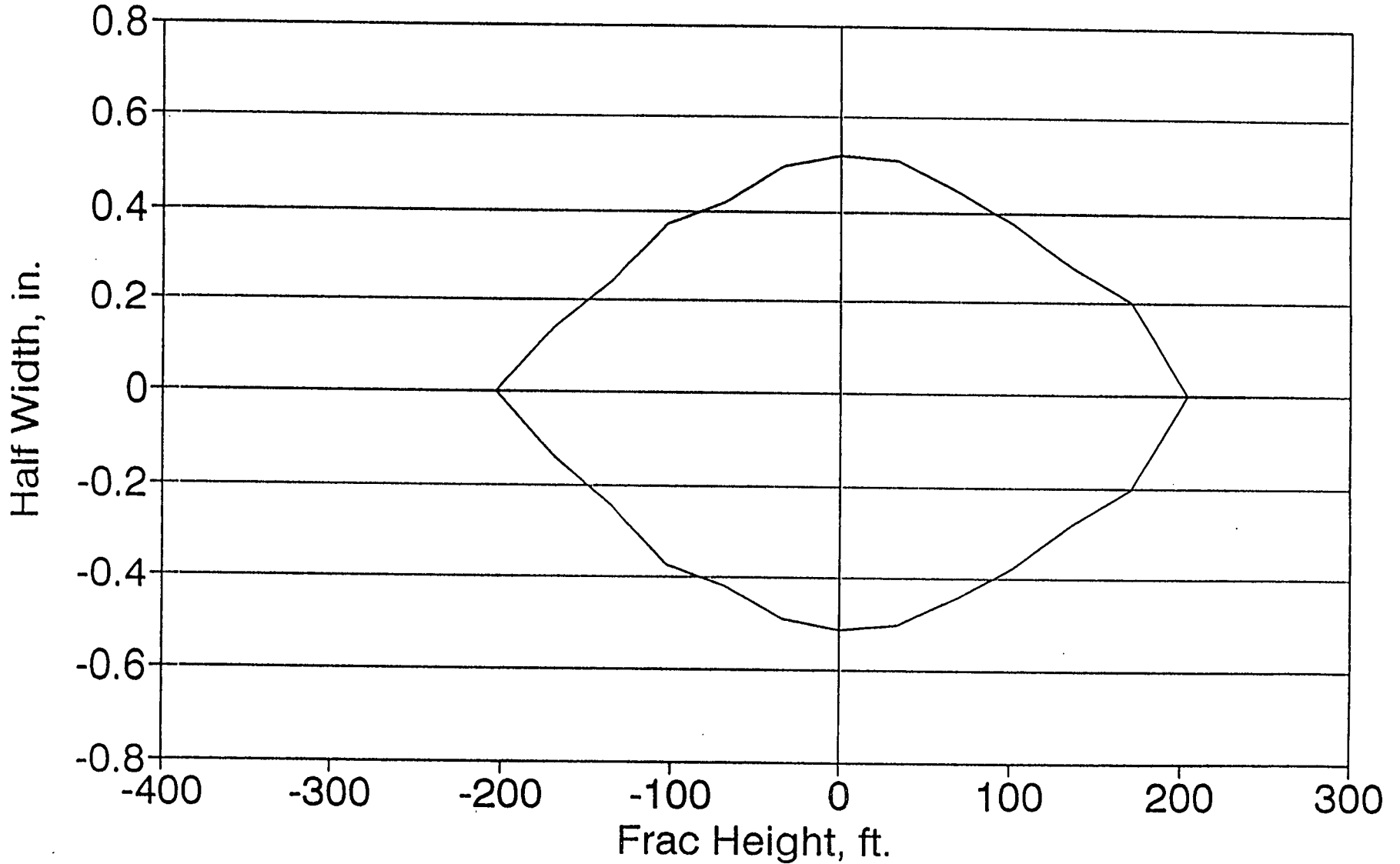


Figure E2 Width profile - case 5

GRI/SFE #3 Case 6 - 3 Layer Variable Visc.

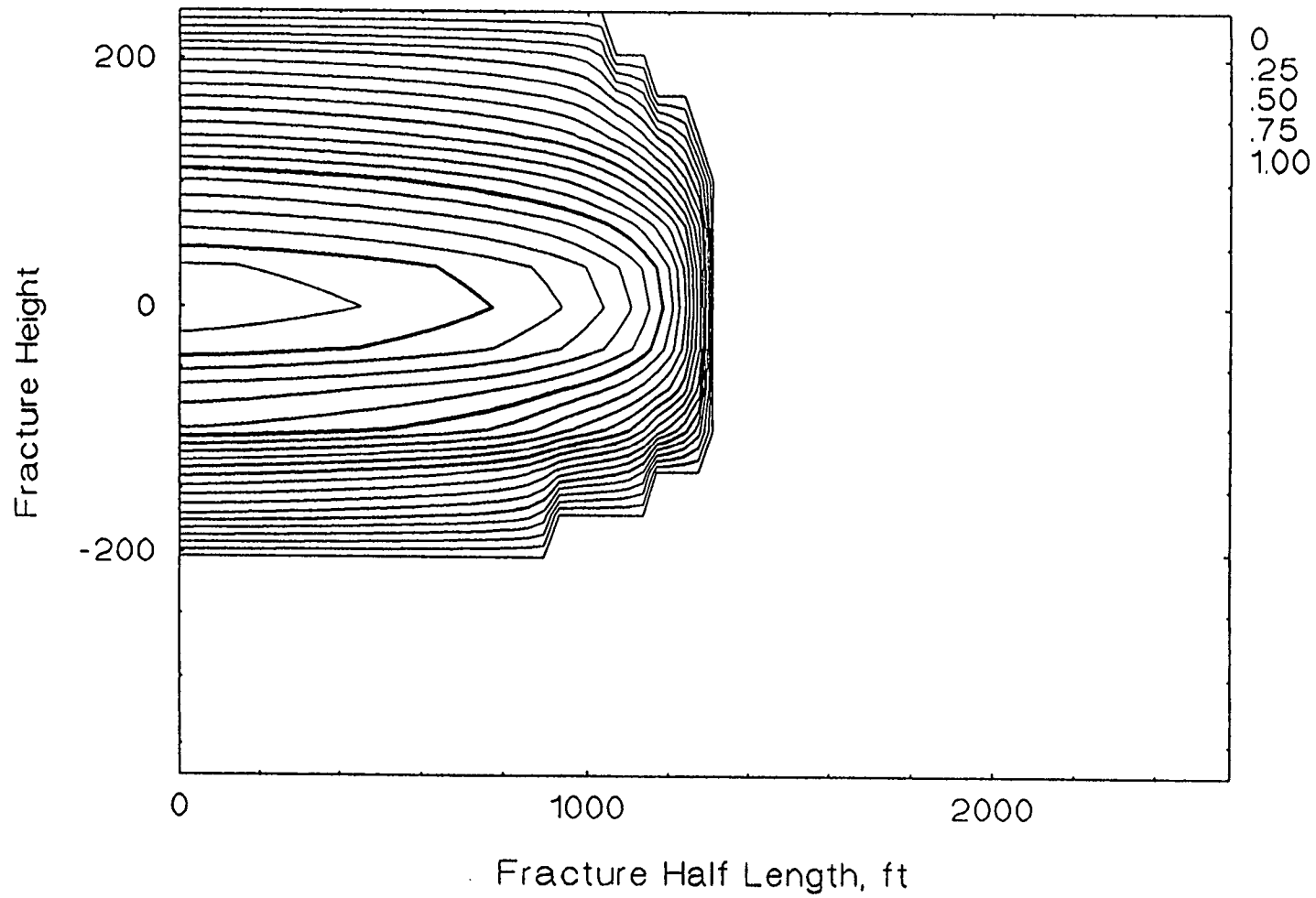


Figure E3 Height profile - case 6

# GRI/SFE #3 Case 6 - 3 Layer Var. Visc.

## Width Profile at Well

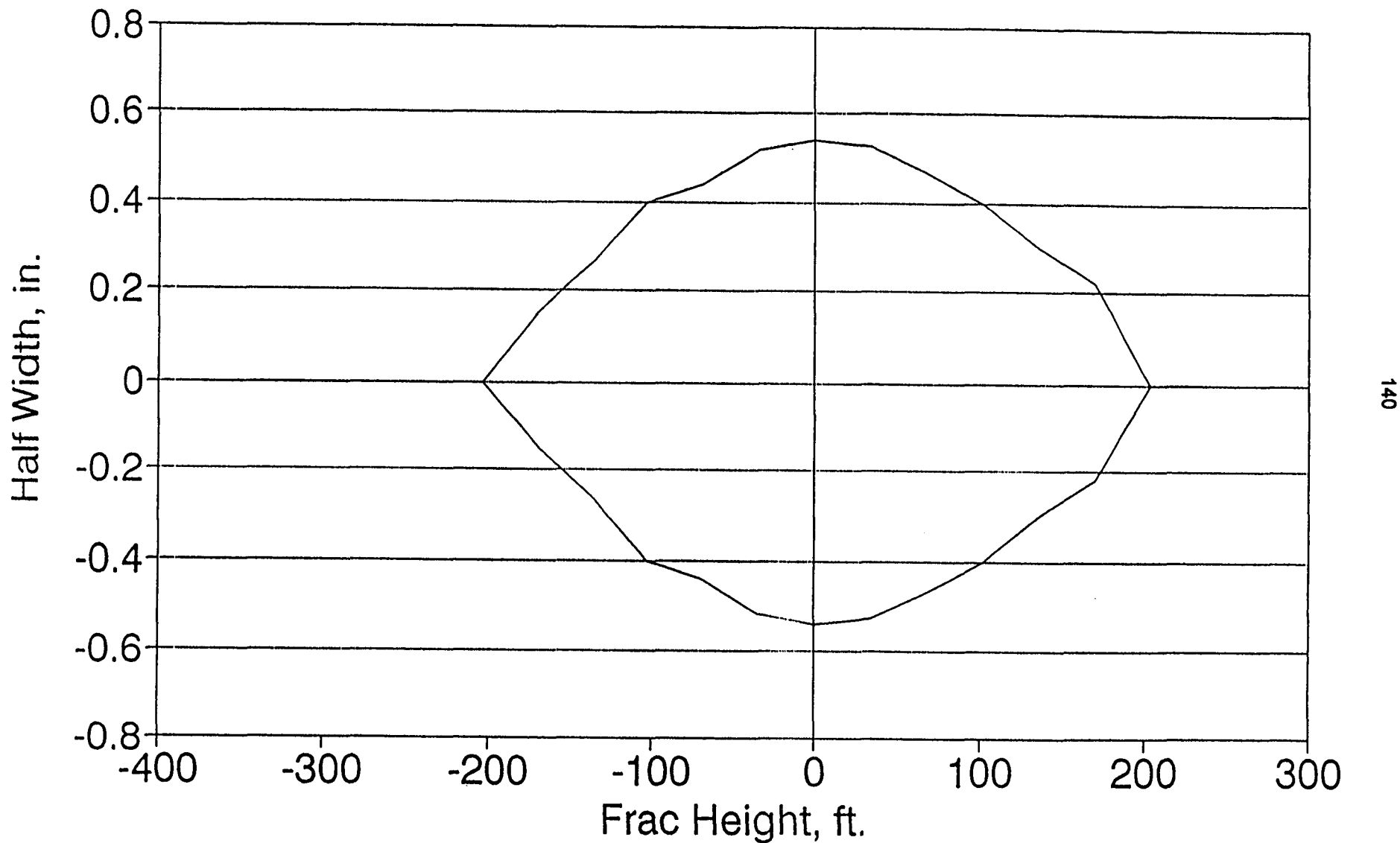


Figure E4 Width profile - case 6

GRI/SFE #3 Case 7 - 5 Layer Const Visc.

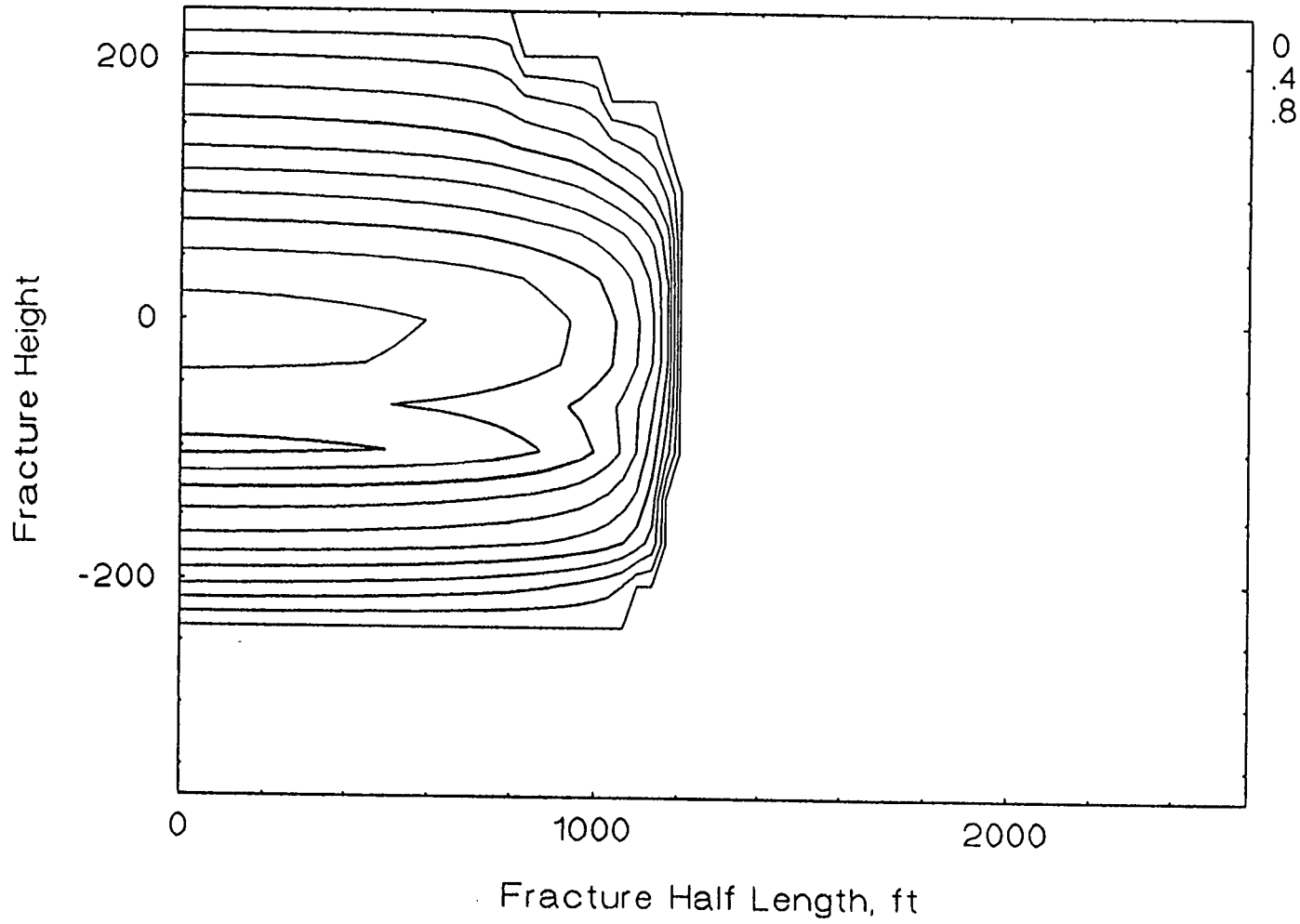
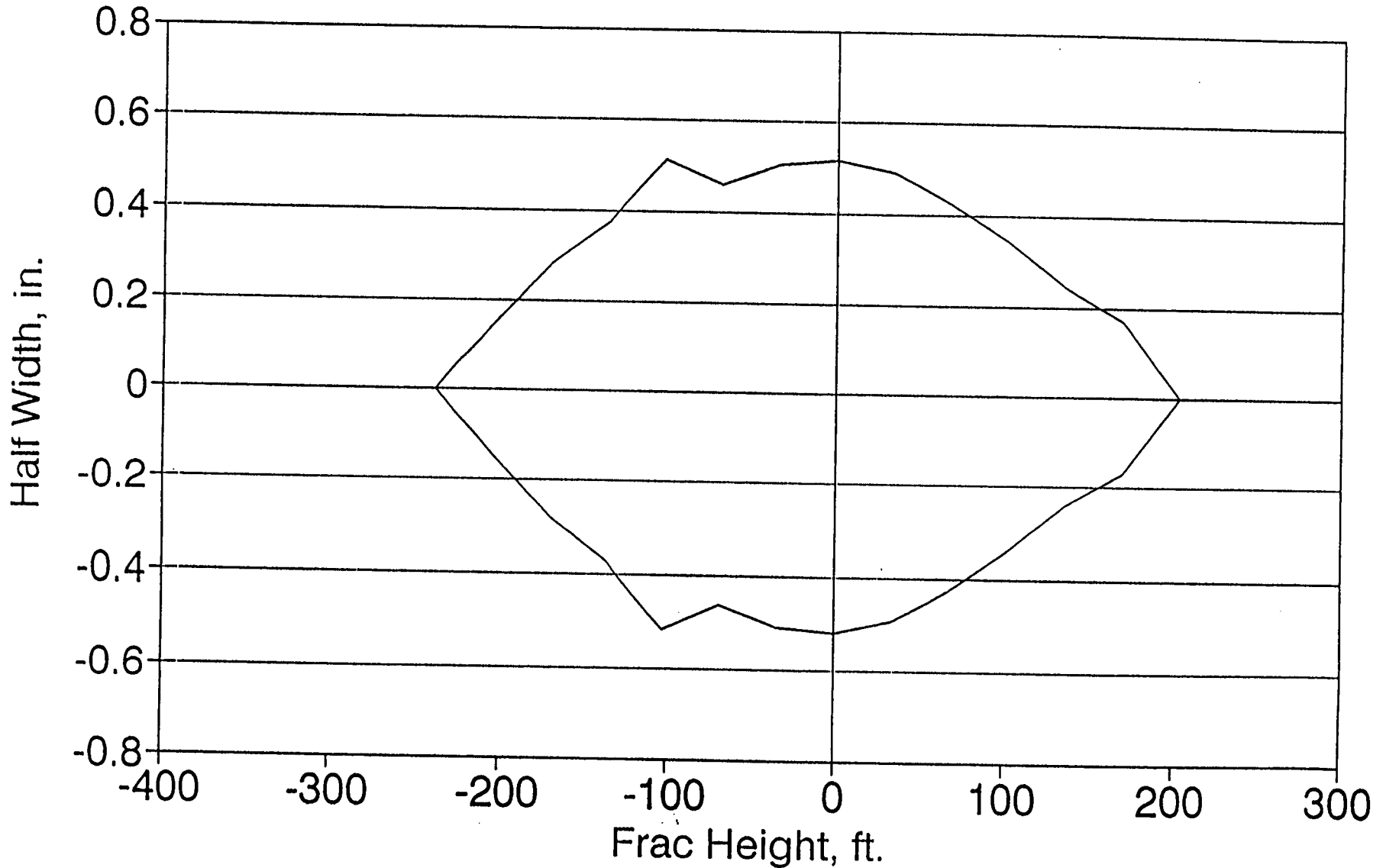


Figure E5 Height profile - case 7

# GRI/SFE #3 Case 7 - 5 Layer Const Visc.

## Width Profile at Well



142

Figure E6 Width profile - case 7

GRI/SFE #3 Case 8 - 5 Layer Variable Visc.

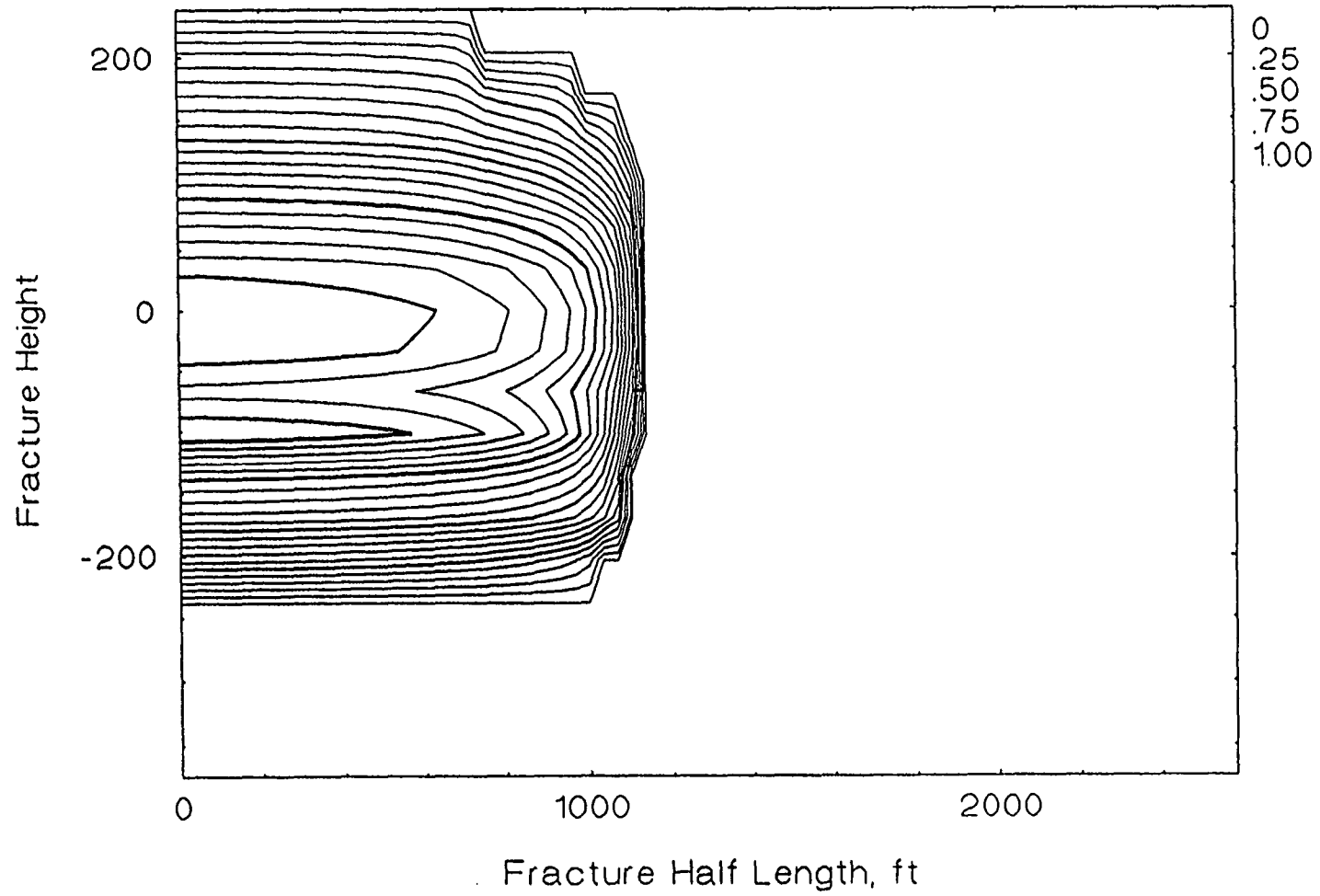


Figure E7 Height profile - case 8

# GRI/SFE #3 Case 8 - 5 Layer Var. Visc.

## Width Profile at Well

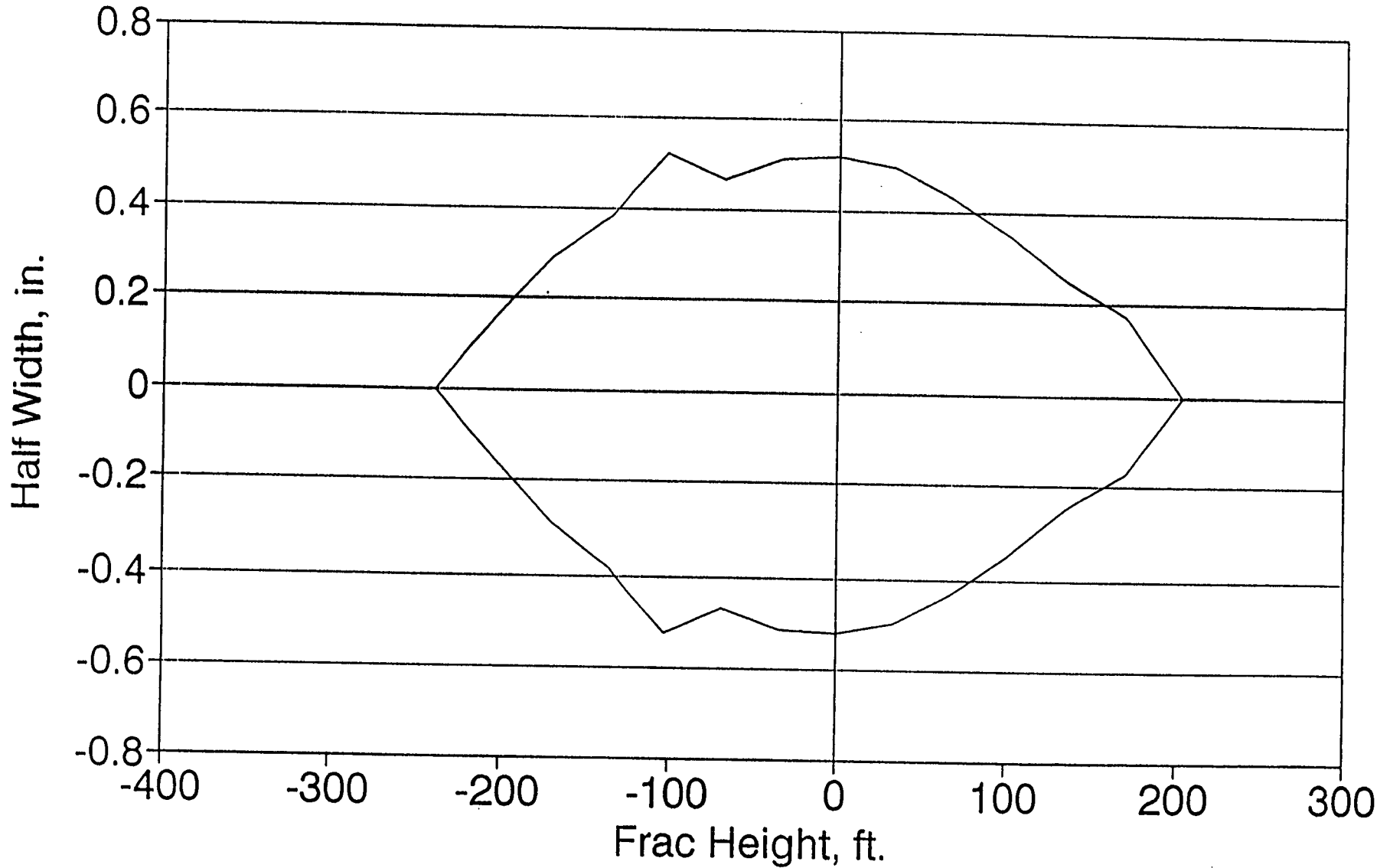


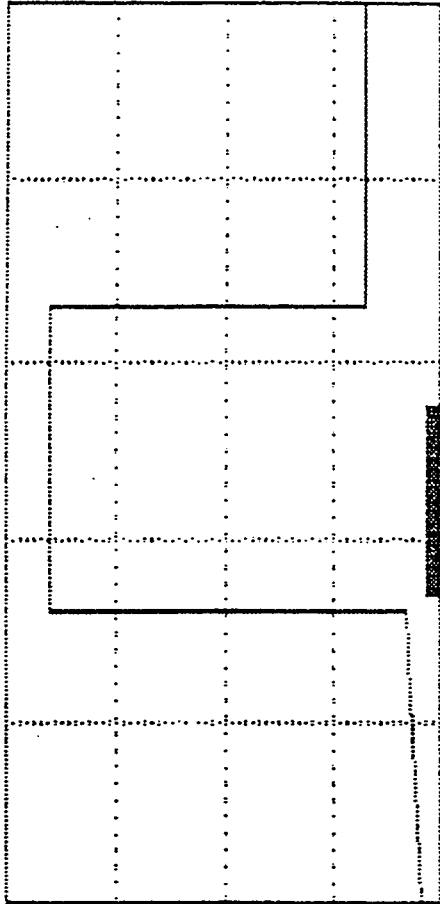
Figure E8 Width profile - case 8

**Appendix F Width and height profiles for ARCO (Stimplan & TerraFrac)**

Figure F1-F8 give the height profiles and width profiles as a function of length for cases 5-8 using Stimplan. Figure F9 gives the height profile as a function of length for case 8 using TerraFrac. These profiles were provided by ARCO and have not been changed for publication.

SFE #3 (3-layer, Const. Visc.)

5500 Stress (psi) 7500 -0.50 Width (in) 0.50

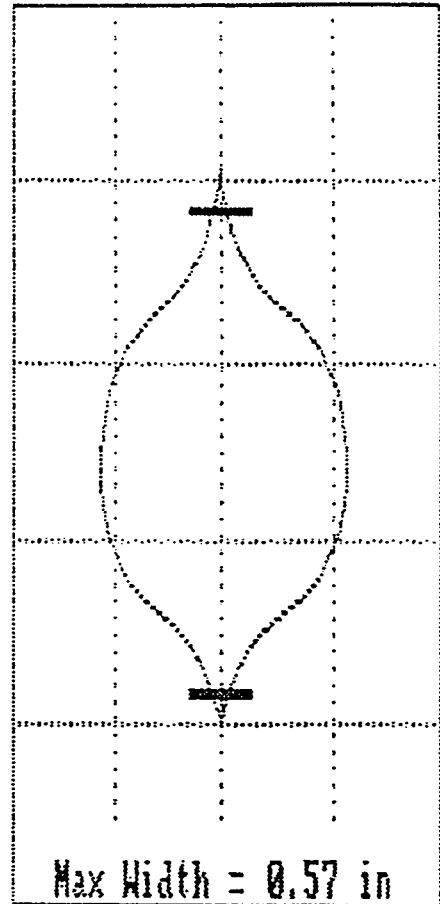


9100

9200

9300

9400



Max Width = 0.57 in

Figure F1 Height profile (Stimplan) - case 5

SFE#3 (3-Layer, 200 cp)

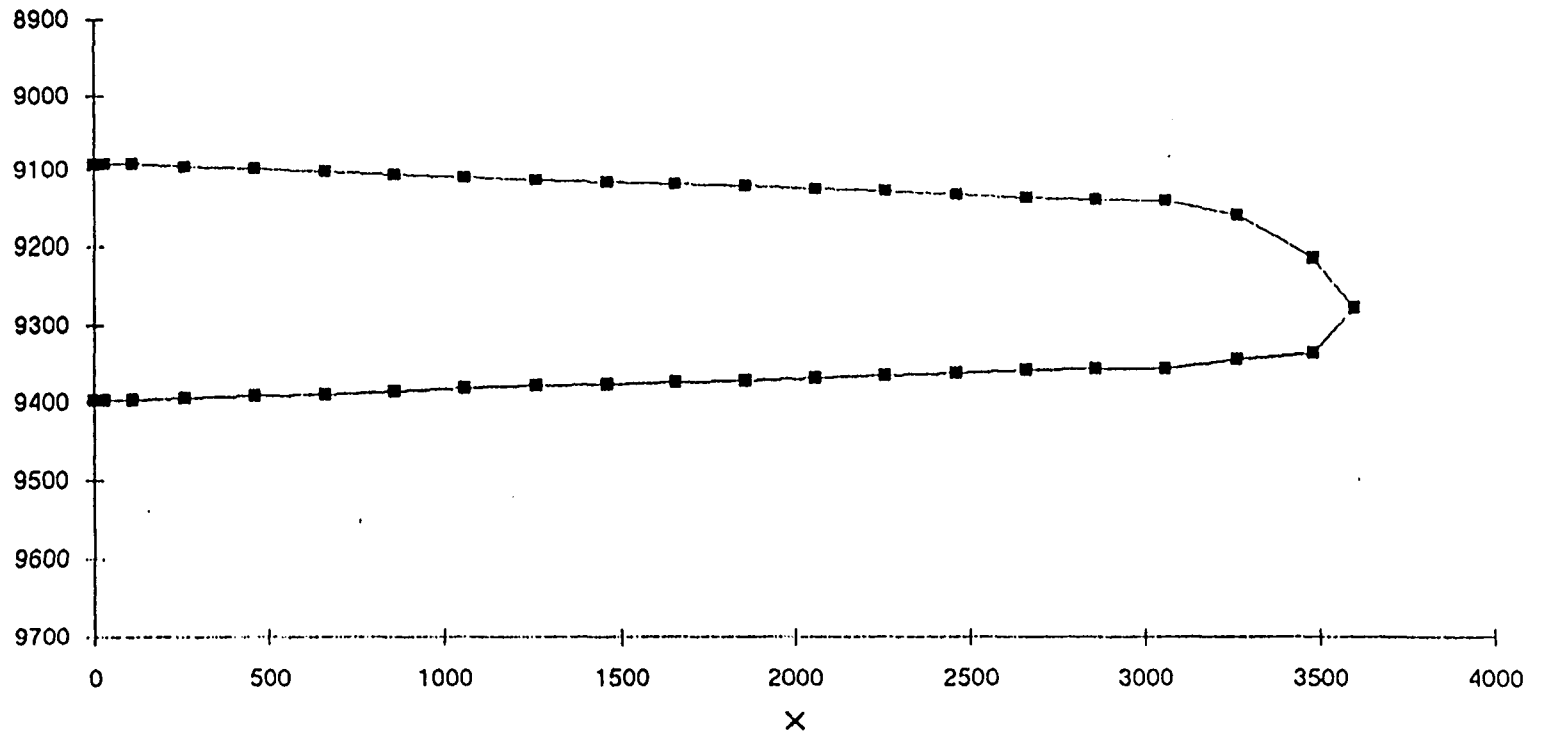


Figure F2 Width profile (Stimplan) - case 5

SFE #3 (3-layer, Var. Visc)

5500 Stress (psi) 7500 -0.50 Width (in) 0.50

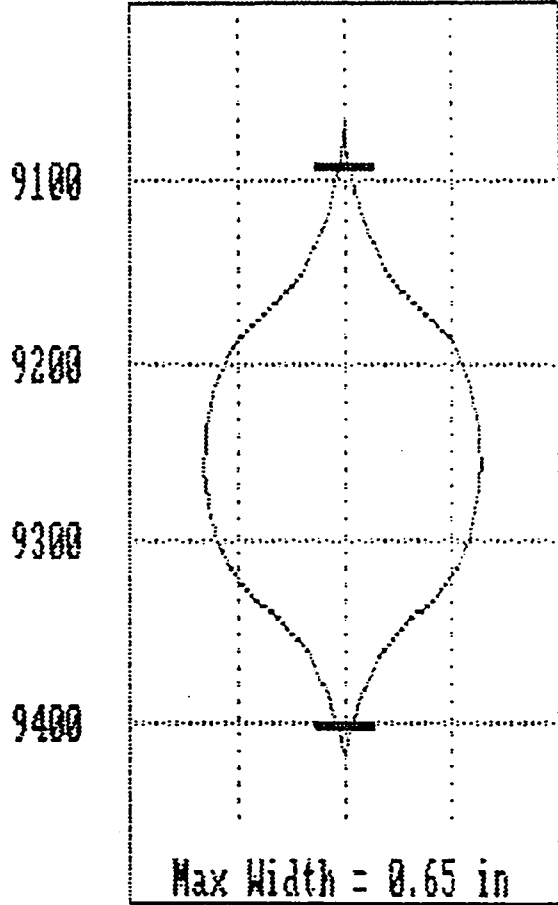
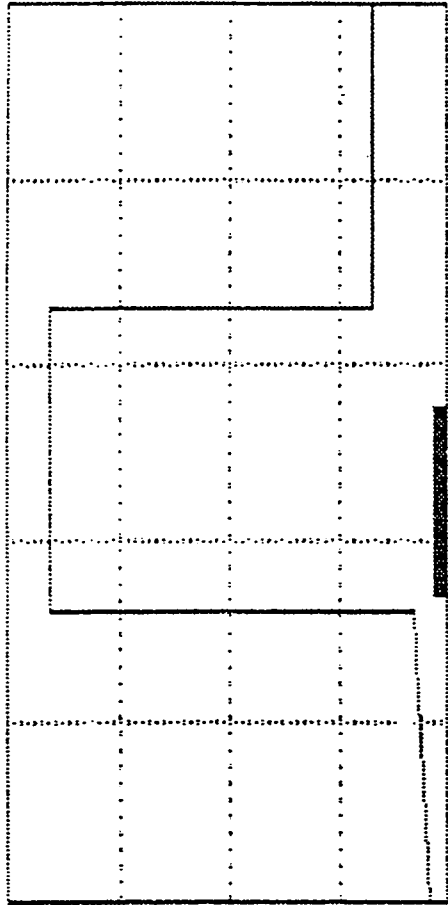


Figure F3 Height profile (Stimplan) - case 6

SFE#3 (3-Layer, Var. Visc.)

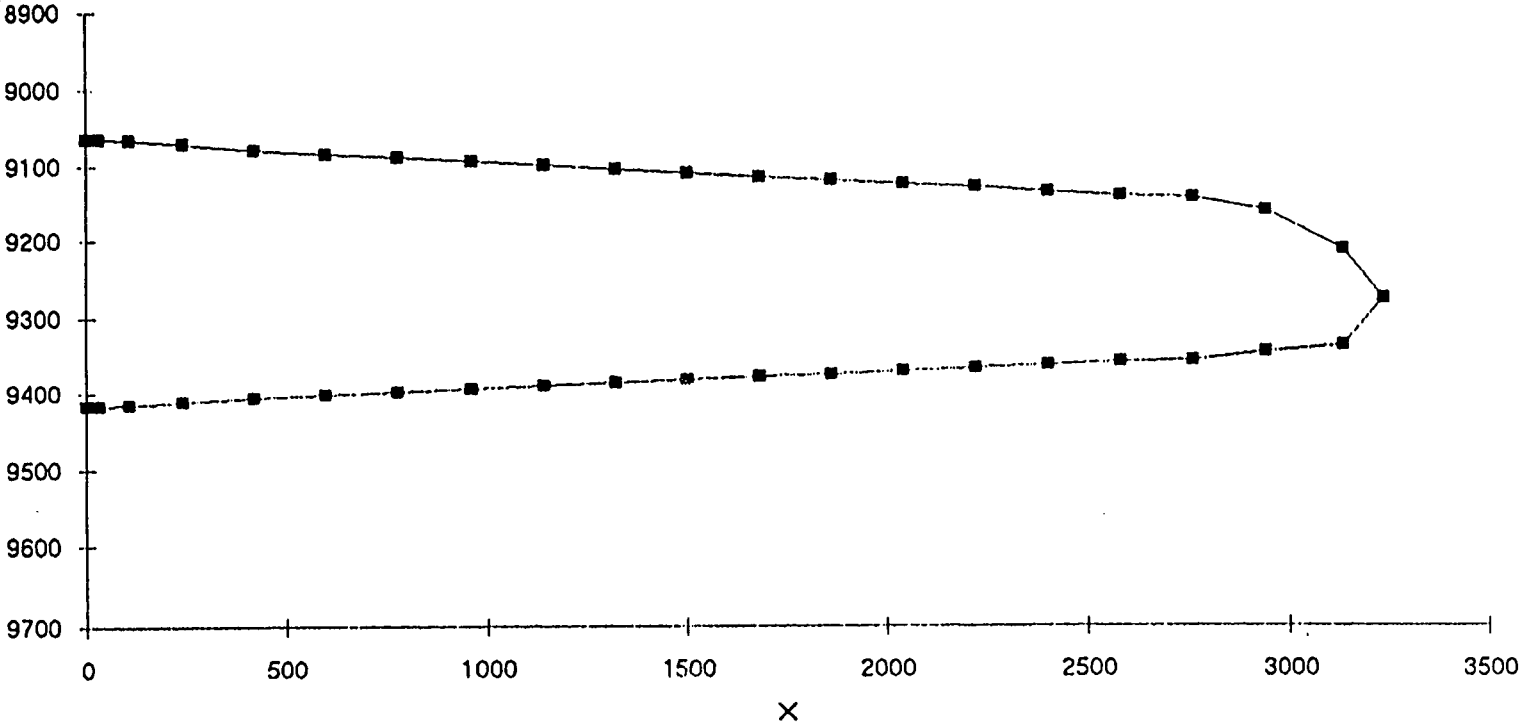


Figure F4 Width profile (Stimplan) - case 6

SFE #3 (5-layer, Const. Visc)

5500 Stress (psi) 8500 -0.50 Width (in) 0.50

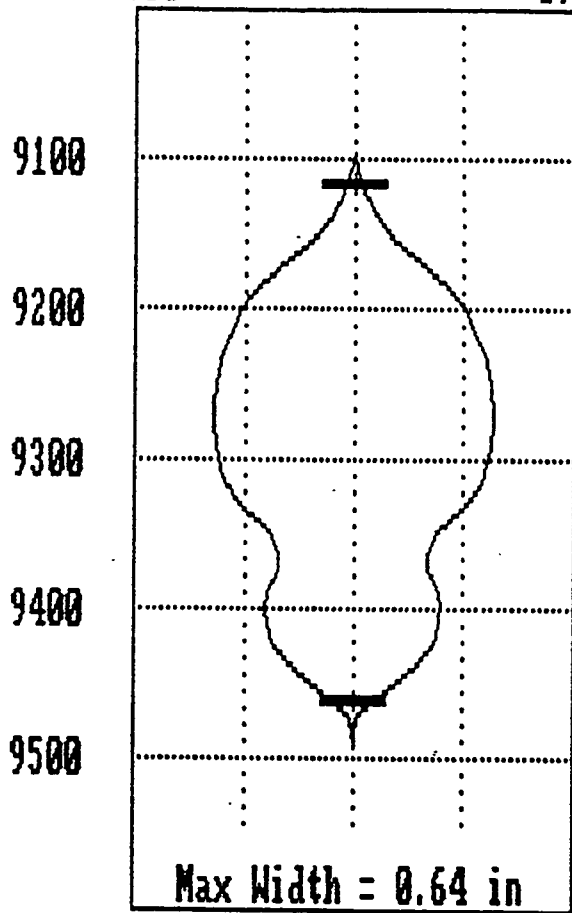
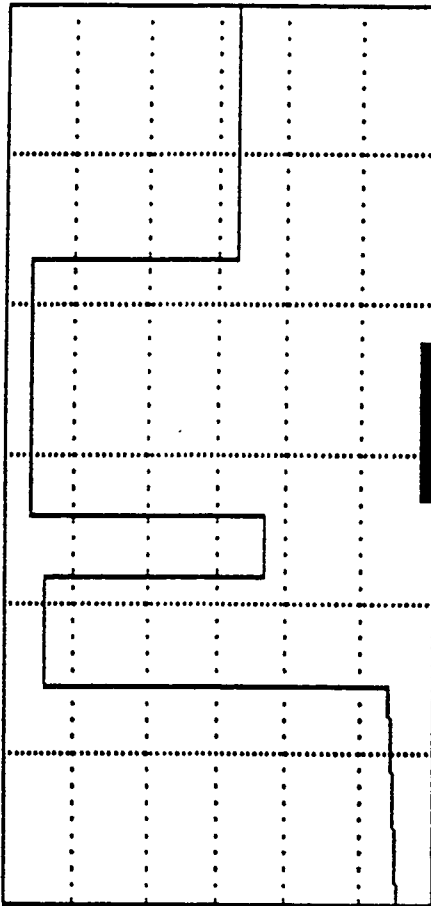


Figure F5 Height profile (Stimplan) - case 7

STIMPLAN, SFE#3 (5-Layer, 200 cp)

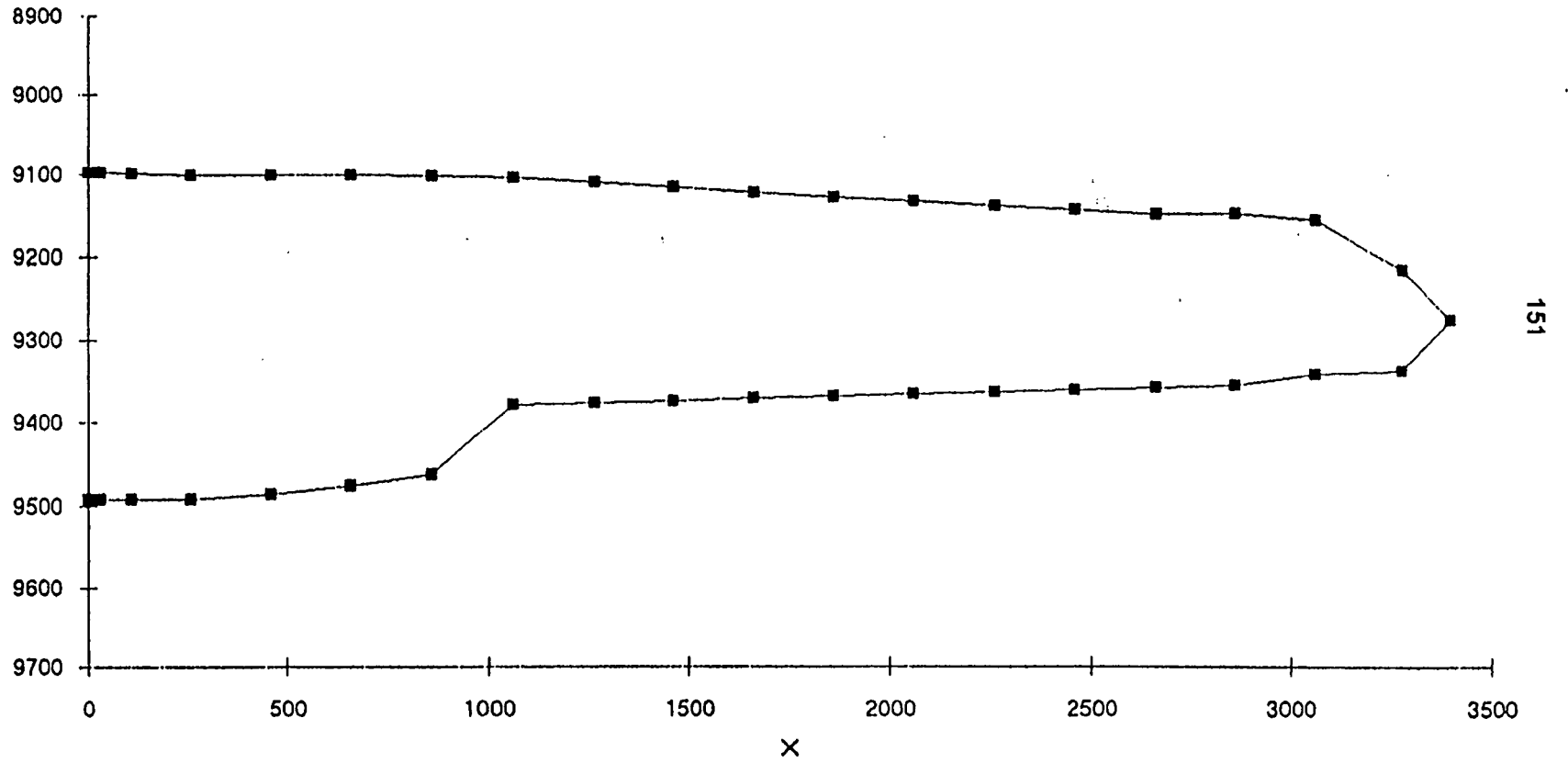


Figure F6 Width profile (Stimplan) - case 7

SFE #3 (5-layer, Var. Visc)

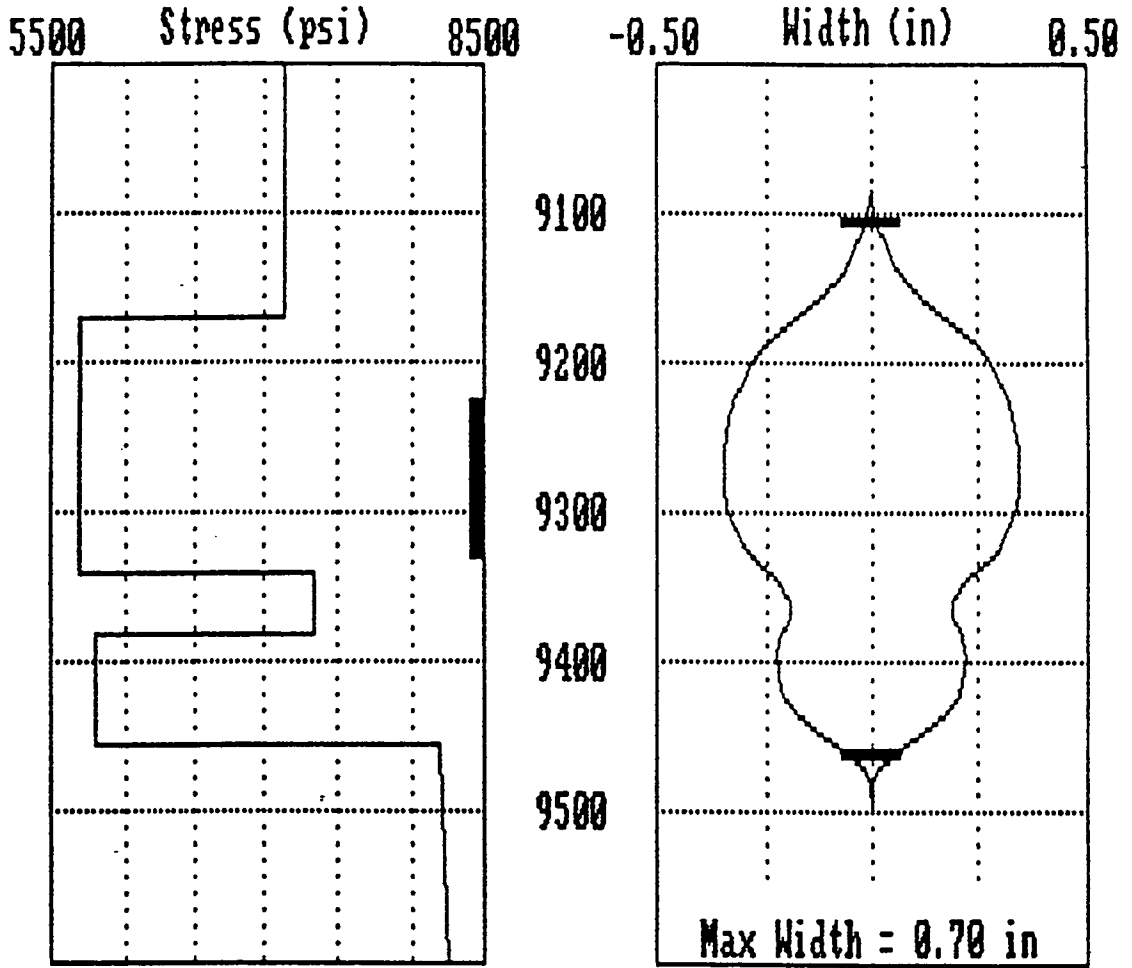
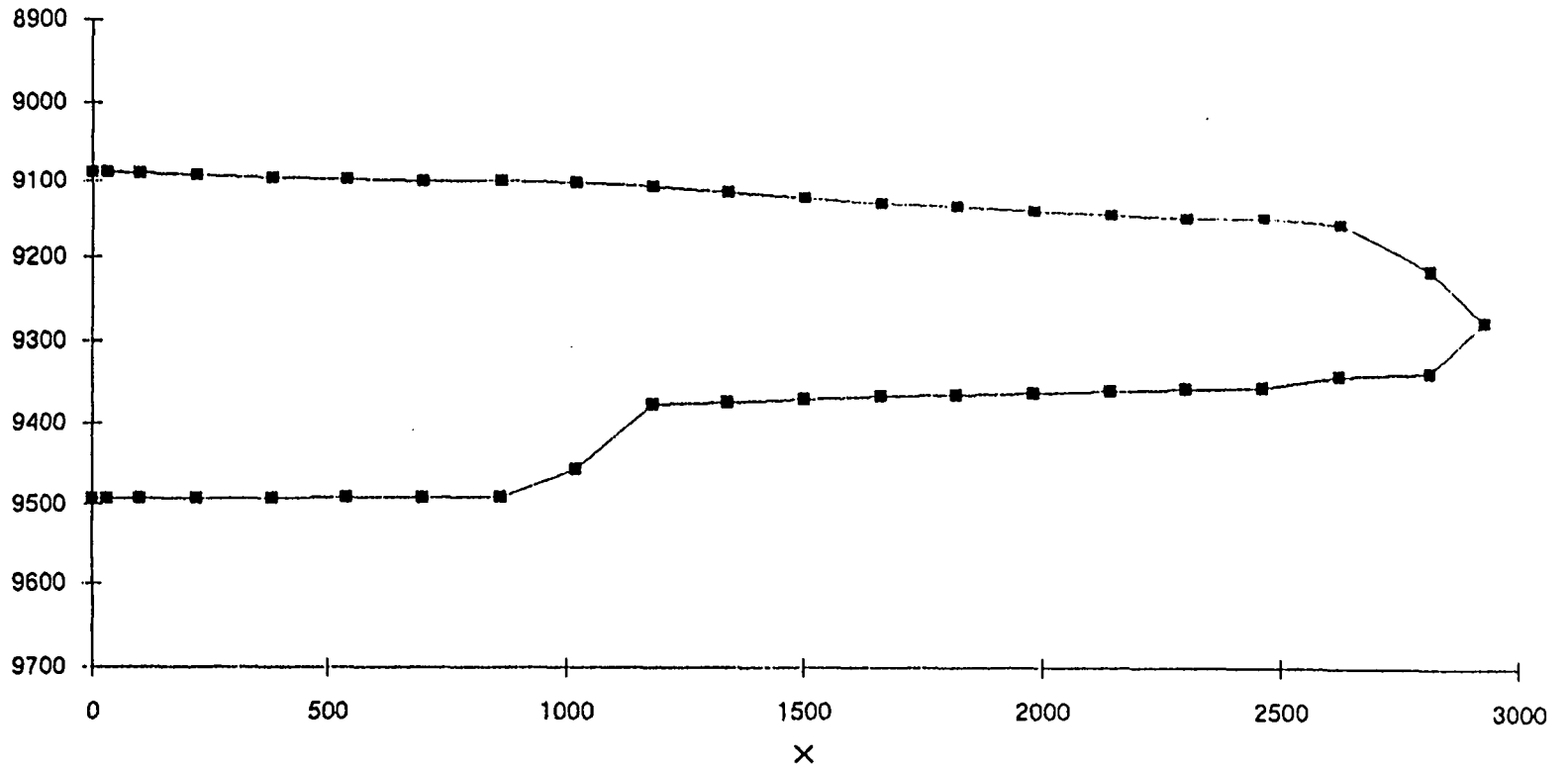


Figure F7 Height profile (Stimplan) - case 8

SFE#3 (5-Layer, Var. Visc.)



153

Figure F8 Width profile (Stimplan) - case 8

Well I.D.:SFE#3

File Name:

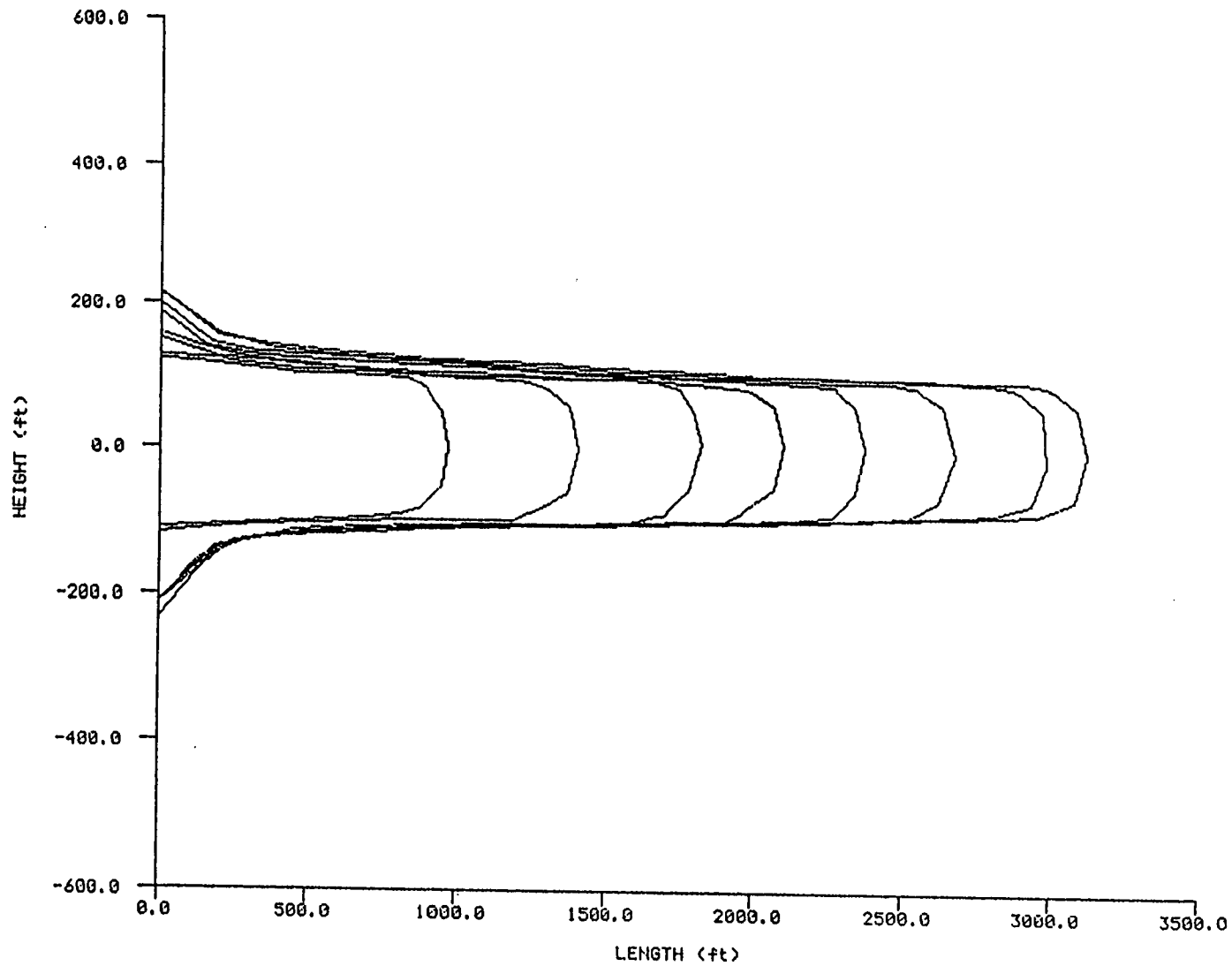


Figure F9 Height profile (TerraFrac) - case 8

**Appendix G Width and height profiles for RES Fracpro**

Figure G1-G8 give the height profiles and width profiles calculated by Fracpro as a function of length for cases 5-8. These profiles were provided by RES and have not been changed for publication.

# CASE 5: 200 CP; 3-LAYER

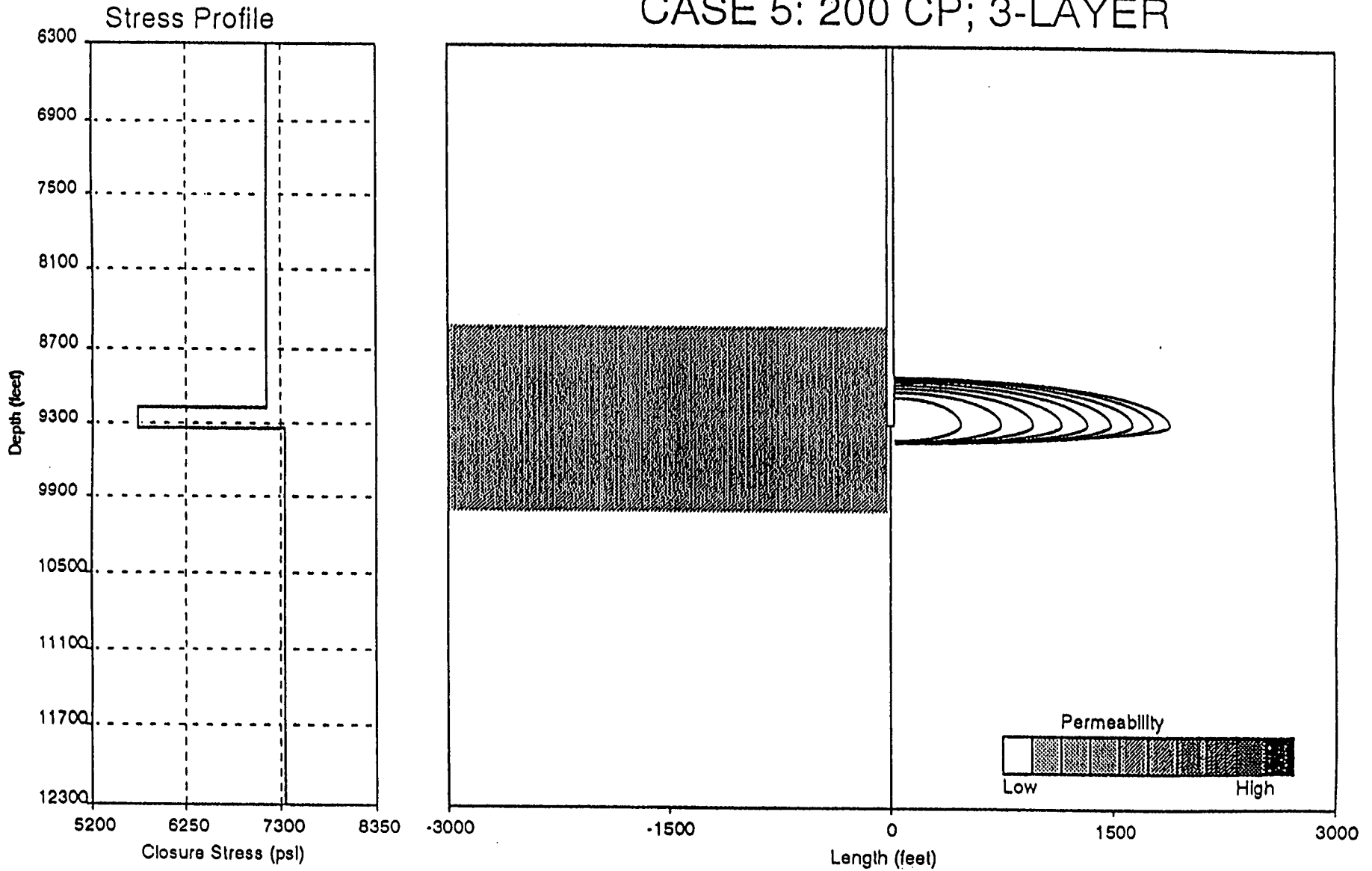


Figure G1 Height profile - case 5

# CASE 5: 200 CP; 3-LAYER

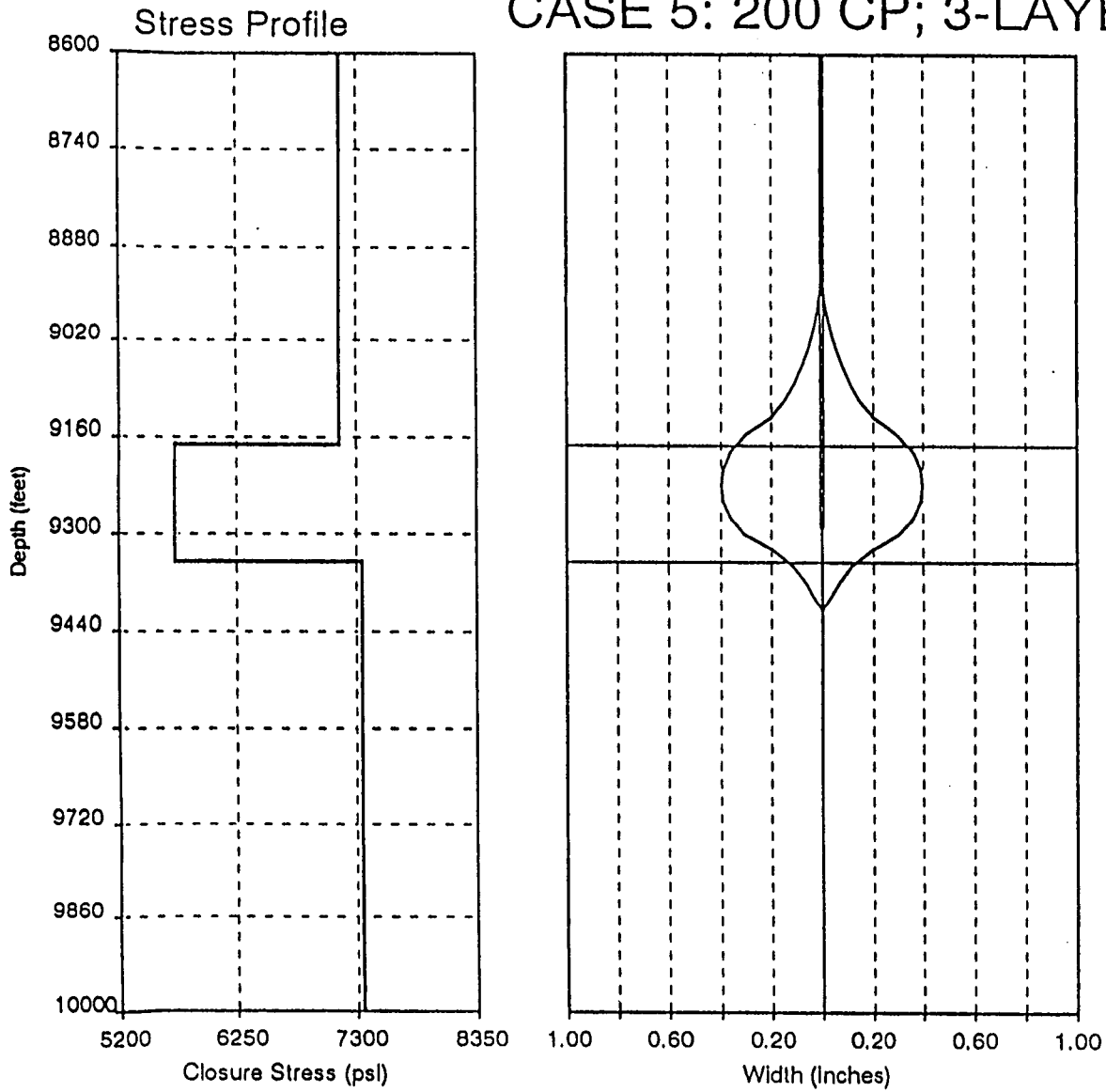


Figure G2 Width profile - case 5

# CASE 6: 40# X-1 VIS; 3-LAYER

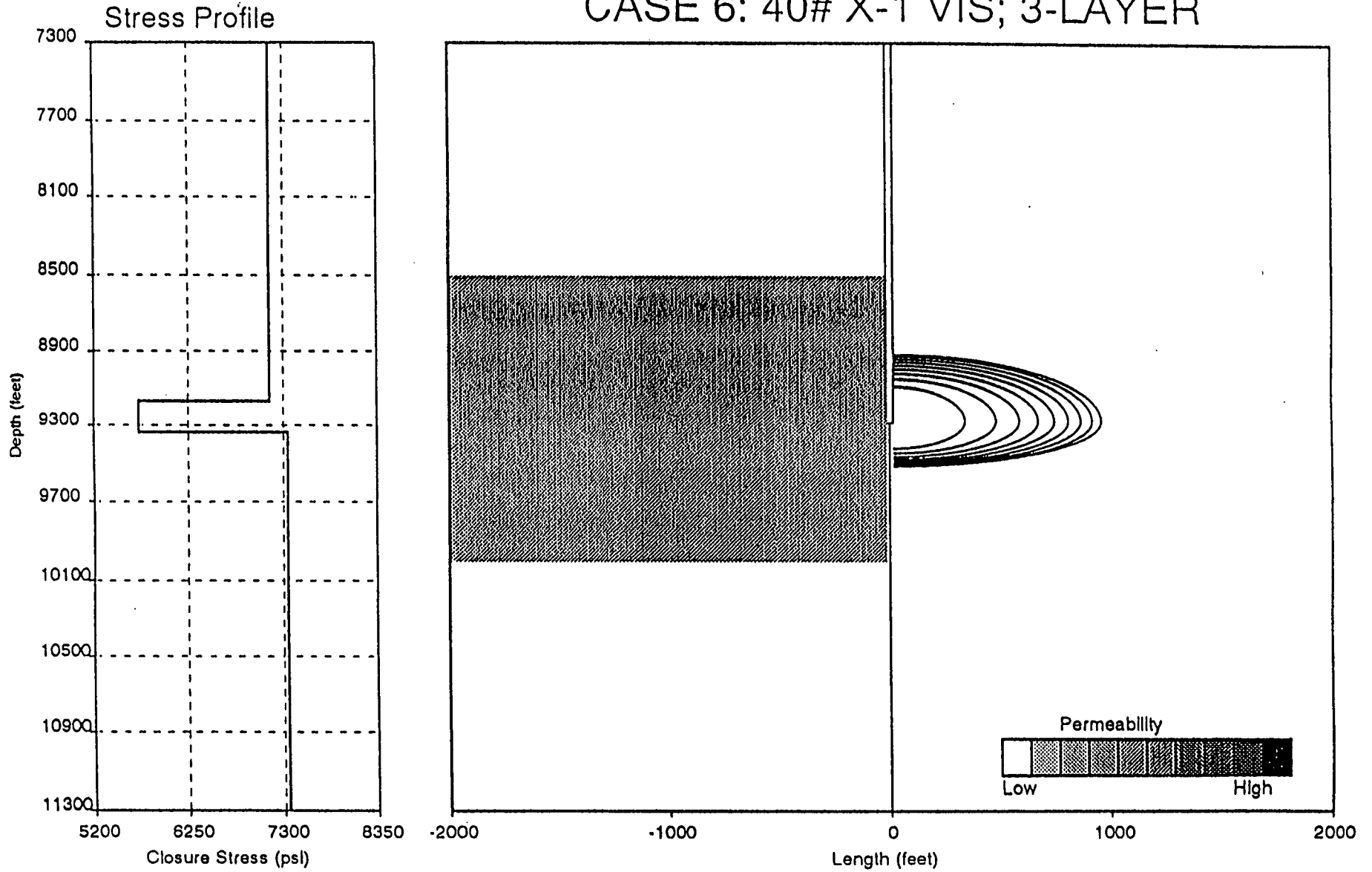


Figure G3 Height profile - case 6

# CASE 6: 40# X-1 VIS; 3-LAYER

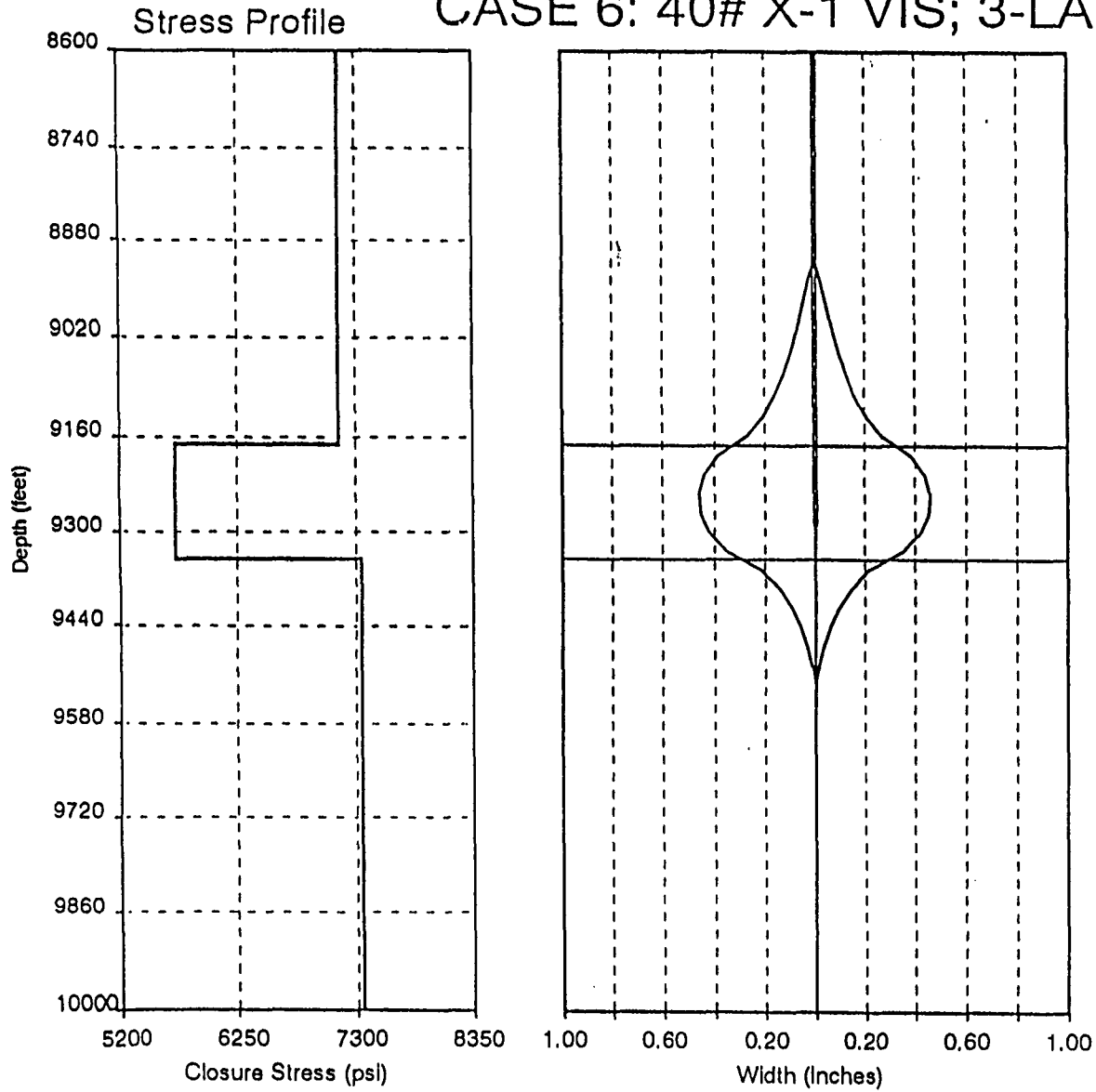


Figure G4 Width profile - case 6

# CASE 7: 200 CP; 5-LAYER

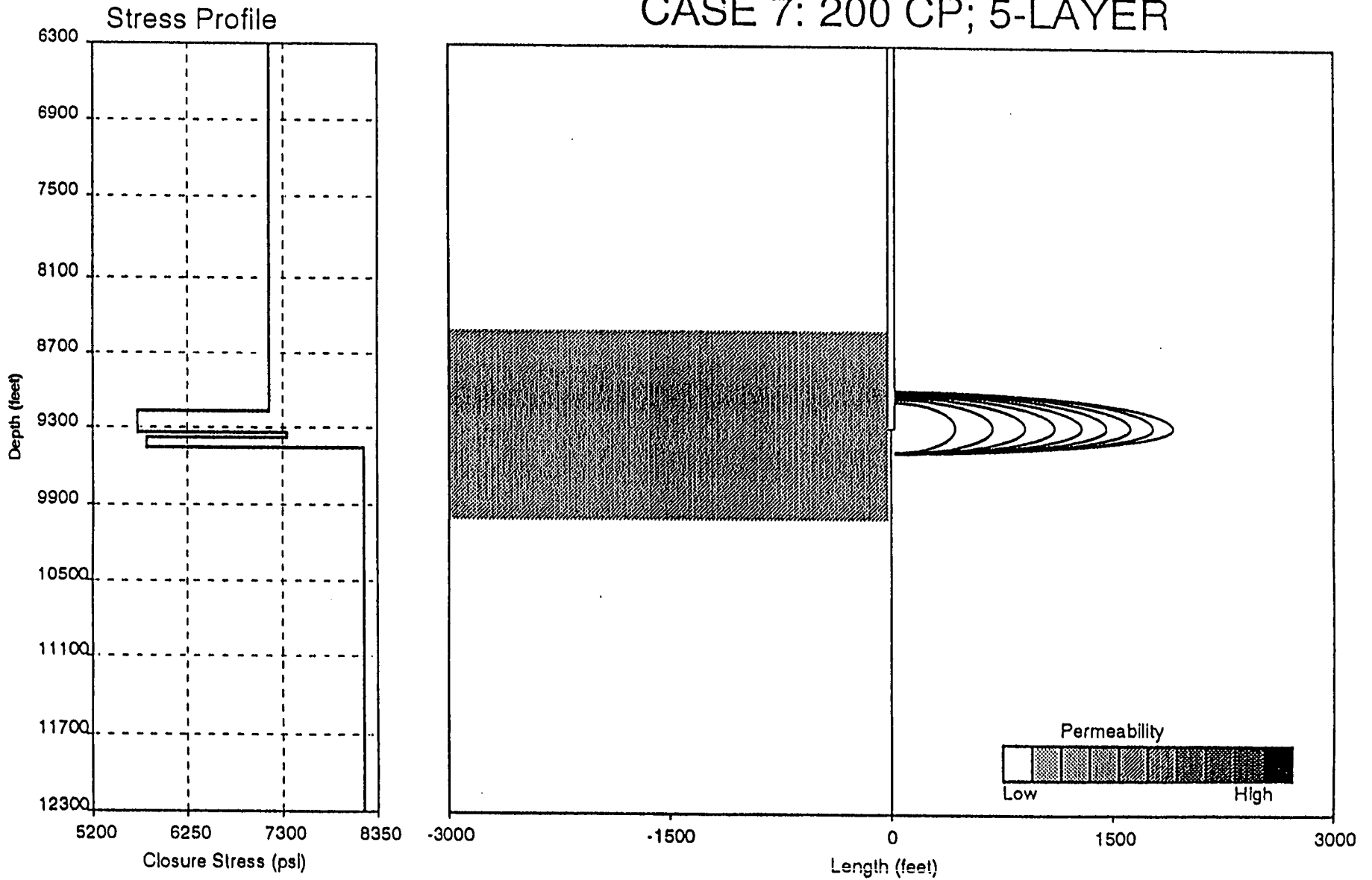


Figure G5 Height profile - case 7

# CASE 7: 200 CP; 5-LAYER

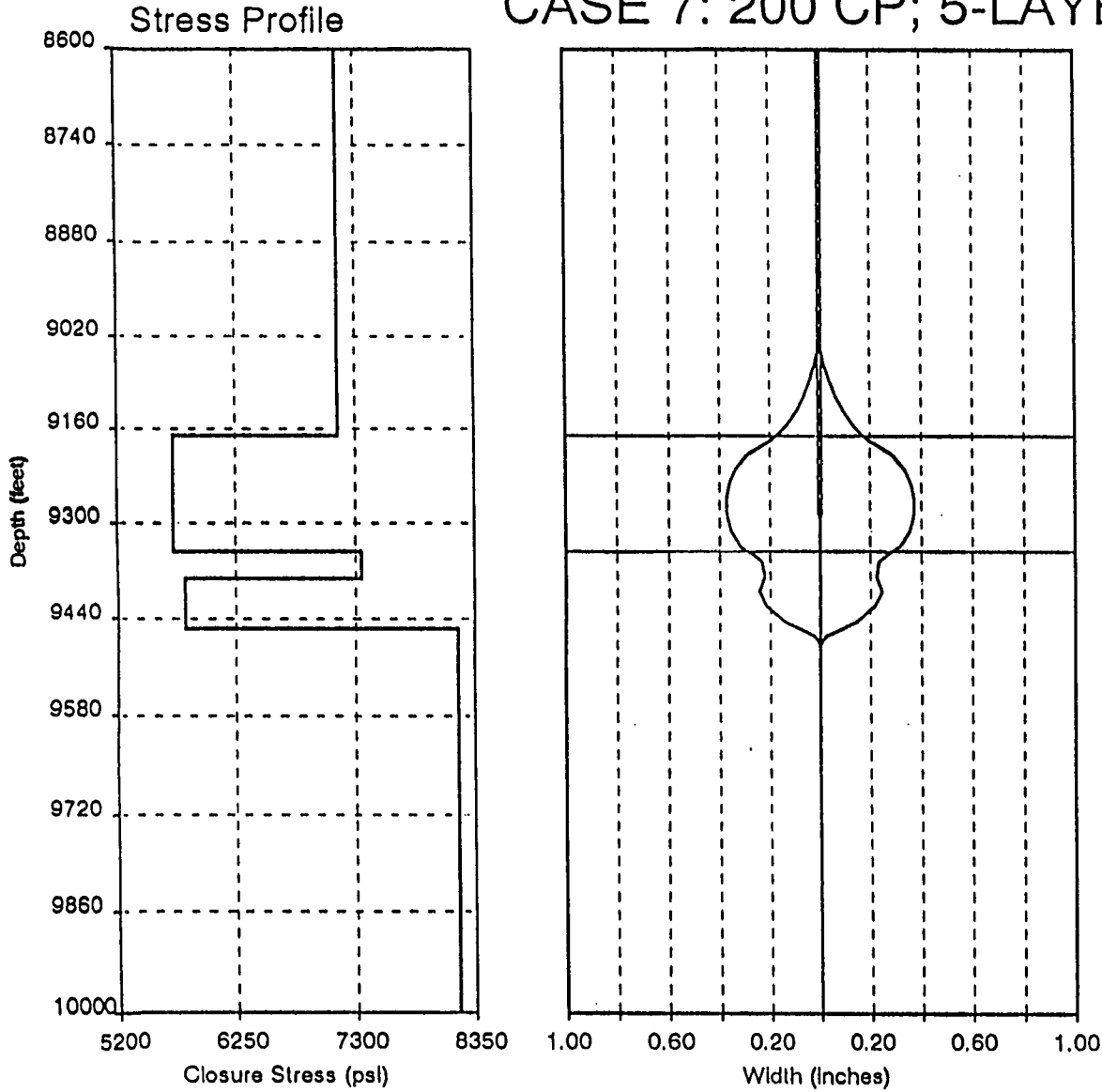


Figure G6 Width profile - case 7

# CASE 8: 40# X-1; 5-LAYER

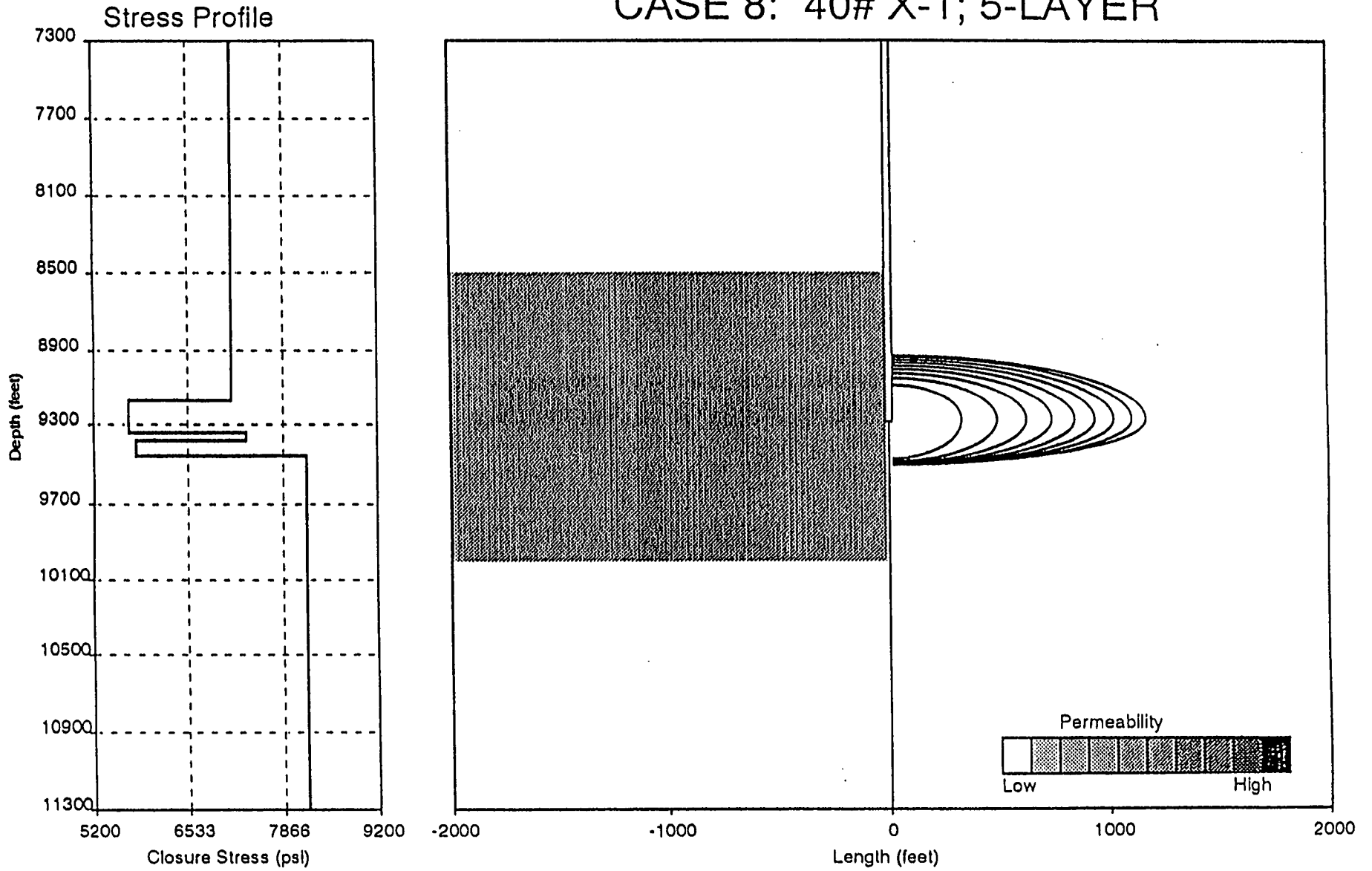


Figure G7 Height profile - case 8

# CASE 8: 40# X-1; 5-LAYER

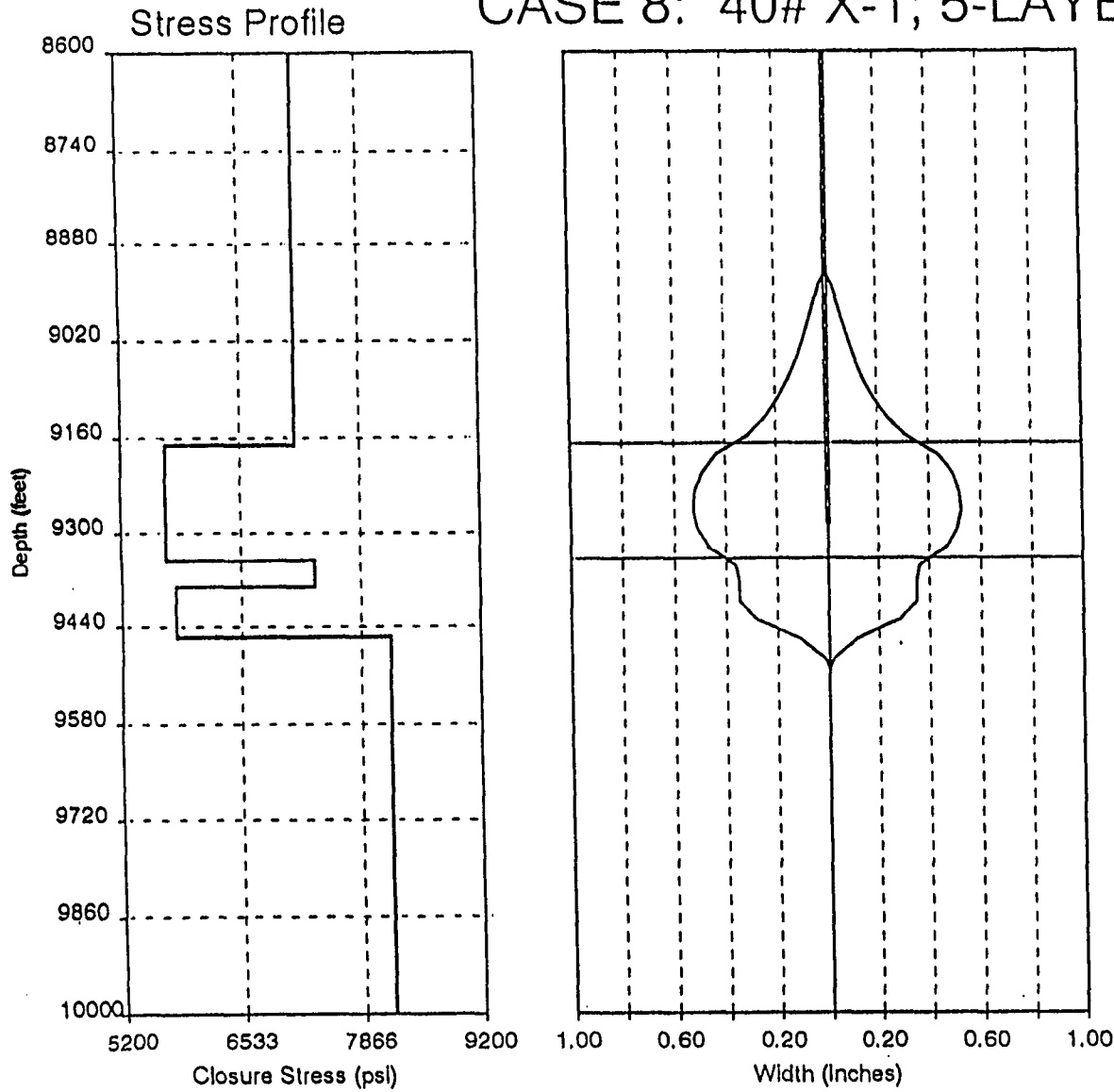


Figure G8 Width profile - case 8

**THIS PAGE INTENTIONALLY LEFT BLANK**